

พฤติกรรมทางสัณฐานวิทยาของอนุภาคพอลิเมอร์สององค์ประกอบที่มีพลาสติกไซเซออร์
ไดออกทิลทาเลต



นางสาวรุ่งกานต์ น้อยสินธุ์

สถาบันวิทยบริการ
จุฬาลงกรณ์มหาวิทยาลัย
วิทยานิพนธ์นี้เป็นส่วนหนึ่งของการศึกษาตามหลักสูตรปริญญาวิทยาศาสตรดุษฎีบัณฑิต

สาขาวิชาวัสดุศาสตร์ ภาควิชาวัสดุศาสตร์

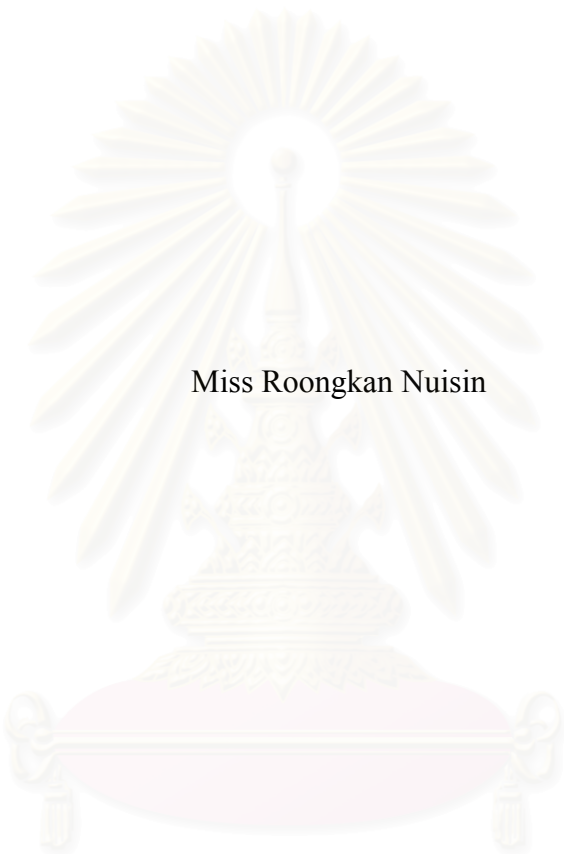
คณะวิทยาศาสตร์ จุฬาลงกรณ์มหาวิทยาลัย

ปีการศึกษา 2546

ISBN 974-17-5055-2

ลิขสิทธิ์ของจุฬาลงกรณ์มหาวิทยาลัย

MORPHOLOGICAL BEHAVIOR OF BI-COMPONENT POLYMERIC
PARTICLES WITH DIOCTYL PHTHALATE PLASTICIZER



Miss Roongkan Nuisin

สถาบันวิทยบริการ
จุฬาลงกรณ์มหาวิทยาลัย

A Dissertation Submitted in Partial Fulfillment of the Requirements
for the Degree of Doctor of Philosophy in Materials Science

Department of Materials Science

Faculty of Science

Chulalongkorn University

Academic year 2003

ISBN 974-17-5055-2

Thesis title MORPHOLOGICAL BEHAVIOR OF BI-COMPONENT
POLYMERIC PARTICLES WITH DIOCTYL PHTHALATE
PLASTICIZER
By Miss Roongkan Nuisin
Field of Study Materials Science
Thesis Advisor Professor Suda Kiatkamjornwong, Ph.D.
Thesis Co-Advisor Professor Shinzo Omi, Ph.D.

Accepted by the Faculty of Science, Chulalongkorn University in Partial
Fulfillment of the Requirements for the Doctor's Degree

.....Dean of Faculty of Science
(Professor Piamsak Menasveta, Ph.D.)

THESIS COMMITTEE

..... Chairman
(Associate Professor Saowaroj Chuayjuljit, M.Sc.)

..... Thesis Advisor
(Professor Suda Kiatkamjornwong, Ph.D.)

..... Thesis Co-Advisor
(Professor Shinzo Omi, Ph.D.)

..... Member
(Associate Professor Werusak Udomkichdecha, Ph.D.)

..... Member
(Mr. Nopporn Pramojaney, Ph.D.)

..... Member
(Assistant Professor Vimolvann Pimpan, Ph.D.)

..... Member
(Lecturer Nantana Jiratumnukul, Ph.D.)

รุ่งกานต์ นุ้ยสินธุ์ : พฤติกรรมทางสัณฐานวิทยาของอนุภาคพอลิเมอร์สององค์ประกอบ
ที่มีพลาสติกไซเซออร์ไดออกทิลทาเลต. **(Morphological Behavior of Bi-
Component Polymeric Particles with Dioctyl Phthalate Plasticizer)** อ. ที่
ปรึกษา : ศ.ดร. สุดา เกียรติกำจรวงศ์, อ. ที่ปรึกษาร่วม: ศ.ดร. ชินไชยะ โอมิ จำนวนหน้า
180 หน้า. ISBN 974-17-5055-2

การศึกษาสัณฐานของพอลิเมอร์สององค์ประกอบประเภทสไตรีนและอะครีเลตนั้น วัตถุประสงค์ที่
หนึ่งประกอบด้วยมอนอเมอร์เมทิลอะครีเลต บิวทิลอะครีเลต หรือบิวทิลเมทาครีเลต วัตถุประสงค์ที่สอง
ประกอบด้วยสไตรีน หรือเมทิลเมทาครีเลต สามารถทำให้หยดของมอนอเมอร์ขนาดเท่า ๆ กันเกิดขึ้น
โดยใช้ชิราสุพอร์สกลาสส์เมมเบรน (เอสพีจี) ที่มีขนาดรูพรอง 0.51 หรือ 0.90 ไมโครเมตร โดยการทำ
อิมัลชันพีเคชันหนึ่งครั้ง ขั้วหยดของเหลวที่ถูกขั้วผ่านรูพรองของเมมเบรน ซึ่งประกอบด้วยมอนอเมอร์
เป็นส่วนใหญ่ สารเติมแต่งประเภทไม่ชอบน้ำ และสารริเริ่มประเภทละลายในน้ำมัน แขนงลอยอยู่
ในวัฏภาคของน้ำที่มีสารคงเสถียรภาพและตัวยับยั้งบรรจุอยู่ หลังจากนั้น ถ่ายของผสมสู่ปฏิกรณ์
และทำพอลิเมอร์เชชัน ได้อนุภาคของพอลิ(สไตรีน-โค-อะครีเลต) ที่มีเส้นผ่านศูนย์กลางในช่วง 3 ถึง
10 ไมโครเมตร และมีการกระจายของขนาดอนุภาคแคบ โดยค่าสัมประสิทธิ์ของการเปลี่ยนแปลง
ไกล์ร้อยละ 10 ขึ้นอยู่กับชนิดของมอนอเมอร์และองค์ประกอบ ศึกษาผลของอุณหภูมิการเปลี่ยนสถานะ
คล้ายแก้วของโคพอลิเมอร์ โดยเทคนิคดิฟเฟอเรนเชียลสแกนนิ่งคาลอริเมทรี พบว่าโคพอลิเมอร์ที่
ประกอบด้วยเมทิลอะครีเลตเข้ากันได้ดีกับเมทิลเมทาครีเลต มากกว่ากับสไตรีนที่มีพลาสติกไซเซออร์
ไดออกทิลทาเลต ค่าอุณหภูมิการเปลี่ยนสถานะคล้ายแก้วของพอลิ(เมทิลเมทาครีเลต-โค-เมทิลอะครีเลต)
ขึ้นกับองค์ประกอบลอยเลื่อน เนื่องจากความแตกต่างของสัดส่วนความว่องไวของมอนอเมอร์ การเติม
พลาสติกไซเซออร์ลงในพอลิ(เมทิลเมทาครีเลต-โค-เมทิลอะครีเลต) มีผลต่อค่าอุณหภูมิการเปลี่ยนสถานะ
คล้ายแก้วน้อยกว่าต่อพอลิ(สไตรีน-โค-เมทิลอะครีเลต) การใช้พอลิเมอร์ที่มีหมู่อะครีเลตโซ่ยาว เช่น
บิวทิลเมทาครีเลต หรือบิวทิลอะครีเลตในโคพอลิเมอร์ มีผลต่ออุณหภูมิการเปลี่ยนสถานะคล้ายแก้วมาก
กว่าการใช้พลาสติกไซเซออร์ไดออกทิลทาเลต ยังควบคุมสัณฐานของอนุภาคพอลิเมอร์ได้โดยการเติมพอลิ
เมอร์ที่มีน้ำหนักโมเลกุลต่ำ เช่น พอลิสไตรีน โดยอัตราส่วนของพอลิสไตรีนและมอนอเมอร์สไตรีน ทำ
ให้ความหนืดของวัฏภาคกระจายเพิ่มขึ้น พบพอลิเมอร์ที่มีสัณฐานแบบแกนเปลือกหรือโครงสร้างแบบ
สะเกลามิ ได้ศึกษาการเกิดเป็นฟิล์มของพอลิเมอร์และสัณฐานวิทยาที่ผิวโดยเทคนิค ไมโครสโกปี

ภาควิชา วัสดุศาสตร์
สาขาวิชาวัสดุศาสตร์
ปีการศึกษา 2546

ลายมือชื่อนิสิต.....
ลายมือชื่ออาจารย์ที่ปรึกษา.....
ลายมือชื่ออาจารย์ที่ปรึกษาร่วม.....

#4373831623: MAJOR MATERIALS SCIENCE

KEY WORD: PARTICLE MORPHOLOGY / SPG (SHIRASU POROUS GLASS)
MEMBRANE EMULSIFICATION / SUSPENSION / STYRENE /
ACRYLATE / PLASTICIZER

ROONGKAN NUISIN: THESIS TITLE. MORPHOLOGICAL
BEHAVIOR OF BI-COMPONENT POLYMERIC PARTICLES WITH
DIOCTYL PHTHALATE PLASTICIZER. THESIS ADVISOR : PROF.
SUDA KIATKAMJORNWONG, Ph.D., THESIS COADVISOR : PROF.
SHINZO OMI, Ph.D. 180 pp. ISBN 974-17-5055-2.

Two-phase copolymers containing styrene-acrylate were synthesized with a soft phase consisting of methyl acrylate, butyl acrylate, or butyl methacrylate. Besides the styrenic copolymers, the copolymers containing a hard phase of methyl methacrylate were also synthesized. Comonomer droplets with a narrow size distribution were prepared using Shirasu Porous Glass (SPG) membrane having pore size 0.51 or 0.90 μm . After a single-step SPG emulsification, the emulsion droplets composing mainly of monomers, hydrophobic additives, and an oil-soluble initiator were suspended in the aqueous phase containing a stabilizer and an inhibitor. It was then transferred to a reactor, and subsequent suspension polymerization was carried out. Uniform copolymer particles poly(styrene-*co*-acrylate)s with a mean diameter ranging from 3 to 10 μm with a narrow particle size distribution or a coefficient of variation close to 10% were achieved depending on comonomer compositions and the recipe. The glass transition temperature measured by differential scanning calorimetry indicated that the resulting copolymer particles contained a soft phase of methyl acrylate compatibilized better with a hard phase of methyl methacrylate than styrene with dioctyl phthalate addition. Glass transition temperatures of poly[(methyl methacrylate)-*co*-(methyl acrylate)] particles were strongly affected by the composition drift in the copolymer caused by their high difference in reactivity ratio. Incorporation of dioctyl phthalate in the copolymer particles did not significantly affect the glass transition temperature of methyl methacrylate- or methyl acrylate-containing copolymer particles, but it did affect the styrene-containing copolymer and particle morphology of the copolymers observed by TEM technique. Incorporation of a long-side chain monomer such as butyl methacrylate or butyl acrylate in copolymerizing with styrene was more effective plasticized than that adding an external plasticizer like dioctyl phthalate. The particle morphologies were also controlled by the addition of low-molecular weight polystyrene. When viscosity of the dispersion phase was high, different morphologies such as core-shell or salami structure were observed. The film formation of copolymer and their surface morphology were studied by microscopic techniques.

Department Materials Science

Student's signature.....

Field of study Materials Science

Advisor's signature.....

Academic year 2003

Co-advisor's signature.....

ACKNOWLEDGEMENTS

I would like to use this opportunity to thank everybody without whose help this work would have not been realized.

First of all, I wish to express my deep gratitude to my advisor Prof. Suda Kiatkamjornwong, Ph.D. for her guidance and kindness throughout the course of study. Her advice, support and encouragement were invaluable and indispensable at all times. I would like to express my sincere gratitude to my overseas advisor Prof. Shinzo Omi, Ph.D. for valuable advice and comments, and very importantly, his kindness and attention throughout the years of the research work in Japan. I am also thankful to him for exposing me to other aspects of polymer science and membrane technology. I would like to take this opportunity to thank Prof. Guang Hui Ma, Ph.D., Dr. Yong Zhong Du, Dr. Naohiro Yamazaki, Dr. Fuminori Ito, and Mr. Kenji Kusunoki for their helpful discussions and suggestions. I am very grateful to Prof. Yasushi Hoshino, Ph.D., and Mr. Ryo Kuroda, Nippon Institute of Technology for carrying out the film characterization by AFM microscopy.

I am grateful to the Department of Materials Science, the Department of Imaging and Printing Technology of the Faculty of Science, the Graduate School of Chulalongkorn University, and Graduate School of Bio-Applications and Systems Engineering (BASE), Tokyo University of Agriculture and Technology for the generous access to research facilities and financial support. I would like to thank the Thailand Research Fund for providing a special research grant in the Program of Golden Jubilee Scholarship, PHD/0041/2543 over the years of study.

I am also thankful to my committee members: Assoc. Prof. Saowaroj Chuaychuljit, M.Sc., Assoc. Prof. Werasak Udomkichdecha, Ph.D., Dr. Nopporn Pramojaney, Asst. Prof. Vimolvan Pimpan, Ph.D., and Lecturer Nantana Jiratumnukul, Ph.D. for their help and advice.

Finally, I am grateful to my parents for their endless support and encouragement over the years. My sincere thanks are also extended to my friends in Thailand and in Japan for their helpful support during the years of hard work. Thanks to Mr. Wiyong Kangwansupamonkon and Ms. Prodepran Thakeaw for their help and support.

CONTENTS

| | Page |
|---|-------------|
| ABSTRACT (IN THAI)..... | iv |
| ABSTRACT (IN ENGLISH)..... | v |
| ACKNOWLEDGEMENTS..... | vi |
| CONTENTS..... | vii |
| LIST OF TABLES..... | xiii |
| LIST OF FIGURES..... | xv |
| LIST OF ABBREVIATIONS AND SYMBOLS..... | xxiv |
| CHAPTER | |
| 1. INTRODUCTION..... | 1 |
| 1.1 Objectives..... | 4 |
| 1.2 Scope of the Research Work..... | 4 |
| 2. THEORY AND LITERATURE SURVEY..... | 5 |
| 2.1 Free-radical Polymerization..... | 5 |
| 2.1.1 Copolymerization Equation..... | 6 |
| 2.1.2 Copolymer Composition Drift..... | 10 |
| 2.2 Particle Morphology..... | 10 |
| 2.2.1 Thermodynamic Considerations..... | 10 |
| 2.2.2 Various Types of Particles and Their Applications.. | 14 |
| 2.3 Plasticizer..... | 15 |
| 2.3.1 Theories of Plasticization..... | 16 |
| 2.3.2 Plasticizer Performance Criterion..... | 17 |
| 2.3.3 Solubility Parameter..... | 18 |

CONTENTS (Continued)

| | |
|---|----|
| 2.3.4 Durability..... | 18 |
| 2.4 Glass-Transition Behavior..... | 19 |
| 2.5 Thermodynamics of Mixing Polymer and Plasticizer..... | 20 |
| 2.6 Membrane Emulsification..... | 22 |
| 2.6.1 The Theory of SPG Emulsification..... | 25 |
| 2.6.2 The Formation of Droplets..... | 27 |
| 2.6.3 Preparation of Emulsion Types by SPG Emulsification..... | 31 |
| 2.6.3.1 Preparation of an Oil-in-Water (O/W) Emulsion..... | 31 |
| 2.6.3.2 Preparation of a Water-in-Oil (W/O) Emulsion..... | 32 |
| 2.6.3.3 Preparation of a Water-in-Oil-in-Water (W/O/W) Emulsion..... | 32 |
| 2.6.4 Emulsifier..... | 33 |
| 2.7 Suspension Polymerization..... | 33 |
| 2.8 Film Formation of the Polymer..... | 34 |
| 2.9 Literature Reviews..... | 37 |
| 3. EXPERIMENTAL..... | 44 |
| 3.1 Materials, Apparatus, and Analytical Instruments..... | 44 |
| 3.1.1 Materials..... | 44 |
| 3.1.1.1 Monomers..... | 44 |
| 3.1.1.2 Crosslinking Agent..... | 45 |

CONTENTS (Continued)

| | | |
|---------|---|----|
| 3.1.1.3 | Initiators..... | 45 |
| 3.1.1.4 | Plasticizer and Hydrophobic Additives..... | 45 |
| 3.1.1.5 | Stabilizers..... | 46 |
| 3.1.1.6 | Solvents..... | 46 |
| 3.1.1.7 | Other Chemicals..... | 46 |
| 3.1.2 | Apparatus..... | 47 |
| 3.1.2.1 | SPG Emulsification Apparatus..... | 47 |
| 3.1.2.2 | Polymerization Kit..... | 47 |
| 3.1.3 | Analytical Instruments..... | 48 |
| 3.2 | Experimental..... | 48 |
| 3.2.1 | Emulsification Procedure..... | 48 |
| 3.2.2 | Polymerization..... | 52 |
| 3.3 | Characterization..... | 52 |
| 3.3.1 | Conversion of Monomers..... | 52 |
| 3.3.2 | Surface Morphology..... | 52 |
| 3.3.3 | Internal Morphology of the Particles..... | 53 |
| 3.3.4 | Size and Size Distribution of Emulsion Droplets and Polymer Particles..... | 54 |
| 3.3.5 | Molecular Weights and Distribution..... | 55 |
| 3.3.6 | Glass Transition Temperature..... | 55 |
| 3.3.7 | Nuclear Magnetic Resonance Spectroscopy..... | 56 |
| 3.3.8 | Functional Group of Copolymer..... | 56 |
| 3.3.9 | Atomic Force Microscopy..... | 57 |

CONTENTS (Continued)

| | | |
|--------|--|----|
| 3.3.10 | Film Formation and Characterization | 58 |
| 4. | RESULTS AND DISCUSSION..... | 60 |
| 4.1 | Effect of DOP on Styrene Homopolymerization..... | 60 |
| 4.1.1 | Dependence of Styrene Homopolymerization on Initiator Type..... | 65 |
| 4.1.2 | Effect of Inhibitor on Polymerization and Polymer Particles..... | 69 |
| 4.1.3 | Detection of DOP Incorporation in the Copolymer by ^1H NMR..... | 71 |
| 4.2 | Effect of the Amount of DOP Plasticizer on Poly(styrene- <i>co</i> -MMA) Particles..... | 74 |
| 4.3 | Effect of DOP on Properties of Poly(Styrene- <i>co</i> -MA) and Poly(MMA- <i>co</i> -MA) Particles..... | 76 |
| 4.3.1 | Particle Morphology..... | 76 |
| 4.3.2 | Glass Transition Temperature..... | 81 |
| 4.3.3 | Effect of Monomer Composition on Glass Transition Temperature..... | 88 |
| 4.3.4 | Effect of Monomer Composition on Molecular Weight of Polymer..... | 91 |
| 4.3.5 | Internal Morphology of Poly(St- <i>co</i> -MA)..... | 92 |
| 4.3.6 | Poly(St- <i>co</i> -MA)/PSt Composite..... | 93 |
| 4.3.7 | Copolymer Composition by ^1H -NMR..... | 97 |

CONTENTS (Continued)

| | |
|--|-----|
| 4.4 Synthesis of Poly(Styrene- <i>co</i> -BMA)..... | 100 |
| 4.4.1 Effect of Initiator Type on Molecular Weight and Molecular Weight Distribution..... | 100 |
| 4.4.2 Effect of the Addition of Polystyrene on Properties of Poly(St- <i>co</i> -BMA) Copolymers..... | 101 |
| 4.4.3 Effect of Polystyrene on Molecular Weight and Molecular Weight Distribution | 109 |
| 4.4.4 Poly(St- <i>co</i> -BMA)/PSt Composite..... | 110 |
| 4.4.5 Glass Transition Temperature of Poly(St- <i>co</i> -BMA) | 113 |
| 4.4.6 Effect of Stabilizer Concentration on Molecular Weight and Molecular Weight Distribution..... | 114 |
| 4.5 Synthesis of Poly(Styrene- <i>co</i> -BA)..... | 115 |
| 4.5.1 Effect of DOP on Properties of Poly(St- <i>co</i> -BA) Copolymer..... | 116 |
| 4.5.2 Effect of Polystyrene Bulky Molecule on Molecular Weight and Molecular Weight Distribution of Poly(St- <i>co</i> -BA)..... | 118 |
| 4.5.3 Internal Morphology of Poly(St- <i>co</i> -BA)/PSt Composites..... | 119 |
| 4.6 Synthesis of poly(MMA- <i>co</i> -MA)..... | 120 |
| 4.6.1 Effect of Stabilizer Type on Molecular Weight and Morphology of Copolymer..... | 121 |

CONTENTS (Continued)

| | |
|--|-----|
| 4.6.2 Effect of Stabilizer on Monomer Droplet Size, Droplet Size Distribution, Polymer Particle Size and Particle Size Distribution..... | 125 |
| 4.6.3 Effect of Monomer Composition on Average Molecular Weight, Molecular Weight Distribution, and Glass Transition Temperature.... | 129 |
| 4.6.4 Effect of Initiator Concentration on Polymer Morphology..... | 131 |
| 4.6.5 Synthesis of Poly(MMA- <i>co</i> -MA) with Various Additives..... | 136 |
| 4.7 Synthesis of Poly(MMA- <i>co</i> -BA) and Poly(MMA- <i>co</i> - BMA) Particles..... | 139 |
| 4.8 Film Formation and Characterization | 143 |
| 4.8.1 Polystyrene Cast Film..... | 143 |
| 4.8.2 Poly(St- <i>co</i> -MA) Cast Film..... | 145 |
| 4.8.3 Structure of Film Surfaces Studied by Atomic Force Microscopy..... | 150 |
| 5. CONCLUSIONS..... | 151 |
| REFERENCES..... | 156 |
| APPENDICES..... | 172 |
| VITA..... | 180 |

LIST OF TABLES

| TABLE | | PAGE |
|-------|---|------|
| 2.1 | Glass transition temperature (°C) for homopolymers from various monomers..... | 20 |
| 2.2 | Solubility parameter of monomer and plasticizer..... | 22 |
| 2.3 | Comparison of characteristics of different polymerization processes..... | 24 |
| 3.1 | A selected recipe for the SPG emulsification | 52 |
| 4.1 | Recipe and experimental results for styrene..... | 63 |
| 4.2 | Calculated amounts of DOP in polystyrene..... | 72 |
| 4.3 | A standard recipe for the SPG..... | 74 |
| 4.4 | A recipe of the continuous phase for the SPG emulsification with the SPG membrane pore size of 1.42 μm | 75 |
| 4.5 | Recipe and results of styrene and methyl acrylate copolymerization..... | 78 |
| 4.6 | Recipe and results of methyl methacrylate and methyl acrylate copolymerization..... | 80 |
| 4.7 | Monomer reactivity ratios for free-radical copolymerization at 60°C..... | 82 |
| 4.8 | Calculated and experimental compositions in radical copolymerization of St and MA..... | 98 |
| 4.9 | Styrene and BMA copolymerization recipe and results..... | 104 |
| 4.10 | Recipe and experimental results for styrene and butyl acrylate copolymerization | 117 |

LIST OF TABLES (Continued)

| | | |
|------|--|-----|
| 4.11 | Recipe and results of methyl methacrylate and methyl acrylate using various stabilizer types..... | 122 |
| 4.12 | Recipe and results of methyl methacrylate and methyl acrylate copolymerization using various amounts of initiator | 133 |
| 4.13 | Recipe and results for methyl methacrylate and methyl acrylate using various additives..... | 138 |
| 4.14 | Recipe and results of methyl methacrylate and butyl acrylate, methyl methacrylate and butyl methacrylate copolymerization..... | 142 |
| 4.15 | Summary of AFM observations..... | 149 |
| A-1 | Numeric data for cumulative composition in poly(St-co-MA); Y_A vs x_M | 174 |
| A-2 | Calculated styrene fraction in unreacted monomers. For poly(St-co-MA); z_A vs x | 175 |
| A-3 | Numeric data for instantaneous composition of styrene in the copolymer; y_A vs x_M | 176 |
| A-4 | Numeric data for cumulative composition in poly(MMA-co-MA); Y_A vs x_M | 177 |
| A-5 | Calculated MMA fraction in unreacted monomer. For poly(MMA-co-MA); z_A vs x | 178 |
| A-6 | Numeric data for instantaneous composition of MMA in poly(MMA-co-MA); y_A vs x_M | 179 |

LIST OF FIGURES

| FIGURE | | PAGE |
|--------|--|------|
| 2.1 | Initial and final stages for the morphology development (basic morphologies)..... | 12 |
| 2.2 | Radii of core-shell and inverted morphologies..... | 14 |
| 2.3 | Reaction of phthalate plasticizers..... | 15 |
| 2.4 | Flow of manufacturing Shirasu porous glass (SPG)..... | 26 |
| 2.5 | SPG membrane: a) a cross section image from SEM, and b) SPG membrane (cylinder)..... | 26 |
| 2.6 | Sketch of the applied pressure corresponding to formation of the emulsion droplets..... | 29 |
| 2.7 | Average diameters of emulsion droplets as a function of pore size of SPG membrane..... | 30 |
| 2.8 | Sketch of the surface of a microporous membrane at the moment t_0 and in subsequent moment $t_0 + \Delta t$ emulsification. a) The dynamic contact angle α is small and the contact line membrane-water-oil phase is fixed at the pore diameter. b) The angle α is larger and facilitates the contact-line expansion in the course of growth of the drop; the latter may span two or more pores..... | 31 |
| 2.9 | The various stages in the formation of a film during the drying of an aqueous dispersion of a soft latex..... | 36 |
| 3.1 | A schematic diagram of an SPG emulsification kit..... | 51 |
| 3.2 | Sample preparation for AFM measurements..... | 57 |

LIST OF FIGURES (Continued)

| | | |
|-----|--|----|
| 4.1 | SEM photographs of polystyrene incorporated with DOP: a) DOP 2.5 wt% (Run 2013); b) DOP 5 wt% (Run 2012, ADVN as initiator); c) DOP 5 wt% (Run 2014, BPO as initiator); d) DOP 5 wt% (Run 2016, ADVN as initiator and PDA as inhibitor); e) DOP 10 wt% (Run 2056, BPO as initiator); and f) DOP 15 wt% (Run 2057, BPO as initiator)..... | 62 |
| 4.2 | Relationship between emulsification time with: a) droplets size; b) standard deviation; and c) coefficient of variation of droplets..... | 64 |
| 4.3 | Normalized GPC chromatograms of polystyrene particles showing effects of the different initiator types..... | 66 |
| 4.4 | Relationship between T_g and DOP concentration (wt%) based on the monomer: a) clean, and b) unclean particles..... | 68 |
| 4.5 | Appearance of the polymer latex stability after 24 hours of polymerization: a) ADVN, NaNO_2 (Run 2011); b) ADVN, NaNO_2 (Run 2012); c) ADVN, NaNO_2 (Run 2013); d) BPO, NaNO_2 (Run 2014); and e) ADVN, PDA (Run 2016)..... | 70 |
| 4.6 | Normalized GPC chromatograms of polystyrene particles showing effects of the inhibitor type..... | 71 |
| 4.7 | Chemical structures of DOP and polystyrene..... | 72 |
| 4.8 | ^1H NMR spectra of polystyrene incorporated with DOP, a) 5 wt% (Run 2016); b) 10 wt% (Run 2056); and c) 15 wt% (Run 2057)..... | 73 |

LIST OF FIGURES (Continued)

| | | |
|------|---|----|
| 4.9 | SEM photographs of the plasticized copolymers: a) polystyrene with DOP 5 wt%; b) polystyrene with DOP 10 wt%; c) polystyrene with DOP 20 wt%; and d) poly(St- <i>co</i> -MMA), St:MMA of 80:20 with 5 wt% of DOP..... | 75 |
| 4.10 | SEM photographs of poly(St- <i>co</i> -MA): a) St:MA, 50:50; b) St:MA, 75:25; c) St:MA, 52:48 with DOP; d) St:MA, 75:25 with DOP; e) St:MA:PSt, 37.5:50:12.5; f) St:MA:PSt, 62.5:25:12.5; g) St:MA:PSt, 37.5:50:12.5 with DOP; and h) St:MA:PSt, 62.5:25:12.5 with DOP..... | 77 |
| 4.11 | SEM photographs of poly(MMA- <i>co</i> -MA): a) PMMA-DOP, b) MMA:MA, 75:25; c) MMA:MA, 50:50; d) MMA:MA, 25:75; e) MMA:MA, 50:50 DOP 5 wt%; f) MMA:MA, 75:25 DOP 5 wt%; and g) MMA:MA, 75:25 DOP 10 wt%..... | 79 |
| 4.12 | Composition drift of poly(St- <i>co</i> -MA), St:MA: a) 50:50 wt%; b) 75:25 wt%..... | 85 |
| 4.13 | Composition drift of poly(MMA- <i>co</i> -MA), MMA:MA: a) 50:50 wt%; b) 75:25 wt%..... | 86 |
| 4.14 | DSC thermograms of a) poly(St- <i>co</i> -MA), and b) poly(MMA- <i>co</i> -MA), with 5 wt% of DOP (based on the monomer concentrations) for all experiments..... | 87 |
| 4.15 | Relationship between T_g and styrene contents with different treatments: a) Poly(St- <i>co</i> -MA) with DOP, and b) without DOP..... | 90 |

LIST OF FIGURES (Continued)

| | | |
|------|--|----|
| 4.16 | Normalized GPC chromatograms of poly(St- <i>co</i> -MA) particles showing the effects of monomer compositions. | 91 |
| 4.17 | Normalized GPC chromatograms of poly(St- <i>co</i> -MA)/PSt particles showing the effects of monomer compositions..... | 92 |
| 4.18 | Microtomed and RuO ₄ -stained TEM photographs of poly(St- <i>co</i> -MA) particles: a) St:MA, 50:50 (Run 2018); and b) St:MA, 75:25 (Run 2019)..... | 93 |
| 4.19 | Demonstration of crosslinking reaction of polymer chains and OsO ₄ | 94 |
| 4.20 | Microtomed and OsO ₄ -stained TEM photographs of poly(St- <i>co</i> -MA)/PSt composite polymer particles: a) St:MA:PSt, 37.5:50:12.5 without DOP (Run 2024); b) St:MA:PSt, 37.5:50:12.5 with DOP (Run 2029); c) St:MA:PSt, 62.5:25:12.5 without DOP (Run 2025); and d) St:MA:PSt, 62.5:25:12.5 with DOP (Run 2030)..... | 96 |
| 4.21 | Microtomed and OsO ₄ -stained TEM photographs of poly(St- <i>co</i> -MA) copolymer particles: a) St:MA, 50:50 without DOP (Run 2022); b) St:MA, 50:50 with DOP (Run 2046); and c) St:MA, 75:25 without DOP (Run 2023)..... | 97 |
| 4.22 | Typical ¹ H NMR spectra of St/MA copolymer in CDCl ₃ at 40°C: a) polystyrene; b) poly(St- <i>co</i> -MA), St:MA of 50:50; and c) poly(St- <i>co</i> -MA), St:MA of 75:25 | 99 |

LIST OF FIGURES (Continued)

| | | |
|------|--|-----|
| 4.23 | Normalized GPC chromatograms of poly (St- <i>co</i> -BMA) particles the ratio of St:BMA, 50:50 showing the effects of initiator type. | 101 |
| 4.24 | SEM photographs of poly(St- <i>co</i> -BMA) particles: a) St:BMA, 50:50; b) 75:25; c) 75:25, DOP 5 wt%; d) 50:50, DOP 5 wt% (ADV N as initiator); e) 50:50, DOP 5 wt% (BPO as initiator); f) St:BMA:PSt, 62.5:25:12.5; and g) St:BMA:PSt, 62.5:25:12.5, DOP 5 wt%..... | 103 |
| 4.25 | A schematic model for the phase separation of the poly(St- <i>co</i> -BMA)/PSt..... | 105 |
| 4.26 | Conversion profile for methyl methacrylate polymerization depicting different phases of reaction. (o) data from Balke and Hamielec at 90°C, and 0.3% AIBN, (—) model prediction..... | 106 |
| 4.27 | “Scaling model” demonstrated by Sundberg: a) A schematic model for the path of gel effect; b) Illustration of morphological development..... | 108 |
| 4.28 | Normalized GPC chromatograms of poly(St- <i>co</i> -BMA) and poly(St- <i>co</i> -BMA)/PSt..... | 110 |
| 4.29 | Microtomed and OsO ₄ -stained TEM photographs of poly(St- <i>co</i> -BMA)/PSt composite particles: a) St:BMA:PSt, 62.5:25:12.5 without DOP (Run 2051); and b) St:BMA:PSt, 62.5:25:12.5 with DOP (Run 2052)..... | 112 |

LIST OF FIGURES (Continued)

| | | |
|------|--|-----|
| 4.30 | Microtomed and OsO ₄ -stained TEM photographs of poly(St- <i>co</i> -BMA) copolymer particles: St:BMA, 75:25 (Run 2054); and b) St:BMA, 75:25 with DOP 5 wt% of monomer (Run 2059)..... | 113 |
| 4.31 | Normalized GPC chromatograms of poly(St- <i>co</i> -BMA) with the ratio of St:BMA, 50:50 showing the effects of PVA-217 concentrations..... | 115 |
| 4.32 | SEM photographs of poly(St- <i>co</i> -BA) and poly(St- <i>co</i> -BA)/PSt particles: a) St:BA, 75:25; b) St:BA, 75:25, DOP 5 wt%; c) St:BA:PSt, 62.5:25:12.5; and d) St:BA:PSt, 62.5:25:12.5, DOP 5 wt%..... | 118 |
| 4.33 | Normalized GPC chromatograms of poly(St- <i>co</i> -BA) and poly(St- <i>co</i> -BA)/PSt | 119 |
| 4.34 | Microtomed and OsO ₄ -stained TEM photographs of poly(St- <i>co</i> -BA)/PSt composite particles: a) St:BA:PSt, 62.5:25:12.5 without DOP (Run 2049); and b) St:BA:PSt, 62.5:25:12.5 with DOP (Run 2050)..... | 120 |
| 4.35 | SEM photographs of poly(MMA- <i>co</i> -MA): a) poly(MMA- <i>co</i> -MA), MMA:MA 50:50, PVA-217:1.1 wt%; b) poly(MMA- <i>co</i> -MA), MMA:MA, 75:25, PVA-217:0.54 wt%; c) poly(MMA- <i>co</i> -MA), MMA:MA 75:25, PVA-217:1.1 wt%; d) poly(MMA- <i>co</i> -MA), MMA:MA 50:50, PVP K-30:1.1 wt%; and e) poly(MMA- <i>co</i> -MA), MMA:MA, 75:25, PVP K-30:1.1 wt%.. | 123 |

LIST OF FIGURES (Continued)

| | | |
|------|--|-----|
| 4.36 | Optical micrographs of poly(MMA- <i>co</i> -MA): a) poly(MMA- <i>co</i> -MA), MMA:MA 50:50, PVA-217 (Run 2035); b) poly(MMA- <i>co</i> -MA), MMA:MA of 50:50, PVP K-30 (Run 2042); c) poly(MMA- <i>co</i> -MA), MMA:MA of 75:25, PVA-217 (Run 2034); and d) poly(MMA- <i>co</i> -MA), MMA: MA of 75:25, PVP K-30 (Run 2041)..... | 124 |
| 4.37 | Normalized GPC chromatograms of poly(MMA- <i>co</i> -MA) at the ratio of MMA:MA is 50:50 showing the effect of stabilizer type. | 126 |
| 4.38 | Normalized GPC chromatograms of poly(MMA- <i>co</i> -MA) at the ratio of MMA:MA is 75:25 showing the effect of stabilizer type..... | 126 |
| 4.39 | Comparison of particle size distribution of poly(MMA- <i>co</i> -MA) with different stabilizer types by the SPG membrane pore size of 0.90 μm , the ratio of MMA:MA is a) 50:50; and b) 75:25..... | 127 |
| 4.40 | Comparison of droplet size distribution of poly(MMA- <i>co</i> -MA) with different stabilizer types by the SPG membrane pore size of 0.90 μm , the ratio of MMA:MA is a) 50:50, and b) 75:25..... | 128 |
| 4.41 | Normalized GPC chromatograms of poly(MMA- <i>co</i> -MA) particles showing the effects of monomer compositions..... | 130 |

LIST OF FIGURES (Continued)

| | | |
|------|--|-----|
| 4.42 | Glass transition temperatures of poly(MMA- <i>co</i> -MA) at various monomer compositions (DOP including 5 wt% by weight of the mixed monomer)..... | 131 |
| 4.43 | SEM photographs of poly(MMA- <i>co</i> -MA) for a) PMMA, ADVN 5 wt%; b) P(MMA- <i>co</i> -MA), MMA:MA 75:25, ADVN 0.62 wt%; c) P(MMA- <i>co</i> -MA), MMA:MA 75:25, ADVN 1.25 wt%; and d) P(MMA- <i>co</i> -MA), MMA:MA 75:25, ADVN 2.50 wt%..... | 132 |
| 4.44 | Normalized GPC chromatograms of poly(MMA- <i>co</i> -MA) particles showing the effects of ADVN concentrations..... | 134 |
| 4.45 | Particle size distribution of poly(MMA- <i>co</i> -MA) with different amounts of initiator..... | 135 |
| 4.46 | SEM photographs of poly(MMA- <i>co</i> -MA): a) poly(MMA- <i>co</i> -MA), MMA:MA of 75:25; b) poly(MMA- <i>co</i> -MA)/EGDMA/HD, MMA:MA of 50:50; c) poly(MMA- <i>co</i> -MA)/EGDMA, MMA:MA of 75:25; and d) poly(MMA- <i>co</i> -MA)/HD, MMA:MA of 75:25, DOP was added at 5 wt% of the monomer in each experiment..... | 139 |
| 4.47 | SEM photographs of a) poly(MMA- <i>co</i> -BA), MMA:BA of 75:25; ADVN initiator; b) poly(MMA- <i>co</i> -BA), MMA:BA of 75:25, BPO as initiator; c) poly(MMA- <i>co</i> -BMA), MMA:BMA of 50:50; BPO initiator..... | 141 |

LIST OF FIGURES (Continued)

| | | |
|------|--|-----|
| 4.48 | OM and SEM photographs of polystyrene film cast on the glass substrate: a) Run 2013 (a magnified image of secondary particles in the left corner); b) Run 2014; and c) Run 2015; and d) Run 2016 (Preparative conditions are in Tables 4.1 and 4.3)..... | 144 |
| 4.49 | OM (left) and SEM photographs (right) taken at an angle of 40° of poly(St- <i>co</i> -MA) particles: a) St:MA 50:50 (Run 2018); and b) St:MA 75:25 (Run 2019), SPG pore size of 0.51 μm..... | 145 |
| 4.50 | SEM photographs (left taken at an angle of 40°): a) poly(St- <i>co</i> -MA)/PSt, St:MA:PSt 62.5:25:12.5 (Run 2025); b) poly(St- <i>co</i> -MA), St:MA 75:25 (Run 2023); SPG pore size of 0.90 μm..... | 146 |
| 4.51 | SEM photographs (left photographs were taken at angle of 30°): a) Poly(St- <i>co</i> -BMA)/PSt (Run 2051); b) Poly(St- <i>co</i> -BA)/PSt, (Run 2049); and c) Poly(St- <i>co</i> -BA)/PSt/DOP (Run2050)..... | 148 |
| 4.52 | AFM image (2.5 μm × 2.5 μm; z-range 5 μm) recorded in air for poly(St- <i>co</i> -MA)/PSt, St:MA:PSt, 62.5:25:12.5 (Run 2025)... | 149 |

LIST OF ABBREVIATIONS AND SYMBOLS

LATIN

| | |
|-------------|--|
| SPG | Shirasu porous glass |
| k | rate constant |
| r_i | the ratio of the rates of growing radical; i for self-propagation to cross-propagation |
| G | Gibb's free energy of the system (J) |
| A_{ij} | corresponding interface between phases i and j |
| r | radii of particle (m) |
| ΔH | heat of mixing (J) |
| ΔS | entropy of mixing ($J K^{-1}$) |
| T | temperature (K) |
| z | lattice coordination number |
| W_{12} | energy of formation of a polymer segment/solvent interaction |
| X_1 | number of sites occupied by a solvent molecule |
| ΔP | transmembrane pressure or critical pressure ($kgf cm^{-2}$) |
| P_d | pressure of the dispersed phase outside the membrane |
| $P_{c,1}$ | pressures at the ends of the membrane pore |
| $P_{c,2}$ | pressures at module |
| \bar{D}_m | membrane pore diameter |
| P_c | critical pressure ($kgf cm^{-2}$) |
| x | numerical factor |
| \bar{D}_e | average diameter of emulsion droplets |

LIST OF ABBREVIATIONS AND SYMBOLS

| | |
|-------------|---|
| \bar{D}_p | average diameter of polymer particles |
| St | styrene |
| MMA | methyl methacrylate |
| MA | methyl acrylate |
| BMA | <i>n</i> -butyl methacrylate |
| BA | butyl acrylate |
| EGDMA | ethyleneglycol dimethacrylate |
| DOP | dioctyl phthalate |
| BPO | benzoyl peroxide |
| AIBN | 2,2'-azo-bis-isobutyronitrile |
| ADVN | 2,2'-azo-bis-2,4-dimethylvaleronitrile |
| HD | hexadecane |
| SLS | sodium dodecyl sulphate |
| PVA | poly(vinyl alcohol) |
| PVP | poly(vinyl pyrrolidone) |
| HQ | hydroquinone |
| PDA | <i>p</i> -phenylenediamine |
| wt | weight (g) |
| CV | coefficient of variation (%) |
| \bar{M}_n | number-average molecular weight (g mol^{-1}) |
| \bar{M}_w | weight-average molecular weight (g mol^{-1}) |
| k_d | decomposition rate constant of initiator |

LIST OF ABBREVIATIONS AND SYMBOLS

| | |
|-------|---|
| f | feed composition |
| F | copolymer composition |
| T_g | glass transition temperature |
| OM | optical microscopy |
| SEM | scanning electron microscopy |
| GPC | gel permeation chromatography |
| NMR | nuclear magnetic resonance spectroscopy |
| DSC | differential scanning calorimetry |
| FT-IR | Fourier-transform infrared spectroscopy |
| AFM | atomic force microscopy |

GREEK

| | |
|---------------|--|
| χ | Flory-Huggins parameter |
| δ | solubility parameter, (MPa) ^{1/2} |
| γ_{12} | interfacial tension between phases 1 and 2 |
| μm | micrometer |
| nm | nanometer |
| θ | contact angle |
| γ | interfacial tension |
| σ | standard deviation |
| δ | chemical shift |

CHAPTER 1

INTRODUCTION

The preparation of polymeric microspheres was developed for more than decades. Typically, polymer lattices containing uniform polymeric particles in a submicron-size range are produced by emulsion polymerization. This kind of polymerization is used to prepare dispersions and particles according to the invention involved and their advantages of techniques and product used. For several purposes, it is desirable to prepare larger particles ($\geq 2 \mu\text{m}$) having a uniform particle size, for instance as standards for microscopy, as model systems for separation, fluid flow, centrifugation, diffusivity measurement and dust investigations. Further, the particles may be used in electrokinetic studies and also in photography, for instance as a coating layer. They may also be used within bio-applications as a means for drug controlled release, for instance. Monodisperse particles may be used as a flattening agent for paint, and powder paint. They may also be used as toners, for example in xerography. Moreover, the large monodisperse particles may also be used for the preparation of stationary material in gel permeation chromatography wherein it is preferred that the particles are monodisperse to attain a minimum pressure drop in the column.

Polymer lattices are essential materials of the surface coating industry. A large proportion of the commercially produced latex polymer has typically been utilized by being cast into films or acting as binders. Recent concerns for the environmental and safety effects have emerged by highly volatile organic compounds used in the traditional coating industry. The demanding growth of water-borne

coatings thus allows the substitution of a solvent-based coating. The properties of film are affected by polymer type and its nature, and film-preparing condition. A coalescing agent is therefore required to enable the latex particles to attract each other to form a continuous film. The core-shell polymer can be used to lower the need for such a coalescing solvent [1,2]. Such heterogeneity could provide uniquely tailored properties, e.g. dispersion of a soft, lower glass transition temperature (T_g) latex, or a soft particle core entrapped in a matrix of a harder polymer shell, which can prevent cracks in the film as an impact modifier [3-7].

However, the emulsion polymerization has a limitation in preparation of the particles with a larger size. Then, the polymer product from the first step may be employed in a subsequent step for preparing particles of larger than 5 μm in high yields, and with a high degree of monodispersity. Over the last 10 years, there has been an increasing interest in a technique for making emulsions known as ‘membrane emulsification’ [8,9]. The Shirasu Porous Glass (SPG) membrane emulsification technique is a promising one to yield monodisperse droplets continuously both in an oil-in-water (O/W) emulsion [8-10] and a water-in-oil (W/O) emulsion systems [11,12]. This method involves a usage of a low pressure to force the dispersed phase to permeate through a membrane, having a uniform pore-size distribution, into the continuous phase. The concept is that the resulting droplet size is controlled primarily by the choice of membrane. The technique is attractive due to its simplicity, consumption of lower energy, and a less amount of surfactant, and a narrow droplet size distribution. By applying this technique, polymeric microspheres with a diameter range of about 3 to 100 μm have been successfully prepared by several research groups [13-16]. However, a little systematic work has been reported in details on

membrane emulsification, when plasticizers are added on many viscous liquids used as the dispersion phase.

In the present dissertation, the SPG emulsification technique and subsequent suspension polymerization were used in the synthesis of poly(St-*co*-MA), poly(St-*co*-MA)/PSt, poly(MMA-*co*-MA), poly(St-*co*-BMA), poly(St-*co*-BMA)/PSt, poly(St-*co*-BA), poly(St-*co*-BA)/PSt, poly(MMA-*co*-BA), and poly(MMA-*co*-BMA) in the presence of *n*-dioctyl phthalate (DOP). Since SPG membrane emulsification is a low shear process, the dispersion phase is permeated through the pores to an aqueous solution of the stabilizers by applying an adequate pressure to the dispersion phase. Fairly uniform dispersion droplets are obtained with good stability because of the uniformity of droplet size and the presence of non-ionic stabilizer such as polyvinyl alcohol. Effects of the added DOP plasticizer on copolymer morphology, glass transition temperature, molecular weight, molecular weight distribution, particle size, and particle size distribution were studied. Moreover, the effects of initiator and stabilizer on polymer morphology development were also studied. Transmission electron microscopy (TEM) and scanning electron microscopy (SEM) techniques have been applied to gain information on the particle morphology. In combination with nuclear magnetic resonance spectroscopy (¹H NMR), we were able to determine quantitatively the amount of comonomer content in the copolymer and observe the existence of DOP. The film formation of polymer particles was investigated using optical microscope (OM), SEM, and atomic force microscopy (AFM) for their application for surface coating when external plasticizer was used.

1.1 Objectives:

The syntheses of bi-component polymer latexes comprising styrene/acrylate copolymer incorporated plasticizers were focused on the basic contribution of mixed monomer pairs in the dispersion phase to the monodispersity of droplet formation. Membrane emulsification is conducted at a variety of ratios of a main component of styrene and acrylate monomers as the second component. The polymer particles were investigated for the particle morphology and mechanism of the morphology development. It was anticipated that the composition of the dispersion phase, the addition of DOP as an external plasticizer, and the hydrophobicity of the dispersion phase govern the interfacial properties, and hence the droplet size and its distribution as well.

1.2 Scope of the Research Work:

Particle morphology affected by the structure of polymer particles was studied. This is done by mainly varying the copolymer composition and plasticizer amount. In summary, the factors investigated in this research work are as follows:

- 1.) Effect of copolymer composition on external and internal morphology of copolymer.
- 2.) Effect of copolymer composition and the addition of low molecular weight polystyrene on particle morphology, particle size, size distribution and average molecular weights.
- 3.) Effect of plasticizer on glass transition temperature of polymer.

CHAPTER 2

THEORY AND LITERATURE SURVEY

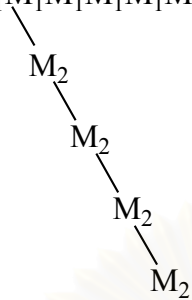
2.1 Free-radical Polymerization

In chain copolymerization, a mixture of two comonomers is able to produce polymeric products with two different structures in polymer chains. As shown in Eq. 2.1, copolymer molecule contains both monomers. The chain polymerization is termed as a copolymerization in which the product is a copolymer.



The random copolymer of different monomers can be carried out with mixtures of two or more monomers. The two monomers incorporated into the copolymer can be determined by the relative concentrations and reactivities [17]. A statistical copolymer has a distribution of the two monomer units along the copolymer chain which follows the statistical law. Where the two monomers units distributed randomly and followed zero-order Markov statistics, the polymer is referred as random copolymer. There are three types of particular copolymer structures, other than the random copolymer, as shown below:

- a. $M_1M_2M_1M_2M_1M_2M_1M_2M_1M_2M_1M_2$ alternating copolymer
- b. $M_1M_1M_1M_2M_2M_2M_1M_1M_1M_2M_2M_2$ block copolymer
- c. $M_1M_1M_1M_1M_1M_1M_1M_1M_1M_1M_1M_1M_1M_1M_1M_1$ graft copolymer



2.1.1 Copolymerization Equation

The different types of monomer have specific tendencies to copolymerization. The composition of monomer in a copolymer is usually different from that of comonomer from which it is produced in feed, as referred to *the first-order Markov or terminal model of copolymerization*. In case of two monomers M_1 and M_2 without any specificity in the mode of initiation, the copolymerization of two monomers lead to two types of propagating species, one with M_1^* at the propagating end and the other with M_2^* . The monomer radical will be represented as M_1^* or M_2^* . It is assumed that the reactivity of the propagating species only depends on the monomer unit at the end of the chain. The four propagation reactions are as follows.



Where k_{11} is the rate constant for a propagating chain ending in M_1 adding monomer M_1 , and so on.

Monomer M_1 disappears by reactions 2.2 and 2.4 and monomer M_2 disappears by reactions 2.3 and 2.5. The propagation rate of monomers to be incorporated in the copolymers is given by Eqs. 2.6 and 2.7.

$$\frac{-d[M_1]}{dt} = k_{11}[M_1^*][M_1] + k_{22}[M_2^*][M_1] \quad (2.6)$$

$$\frac{-d[M_2]}{dt} = k_{12}[M_1^*][M_2] + k_{22}[M_2^*][M_2] \quad (2.7)$$

Equation 2.6 is divided by 2.7 to yield the copolymer composition expressed as the ratio of the rates at which the two monomers enter the copolymer:

$$\frac{d[M_1]}{d[M_2]} = \frac{k_{11}[M_1^*][M_1] + k_{21}[M_2^*][M_1]}{k_{12}[M_1^*][M_2] + k_{22}[M_2^*][M_2]} \quad (2.8)$$

The concentrations of reactive species of M_1^* and M_2^* were assumed to be in a *steady state concentration*. Then, the rates of reactions expressed in Eqs. 2.3 and 2.4 are equal as shown in Eq. 2.9.

$$k_{21}[M_2^*][M_1] = k_{12}[M_1^*][M_2] \quad (2.9)$$

Equation 2.8 is combined with Eq. 2.9 to yield

$$\frac{d[M_1]}{d[M_2]} = \frac{\frac{k_{11}k_{21}[M_2^*][M_1]^2}{k_{12}[M_2]} + k_{21}[M_2^*][M_1]}{k_{22}[M_2^*][M_2] + k_{21}[M_2^*][M_1]}$$

$$= \frac{k_{11}k_{21}[M_1]^2 + k_{12}k_{21}[M_1][M_2]}{k_{21}[M_1] + k_{22}[M_2]} \quad (2.10)$$

Let us define,

$$\frac{[M_1^*]}{[M_2^*]} = \frac{k_{21}[M_1]}{k_{12}[M_2]}$$

$$r_1 = \frac{k_{11}}{k_{12}}, \text{ and } r_2 = \frac{k_{22}}{k_{21}} \quad (2.11)$$

r_i is the ratio of the rates of growing radical i for self-propagation to cross-propagation. The type of copolymer formed is a function of r_1 and r_2 , a value greater than one indicates a preference for homopolymerization, and a value less than one indicates a preference for reaction with the other monomer. The copolymer types are known to be classified as follows.

Case 1: $r_1 \approx r_2 \approx 1$. This means that there is no preference for either monomer to add onto either of the free radical centers. The copolymer formed is completely random.

Case 2: $r_1 \approx r_2 \approx 0$. This means that both propagating free-radicals have a strong tendency to react with the opposite monomer. An alternating copolymer results in.

Case 3: $r_1 \ll 1; r_2 \gg 1$. This is the case when a pair of monomers copolymerized poorly. Radicals with M_2 unit have a strong preference to react with themselves. Very few M_1 radicals are formed, and those that do also have a strong tendency to react with M_2 . The result is the formation largely of M_2 homopolymer.

This is generally the situation when monomers with very different ability to stabilize free radicals are involved.

Case 4: $r_1 \approx r_2 \gg 1$. This case has been observed rarely and never in free radical polymerization. It results in a simultaneous formation of homopolymer.

Using the parameter in Eq. 2.11, the Eq. 2.10 can be rearranged to,

$$\frac{d[M_1]}{d[M_2]} = \frac{[M_1](r_1[M_1] + [M_2])}{[M_2]([M_1] + r_2[M_2])} \quad (2.12)$$

Equation 2.12 is the copolymerization composition equation, where $\frac{d[M_1]}{d[M_2]}$ is the molar ratio of the two monomer units incorporated in the copolymer at any instant. The parameters r_1 and r_2 reflect the tendency of monomer to add the other monomer.

The instantaneous copolymer composition equation can be expressed in terms of mole fraction as

$$f_1 = 1 - f_2 = \frac{[M_1]}{[M_1] + [M_2]} \quad (2.13)$$

$$F_1 = 1 - F_2 = \frac{d[M_1]}{d[M_1] + d[M_2]} \quad (2.14)$$

where f_1 and f_2 are the mole fraction of monomers M_1 and M_2 in the feed and F_1 and F_2 are the mole fraction of monomers in the copolymer.

Combining Eqs. 2.13 and 2.14 with Eq. 2.12 yields

$$F_1 = \frac{r_1 f_1^2 + f_1 f_2}{r_1 f_1^2 + 2 f_1 f_2 + r_2 f_2^2} \quad (2.15)$$

Equation 2.15 gives the copolymer composition as the mole fraction of monomer M_1 in the copolymer and is more convenient to use this equation for further calculation.

2.1.2 Copolymer Composition Drift

One monomer is consumed preferentially, causing f_1 to change as the overall monomer conversion increases. The change in f_1 gives rise to a variation in F_1 with conversion. Copolymer composition drift leads to copolymers with significantly different compositions. The method to avoid copolymer composition drift can be arranged as follows:

- i) Terminate copolymerization reaction at low monomer conversion ($\leq 5\%$)
- ii) Add the preferentially consumed monomer to maintain f_1 constant

2.2 Particle Morphology

2.2.1 Thermodynamic Considerations

It has long been recognized that copolymerizations of two monomers by emulsion, seed, or suspension technique, can lead to the production of polymer particles with different types of morphology. Some composite polymer particles having heterogeneous structures such as core-shell with various types of particle morphologies [14,18,19]. Those morphologies were depended upon the nature of the monomers and polymer formed, the experimental condition and type of

polymerization process [20]. Theoretical predictions of the particle morphologies have gained much interest in recent years. In the past decade, the studies have been devoted to the theory of the various thermodynamics, kinetic parameters, and dynamic mathematical models [21].

An analysis of the thermodynamics dealing with a two-stage particle formation has been developed by Sundberg et al. [22] and Muscato et al. [23] in which the system was considered in terms of the free energy changes at the interfaces of a three phase system (i.e. polymer 1, polymer 2, and water). These interfaces are polymer 1/water, polymer 2/water, and polymer 1/polymer 2. Accordingly, the total free energy change for any of the configurations is shown in Figure 2.1, and the change of the free energy morphology development can be expressed as follows:

$$\Delta G = \sum \gamma_{12}A_{12} - \gamma'_{12}A'_{12} \quad (2.16)$$

where: ΔG is the change in the Gibb's free energy of the system

γ_{12} is the interfacial tension between phases 1 and 2

A_{12} is corresponding to interfacial area between phases 1 and 2

γ'_{12} is the interfacial tension against the aqueous phase (containing surfactant)

A'_{12} is interfacial area of the initial latex particle

Eq. 2.16 was applied to any morphological structures in Figure 2.1 and requires that particle morphology has developed slowly enough so that equilibrium conditions have applied throughout its development. It is considered to modify Eq. 2.16 by dividing through A'_{12} and thus achieve a free energy expression that is independent of particle size. Then, the free energy change is

$$\Delta\gamma = \sum \gamma_{12} A_{12} / A'_{12} - \gamma' \quad (2.17)$$

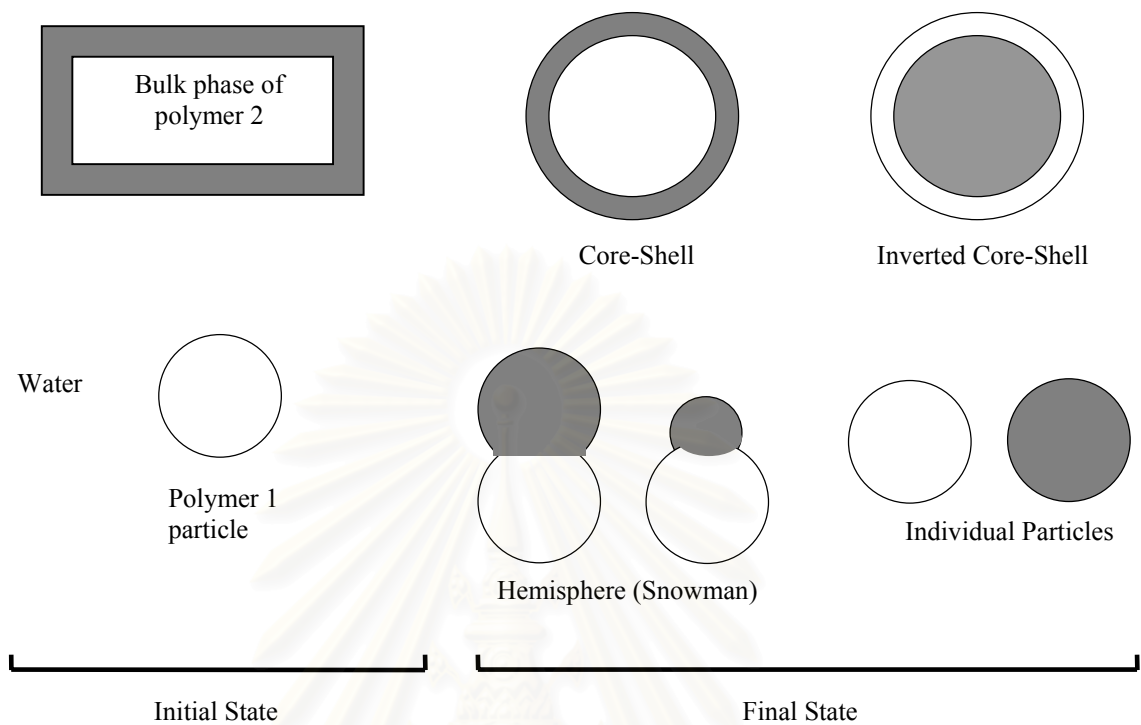


Figure 2.1 Initial and final stages for the morphology development (basic morphologies) [22].

The $\Delta\gamma$ values so calculated will depend upon the particular choice of which polymeric constituents are designated to be component 1 or 2. Each of the morphologies depicted in Figure 2.1 has different combinations of $\gamma_{12}A_{12}$ according to each particular morphological configuration. The morphology of the thermodynamically preferred system is that has the minimum interfacial free energy. For example, the different values for G , the free energy of the extreme morphologies, the core-shell and the inverted configurations, can be calculated using Eq. 2.16 as:

$$\Delta G_{\text{core-shell}} = \gamma_{12}4\pi r_1^2 + \gamma_{2w}4\pi r_2^2 \quad (2.18)$$

$$\Delta G_{\text{inverted}} = \gamma_{12}4\pi r_2^2 + \gamma_{2w}4\pi r_1^2 \quad (2.19)$$

Where r_1 and r_2 are the appropriate radii shown in Figure 2.2. Chen et al. [25] developed a thermodynamically-based mathematical model to describe free energy differences between different possible morphological structures. Sundberg and Sundberg [26] extended the model of morphological studies of two-component pairs of polymer to three-component composites. Those morphologies were classified in 22 possible equilibrium morphologies. The final morphological state can be expressed up to 22 equations.

Thermodynamical treatment for the prediction of particle morphology is favored based on the equilibrium state, the kinetic morphological development also still exists. Since the polymeric phases are subject to serious diffusional limitations, therefore, kinetic factors also play a role in investigating the particle morphology [27]. Winzor et al. [28,29] described the phase structure development within composite latex particles during the polymerization process and was potentially dependent upon both the latex recipe and the polymerization process characteristics. An equilibrium thermodynamic approach was presented to predict the particle morphology as a function of the extent of conversion of a seed latex polymerization reaction. Recently, Kirsch et al. [30] represented the simulation work in different experimental parameters and the results were checked with respect to their final particle morphology. A combination of thermodynamic and kinetic aspects are able to predict the experimental structure. All morphologies are within a small range of Gibb's free

energy change. Hence, minor changes in the reaction parameters may result in an altered morphology.

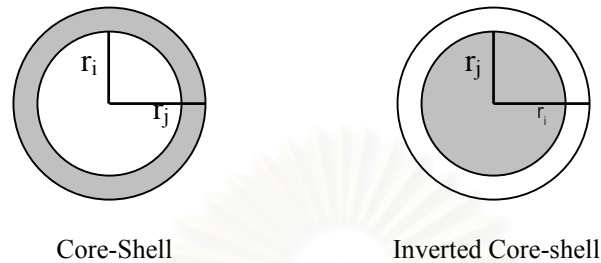


Figure 2.2 Radii of core-shell and inverted morphologies [24].

2.2.2 Various Types of Particle and Their Applications

Particles in a size range up to 10 μm have been synthesized by Ugelstad et al. [31], the coefficient of variation in particle size was found to be about 1%. The results confirmed the high monodispersity of the particles. The size distribution was reported to be too narrow for optimal use in Coulter Counters.

The new methods have been used to prepare particles with various groups on the surface. Such particles may also be built up as core and shell particles. Particles with various densities and hydrophilic surface groups were also prepared. These particles have turned out to be very useful for a number of immunoassay applications. Ugelstad et al. [32] prepared monodisperse particles containing magnetite incorporating amounts were more than 30% iron. The particles have been applied in cell separation [33]. The methods of preparation of monodisperse polymer particles have proved to be especially well suited for preparation of monodisperse highly porous particles of sizes from 1 to 50 μm [34,35]. Such particles have been applied in development of new, highly effective systems for liquid chromatography

[36]. The high monodispersity leads to a very uniform solid phase to optimal packing of the column, which greatly improves both separation efficiency and flow properties.

2.3 Plasticizers

Diethyl phthalate (2-ethylhexyl phthalate) is an ester manufactured from phthalic acid and 2-ethylhexanol. Phthalic anhydride is produced by catalytic oxidation of either naphthalene from coal tar distillation or, more commonly today, by oxidation of *o*-xylene. 2-Ethylhexanol is manufactured from propylene. The formation of the monoalkyl phthalate occurs rapidly at relatively low temperature by ring opening of phthalic anhydride as shown in Figure 2.3. Conversion to the diester is slower, required heating to 140 to 150°C in the presence of a catalyst [37]. The use of a catalyst reduces reaction temperature, thereby minimizing loss of the volatile alcohol. Sulfuric acid and *p*-toluenesulfonic acid are the most commonly used catalysts. Equilibrium is driven towards complete phthalate formation by removal of water, usually under vacuum. Excess amount of 2-ethylhexanol is introduced to ensure complete conversion of phthalic anhydride. The unused alcohol is recycled after esterification is complete. After purification, commercial grades of DOP contain less than 0.1 % of the unreacted 2-ethylhexanol.

Figure 2.3 Reaction of phthalate plasticizers

A plasticizer or softener is a substance or material incorporated in a material to increase its flexibility, workability, or elastibility. In general, a plasticizer is a high boiling point organic substance (liquid phase) or in some circumstances an organic solid. The effect of this softening results in the following actions, e.g. to reduce tensile strength, increase elongation, reduce glass transition temperature, or reduce hardness.

Plasticizers are used primarily in thermoplastic polymers and for the most part plasticize the amorphous part of these polymers for example in poly(vinyl chloride) (PVC) production. However, some type of plasticizer gives preference to crystallize polymers. Plasticizers are also used in thermosetting materials such as rubber or phenol-formaldehyde resins. Moreover, plasticizers are used in both homopolymer and copolymer systems. Copolymers generally require the use of less plasticizer (or no plasticizer) to achieve the same degree of flexibility as homopolymers. Copolymers are internally plasticized by the comonomer incorporated in part of polymer backbone. Plasticizers are usually external to the polymer and are not bound to the polymer by primary chemical bonds but the physical interaction instead. The above actions assume polymer/plasticizer compatibility.

available to replace it to mask the force centers and provides flexibility of the plasticized polymer system.

2.3.2 Plasticizer Performance Criterion

For the use of a particular plasticizer for an application, there are four basic parameters that must be considered. These parameters are compatibility, efficiency, durability, and processability. Compatibility of an external plasticizer with a polymer may be defined as the combinations of the polymer and plasticizer to form a homogenous compound that will stay homogeneously and provide useful plastic properties [41]. The compatibility of a plasticizer with a polymer is affected by the factors such as temperature, pressure, UV light radiation, oxidation, and nature of polymer and plasticizer.

2.3.3 Solubility Parameter

The solubility parameter of a plasticizer is useful in predicting polymer compatibility. The solubility parameter of a solvent is the square root of a solvent's cohesive energy density, which is calculated from a solvent's heat of vaporization. If a plasticizer has a solubility parameter similar to a polymer, it should be compatible. In contrast for the high boiling point plasticizers, it is not easy to determine heat of vaporization and difficult to be compatible. Solubility parameters can be estimated from the molar attraction constants by Small's method.

Another method is the thermodynamic method of estimating compatibility by considering the Flory-Huggins interaction parameter. The interaction parameter can be calculated for resin/plasticizer blends by observation of osmotic pressure, equilibrium swelling, vapor pressures and depression of freezing or

elevation of melting points. Dielectric constants of plasticizers are also indicators of compatibility. Dielectric constants are indicators of weak forces associated with polymer force centers. If a plasticizer is to be compatible, it should have a dielectric constant similar to the polymer.

2.3.4 Durability

Plasticizers are physically bound to polymers. Therefore, in plasticized systems, a plasticizer can and will leave the system known as “migration” and the plasticized polymers will become brittle. Plasticized polymers are sometimes exposed to liquid media and plasticizer will be extracted. Plasticizers can also migrate from one plasticized material to another substrate. If a plasticizer volatilizes off or migrates out, the polymer becomes hard, and therefore the plasticizing property is inefficient. Incompatible plasticizers will exude from the system, and therefore will not remain permanent. The ASTM methods such as ASTM D-1239 are useful in measuring these parameters [42].

2.4 Glass Transition Behavior

Latex particle morphology is essential for assessing for polymer compatibility. It is well known that various morphologies can be achieved according to the nature, reactivity and polymerization process. The glass transition behavior (T_g) of copolymers has appeared to be influenced by polymer compatibility [43,44]. In emulsion copolymer, T_g data have been investigated from theoretical and experimental basis and compared with colloidal properties, which should also be influenced by the particle morphology.

In random copolymers, the glass transition behaviors of copolymer are closely connected with the sequence distribution and individual copolymer chain microstructure controlled by the composition drift allowed by polymerization process. The glass transition behavior may be accurately predicted. The basic assumption is that any chain keeps its own calorimetric characteristics in the copolymer sample as if it was segregated in an isolated domain.

Few systems follow the classical and simple additive rule of the Fox's equation [45] as shown in Eq. 2.20, which relates copolymer or homopolymer's T_g values and the overall composition.

$$\frac{1}{T_{g \text{ copolymer}}} = \frac{W_1}{T_{g1}} + \frac{W_2}{T_{g2}} + \dots \quad (2.20)$$

where W_i is the weight fraction of monomer i in the copolymer and $T_{g i}$ is the glass transition temperature of homopolymer i . The glass transition temperature must be expressed in Kelvin. The equation gives fairly accurate prediction of T_g for high molecular weight polymers, since T_g decreases as molecular weight is reduced. The sample of polymer T_g is shown in Table 2.1.

สถาบันวิทยบริการ
จุฬาลงกรณ์มหาวิทยาลัย

Table 2.1 Glass transition temperature (°C) for homopolymers from various monomers [46,47]

| Acrylic and methacrylic acids and esters | | |
|--|--------------|----------|
| Monomer | Methacrylate | Acrylate |
| Methyl | 105 | 8 |
| Ethyl | 65 | -22 |
| <i>n</i> -Butyl | 20 | -54 |
| Isobutyl | 64 | -43 |
| <i>t</i> -Butyl | | 74 |
| 2-Ethylhexyl | -10 | -85 |
| 2-Hydroxyethyl | 55 | |
| 2-Hydroxypropyl | 73 | |
| Other monomers | | |
| Styrene | 100 | |
| Vinyl acetate | 29 | |
| Vinyl chloride | 81 | |
| Vinylidene chloride | -18 | |

2.5 Thermodynamics of Mixing of Polymer and Plasticizer

From a thermodynamic viewpoint, the free energy of mixing polymer (ΔG_{mix}) and plasticizer contains enthalpic (ΔH) and entropic (ΔS) components. To describe the phase behavior of the system, the enthalpic and entropic contributions must be related to the molecular characteristics of the components. By estimating the entropy and enthalpy of mixing monomers and DOP, the free energy of mixing, ΔG_{mix} at absolute

temperature T may be derived as in Eq. 2.21. Basic thermodynamics indicate that two substances will be miscible when the free energy of mixing is negative.

$$\Delta G_{\text{mix}} = \Delta H_{\text{mix}} - T\Delta S_{\text{mix}} \quad (2.21)$$

Considering the mixtures of plasticizer and polymer as semi-diluted or concentrated solutions, the simple Flory-Huggins model can be applied. Due to its relative simplicity, the Flory-Huggins model has been used extensively in research and industry to predict the compatibility between polymers and plasticizers or solvents and thus select the best matches.

The Flory-Huggins parameter χ is a dimensionless measure of the strength of the interaction between polymer chains and plasticizer molecules. The basic premise for the Flory-Huggins theory [48] is that the polymer molecules behave like a freely jointed chain composed of discrete segments, which together with the plasticizer molecules, occupy sites on a lattice. Each lattice site must be occupied by either a polymer chain segment or a plasticizer molecule, so that there are no vacancies. In addition, adjacent segments of polymer occupy adjoining lattice sites. The Flory-Huggins parameter is derived from the enthalpy of mixing and may be calculated from the Eq. 2.22:

$$\chi = (z\Delta W_{12}X_1)/kT \quad (2.22)$$

where z is a lattice coordination number

W_{12} is the energy of formation of a polymer segment/solvent interaction

X_1 is the number of sites occupied by a solvent molecule

Plasticizer no longer boils off at 400°C, pure DOP produces an identified phthalic anhydride and octenes in the gas phase. The solubility parameters of monomer and plasticizer are presented in Table 2.2.

Table 2.2 Solubility parameter of monomer and plasticizer [49].

| Chemicals | Solubility parameter, δ | | H-bonding group |
|---------------------|--------------------------------|-------------------------|-----------------|
| | (MPa) ^{1/2} | (cal/cm) ^{1/2} | |
| Butyl acrylate | 18.0 | 8.8 | m |
| Butyl methacrylate | 16.8 | 8.2 | m |
| Methyl acrylate | 18.2 | 8.9 | m |
| Methyl methacrylate | 18.0 | 8.8 | m |
| Styrene | 19.0 | 9.3 | p |
| Dioctyl phthalate | 24.8 | 12.1 | m |
| Water | 47.9 | 23.4 | s |

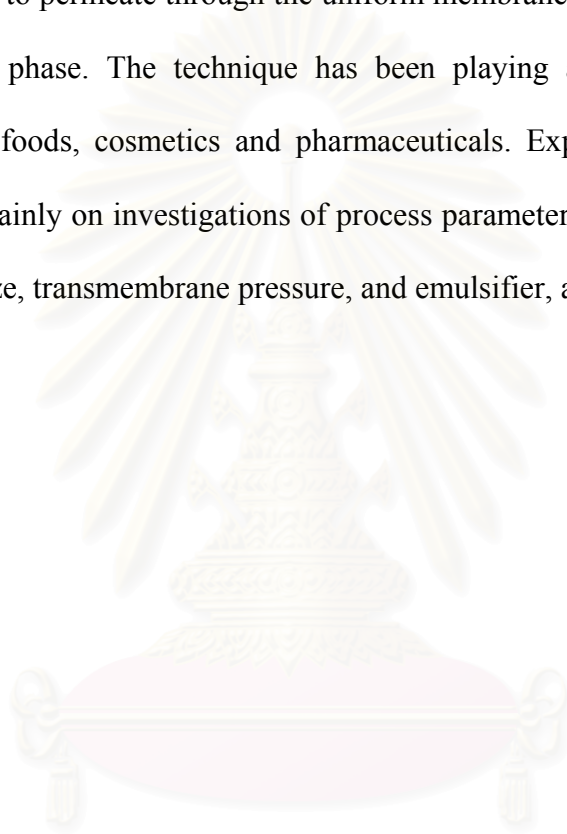
H-bonding: p = poor; m = moderate; s = strong.

2.6 Membrane Emulsification

Over the past two decades, there has been considerable interest in preparation of monodisperse polymer particles since these find applications in science, medicine and industry. In general, most of the research work is concerned with the preparation of monodisperse polymer particles via polymerization process. The polymerization can be emulsion polymerization, emulsifier-free emulsion polymerization, dispersion polymerization, suspension polymerization, seeded emulsion polymerization, precipitation polymerization, microemulsion polymerization, and miniemulsion

polymerization. The important factors of each system are divided into reaction characteristics and mechanism of nuclei growth. The characteristics of particle size, and particle size distribution are shown in Table 2.3.

Besides, there has been an increasing interest in the technique called *membrane emulsification*. This method involves using the low pressure to force the dispersed phase to permeate through the uniform membrane pore and distribution into the continuous phase. The technique has been playing an important role in the formulation of foods, cosmetics and pharmaceuticals. Experimental studies, which have focused mainly on investigations of process parameters such as membrane type, average pore size, transmembrane pressure, and emulsifier, are reviewed [50].



สถาบันวิทยบริการ
จุฬาลงกรณ์มหาวิทยาลัย

2.6.1 The Theory of SPG Emulsification

SPG is an abbreviation of Shirasu Porous Glass. Membrane emulsification is a new emulsification technique, especially suitable for the production of highly uniform particles or droplets of controlled mean size [51]. The membrane is fabricated from a spinodal decomposition of the mixture of CaO-Al₂O₃-B₂O₃-SiO₂, with a subsequent removal of the CaO-B₂O₃ phase by an acid treatment. This membrane possesses a unique porous structure in a cylindrical shape of the membrane, consisting of hydrophilic Al₂O₃-SiO₂ as shown in Figure 2.4. Due to uniform pores, a wide range of available mean pore size from 0.05 to 30 μm and the possibility of surface modification are found in market place, the SPG membrane developed by Nakashima and Shimizu [52], is a potentially suitable membrane for emulsification. When the porous glass membrane has an average pore diameter of less than 0.1 μm, the permeation of dispersion phase requires a prolonged period. Thus, a glass membrane having an average pore diameter less than 0.1 μm is not preferable from the viewpoint of productivity. A glass membrane having an average pore diameter exceeding 10 μm is not preferable either, since use thereof makes it very difficult to obtain droplets with a uniform diameter [53]. In this research, the pore sizes of SPG membrane ranging from 0.5 and 0.9 μm were used to produce a stable oil-in-water (O/W) emulsions. The cross section of membrane is shown in Figure 2.5.

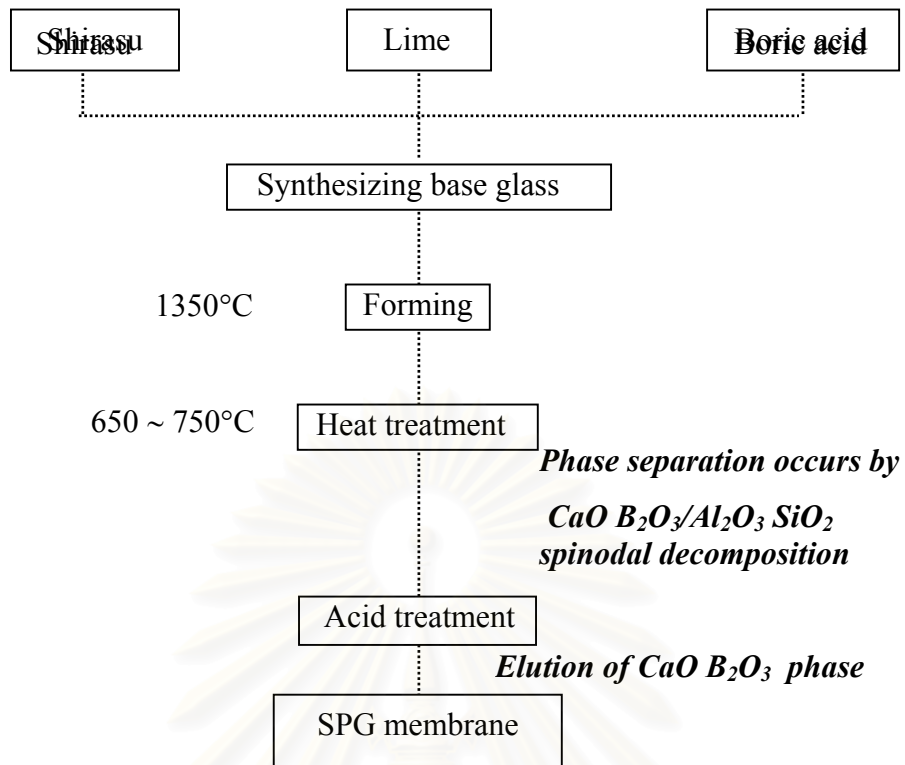


Figure 2.4 Flow of manufacturing Shirasu porous glass (SPG) [54]

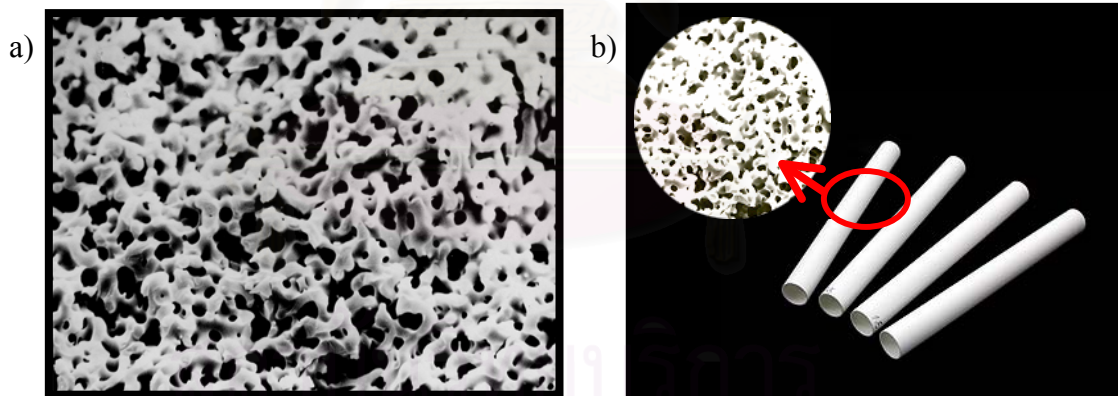


Figure 2.5 SPG membrane: a) a cross section image from SEM, and b) SPG membrane (cylinder)

SPG emulsification method produces emulsions by permeating two immiscible liquids (referred to as a dispersion phase which is consisted of a water-insoluble monomer and an initiator) into the other phase (referred to as a continuous

phase which is consisted of water and a stabilizer) through a membrane having a relative uniform pore diameter. The membrane emulsification method makes it possible to produce monodisperse emulsions consuming less energy by applying pressure to permeate the dispersion phase through the membrane.

2.6.2 The Formation of Droplets

Although much of the early work on membrane emulsification is of a rather empirical nature, more systematic studies have been done and the important process controlling parameters and conditions identified [51]. These are membrane pore size distribution, membrane porosity, membrane surface type, emulsifier type and concentration, dispersed phase flux, velocity of the continuous phase and transmembrane pressure [55-57]. Transmembrane pressure ΔP is defined as Eq. 2.23 [58]:

$$\Delta P = \frac{P_d - (P_{c,1} + P_{c,2})}{2} \quad (2.23)$$

where P_d is the pressure of the dispersed phase outside the membrane, $P_{c,1}$ and $P_{c,2}$ are the pressures at both ends of the membrane module. When the pressure is applied to the dispersion phase, the liquid is penetrated into the micropores. The protrusion of liquids, depends on the pore diameter (\bar{d}_m) and the pressure at which the dispersed phase droplet is released from the pores, can be theoretically derived in Eq. 2.24:

$$P_c = 4\gamma\cos\theta/\bar{d}_m \quad (2.24)$$

where P_c is the minimum pressure or critical pressure in which the dispersion phase is pushed out, γ is the dispersed/water interfacial tension, and θ is the contact angle between the dispersed phase and the membrane surface, P_c is also referred to as the critical pressure.

It is generally necessary to find a balance between all of the above-mentioned parameters to achieve the desired result, often considered as the formation of an emulsion with the smallest droplet size and narrowest size distribution. In reality, this will be dictated by the demands of the product and the rate of emulsion production. Omi et al. [13] found that the droplet formation started at a critical permeation pressure. The rate of emulsification increased as the pressure increased from the critical value. With an excess permeation pressure, the non-uniform size distribution of the droplets was obtained.

As shown in Figure 2.6, when the applied pressure is lower than P_c , the dispersion phase does not permeate through the membrane. In contrast, when the applied pressure is higher than P_c , the dispersion phase is able to protrude through the membrane pore. The creation of droplets into the continuous phase occurs. The size of emulsion droplets changes depending on the pore size of the membrane as shown in Figure 2.7 and Eq. 2.26 to correlate \bar{D}_e with \bar{D}_m in a linear relationship:

$$\bar{D}_e = x\bar{D}_m \quad (2.25)$$

where \bar{D}_e is an average diameter of emulsion droplets and x can range typically from 3 to 7 [13,51,59]. The coefficient 6.62 was presented by Omi et al. [13], which is demonstrated in Figure 2.7. Also, Nakashima et al. [51] claimed that the coefficient was 3.25. The difference of the values is probably due to the difference in the opening

of micropores as reported by Omi et al. [13]. Monomer droplets with a narrower particle size distribution can be efficiently obtained when the pressure is 1.05 to 1.50 times the critical pressure (the lowest pressure which can pass the dispersion phase through the pores of porous membrane) [53]. The temperature of the dispersion and aqueous phase during the dispersion is not limited, normally as the dispersion phase is stably dispersed without initiating polymerization. It is preferable to maintain the dispersion and continuous phase at the temperature ranging from 0°C to 60°C [53]. The temperature used should be within optimum conditions in conjunction with the decomposition temperature and half-life of polymerization initiator, the boiling point of organic solvent, and etc. Normally, emulsification process was carried out at ambient temperature [13,51]. During the dispersion process, the period for emulsifying the dispersion phase can be suitably determined without limitations unless the polymerization is induced.

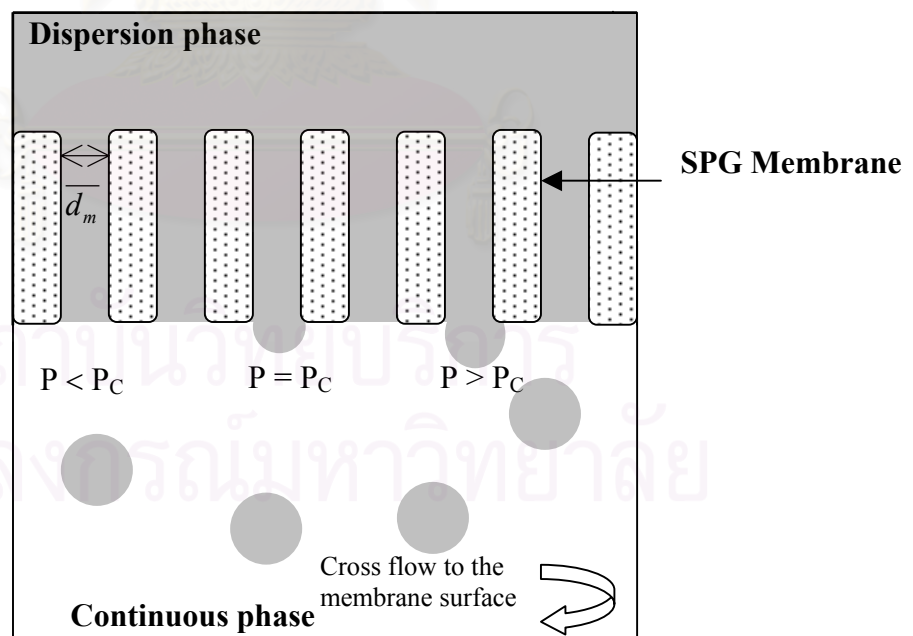


Figure 2.6 Sketch of the applied pressure corresponding to formation of the emulsion droplets

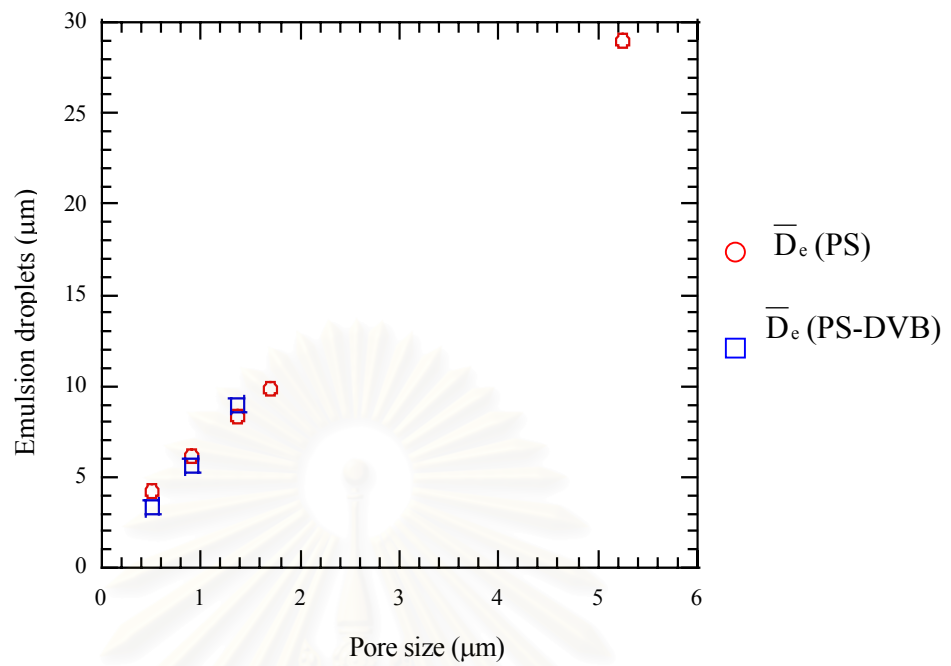


Figure 2.7 Average diameters of emulsion droplets as a function of pore size of SPG membrane [13].

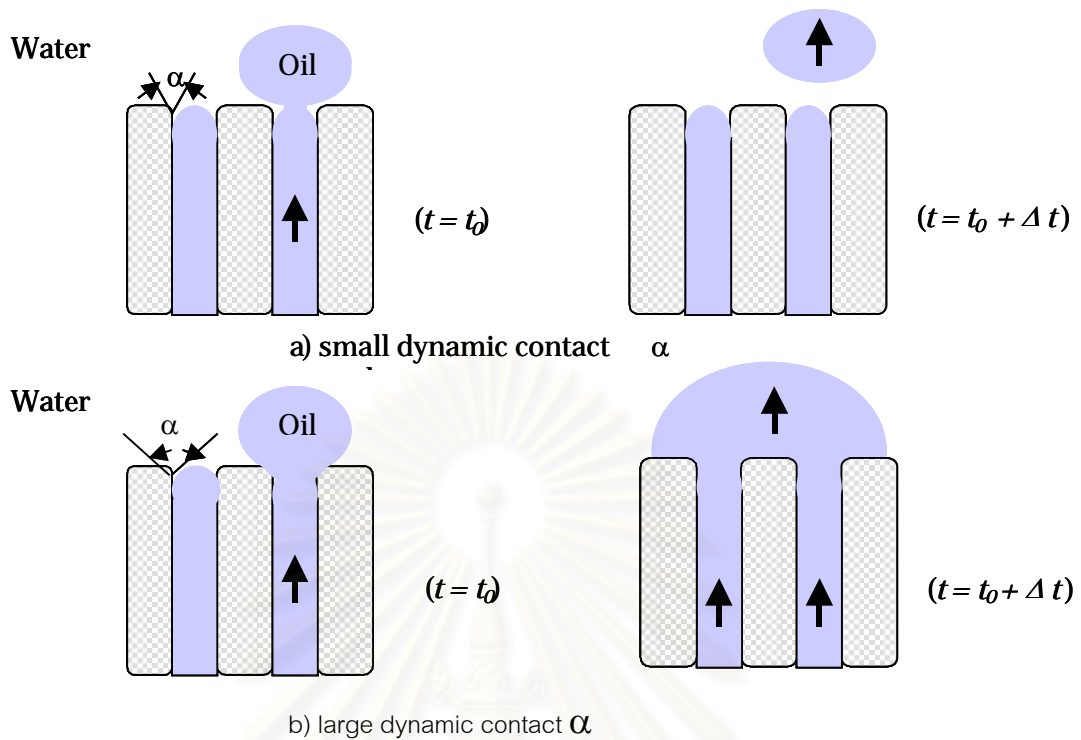


Figure 2.8 Sketch of the surface of a microporous membrane at the moment t_0 and in subsequent moment $t_0 + \Delta t$ emulsification. a) The dynamic contact angle α is small and the contact line membrane-water-oil phase is fixed at the pore diameter. b) The angle α is larger and facilitates the contact-line expansion in the course of growth of the drop; the latter may span two or more pores [60].

2.6.3 Preparation of Emulsion Types by SPG Emulsification

2.6.3.1 Preparation of an Oil-in-Water (O/W) Emulsion

An ordinary membrane, composed of $\text{Al}_2\text{O}_3\text{-SiO}_2$. The microporous membrane has a hydrophilic property by itself. For the continuous phase, water is usually used. The membrane is set in the stainless steel module and immersed in the continuous phase. Then, the dispersion phase is loaded into the oil vessel. Dispersion phase is a hydrophobic substance such as a water insoluble monomer or an organic solvent. As a rule, the disperse phase should not wet the membrane pores.

This means that hydrophilic membranes are more suited to making the O/W than W/O emulsions. Besides, the selection of a suitable emulsifier and a stabilizer added in the continuous phase should be carefully considered [51].

2.6.3.2 Preparation of a Water-in-Oil (W/O) Emulsion

The preparation of W/O emulsion has been done using a hydrophobic membrane. The membrane can be modified by heating the hydrophilic type membrane at 437 K for 48 h in vacuum. Then, it is dipped in toluene to which 5% by volume of octadecyltrichlorosilane (ODS) was added, and heated to reflux at 383 K for 8 h. The membrane was rinsed in dried toluene in which 1% by volume of trimethylchlorosilane (TMS) was added at room temperature for 2 h. Membrane was rinsed in dried toluene, a hydrophobic membrane is thus obtained.

The hydrophobic membrane wetted with the oil phase was set in the module and immersed in the oil phase. The water phase was loaded into the storage vessel. Generally, monodisperse emulsion droplets can be produced by adding a non-ionic emulsifier to the oil phase and dissolving inorganic salts in the water phase. The W/O emulsions have also been made using hydrophilic membranes. However, the resultant droplet size is less than the pore size and is apparently dependent on the structure of the pore outlets and not strictly on the diameter [61,62].

2.6.3.3 Preparation of an Water-in-Oil-in-Water (W/O/W)

Emulsion

The double emulsification technology based on the application of SPG membrane is to produce W/O/W emulsion capsules of uniform droplet

diameter using the SPG membrane having uniform micropores. The formulation could be used in the cancer therapy by drug injection to hepatic artery [54,63].

2.6.4 Emulsifier

Emulsifiers have two main roles to play in the formation of an emulsion. Firstly, they lower the interfacial tension between oil and water. This facilitates droplet disruption and in the case of membranes lowers the minimum emulsification pressure. Vladisavljevic and Schubert [64] have suggested that the interfacial tension is one of the essential forces holding a droplet at a pore. The larger droplets are produced, the higher equilibrium interfacial tension. Secondly, emulsifiers stabilize the droplets against coalescence and/or aggregation. This will depend on both the type of emulsifier and the concentration. Yuyama et al. [65] investigated that the droplet size and size distribution were significantly affected by the hydrophobicity of the dispersion phase and the concentration of the mixed surfactant by which the interfacial tension between the continuous and the dispersion phase was changed. The interfacial tension increased in the presence of poly(vinyl alcohol) and sodium dodecyl sulphate (PVA-SLS) complex, which is located at the adsorbed layer formed by molecules of the surfactant at various concentrations.

2.7 Suspension Polymerization

The monomer droplets obtained from the membrane emulsification can be polymerized by a suspension polymerization. Suspension polymerization differs from emulsion polymerization in that monomer-soluble free radical polymerization initiators are utilized to polymerize essentially water insoluble monomers. The

polymerization can be regarded as a set of bulk polymerization taking place in each monomer droplet, and thus molecular weight is inversely proportional to initiator concentration and polymerization rate as it is typical of a bulk radical polymerization. Particle stabilization is usually maintained through the adsorption of water-soluble polymers such as partially hydrolyzed poly(vinyl acetate) and acrylic acid copolymers, and particle size is generally in the range 0.01 to 1 μm . The relatively large particle size of suspension polymerization polymers facilitates the isolation of polymer particle (e.g., by centrifugation) and such “beads” are widely utilized in solvent-borne surface coatings and in photocopy or xerographic toner resins. Suspension copolymers containing sufficient carboxylic acid comonomer to be alkali-soluble are utilized in printing inks at alkaline pH. As a result of the large particle size, suspension polymers are rarely directly utilized in the form of the aqueous dispersion because settling and film-forming problems would be expected.

2.8 Film Formation of the Polymer

The replacement of solution cast-films by water-borne coatings of latex is an important contribution to the reduction of air pollution by decreasing the use of volatile organic solvents. However, due to additives, latex films often do not attain the quality and stability of their counter parts cast from solution. Another disadvantage of water-borne coatings is that film formation proceeds at temperatures above the so-called minimum film-forming temperature (MFT), which is close to the glass transition (T_g) of the polymer, but desired film properties often require T_g 's above ambient temperature. The market requires application limits and disadvantages of latex films to be eliminated at the lowest possible cost [66-68].

Film formation of water-borne coatings is a complex process and may be viewed as a succession of different steps, including concentration of dispersion, particle packing, particle deformation and finally interdiffusion or adhesion. Observations differ with regard to whether these stages proceed in this sequence or partially overlap. Water evaporation starts once the dispersion is spread on a substrate. As the solid content of the dispersion increases, particles approach a critical spacing and coagulation sets in [69].

In order to apply polymer lattices for coating, their film formation behavior should be investigated. To understand the fundamental mechanism of film formation is important for designing a coating formulation. The latex particles must be soft enough to deform and pack into a layer in which depends on polymer T_g . The T_g is the temperature at which polymer chain segment begins moving and molecules can interdiffuse. The T_g is a particularly useful parameter to describe polymer ability to form a film [70]. Then, the addition of plasticizer is affect to the polymer T_g . Particle deformation behavior depends on the polymer T_g and viscosity, the plasticizing effect due to plasticizer type, water, surfactant, and the total driving force for particle deformation. In addition, it is temperature and time dependent [71]. Thus, T_g is essentially a very useful parameter to describe an ability of polymer to form a film [72]. The film formation process is depicted by the various stages as shown in Figure 2.9. Initially the latex particles are present as a dispersion in water. As the water evaporates, the particles eventually come into contact and form a close-packed array. If the T_g of the latex in the presence of water is below room temperature, the particles will deform to fill all available space, yielding an interdiffusion across particle boundaries, causing coalescence and the creation of a continuous film.

In this research, the SPG emulsification technique and subsequent suspension polymerization were applied for the preparation of polymer latex. The limitations of this technique were found on the low solid content of latex and a small volume of the latex produced in each batch.

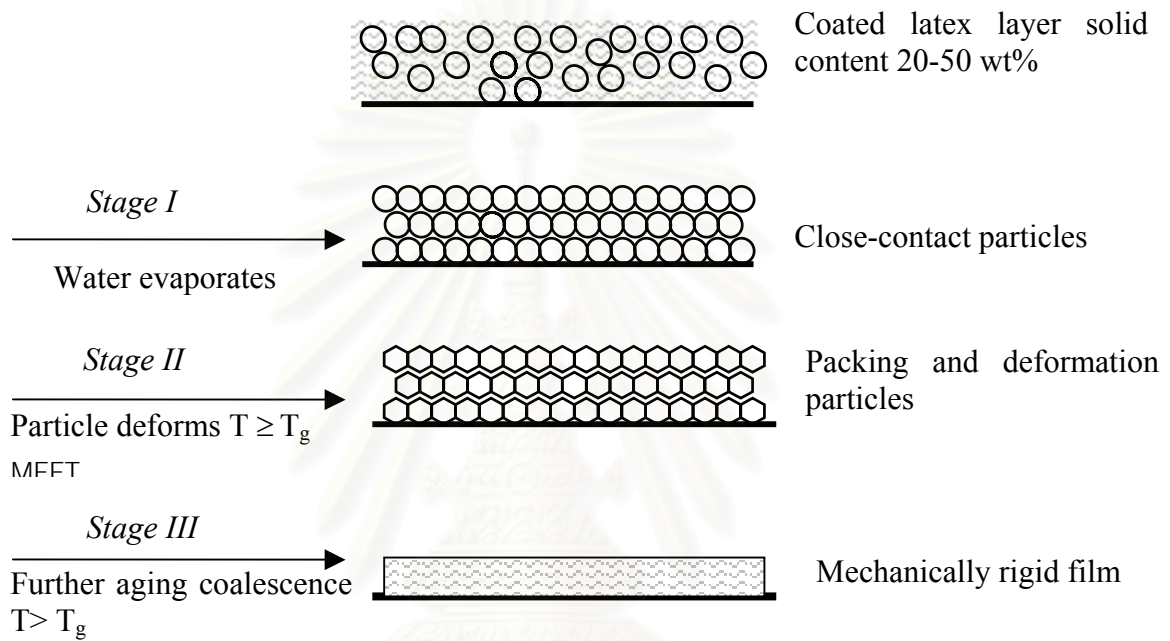


Figure 2.9 The various stages in the formation of a film during the drying of an aqueous dispersion of a soft latex [73-75].

For a film formation to be successful, the film must be formed at or above the MFT. This is normally taken to be the minimum temperature at which the dry film is transparent and crack-free. The plasticizer is added to improve the filming properties of the coating [71]. In bulk polymer samples, plasticizers lower the T_g . Since the elastic modulus of a polymer decreases by several orders of magnitude as the temperature is raised above T_g and promoted the ease of polymer deformation in latex film formation.

2.9 Literature Reviews

The technology of membrane emulsification, proposed by Nakashima et al. [9,51,52], has found a considerable development and many applications during the last decade [6-16,18,50-65]. The influence of different factors on the process of emulsification by microporous membranes has been investigated in the works by Kandori et al. [8,11], Schubert and Schröder [50,57], and Yuyama et al. [65]. The method has been applied in many fields, in which monodisperse emulsions are needed. An example is the application in food industry for production of oil-in-water (O/W) emulsions: dressings, artificial milk, cream liqueurs, as well as for preparation of some water-in-oil (W/O) emulsions: margarine and low-fat spreads. Shiomori et al. [76] studied the hydrolysis of olive oil by lipase in a homogenizer and in a monodisperse emulsion system. The effects of substrate, concentration, droplet diameters and interfacial area on hydrolysis rate were studied. Kandori et al. [11] prepared fine and monodisperse water-in-oil (W/O) emulsions using the Shirasu Porous Glass (SPG) emulsification technique with a copolymer-type surfactant. The W/O emulsions were prepared by two kinds of SPG emulsification techniques using batch and continuous methods. Highly monodisperse W/O emulsions were formed and there was no difference in the size of the water droplets produced by these two methods. The dispersion stability of W/O emulsions prepared by this technique with a concentration of copolymer-type surfactant above 7.5 wt% was extremely good. This remarkable stability was described to the low interfacial tension in addition to the formation of a viscoelastic adsorbed film of copolymer-type surfactants on the water droplets.

Another application of this method is for fabrication of monodisperse colloidal particles; silica-hydrogel and polymer microspheres; porous and crosslinked polymer

particles; microspheres containing carbon black for toners, etc. Ha et al. [77] reported in the synthesis of carbon black/monomer solution using the membrane emulsification. The uniform microspheres of poly(styrene-*co*-butylacrylate) containing carbon black were carried out for the toner application. Hosoya et al. [78] illustrated the uniformly-sized polymer particles by preparing either a two-step swelling and polymerization method or SPG technique. The suitability as a uniformly-sized packing material for small-scaled high-performance liquid chromatography (HPLC) was investigated. In HPLC, the column packed with the 3 μm particles prepared by the SPG technique proved to have a fairly high column efficiency with good column stability.

A third field of utilization is for obtaining multiple emulsions and microcapsules, which have found applications in pharmacy and chemotherapy [12,79-82]. Baba et al. [12] prepared monodispersed chitosan microspheres using SPG to examine the effect of preparation conditions on physiochemical properties of the microspheres. The W/O emulsion of organic acid solutions of chitosan was prepared. The monodispersed chitosan microspheres with the arbitrary size, diameter and porosity could be easily prepared by selecting a proper experimental conditions. The application for release of butyric acid from the chitosan microspheres was revealed.

Closely related to the membrane emulsification is the method employing capillary tubes and microchannels to produce monodisperse emulsions [83-87]. The use of microfluidic systems, dispersed phase liquids and continuous phase liquids were injected into the separated microchannels, and droplets are rapidly and reproducibly formed at the junction of the channels. The resulting droplets were accurately uniform in size, and the size is easily varied by controlling the flow speed in the channels. The production of O/W droplets was realized.

Some comparisons between membrane emulsification and so-called rotating stirrer methods and homo-mixers can be found in many literatures. Also, Partch et al. [88] have described the preparation of polymer colloids by chemical reactions in aerosols. Panagiotou and Levendis [89] reported that monodisperse particles of polystyrene and poly(methyl methacrylate) in the size range of 30 to 60 μm were produced using an acoustically oscillating aerosol generator. The device consists of an oscillating orifice plate and a spray drying tower. The liquid was oscillated at a high frequency, which was the vibration created an instability of small liquid droplets. Uniformity of the droplet sizes was controlled by the size of orifice, the oscillator frequency and the liquid feed rate. By this method, production of low molecular weight polymers is a disadvantage.

The polymer morphology and the polymer phase separation taking place during polymerization within composite latex particles were introduced for artificial latex processing. The choice of the type of solvent has an influence upon the particle morphology as it develops during processing. Tawonsree et al. [90] and Ma et al. [91], studied the polystyrene hollow particles by combining a Shirasu Porous Glass emulsification technique and subsequent suspension polymerization. The performed polymers are dissolved in a mutual solvent and the solvent subsequently removed by evaporation. The formation of hollow particles occurred from the rapid phase separation between PSt and hexadecane (HD). Rapid phase separation confined the HD inside the droplets, it belonged to a non-equilibrium morphology. The HD/St ratio was increased to a high value to confirm the above proposition by promoting rapid phase separation further between HD and PSt, to prevent monomer diffusion into aqueous phase, and to obtain hollow particle with a large hole. Recently, Ma et al. [92,93] studied the addition of 2-diethylaminoethyl methacrylate (DMAEMA) to

allow the hollow particles to be formed more easily by decreasing the interfacial tension between the copolymer and aqueous phase. HD was more easily encapsulated by the polymer when the conversion was quite high, irrespective of whether the DMAEMA hydrophilic monomer was incorporated into the polymer.

Kiatkamjornwong et al. and Nuisin et al. [94,95] investigated the effects of additives and initiator efficiency for producing polymeric particles of poly[styrene-*co*-(methyl methacrylate)] by the SPG emulsification technique followed by suspension copolymerization. Initiators like benzoyl peroxide (BPO), 2,2'-Azo-bis-2,4-dimethylvaleronitrile (ADVN), or 2,2'- azo-bis-isobutyronitrile (AIBN) was used and found that BPO was the most suitable initiator in terms of fairly uniform particle size and size distribution. Besides, copolymers for various feed ratios of styrene/methyl methacrylate were synthesized. Then, *n*-butyl methacrylate (*n*-BMA) or 2-ethylhexyl methacrylate (EHMA) was added as the third monomer to decrease the terpolymer glass transition temperature. Various microspheres with different morphologies were obtained depending on the composition of the oil phase. It was found that the particle size decreased with a narrower size distribution when the additives were changed from long-chain alkanes to long-chain alcohols and long-chain esters, respectively. The spherical poly[(styrene-*co*-methyl methacrylate)] particles without phase separation were obtained when using an adequate amount of the crosslinking agent and methyl palmitate as an additive.

Omi et al. [96] employed the SPG membrane to form uniform size droplets having the coefficient of variation (CV) of around 10%. Styrene (St) and acrylic monomers were used as monomers, and their polymers were dissolved in the droplets to investigate the development of phase separation. The hydrophilic methyl methacrylate (MMA) was polymerized in the droplets with a mixed solvent consisting

of hydrophilic hexanol (HA) and hydrophobic benzene and hexadecane (HD), the resulting morphology shifted from hemisphere to sandwich and eventually to PMMA/solvent core-shell with increasing hydrophilicity of the mixed solvent. As styrene was added to MMA, the morphology shifted from hemisphere core/solvent shell to raspberry core/solvent shell as the fraction of St increased. When a mixed monomer of styrene and MMA dissolving polystyrene (PSt) was polymerized, the resulting morphology shifted from salami to core-shell with increasing the MMA fraction in the comonomer. Their effects on glass transition temperature of the polymers, molecular weight, and the composition of copolymers were also taken in consideration whenever the final morphologies were discussed.

Ma et al. [97] prepared PSt-PMMA composite microspheres with lauryl alcohol, LOH, cosurfactant dissolved in dichloromethane (DCM) as a dispersed phase. When the polymer concentration was low, PSt-PMMA core-shell particles always were obtained in the absence of LOH, irrespective of PSt-PMMA ratio. Different morphologies such as multiplet, and inverted core-shell were observed when the polymer concentrations were high.

Tokarev et al. [98] studied the new approach to the synthesis of core-shell lattices using peroxide macro-initiators for the formation of the seed particles. The peroxide tethered to the surface of particles and the chain-growing reactions of the shell polymerization are localized. The consumption of shell-forming monomer allowed the encapsulation of a core polymer and formation of the shell polymer to improve the properties of the polymer as a whole.

Ma et al. [99] studied the influences of a polar plasticizer containing glycerol, and a nonpolar plasticizer of dioctyl phthalate (DOP) on the microstructure, and relaxation properties of poly(methyl methacrylate) ionomers were investigated by

dynamic mechanical thermal analysis. The results indicated that glycerol moiety strongly interacted with and weakened the ionic cluster 'phase', and also significantly increased the mobility of the backbone hydrocarbon chains in the multiplet-containing matrix phase. In contrast, the nonpolar plasticizer DOP was more suitable in that it appreciably reduced the glass transition temperature of the hydrocarbon-rich matrix phase, but had a much smaller effect than glycerol on the glass transition temperature of the ion-rich cluster 'phase'. The results were compared which was found a contrast effect of the two plasticizers on polystyrene ionomers.

Lin et al. [100] investigated the effects of four organic esters used as plasticizers [triacetin, diethyl phthalate (DEP), dibutyl phthalate (DBP) and tributyl citrate (TBC)] on the water absorption behavior and adhesive property of PMMA (Eudragit®) films, on the T_g , and on plasticizer permanence of Eudragit E film. The result indicated that the water absorption of these Eudragit films was dependent on the type of Eudragit polymers and plasticizers used. Eudragit E film plasticized with triacetin showed a slight water absorption, but did not absorb any water when plasticized with DEP, DBP, or TBC. The TBC may be the best choice of plasticizer for Eudragit film, particularly for the Eudragit E film.

Shieh and Liu [101] investigated the influences of contents and molecular weights of low-density polyethylene (LDPE) on dioctyl phthalate (DOP) plasticization in the poly(vinyl chloride) (PVC) plastisol (PVC/DOP/AO = 100/30/6.5) using DMA and DSC techniques. The plasticization effects of DOP on the PVC plastisol were found to decrease with increasing LDPE content. A negligible plasticization effect of DOP on the PVC plastisol was found when the LDPE content was equal to or higher than 75 parts per 100 parts by weight of LDPE and the PVC plastisol. The interaction enabled the incorporation of DOP into LDPE and decreased

the plasticization effects of DOP on the PVC plastisol. A further decrease in the plasticization effects of DOP on the PVC plastisol by the presence of LDPE was found with increasing LDPE molecular weights.

Kovačić and Mrklič [102] studied the process of loss of plasticizers: dioctyl phthalate, diisononyl phthalate, benzylbutyl phthalate, dioctyl adipate, phosphate plasticizer Reofos, polymeric plasticizer Reoplex and epoxidized soybean oil from plasticized poly(vinyl chloride) foils by the method of isothermal thermogravimetry in the temperature range of 120 to 150°C. The investigated samples contained ca. 10 to 40 wt% of plasticizers. The rate constants of the process of loss of plasticizers were calculated, and the dependences of the rate constant on temperature and on the initial concentration of plasticized PVC were mathematically defined. The activation energy of the process was calculated from the exponential dependence of the rate constant of evaporation on temperature. Compensation parameters were also calculated as a measure of reaction ability of the system. The roles of various parameters i.e. molecular weight, structure of polymer, polarity on the kinetics of evaporation of plasticizers were discussed.

Meincken et al. [72] investigated the influence of particle size and morphology of a synthetic polymer latex on film formation behavior by atomic force microscopy (AFM). Theoretical models predicted that small particles coalesced more easily than did the large colloids. Sequences of AFM images were acquired over a certain temperature range or at room temperature as a function of time. From the resulting images, the average particle diameter of the latex in the surface layer was determined as a function of the time or temperature. The resulting curves could be compared to observe differences in the film formation kinetics of the different lattices. These AFM studies confirmed that the film formation behavior was influenced by the particle size

and particle morphology, but the core/shell ratio of core-shell particles did not significantly influence the film formation kinetics.



สถาบันวิทยบริการ
จุฬาลงกรณ์มหาวิทยาลัย

CHAPTER 3

EXPERIMENTAL

3.1 Materials, Apparatus, and Analytical Instruments

3.1.1 Materials

Styrene was reagent grade and stored at -10°C before use. Styrene monomer was distilled before use for Runs 2022 to 2052. Methyl methacrylate, methyl acrylate, butyl acrylate, and butyl methacrylate were reagent grade and distilled to remove inhibitor before use. Polystyrene having an $\overline{M}_n = 4200$, $\overline{M}_w = 40000$, and $\overline{M}_w/\overline{M}_n = 9.54$, was produced in house. Dioctyl phthalate (DOP) was used as a plasticizer. N, N'-azobisisobutyronitrile (ADVN-V65) or benzoyl peroxide (BPO) were used as initiators. Sodium dodecyl sulphate (SLS) and poly(vinyl alcohol) (PVA-217) having a degree of polymerization of 1700, and 88.5% saponification were used as a surfactant and a stabilizer, respectively. Sodium nitrite (NaNO_2) and *p*-phenylenediamine were used as inhibitors. Sodium sulphate (Na_2SO_4) was used as an electrolyte. Methyl alcohol was used as a solvent and non-solvent for the copolymers.

3.1.1.1 Monomers

Styrene (St, $\text{C}_6\text{H}_5\text{CH}=\text{CH}_2$, MW = 104.0), methyl methacrylate (MMA, $\text{CH}_2=\text{C}(\text{CH}_3)\text{COOCH}_3$, MW = 100.12), methyl acrylate (MA, $\text{CH}_2=\text{CHCOOCH}_3$, MW = 86.0), *n*-butyl methacrylate (BMA, $\text{CH}_2=\text{C}(\text{CH}_3)\text{COO}(\text{CH}_2)_3\text{CH}_3$, MW = 142.2), and *n*-butyl acrylate (BA,

$\text{CH}_2=\text{CHCOO}(\text{CH}_2)_3\text{CH}_3$, MW = 128), from Wako Pure Chemicals, Osaka, Japan, were of commercial grade. Each was distilled under reduced pressure, and stored in a freezer at -10°C prior to use.

3.1.1.2 Crosslinking agent

Ethyleneglycol dimethacrylate (EGDMA, $\text{CH}_2=\text{C}(\text{CH}_3)\text{COOCH}_2\text{CH}_2\text{OCOC}(\text{CH}_3)=\text{CH}_2$, MW = 198.22, Wako Pure Chemicals, Osaka, Japan), was commercial grade.

3.1.1.3 Initiators

Benzoyl peroxide (BPO, with 25 wt% moisture content ($\text{C}_6\text{H}_5\text{COO}$)₂, Kishida Chemicals, Osaka, Japan), was reagent grade. 2,2'-Azo-bis-2,4-dimethylvaleronitrile (ADV, V-65, $\text{CH}_3\text{CH}(\text{CH}_3)\text{CH}_2\text{C}(\text{CN})(\text{CH}_3)\text{N}=\text{N}(\text{CH}_3)(\text{CN})\text{CCH}_2(\text{CH}_3)\text{CHCH}_3$, MW = 248.0, Wako Pure Chemicals, Osaka, Japan), was reagent grade. EGDMA was treated with 5% sodium carbonate for 5 times, and then washed with deionized water (DDI) for another 5 times. The inhibitor-free EGDMA was dried with 5 Å molecular sieve.

3.1.1.4 Plasticizer and hydrophobic additives

Diethyl phthalate (bis-(2-ethylhexyl phthalate), DOP, $\text{C}_6\text{H}_4[\text{COOCH}_2\text{CH}(\text{CH}_2\text{CH}_3)(\text{CH}_2)_3\text{CH}_3]_2$, MW = 390.56), Fluka, Buchs, Switzerland and Wako Pure Chemicals, Osaka, Japan, both were chromatography grade and used as a plasticizer. *n*-Hexadecane ($\text{CH}_3(\text{CH}_2)_{14}\text{CH}_3$, MW = 226.45, Tokyo Chemical Industry, Tokyo, Japan) was used as a hydrophobic additive for droplet stabilizer in a dispersion phase.

3.1.1.5 Stabilizers

Poly(vinyl alcohol), PVA-217, degree of polymerization = 1700, 88.5% saponification, Kuraray, Osaka, Japan, was commercial grade and used as a stabilizer in the continuous phase. Poly(vinyl alcohol), PVA, PVA-205S with a degree of polymerization = 500, 86.5% saponification, Air Products and Chemicals, Inc., Pennsylvania, USA, was commercial grade and used as a stabilizer. Sodium Dodecyl Sulfate, Sodium Lauryl Sulfate (SLS, $\text{CH}_3(\text{CH}_2)_{11}\text{OSO}_3\text{Na}$, MW = 288.38, Merck, Darmstadt, Germany) or poly(vinyl pyrrolidone), PVP K-30, $\overline{M}_n = 40,000$ Tokyo Chemical Industries, Tokyo, Japan, was of biochemical grade and used as a surfactant.

3.1.1.6 Solvents

Methyl alcohol, (CH_3OH , MW = 32.4, Kishida Chemicals, Osaka, Japan), was commercial grade and used for precipitating polymer latex.

3.1.1.7 Other chemicals

Sodium sulfate anhydrous, (Na_2SO_4 , MW = 142.04, Kokusan Chemical Works, Osaka, Japan) was commercial grade and used as an electrolyte in the continuous phase. Hydroquinone (HQ, $\text{HO}(\text{C}_6\text{H}_4)\text{OH}$, Kishida Chemicals, Osaka, Japan), Sodium nitrite, (NaNO_2 , MW = 69.0 Chameleon Chemical, Osaka, Japan), and *p*-phenylenediamine (PDA, $\text{NH}_2\text{C}_6\text{H}_4\text{NH}_2$, MW = 108.14, Chameleon Chemicals, Osaka, Japan) were reagent grade and used as inhibitors for suspension polymerization.

3.1.2 Apparatus

3.1.2.1 SPG Emulsification Apparatus

Microporous glass membrane (SPG membrane, Ise Chemical Corp., Tokyo, Japan), an annulus cylinder diameter 10 mm, length 20 mm, pore sizes 0.51 and 0.90 μm

Teflon oil vessel, 20 cm^3

Emulsion storage vessel, 300 cm^3

SPG stainless steel module (for inserting the SPG membrane)

3.1.2.2 Polymerization Kit

| | | |
|--|---|------|
| Three-necked glass separator flask, 300 cm^3 | 1 | unit |
| Dimroth spiral condenser | 1 | unit |
| Nitrogen inlet and outlet nozzle; each | 1 | unit |
| Semicircular anchor-type blade | 1 | unit |
| Thermostat bath with heating coil and circulation pump (Yamato BM-82, Tokyo, Japan) | 1 | unit |
| Nitrogen gas or Air (Tokyo Chemicals Company, Tokyo, Japan) | 1 | unit |

3.1.3 Analytical Instruments

Optical Microscope (OM), Model BHC with Olympus DP-10 CCD camera (Olympus America Inc., New York, USA)

Scanning Electron Microscope (SEM), JEOL JSM-5310 (JEOL, Tokyo, Japan)

Gel Permeation Chromatography (GPC), Tosoh HLCH820 (Tosoh Corporation, Tokyo, Japan)

Nuclear Magnetic Resonance Spectrometer (NMR), JNM A500FT (JEOL, Tokyo, Japan)

Fourier-Transform Infrared Spectrometer (FT-IR), Nicolet (Nicolet Corporation, Wisconsin, USA)

Differential Scanning Calorimeter (DSC), Mac Science 3100 (Mac Science, Tokyo, Japan)

Transmission Electron Microscope (TEM), JEOL JEM 1010 (JEOL, Tokyo, Japan) and JEM 200cx (JEOL-USA, Inc., Massachusetts, USA)

Atomic Force Microscope (AFM), JEOL JSPM-4200 Scanning probe microscope (JEOL, Tokyo, Japan)

3.2 Experimental

3.2.1 Emulsification Procedure

The SPG membrane with a pore size of 0.51 μm or 0.90 μm (Ise Chemical Corp., Tokyo, Japan) was used for the emulsification. A schematic diagram of emulsification kit apparatus is shown in Figure 3.1. This system consists of stop valves (a), a three-digit pressure gauge (b), a clamp (c), the oil vessel (d), the SPG membrane module (e), the emulsion vessel (f), the stirrer (g), the needle valve (h), and a nitrogen gas tank (or air tank) (i). The preparative condition for a one-step emulsification is also shown in Table 3.1. The SPG membrane was pre-wetted in the aqueous phase. The air or N_2 pressure was used to permeate the dispersion phase through the SPG membrane. Three-digit pressure gauge was used. The ranges of

pressure of 1.28 to 1.45 kgf cm⁻² for the 0.51 μm, and 0.30 to 0.70 kgf cm⁻² for 0.90 μm membrane pore size were used. The dispersion phase containing a mixture of the monomers, DOP, and BPO, or ADVN initiator was prepared and stored in 20 cm³ oil storage vessel. Precisely controlled nitrogen or air pressure was applied to the oil storage vessel of the dispersion phase. The dispersion phase was then allowed to permeate through the membrane. The stainless steel module was completely immersed in an emulsion storage vessel containing the continuous phase. In the continuous phase, the PVA stabilizer, SDS surfactant, Na₂SO₄ electrolyte, and NaNO₂ inhibitor were dissolved. The droplets were stabilized by the adsorption of surfactant and electrolyte onto their surfaces. To prevent creaming of the droplets, the continuous phase was gently stirred at 300 rpm with a magnetic bar.

Table 3.1 A selected recipe for the SPG emulsification

| Component | Weight (g) |
|---|---------------------------------------|
| Continuous phase | |
| PVA-217 | 2.00 ^a , 3.00 ^b |
| SLS | 0.10 |
| Na ₂ SO ₄ | 0.10 |
| Inhibitor (NaNO ₂ , or PDA) | 0.04 |
| Water | 230 |
| Dispersion phase | |
| Initiator (BPO, or ADVN) | 0.04 |
| Monomer content (St, MMA, MA, BA, BMA) ^c | 16.0 |
| DOP | 0.8 |

^a SPG membrane pore size 0.9 μm, ^b SPG membrane pore size 0.5 μm

^c The selection of monomer content is given in Chapter 4 in details.

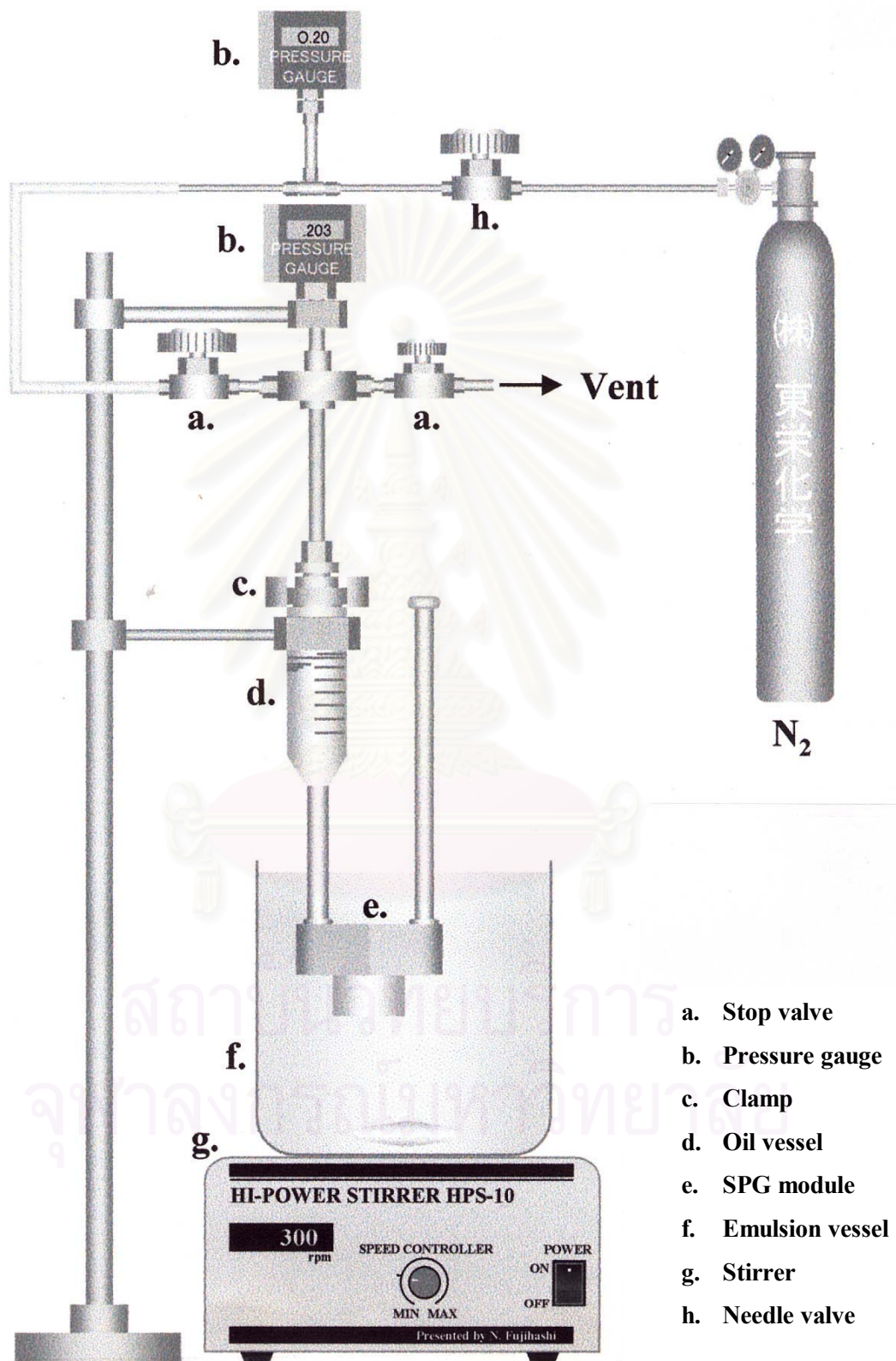


Figure 3.1 A Schematic diagram of an SPG emulsification kit

3.2.2 Polymerization

The emulsion obtained was transferred to a three-necked glass vessel with a capacity of 300 cm³ connected with a semicircular anchor-type blade made of PTFE for agitation, a Dimroth condenser, and a nitrogen inlet nozzle. Nitrogen gas was gently bubbled into the emulsion for 1 h; the nozzle was then lifted above the emulsion level. The temperature was increased to reach 75°C, and controlled at this constant temperature for polymerization. The emulsion was polymerized for 24 h under the nitrogen atmosphere by suspension polymerization.

3.3 Characterization

3.3.1 Conversion of Monomers

Percentage conversion of the monomers was monitored by gravimetric method. Methyl alcohol, a non-solvent was added to precipitate the polymer. The polymer particles were separated by centrifugation at 2000 rpm and washed repeatedly with methyl alcohol for 2-3 times. The polymer particles were then dried in vacuum at room temperature for 48 h and weighed.

3.3.2 Surface Morphology

The external morphology of polymer particles was observed by scanning electron microscope (JEOL, Model JSM-5310, Tokyo, Japan). The specimens were prepared by diluting the polymer latex, from which the diluted suspension was dropped on an aluminum stub surface and coated with a thin layer of gold under reduced pressure (less than 10⁻² Pa) using a fine coater (JEOL, Model JFC-1200, Tokyo, Japan). The magnification was set at 1000× in the SEM photographs taken for

the determination of an average size of the polymer particles with a coefficient of variation (CV).

3.3.3 Internal Morphology of the Particles

The internal morphologies of polymer particles in Runs 2018 and 2019 prepared from St:MA contents of 50:50, and 75:25, with an incorporation of 5% DOP were subjected to TEM observation (Model JEM 1010, JEOL, Tokyo, Japan). The samples were characterized by Actresearch Co., Ltd, Yokkaichi, Japan. The specimens were prepared by embedding in an epoxy resin and curing at ambient temperature. The samples were microtomed and stained with RuO₄, and viewed at a magnification of 20000×.

The internal morphology of other polymer particles was observed by transmission electron microscope, TEM (JEOL-USA, Inc., Model JEM 200cx, Massachusetts, USA). The specimens were prepared by embedding the polymer sample in an epoxy resin and curing at ambient temperature for 8 h. The epoxy resin contained vinyl cyclohexene dioxide (VCD, ERL-4206[®], EMS, South Carolina, USA), epoxy resin (DER-736[®], EMS, South Carolina, USA), nonyl succinic anhydride (NSA, EMS, South Carolina, USA), dimethyl amino ethanol (DMAE, EMS, South Carolina, USA) as a catalyst. The ratio of VCD, to DER-736[®], to NSA was 10.4:62.5:20.1, and 0.4 wt% of the mixed epoxy of DMAE catalyst was then added. The embedded specimens were cured at room temperature for 72 h and cut to a thin section of 50 nm using an ultramicrotome. Then, the ultrathin cross-sectioned specimens were stained by exposing to OsO₄ vapor from the 0.5% OsO₄ solution for 3 h prior to the TEM investigation.

3.3.4 Size and Size Distribution of Emulsion Droplets and Polymer Particles

The monomer droplets before polymerization were observed by an optical microscope (Olympus optical microscope, Model BHC with Olympus DP-10 CCD camera (Olympus America Inc., New York, USA). Diameters of about 150 monomer droplets were measured and calculated for an average diameter and a size distribution. On average, the diameters of about 150 polymer particles were measured and calculated from the SEM photographs. Through the evaluation of the OM and SEM photographs, the number-average diameters of the emulsion droplets (\bar{D}_e) and polymer particles (\bar{D}_p) were calculated according to Eq. 3.1, as well as the standard deviation (σ), and coefficient of variation (CV) were calculated using the formula in Eqs. 3.2 and 3.3:

$$\bar{D}_n = \frac{\sum_{i=1}^n n_i D_i}{\sum_{i=1}^n n_i} \quad (3.1)$$

where n_i is the number of particle diameter, D_i is the diameter of individual particle, and \bar{D}_n corresponds to the mean number of the population. The standard deviation σ is determined from the measured particle diameters from the following equation.

$$\sigma = \left[\frac{1}{n-1} \sum_{i=1}^n (D_i - \bar{D}_n)^2 \right]^{1/2} \quad (3.2)$$

The particle size distribution is reflected in the standard deviation. The breadth of the particle size distribution is proportional to the standard deviation of the particle diameters using the coefficient of variation (CV) as follows:

$$CV (\%) = \sigma / \bar{D}_n \times 100 \quad (3.3)$$

3.3.5 Molecular Weights and Distribution

Gel permeation chromatography (GPC) was used for the examination of average molecular weights and molecular weight distribution. The GPC chromatograms were obtained using Tosoh gel permeation chromatography (Model HLC H820 Chromato column, Tosoh, Tokyo, Japan) at the oven temperature of 40°C, and the injection temperature at 35°C. Pressure was applied to the samples at 16 kgf cm⁻² and the reference at 12 kgf cm⁻². There are two types of GPC columns for sample analysis. The first column (Model GRCX4) and the second column (Model GMMXL) were both packed with mixed gels of crosslinked poly[(divinyl benzene)-*co*-styrene]. Likewise, the reference column (Model GMMXL) was also packed with mixed gels of poly[(divinyl benzene)-*co*-styrene]. Tetrahydrofuran (THF, Wako Chemical Works, Osaka, Japan) was used as a solvent and an eluent. For analysis, one mg of the dried polymer sample was dissolved in two cm³ of THF to obtain an approximate concentration of 0.1 wt%. Then, the polymer solution filtered with 0.2 μm PTFE membrane (Advantec, Tokyo, Japan) was injected into the columns at a flow rate of 0.5 cm³ min⁻¹. The chromatogram was detected using the refractive index detector.

3.3.6 Glass Transition Temperature

Measurement of glass transition temperature (T_g) was performed using a differential scanning calorimeter (DSC) (Model 3100, MAC Science, Tokyo, Japan). The sample was prepared by two methods, the unclean and clean method. For the first method, the polymer latex was dried under vacuum at ambient temperature for 120 h without further cleaning process. The second method, the polymer latex was washed repeatedly with methanol to remove all the surfactants, DOP (partial amount), and stabilizer. Then, the precipitated latex was dried under vacuum at ambient temperature for 48 h. The sample (5 to 10 mg) from each preparation method was placed on the aluminum pan and put on the sample chamber at room temperature along with an empty pan as a reference to adjust the output balance. Measurement of the sample was done at a heating rate of $10^\circ\text{C min}^{-1}$. The range of the temperature was scanned from -30 to 130°C under liquid nitrogen.

3.3.7 Nuclear Magnetic Resonance Spectroscopy

The copolymer composition and DOP were studied by ^1H NMR (Model JNM-A500 FT, JEOL, Tokyo, Japan). The copolymer composition was calculated from the structural components as a chemical shift, commonly measured in ppm from an internal reference. The polymer can provide information on number and type of atoms linked to each particular nucleus. Proton NMR spectra (^1H NMR) are complicated by the presence of coupling effects between the spins of the protons. ^1H NMR spectra were recorded by 500 MHz NMR spectrometer (Model JNM-A500 FT, JEOL, Tokyo, Japan) spectrometer at 45°C using deuterated chloroform (CDCl_3) as the solvent and tetramethylsilane (TMS) as internal reference. The sample concentration was 30% w/v CDCl_3 . A total of 160 scans was accumulated,

corresponding to a spectral width of 10000 Hz, with an acquisition time of 3.2768 s, and a pulse delay of 3.7232 s.

3.3.8 Functional Group of Copolymer

The FT-IR, Nicolet Fourier Transform Infrared Spectrometer was used for characterizing the functional groups of the copolymer. Polymer latices were washed repeatedly by methanol and dried under vacuum for 48 h. The polymer samples were prepared by KBr pellet method.

3.3.9 Atomic Force Microscopy

Atomic force microscopy (AFM) was used to characterize the film formation of the current latices due to its following advantages. First, it is possible to map topology at the surface, which allows one to determine the particle size, roughness of film surface or the height of single particles placed on a flat substrate. Second, it is possible to studying ordering and packing phenomena on surface [103]. Third, resolutions below 10 nm can be refined achieved on the investigated polymer systems. Hence, by AFM of film casting and of film surfaces, the films can be characterized in terms of topology and phase distribution [104,105].

สถาบันวิทยบริการ
จุฬาลงกรณ์มหาวิทยาลัย

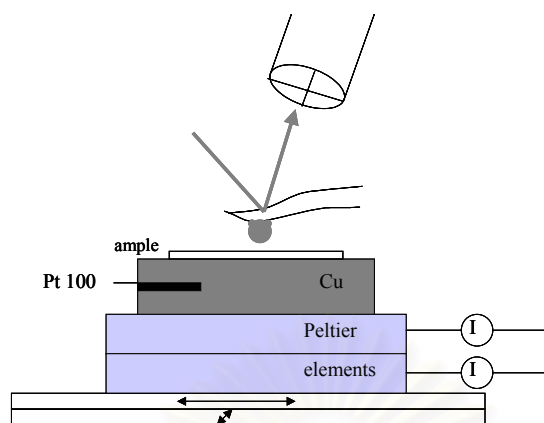


Figure 3.2 Sample preparation for AFM measurements

All AFM data presented was recorded in contact mode. In this mode, imaging the tip is kept in contact with the surface while the sample is scanned laterally. The force pressing against the polymer surface was controlled by the deflection of a cantilever beam and kept at a constant value by a feedback system [106].

Glass plate was a substrate for this experiment because it has a flat, hydrophilic surface that allows good wetting by the aqueous colloidal solution of copolymer prior to evaporation (fast/slow-dried films, which leads to a deposition of the spheres on the substrate). The experimental set up used is shown in Figure 3.2, the polymer sample was placed on a heating/cooling stage, which was located on a x/y translator. The AFM is placed above the sample. Select an initial scan size of $50\ \mu\text{m} \times 50\ \mu\text{m}$ image and a high-resolution image to show the best resolution possible of an individual copolymer latex sphere. The resonance frequency of the low frequency, non-contact silicon cantilevers is about 170 kHz. The cantilever is driven at its resonance frequency with a driving-amplitude of 0.2 mV. The measurements are

performed under ambient conditions. The surface structure of self-assembled latex structure polymers films on a mica (hydrophilic) substrate.

AFM images of the polymer film are acquired at 24 h after casting the film. Until the film had dried, the time between the acquisition of two images was increased to a few hours. The average particle diameter is determined by using line-scan through the image and the peak-to-peak distance measurement.

3.3.10 Film formation and Characterization

Film formation of polystyrene, poly(*St-co-MA*), poly(*St-co-BMA*), and poly(*St-co-BA*) were studied. Surface topography were illustrated using various characterization methods as follows: scanning electron microscopy (SEM), optical microscopy (OM), and atomic force microscopy (AFM). The preparation of OM and SEM observations, a preweighed sample of polymer latex was stirred and agitated for several minutes. A fine-tip dropper was used to suck in and squeeze out the latex several times to let the dispersed particles being sufficiently mixed. The mixed dispersion, having a solid content of ca. 4.5 wt%, was then spread on a glass substrate and allowed to dry at room temperature. In most cases, the substrate with the dispersion was covered with a paper box to slow down the water evaporation rate throughout the drying period. The film thickness varied throughout the film with a range of 5 to 20 μm for one coating layer. The edges of the film were somewhat thinner.

Prior to the SEM measurements, the film was dried in the vacuum oven for 48 h and was then coated with a layer of gold onto the surface to prevent a charging of the films and to slow down the melting of polymer surface under the electron beam.

CHAPTER 4

RESULTS AND DISCUSSION

The polystyrene particles with DOP incorporated were prepared with an SPG membrane pore size of 0.51 μm or 0.90 μm for emulsification. They were subsequently polymerized by suspension polymerization. The preparative conditions for a one-step emulsification of styrene are shown in Table 3.1 and the recipes of copolymer compositions in Table 4.1.

4.1 Effect of DOP on Styrene Homopolymerization

The SEM photographs (Figure 4.1a for Run 2013) show that polystyrene particles incorporating DOP have an average diameter of 3 μm and were irregular in shape. A higher magnification of these particles revealed small particles with an average diameter of less than 0.1 μm . These small particles covered the surface of the big particles. Very interestingly, it could be estimated that emulsion polymerization evidenced by the small particles takes place at the expense of the suspension polymerization for the present case. Secondary particle nucleation in Run 2013 could take place at the longer emulsification time of 20 h using the SPG membrane pore size of 0.51 μm under low pressure (1.3 kgf cm^{-2}). Emulsion droplets with an average diameter of 4.1 μm were obtained resulting in the opalescence of the mixture and formation of small polymer particles. This produces polymers the higher molecular weights with a bimodal molecular weight distribution. Small fraction of high molecular weight polymer may be formed during the long emulsification at room temperature leading to slow termination of polymer's radicals. As the suspension

polymerization proceeds, styrene polymerized much faster and thus excluded DOP behind, leaving it in the aqueous phase due to the latter's moderate hydrogen bonding. The aqueous phase composition of the dissolved styrene monomer and DOP then polymerized to give the minute amount of secondary particles deposited on the bigger primary particles. DOP may provide hydrophobic environment and promote the partition of St in the aqueous phase (which may induce the secondary nucleation).

Glass transition temperatures of the clean composite polymer are shown in Table 4.1 that the T_g 's values for the clean particles of the highly and lowly plasticized portions were 18 and 71°C, respectively, and 6.4 and 86°C for the unclean particles. The DOP could be mixed and in-situ plasticized with styrene so the glass transition temperature values could confirm the polymerization loci. Also, we can anticipate that DOP migration could probably take place during the temperature rise in the course of the DSC measurement. One thing is needed mention to mention as that the droplet size and the droplet size distribution depended on the duration of SPG emulsification process, especially for the use of small pore size of the SPG membrane (0.5 μm). As shown in Figure 4.2c, the coefficient of variation of monomer droplets was broader with emulsification time. The permeation pressure was held at a constant rate of 1.28 kgf cm⁻².

Yuyama et al. [65] described the average droplet size dependence on the medium interfacial tension, which was related to the concentration of surfactant and hydrophobicity of dispersion phase. The PVA and SLS stabilizer used may be considered that the polyelectrolyte stabilizer behaved as the adsorbed layer on the droplet surface. The continuous and dispersion phases were in contact with the SPG membrane until the release of the droplets. Therefore, the longer the droplets stayed in the hydrophilic membrane pore, the interface was possibly affected by the membrane

surface having the silanol functional groups. Then, the average droplet size of the monomer decreased as a function of emulsification time.

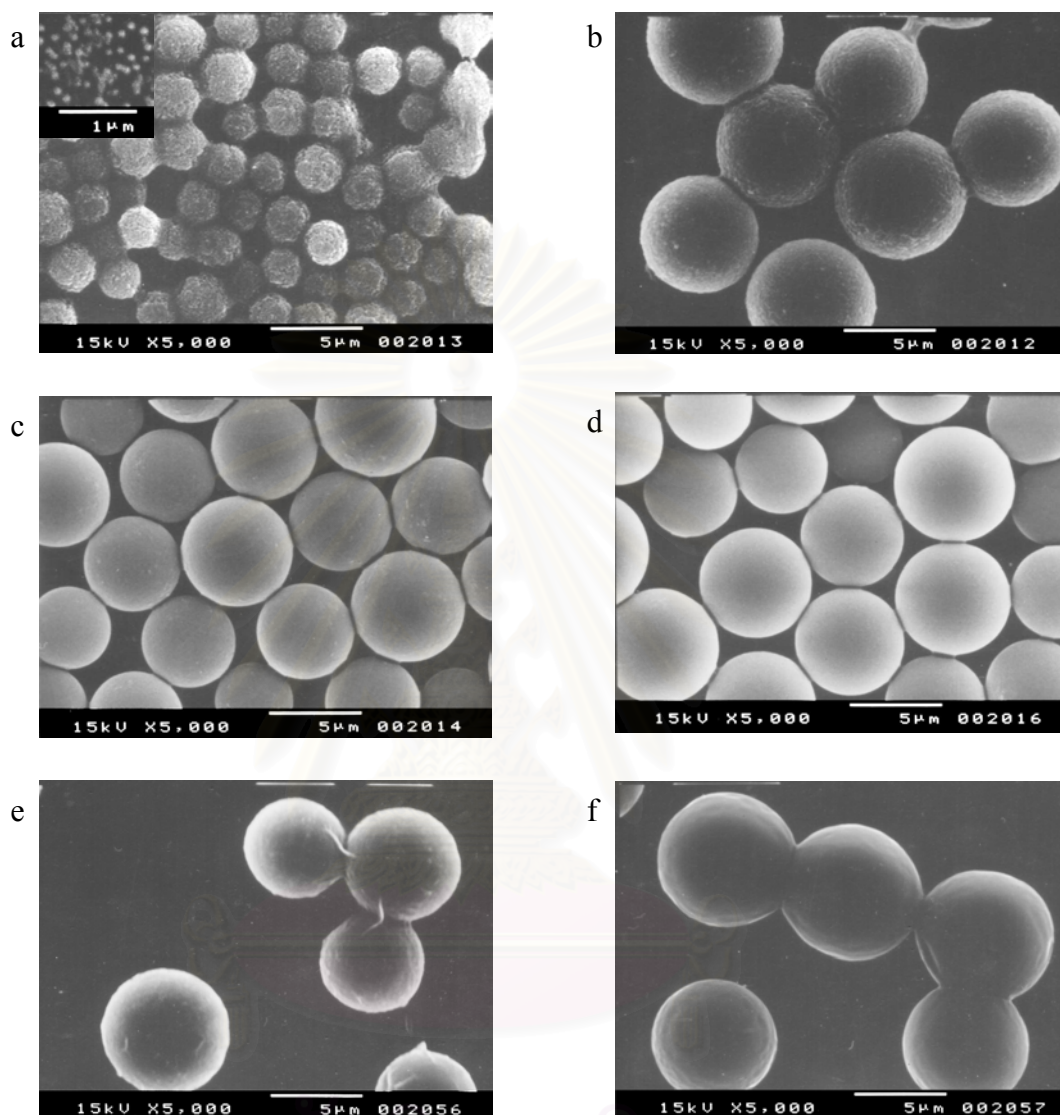


Figure 4.1 SEM photographs of polystyrene incorporated with DOP: a) DOP 2.5 wt% (Run 2013); b) DOP 5 wt% (Run 2012, ADVN as initiator); c) DOP 5 wt% (Run 2014, BPO as initiator); d) DOP 5 wt% (Run 2016, ADVN as initiator and PDA as inhibitor); e) DOP 10% (Run 2056, BPO as initiator); and f) DOP 15 wt% (Run 2057, BPO as initiator).

Table 4.1 Recipe and results for styrene polymerization

| Run No. | Initiator and inhibitor types | DOP (wt.% of monomer) | Monomer conversion (%) | D_e (μm) | CV_e (%) | D_p (μm) | CV_p (%) | $\bar{M}_n \times 10^{-4}$ | $\bar{M}_w \times 10^{-4}$ | PDI | T_g ($^{\circ}\text{C}$) clean | T_g ($^{\circ}\text{C}$) unclean |
|-------------------|-------------------------------|-----------------------|------------------------|-------------------------|------------|-------------------------|------------|----------------------------|----------------------------|------------------|------------------------------------|--------------------------------------|
| 2013 ^a | ADV N, NaNO ₂ | 2.5 | 86.6 | 4.1 | 8.3 | 2.9 | 10.3 | 4.1 | 33.7 | 8.1 ^b | 18.1/71.0 ^c | 6.4/86.0 ^c |
| 2012 ^a | ADV N, NaNO ₂ , | 5 | 74.6 | 8.8 | 18.4 | 7.3 | 18.5 | 1.8 | 8.2 | 4.6 | 3.1/48.2 ^c | 1.0/43.1 ^c |
| 2016 ^a | ADV N, PDA | 5 | 76.0 | 7.1 | 15.9 | 5.8 | 16.1 | 1.7 | 7.5 | 4.5 | 6.3/65.9 ^c | 11.7/54.8 ^c |
| 2014 ^a | BPO, NaNO ₂ | 5 | 76.5 | 6.3 | 15.2 | 5.9 | 11.2 | 1.7 | 3.9 | 2.3 | 9.9/72.6 ^c | 10.3/66.4 ^c |
| 2056 | BPO, NaNO ₂ | 10 | 84.4 | 12.4 | 15.8 | 7.9 | 21.4 | 2.8 | 5.9 | 2.1 | 16.2/45.9 ^c | 10.0/46.8 ^c |
| 2057 | BPO, NaNO ₂ | 15 | 80.6 | 10.9 | 15.8 | 9.2 | 17.9 | 2.5 | 5.2 | 2.1 | 13.5/35.5 ^c | 10.9/38.8 ^c |

Flattened

^a SPG pore size of 0.51 μm , otherwise is 0.90 μm . ^b Bimodal curve. ^c Two separate T_g values were observed.

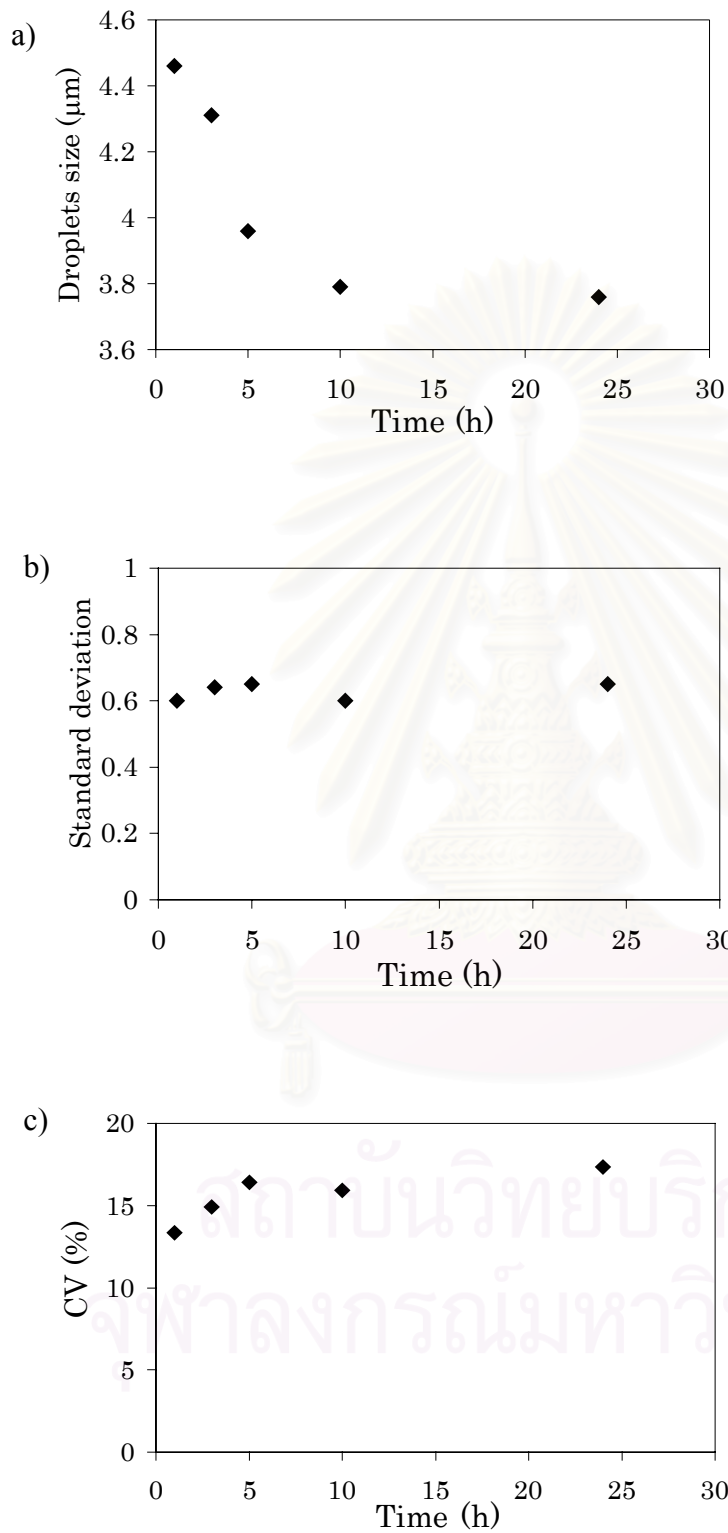


Figure 4.2 Relationship between emulsification time with: a) droplets size; b) standard deviation; and c) coefficient of variation of droplets

4.1.1 Dependence of Styrene Homopolymerization on Initiator Type

Two types of initiator, ADVN (a more aqueous type) and BPO (a non-aqueous type), were used to polymerize DOP plasticized styrene. Oil-soluble initiator having a very low solubility in water, such as BPO, has advantages in comparison with more polar initiators such as ADVN. Not only reducing the risk of formation of new particles in the aqueous phase, but they also reduce the change of bulk polymerization in the monomer droplets. With the less oil-soluble ADVN, it is a stronger requirement that all monomers have been absorbed in the monomer droplets before the polymerization is started by raising the reaction temperature. Similarly, with this initiator type, it must be taken care that the monomer phase could not be formed by evaporation and condensation of the monomer during the polymerization. ADVN are slightly water soluble, which can diffuse into the monomer phase and starts a bulk polymerization, which will result in the formation of large lumps and thereby entail great disadvantages. Using an initiator having a very low solubility in water, such as BPO, all monomers will possibly not diffuse out of the particles through the aqueous phase to the monomer reservoir. Thus, if a certain monomer phase is intermediately present during the polymerization, the only thing which possibly happen is a thermal polymerization therein, and the monomer will primarily be absorbed in the particles containing the initiator as the polymerization proceeds.

The effects of the initiator on the particle size are shown in Table 4.1, from which both initiators produced the similar monomer conversion of 74.6 and 76.5%. The average particle size obtained from the ADVN initiation (Run 2012, Figure 4.1b) was larger than that from the BPO (Run 2014, Figure 4.1c). After the polymer latex had been kept for 24 h, we found that the plasticized polystyrene synthesized with the BPO initiation gave one layer of precipitate residing at the

bottom of the bottle. In contrast, two separate layers of precipitate were observed for the ADVN initiation. The BPO-initiated polystyrene preferred not to suspend in the aqueous phase due to the higher hydrophobicity of both initiator fragments. For the ADVN initiation system, the polystyrene particles with more polar initiator fragments could stay better in the aqueous phase. Therefore, the BPO initiation gave polymers with the lower average molecular weights and narrow molecular weight distribution than those from the ADVN as shown in Figure 4.3. However, the surface morphology of the polymer particles was still similar, because a smooth surface was obtained as shown in Figures 4.1b to 4.1d.

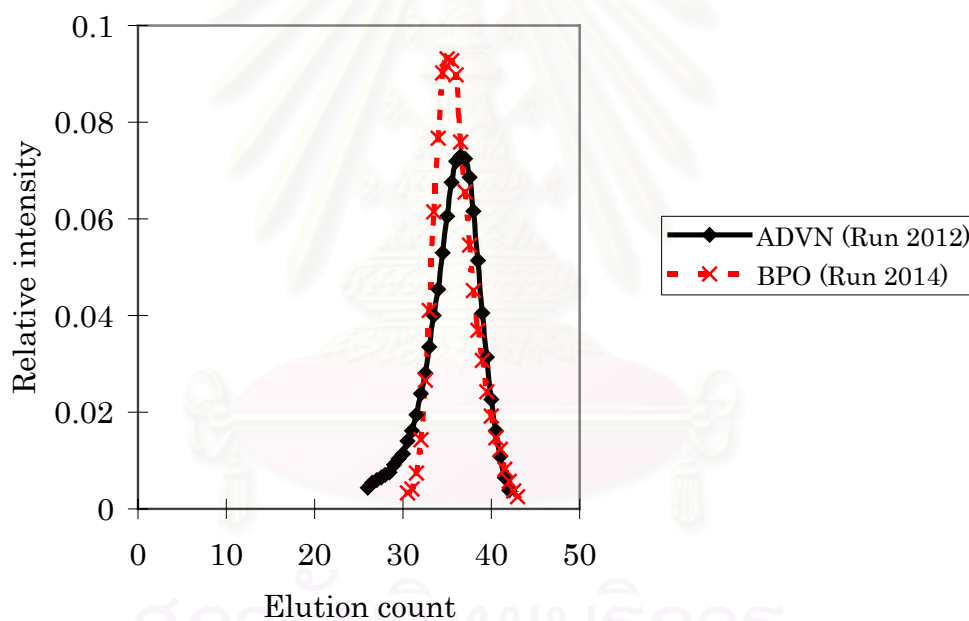


Figure 4.3 Normalized GPC chromatograms of polystyrene particles showing effects of the different initiator types.

The glass transition temperatures of DOP-plasticized polystyrene are presented in Table 4.3. For all experiments, two separate T_g values were found, indicating increasing immiscibility of the styrene monomer (dissolving PS) and DOP

during polymerization as shown in Figure 4.4. At the beginning stage of the polymerization, more concentration of DOP was consumed along with styrene conversion, because the polymer chain lengths were still short, which eased the inclusion of DOP between these chains. At this stage, highly plasticized polystyrene was obtained, yielding a lower glass transition temperature. At the later stage of polymerization, less DOP was retained in the monomer droplets. Less plasticized polystyrene particles (chains) resulted in, and yielded the higher glass transition temperature.



สถาบันวิทยบริการ
จุฬาลงกรณ์มหาวิทยาลัย

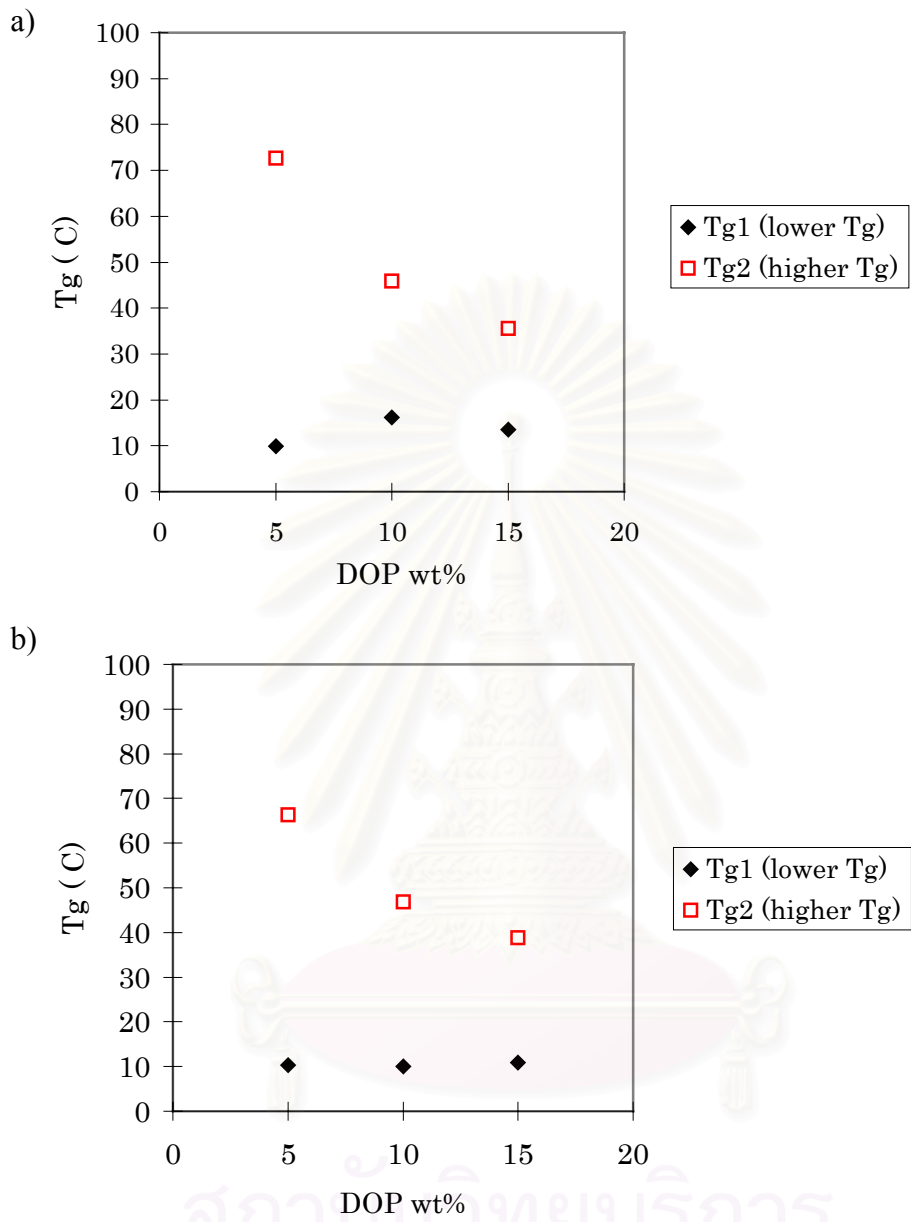


Figure 4.4 Relationship between T_g and DOP concentration (wt%) based on the monomer: a) clean, and b) unclean particles

4.1.2 Effect of Inhibitor on Polymerization and Polymer Particles

Two types of water-soluble inhibitors namely NaNO_2 and PDA were used. An aqueous phase inhibitor, as given a task of preventing the secondary nucleation should possess the properties as follows. First, the inhibitor eliminates particle formation in the aqueous phase by preventing the propagation of any free radicals in this phase. Second, the inhibitor should not obstruct polymerization kinetics in the droplets by inducing an induction period, annihilating free radicals. Finally, it should not affect the stability of particles [107]. In case of NaNO_2 , it undergoes hydrolysis and forms nitrous acid, which dissociates into nitric oxide and nitric acid as the following equations (Eqs. 4.1a to 4.1g) [108]. Uneven electrons of nitric oxides and nitrous oxide promote the coupling reaction with polymeric radicals. However, these radicals are also soluble in the oil phase, and inhibit the polymerization to some extent. From Table 4.1, it was found that the inhibitors did not significantly affect the monomer conversion, molecular weights and molecular weight distribution, and particle morphology. All the synthesized particles had smooth surfaces and spherical shape with an average particle size of 8 μm . One must mention that the latex with the PDA inhibitor exhibited the dark violet color as shown in Figure 4.5e, from which the dark-brown polystyrene particles were formed. For the forthcoming syntheses of plasticized copolymers, only NaNO_2 was justified to be used as an inhibitor.

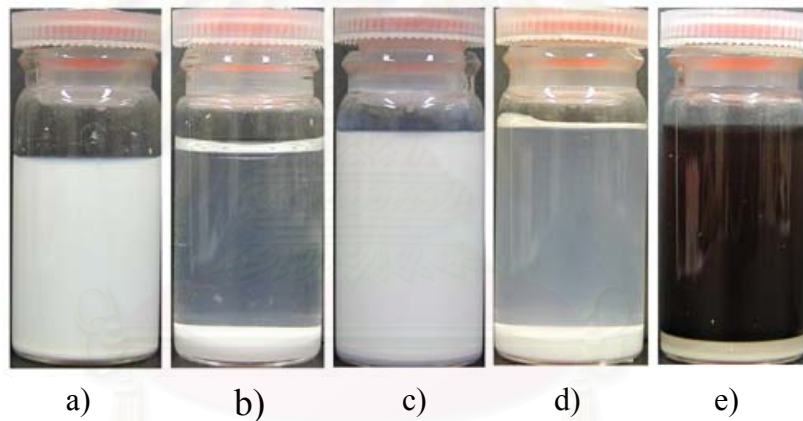


Figure 4.5 Appearance of the polymer latex stability after 24 hours of polymerization: a) ADVN, NaNO₂ (Run 2011); b) ADVN, NaNO₂ (Run 2012); c) ADVN, NaNO₂ (Run 2013); d) BPO, NaNO₂ (Run 2014); and e) ADVN, PDA (Run 2016).

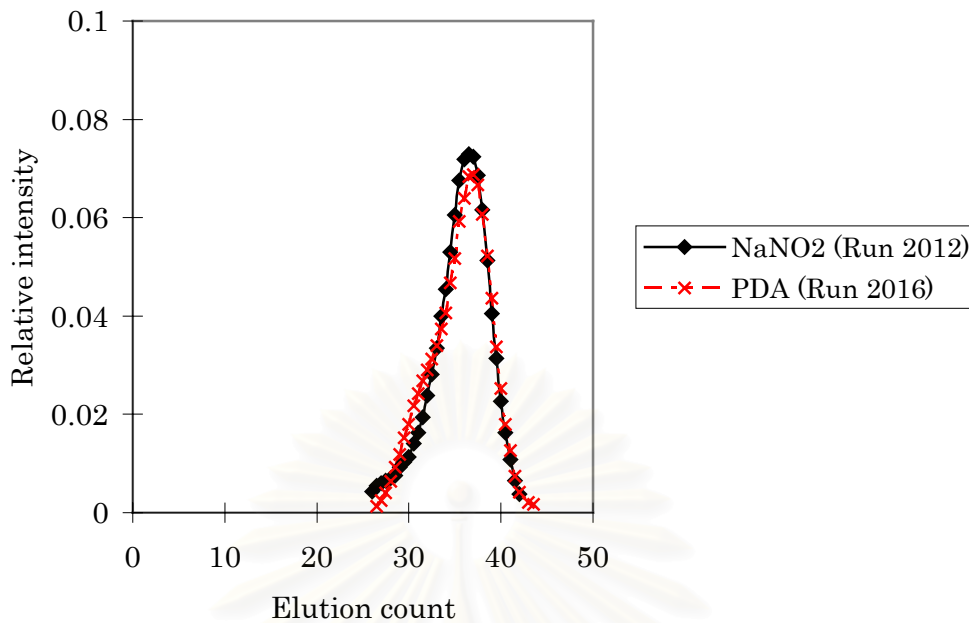


Figure 4.6 Normalized GPC chromatograms of polystyrene particles showing effects of the inhibitor type.

For the effect of the inhibitor type on molecular weight and molecular weight distribution of polystyrene, the similar average-molecular weight and molecular weight distribution was obtained as shown in Table 4.1 and Figure 4.6. The inhibitor molecules are present in the continuous phase and inflict on the conversion, the molecular propagation.

4.1.3 Detection of DOP Incorporation in the Copolymer by ^1H NMR

Assignments of proton positions in the ^1H NMR spectra of polystyrene are shown in Figures 4.7 and 4.8. The resonance signals due to phenyl protons of the styrene unit were observed at the chemical shifts (δ) of 6.3 to 7.2 ppm. For DOP, the resonance signals in the phenyl ring, appearing in the form of triplet within the chemical shifts of 7.5 and 8.0 ppm were resulted from a diamagnetic shielding by the

isolated phenyl ring of DOP. The estimated concentration of DOP in polystyrene is summarized in Table 4.2. The calculated values using Eq. 4.2, revealed a good agreement with the experimental composition.

$$\text{DOP (wt\% in PSt)} = \frac{[A(-C_6H_4)/4]_a + [A(-C_6H_4/4)]_b}{[A(-C_6H_4)_a + A(-C_6H_4)_b]/4 + A(-C_6H_5)/5} \quad (4.2)$$

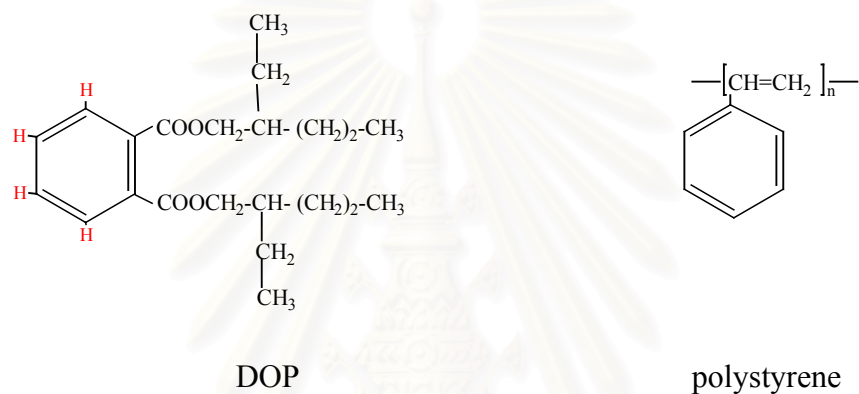


Figure 4.7 Chemical structures of DOP and polystyrene

Table 4.2 Calculated amounts of DOP in polystyrene

| Run No. | DOP in Feed (wt% of monomer) | DOP in Feed (mol%) | DOP (mol%) calculated from Eq. 4.2 |
|---------|------------------------------------|-----------------------|---------------------------------------|
| 2016 | 5 | 1.31 | 0.36 |
| 2056 | 10 | 2.59 | 0.38 |
| 2057 | 15 | 3.84 | 0.44 |

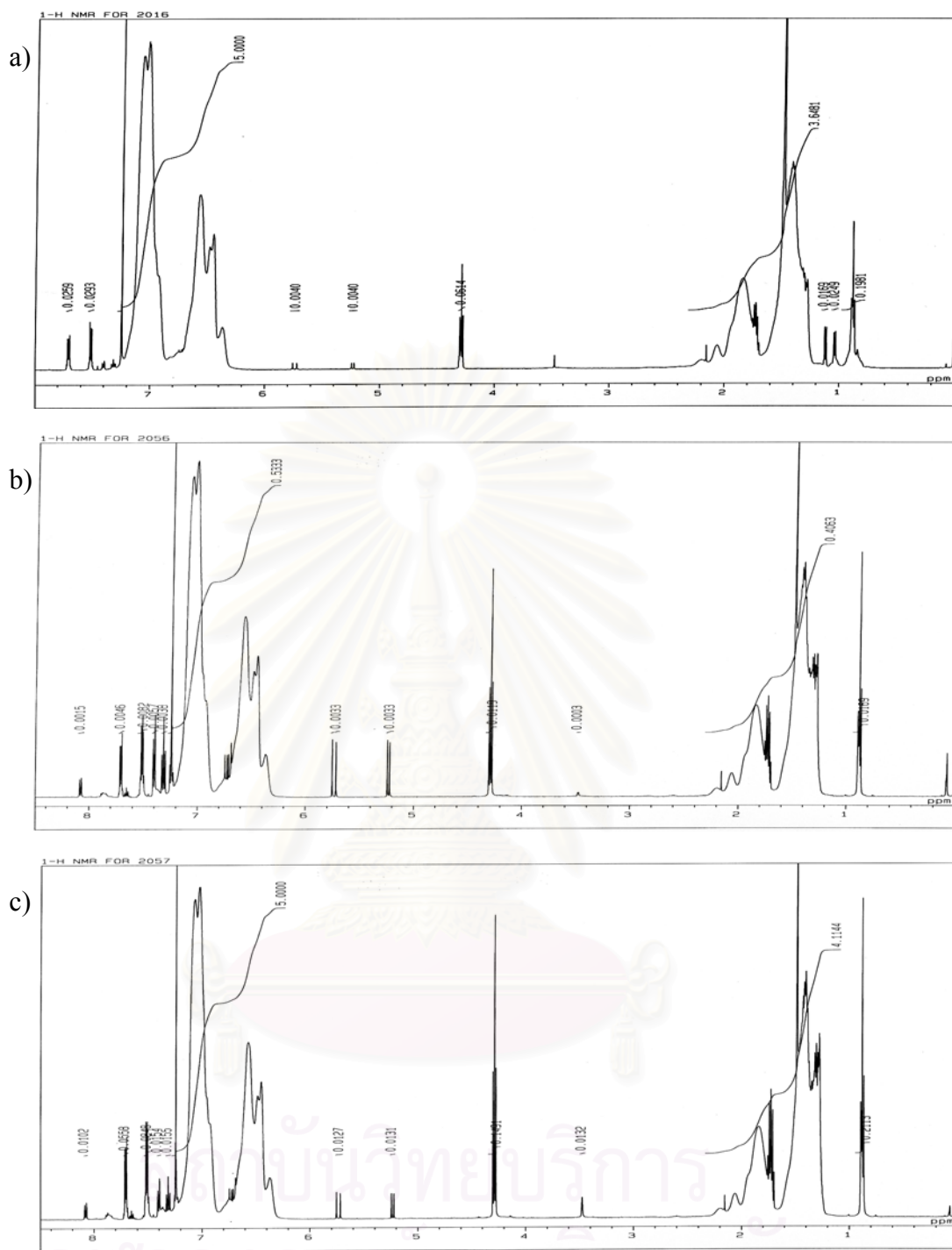


Figure 4.8 ^1H NMR spectra of polystyrene incorporated with DOP, a) 5 wt% (Run 2016); b) 10 wt% (Run 2056); and c) 15 wt% (Run 2057)

4.2 Effect of the Amount of DOP Plasticizer on Poly(styrene-*co*-MMA) Particles

The synthesis of copolymer poly(St-*co*-MMA) has been done using the SPG pore size of 1.42 μm . The ratios of DOP in the copolymer were varied from 5, 10, and 20% by weight of total monomer mixtures, as shown in Table 4.3. The preparative conditions of the continuous phase are shown in Table 4.4. Poly(St-*co*-MMA) particles were retained with a smooth surface and spherical shape when DOP 5 wt% was added as shown in Figures 4.9a to 4.9c. Increasing the amount of DOP to 10 wt% and 20 wt%, the particles had a tendency to be soft and stick with each other. The particles became collapsed and became a rubbery-like material when the 20 wt% of DOP was added. As shown in Figure 4.9b, each particle was stuck together or attached with the other particles, then form a discontinuous film with many voids.

Table 4.3 Polymerization recipe and results of the plasticized poly(St-*co*-MMA)

| Run No. | Composition | Monomer composition (wt%) | Monomer conversion (%) | D_p (μm) | CV_p (%) | $\overline{M}_n \times 10^{-4}$ | $\overline{M}_w \times 10^{-4}$ | PDI |
|---------|-----------------------|---------------------------|------------------------|-------------------------|------------|---------------------------------|---------------------------------|------|
| 103 | Styrene | 100 | 43.0 | na | na | < 0.01 | 1.8 | 18.0 |
| | DOP 5 wt% | | | | | | | |
| 104 | P(St- <i>co</i> -MMA) | 80/20 | 40.2 | 6.4 | 8.2 | < 0.06 | 3.1 | 50.6 |
| | DOP 25 wt% | | | | | | | |
| 105 | P(St- <i>co</i> -MMA) | 50/50 | 23.0 ^a | 5.8 | 16.1 | 1.7 | 7.5 | 8.6 |
| | DOP 5 wt% | | | | | | | |
| 106 | P(St- <i>co</i> -MMA) | 80/20 | 21.8 ^a | 10.0 | 17.7 | < 0.1 | 3.3 | 31.9 |
| | DOP 10 wt% | | | | | | | |

^a Initiator may partially decompose or recombine; na = not available

Table 4.4 A recipe of the continuous phase for the SPG emulsification with the SPG membrane pore size of 1.42 μm .

| Component | Weight (g) |
|--------------------------|-----------------|
| PVA-205 | 1.50 (0.68 wt%) |
| SLS | 0.05 (0.20 wt%) |
| Na_2SO_4 | 0.05 (0.20 wt%) |
| Hydroquinone | 0.0015 |
| Water | 230 |

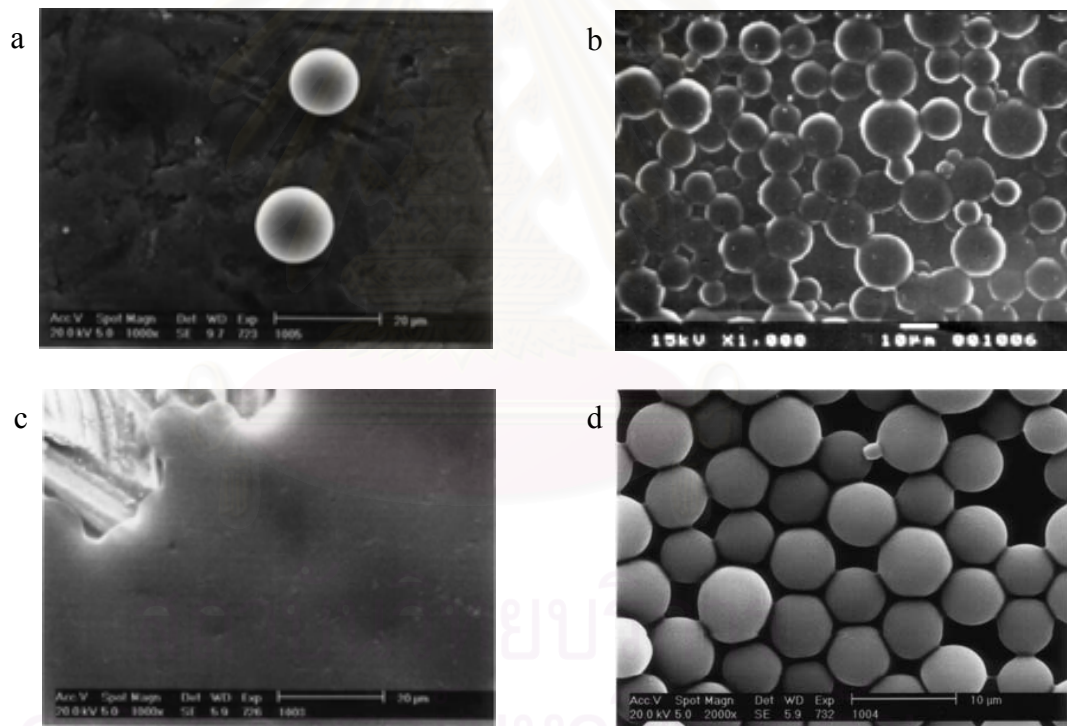


Figure 4.9 SEM photographs of the plasticized copolymers: a) polystyrene with DOP 5 wt%; b) polystyrene with DOP 10 wt%; c) polystyrene with DOP 20 wt%; and d) poly(St-co-MMA), St:MMA of 80:20 with 5 wt% of DOP.

4.3 Effect of DOP on Properties of Poly(St-*co*-MA) and Poly(MMA-*co*-MA) Particles

4.3.1 Particle Morphology

The DOP plasticizer of 5 % by weight of the total monomer was added to 16.0 g of monomer mixtures. Poly(St-*co*-MA) and poly(MMA-*co*-MA) particles were then synthesized with the recipes as shown in Tables 4.5 and 4.6. The SEM photographs for all copolymer particles obtained in each run are shown in Figure 4.10. The particles of poly(St-*co*-MA) remained spherical shape as shown in Figures 4.10a to 4.10d. In the absence of DOP, pin-holes on the particle surfaces were observed in Figure 4.10a for Run 2022. In addition, small flakes were attached to the particle surfaces in Figure 4.10b (Run 2023) when the amount of styrene monomer increased in the absence of DOP. With the addition of DOP, the polymer particles obtained have a spherical shape with a smooth surface. Poly(MMA-*co*-MA) was synthesized by the same experimental methods as for the poly(St-*co*-MA). A smooth and spherical particle surface was obtained from all recipes. However, the particles were soft and easily deformed when they were exposed to a strong electron beam from the SEM apparatus as shown in Figure 4.11. The poly(St-*co*-MA) particles are rather strong and rigid, because its vinyl backbone contains the bulky phenyl moiety as a substituent group for the hydrogen atom, while the poly(MMA-*co*-MA) particles are relatively flexible, with the less stiff and weaker aliphatic functional group. This difference in chain stiffness could be the reason for the polymer surface hardness and resistance to the high energy of irradiation. MMA monomer units are labile to the exposure of electron beam. Even solid PMMA spheres can be observed shrinking after a longer time of SEM observation.

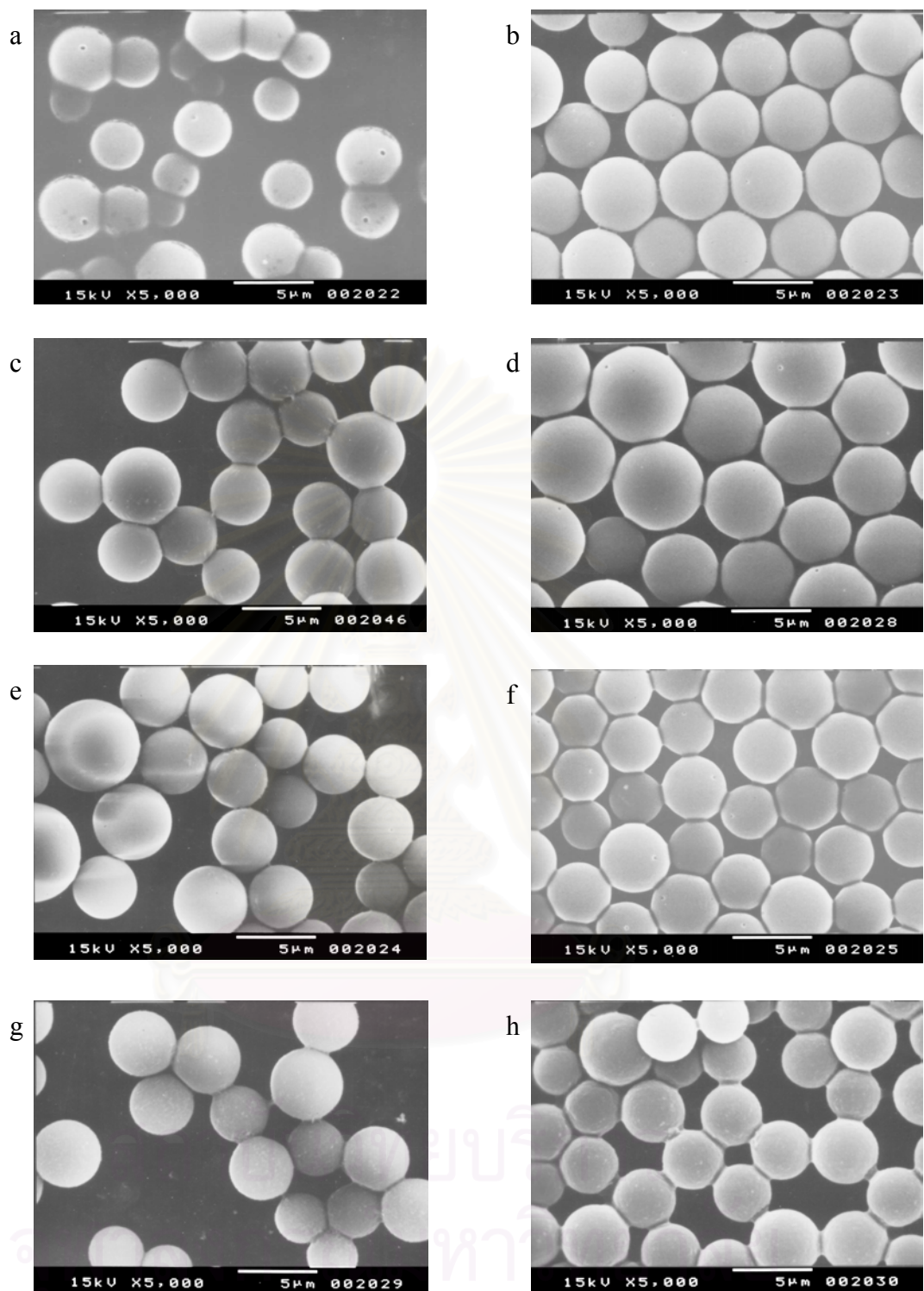


Figure 4.10 SEM photographs of poly(St-co-MA): a) St:MA, 50:50; b) St:MA, 75:25; c) St:MA, 52:48 with DOP; d) St:MA, 75:25 with DOP; e) St:MA:PSt, 37.5:50:12.5; f) St:MA:PSt, 62.5:25:12.5; g) St:MA:PSt, 37.5:50:12.5 with DOP; and h) St:MA:PSt, 62.5:25:12.5 with DOP.

Table 4.5 Recipe and results of styrene and methyl acrylate copolymerization

| Run No. | Composition | Monomer Composition (wt.%) | Monomer Conversion (%) | D _e (μm) | CV _e (%) | D _p (μm) | CV _p (%) | \bar{M}_n ×10 ⁻⁴ | \bar{M}_w ×10 ⁻⁴ | PDI | T _g (°C) clean | T _g (°C) unclean |
|-------------------|------------------------|----------------------------|------------------------|---------------------|---------------------|---------------------|---------------------|-------------------------------|-------------------------------|-----|---------------------------|-----------------------------|
| 2014 ^a | PSt/DOP | 100 | 76.5 | 6.3 | 15.2 | 5.9 | 11.2 | 1.7 | 3.9 | 2.3 | 12.7/77.4 ^c | 10.3/66.8 ^c |
| 2022 | P(St-co-MA) | 50/50 | 93.0 | 8.4 | 21.6 | 3.8 | 13.1 ^b | 2.0 | 4.4 | 2.2 | 23.2/65.4 ^c | 17.5/37.9 ^c |
| 2023 | P(St-co-MA) | 75/25 | 89.7 | 5.8 | 10.0 | 4.8 | 10.8 | 1.6 | 3.9 | 2.4 | 11.2/78.2 ^c | 11.0/47.5 ^c |
| 2046 | P(St-co-MA)/DOP | 52/48 | 17.4 | 6.5 | 15.3 | 5.8 | 16.5 | 0.4 | 1.6 | 4.5 | 21.1/55.1 ^c | 23.1 |
| 2028 | P(St-co-MA)/DOP | 75/25 | 52.2 | 7.1 | 16.1 | 5.9 | 19.7 | 1.6 | 3.6 | 2.3 | 24.9/58.3 ^c | 22.0/60.3 ^c |
| 2024 | P(St-co-MA)/PSt | 37.5/50/12.5 | 89.8 | 7.8 | 21.1 | 5.2 | 15.8 | 1.3 | 3.8 | 2.8 | 26.7/72.2 ^c | 25.4/50.4 ^c |
| 2025 | P(St-co-MA)/PSt | 62.5/25/12.5 | 69.6 | 6.1 | 10.4 | 4.4 | 14.3 | 1.5 | 3.2 | 2.2 | 31.7/53.9 ^c | 20.9/49.9 ^c |
| 2029 | [P(St-co-MA)/PSt]/ DOP | 37.5/50/12.5 | 38.9 | 7.0 | 16.1 | 5.0 | 18.3 | 1.2 | 3.2 | 2.8 | 22.2/50.1 ^c | 22.9/44.2 ^c |
| 2030 | [P(St-co-MA)/PSt]/ DOP | 62.5/25/12.5 | 67.5 | 5.9 | 10.1 | 4.1 | 13.8 | 1.5 | 3.9 | 2.6 | 15.0/51.7 ^c | 14.6/46.9 ^c |

^a SPG membrane pore size of 0.51 μm, otherwise 0.90 μm. ^b Coagulated particles were partially observed. ^c Two separated T_g values were observed.

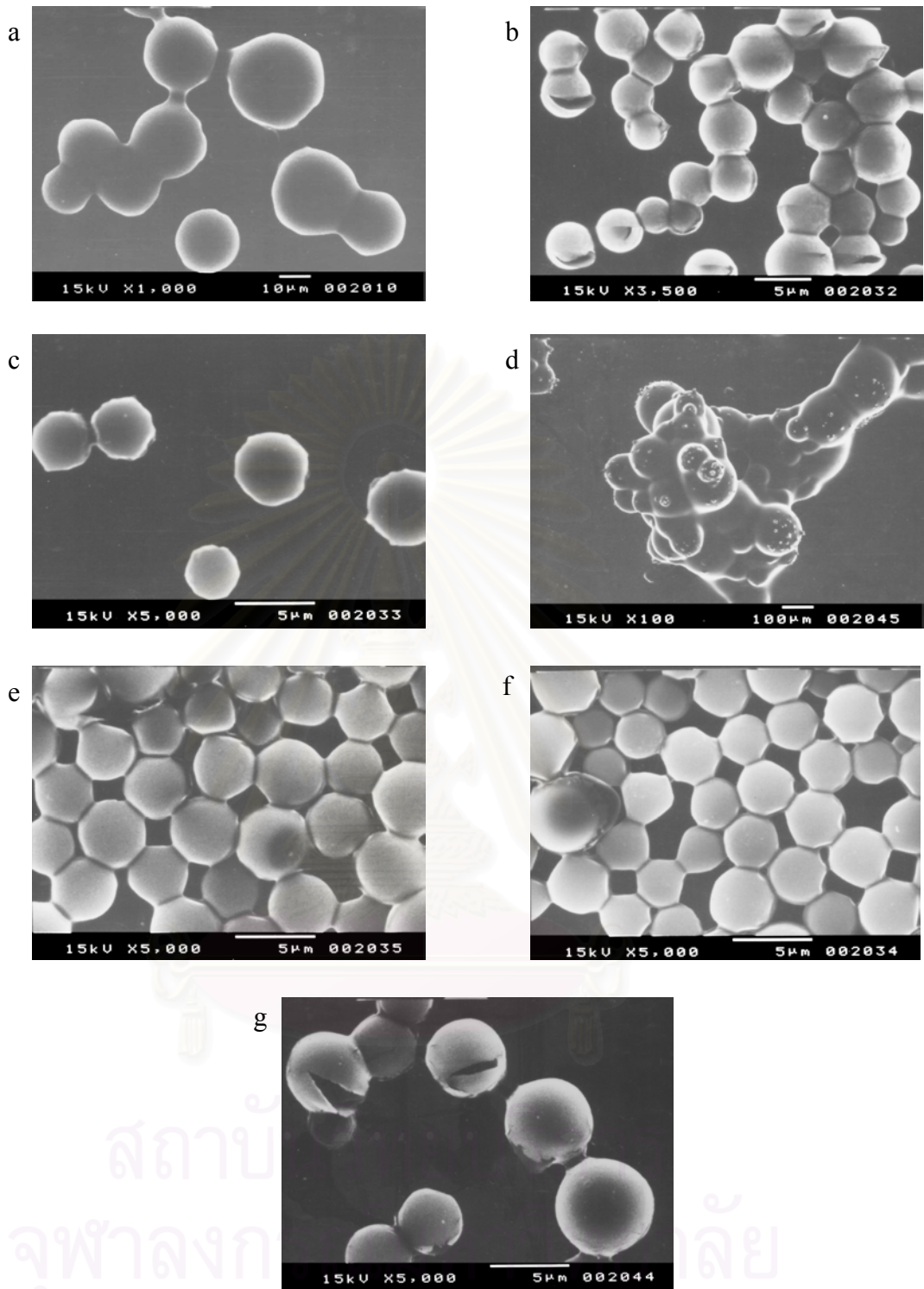


Figure 4.11 SEM photographs of poly(MMA-*co*-MA): a) PMMA-DOP, b) MMA:MA, 75:25; c) MMA:MA, 50:50; d) MMA:MA, 25:75; e) MMA:MA, 50:50 DOP 5 wt%; f) MMA:MA, 75:25 DOP 5 wt%; and g) MMA:MA, 75:25 DOP 10 wt%.

Table 4.6 Recipe and results of methyl methacrylate and methyl acrylate copolymerization

| Run No. | Composition | Monomer Composition (wt.%) | Monomer Conversion (%) | D_e (μm) | CV_e (%) | D_p (μm) | CV_p (%) | $\bar{M}_n \times 10^{-4}$ | $\bar{M}_w \times 10^{-4}$ | PDI | T_g ($^{\circ}\text{C}$) clean | T_g ($^{\circ}\text{C}$) unclean |
|---------|-----------------------------|----------------------------|------------------------|-------------------------|------------|-------------------------|-------------------|----------------------------|----------------------------|-------------------|------------------------------------|--------------------------------------|
| 2010 | PMMA/DOP | 100 | 85.6 | 6.9 | 25.9 | Coag ^a | Coag ^a | 3.7 | 13.0 | 3.5 | 14.0 | 14.0 |
| 2032 | P(MMA-co-MA) | 75/25 | 68.1 | 4.5 | 22.7 | 5.5 | 18.8 | 2.3 | 10.2 | 4.5 | 27.9 | 29.2 |
| 2033 | P(MMA-co-MA) | 50/50 | 73.7 | 7.0 | 39.7 | 5.4 | 26.6 | 3.9 | 62.6 | 16.0 ^b | 25.9 | 29.4 |
| 2045 | P(MMA-co-MA) | 25/75 | 19.4 | 5.9 | 52.5 | 4.5 | 20.6 ^a | 6.4 | 47.4 | 7.4 | 28.0 | 27.9 |
| | | | coagulum | | | | | | | | | |
| 2035 | P(MMA-co-MA)/ DOP 5 wt% | 50/50 | 79.9 | 5.6 | 22.8 | 5.4 | 14.5 ^a | 4.0 | 52.3 | 13.2 ^b | 29.5 | 25.3 |
| 2034 | P(MMA-co-MA)/ DOP 5 wt% | 75/25 | 57.1 | 4.6 | 13.6 | 4.7 | 18.7 | 3.3 | 22.1 | 6.7 | 38.0 | 29.2 |
| 2044 | P(MMA-co-MA)/ DOP 10 wt% | 75/25 | 66.7 | 5.3 | 14.4 | 5.2 | 12.1 | 3.2 | 20.2 | 6.3 | 42.5 | 21.9 |

^a Coagulated particles were partially observed. ^b Bimodal curve

DOP concentration of 5 wt% was based on the monomer concentration.

4.3.2 Glass Transition Temperature

The secondary (higher) T_g value of the unclean poly(St-co-MA) particles was found to be lower than that of the clean polymer as shown in Table 4.5. The glass transition temperature of polymers is of course affected by the addition of DOP plasticizer (5 wt% and 10 wt% of monomer). In general, DOP resides physically inside the polymer chains and reduces the repulsion force between intermolecular chains. It can thus ease the motion of the rigid chains of styrene-MA copolymer. In comparison, some portions of DOP in the polymer latex cleaned by methanol were washed out from the particles during the treatment. The secondary T_g of the clean polymer particles was thus higher than that of the unclean latex, which was close to T_g of the neat polystyrene. Besides the removal by methanol cleaning, migration of the DOP plasticizer to the particle surface according to its general nature may assist in the removal during the cleaning. On the other hand, the primary (lower) T_g values were located close to the T_g of the PMA, depending on MA monomer content in the copolymer. The different increments in T_{g1} (the lower T_g) and T_{g2} (the higher T_g) values depended greatly on the sample preparation methods and the incorporated amount of DOP. The difference between T_{g1} and T_{g2} of the clean particles was larger than that of the unclean particles. In addition, the T_{g1} and T_{g2} of the DOP plasticized polymer particles were found narrower than those of particles without DOP.

Table 4.7 Monomer reactivity ratios for free-radical copolymerization at 60°C [109]

| M_1 | r_1 | M_2 | r_2 | r_1r_2 | Remarks |
|---------------------|-------|---------------------|-------|----------|---------|
| Styrene | 0.84 | Butyl acrylate | 0.18 | 0.151 | |
| Styrene | 0.192 | Methyl acrylate | 0.80 | 0.154 | |
| Styrene | 0.56 | Butyl methacrylate | 0.31 | 0.174 | a |
| Styrene | 0.52 | Butyl methacrylate | 0.47 | 0.244 | b |
| Styrene | 0.74 | Butyl methacrylate | 0.59 | 0.437 | c |
| Styrene | 0.49 | Methyl methacrylate | 0.418 | 0.205 | |
| Methyl methacrylate | 2.15 | Methyl acrylate | 0.40 | 0.86 | |

a, b, and c referred to different calculation methods [109]

Table 4.7 shows the reactivity ratios of the co-monomers using in the present research. Figure 4.12 shows the composition drift of St in the copolymer of poly(St-co-MA). The calculation was carried out based on the terminal model (Eq. 2.12) and the bulk copolymerization. A possible partition of MA in the aqueous phase was not taken in consideration. The reactivity ratios of the two monomers, r_1 (St) = 0.192 and r_2 (MA) = 0.80 [109] indicate that MA is consumed faster than St as shown in Figure 4.12a. The reaction mixture is short of MA, i.e., the polymer propagation chains are rich in MA units at the beginning in Figure 4.12b, and the subsequently growing chains are terminated by the St monomer units when approaching a complete conversion. The composition drift of styrene was more pronounced at the higher styrene concentrations. Based on $r_1r_2 \approx 0.15$, this copolymer lies between the two extremes of ideal and alternating copolymerization. As the r_1r_2 product decreases from unity (1 for an ideal copolymerization; $0 < r_1r_2 < 1$) toward zero [110], there is an increasing tendency towards alternation. However, the whole copolymer is still of a random type. Copolymer composition drift could determine the extent of T_g value in 50:50 wt% of poly(St-co-MA) as shown in Table 4.5.

In the case of poly(MMA-*co*-MA), a single T_g value with a sharp transition was observed for all copolymer compositions as shown in Figure 4.13. The T_g value was close to room temperature. T_g values of the copolymers with and without DOP were observed in the same range, as shown in Table 4.6. Likewise, the T_g value is also controlled by the composition drift in the copolymer. Moreover, a much larger compositional drift in the copolymer is also found in the case of MMA-MA system. The reactivity ratios of MMA (r_1) and MA (r_2) are 2.150 and 0.400 [109,110], as shown in Table 4.7 and Figure 4.13. Based on the $r_1 r_2$ product of 0.86 (approaching 1), poly(MMA-*co*-MA) is an ideal (random) type of copolymer. Since the MMA reactivity ratio is greater than unity, the copolymer contains a larger proportion of MMA as shown in Figure 4.13a. The very high value of r_1 produces the MMA-rich chains at the beginning of the copolymerization in Figure 4.13b, which causes MMA starving in the reaction mixture. At the end of the copolymerization, MA units are thus preferentially consumed, depending on the reaction time. Since the difference in reactivity of the two monomers is very high, it becomes more difficult to produce copolymers having appreciable amounts of the less reactive monomer, unless the copolymerization approaches the end of conversion. Composition drift in the copolymer is thus another factor that controls the glass transition temperature of the copolymer.

In comparison with poly(St-*co*-MA), poly(MMA-*co*-MA) copolymers achieved better compatibility than the St-MA copolymers. This could result from the similar chemical structure of DOP and acrylate monomer. In other words, the DOP mixes more homogeneously in the matrix of poly(MMA-*co*-MA) than it does in the matrix of poly(St-*co*-MA), according to the DSC thermograph shown in Figure 4.14.

However, other factors influencing T_g may be the surfactant and stabilizer in the polymer latex [111], since the PVA and SLS can be physically adsorbed to the polymer surface. If possible, it might be necessary to separate the particles from their serum before proceeding to the subsequent processes. The heating rate during the DSC scanning is also undoubtedly one of the factors that governed the T_g value.



สถาบันวิทยบริการ
จุฬาลงกรณ์มหาวิทยาลัย

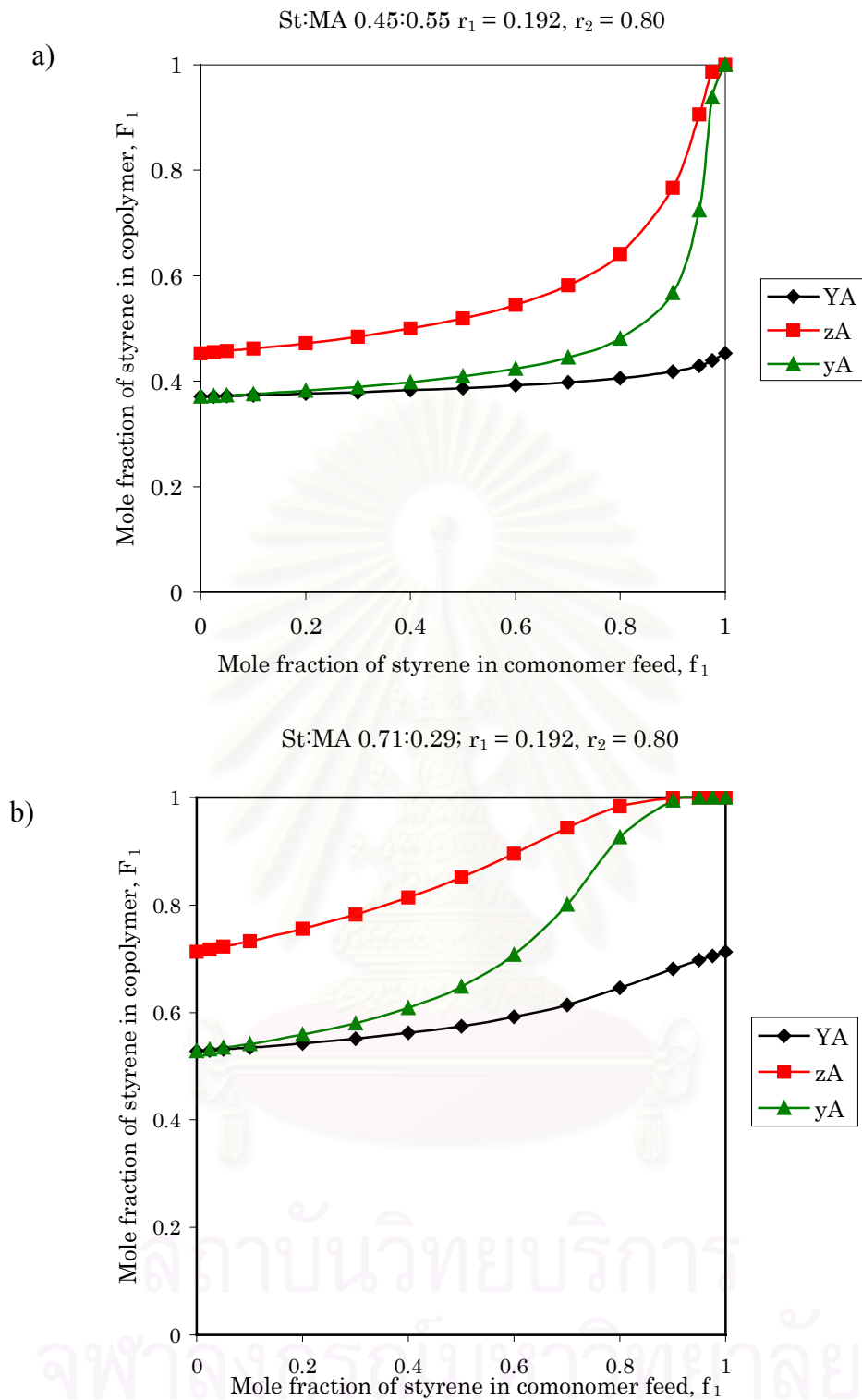


Figure 4.12 Composition drift of poly(St-co-MA), St:MA: a) 50:50 wt%; b) 75:25 wt%, **YA** = cumulative composition of styrene in copolymer.
yA = composition of styrene in unreacted monomer.
zA = instantaneous composition of styrene in copolymer.

MMA:MA 0.46:0.54; $r_1 = 2.15$, $r_2 = 0.40$

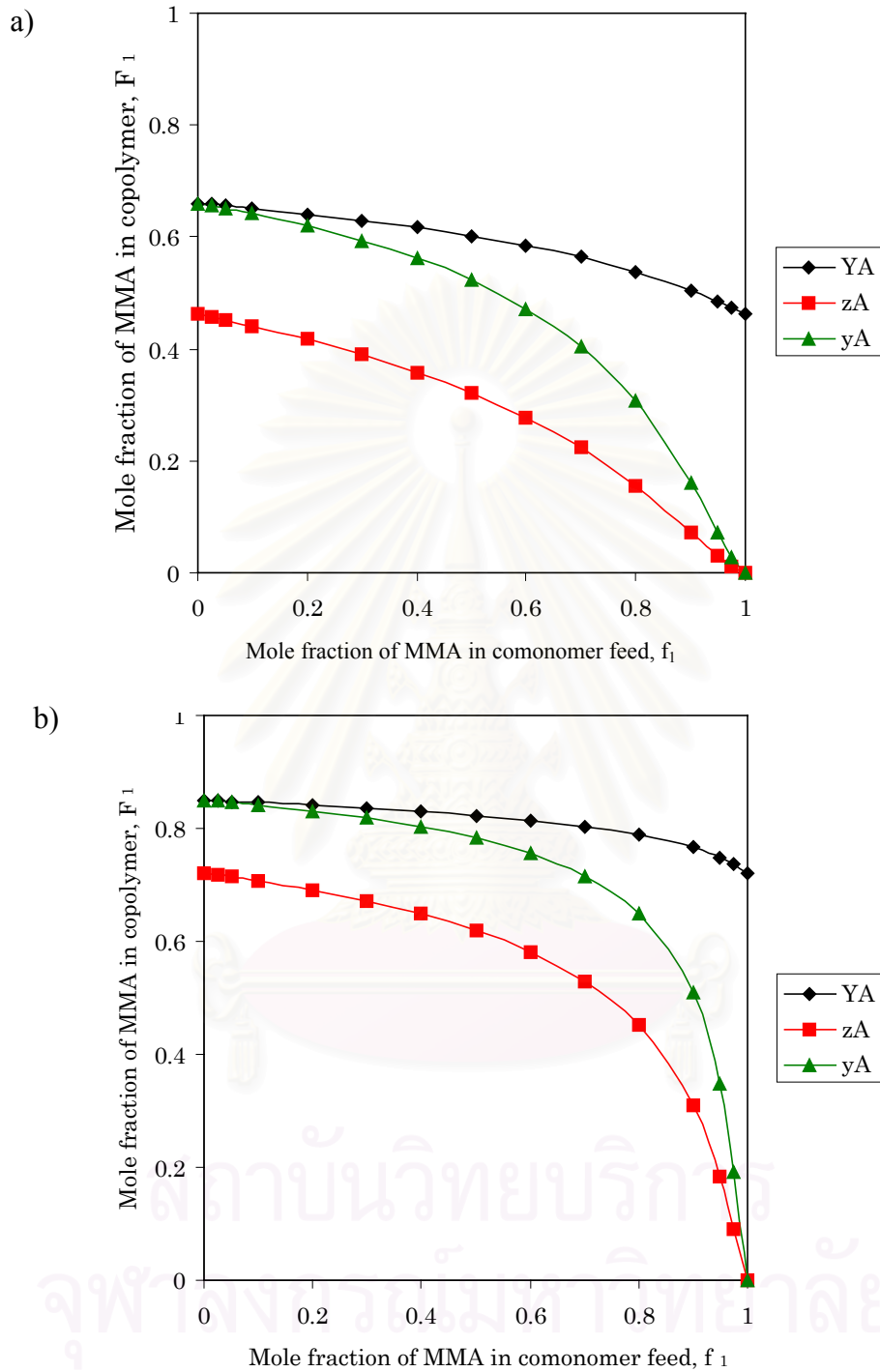


Figure 4.13 Composition drift of poly(MMA-co-MA), MMA:MA: a) 50:50 wt%; b)

75:25 wt%, YA = cumulative composition of MMA in copolymer.

yA = composition of MMA in unreacted monomer.

zA = instantaneous composition of MMA in copolymer

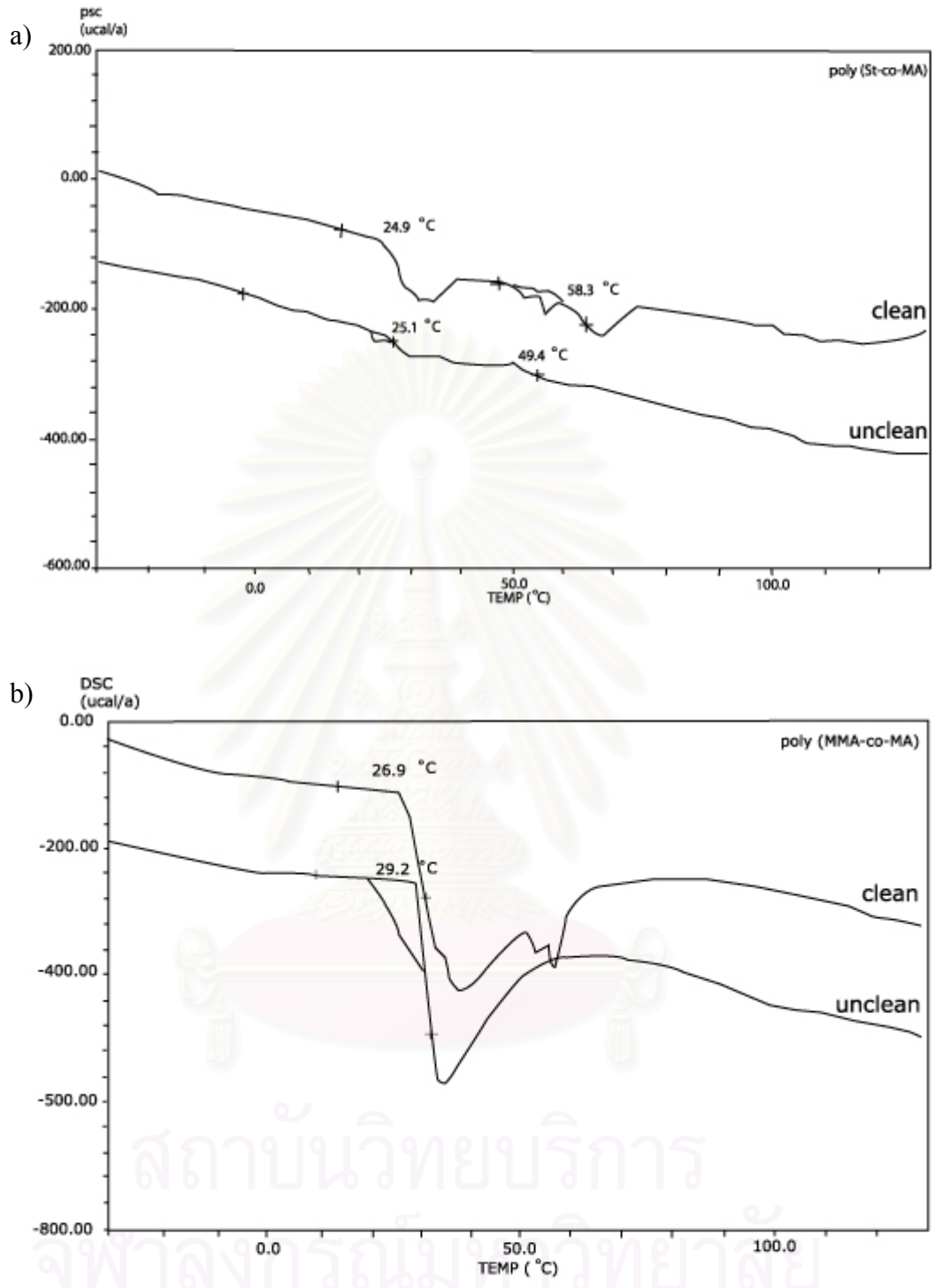


Figure 4.14 DSC thermograms of a) poly(St-co-MA), and b) poly(MMA-co-MA), with 5 wt% of DOP (based on the monomer concentrations) for all experiments.

4.3.3 Effect of the Monomer Composition on Glass Transition

Temperature

The relationship between the copolymer composition and T_g of polymer was studied with the variation of monomer composition. In theory, T_g value of copolymer was affected by the method of sample preparation and measurement method. The measurement was carried out for estimation of the copolymer's T_g using Fox's equation (Eq. 2.20). The sample for the T_g measurement was prepared by two methods. First, the polymer latex was prepared by direct drying of the polymer latex in a vacuum oven for 5 days without cleaning. Second, the polymer latex was repeatedly washed by methanol and dried in the vacuum oven for 2 days. The glass transition temperatures of these two samples as prepared should be in a range between the T_g 's values of PSt and PMA homopolymer. As shown in Figure 4.14, the two separate T_g values were found in both preparation techniques.

The difference of T_{g1} (lower T_g) and T_{g2} (higher T_g) values were also found depending on the sample preparation and the incorporated portion of DOP. The T_{g1} and T_{g2} of the clean particles were greater than those of unclean particles. In addition, the T_{g1} and T_{g2} of the incorporated DOP particles were narrower than the particles without DOP. However, the experimental T_{g2} was close to the calculated value of T_g , while T_{g1} was found lower. However, the other factors affecting T_g value may include the effect of surfactant and stabilizer in polymer latex. Since PVA and SLS can physically attach on the polymer surface. In addition, it might be necessary to separate the particles from their serum.

The lower T_g of the copolymer measured from the dried polymer latex was found slightly lower than those of the clean polymer latex in all compositions. However, the more difference in T_g values was revealed in the higher

T_g , and since, the clean particles represent the secondary T_g (higher T_g) in comparison with the single T_g of unclean particles except the ratio of styrene monomer at 75 wt%. The separate T_g values were found in both preparation methods. Meanwhile, DOP was homogeneously trapped inside the polymer particles. It can ease the rigid chain of styrene-MA copolymer to enforce vibration. In contrast, when the polymer latex was cleaned with methanol, DOP was washed out from the particles during treatment. On the other hand, the copolymer sample was used repeatedly as a secondary measurement, the DOP may also have evaporated or decomposed from the polymer particles. The T_g values were obtained at the higher value in comparison with the untreated particles at the first measurement.

As expected, it was found that poly(St-co-MA) without DOP had T_g values higher than the copolymer with DOP as shown in Figure 4.15b. The secondary T_g value was revealed in the sample prepared by the same drying method for all recipes. All T_g values were also far from the T_g values of plasticized particles.

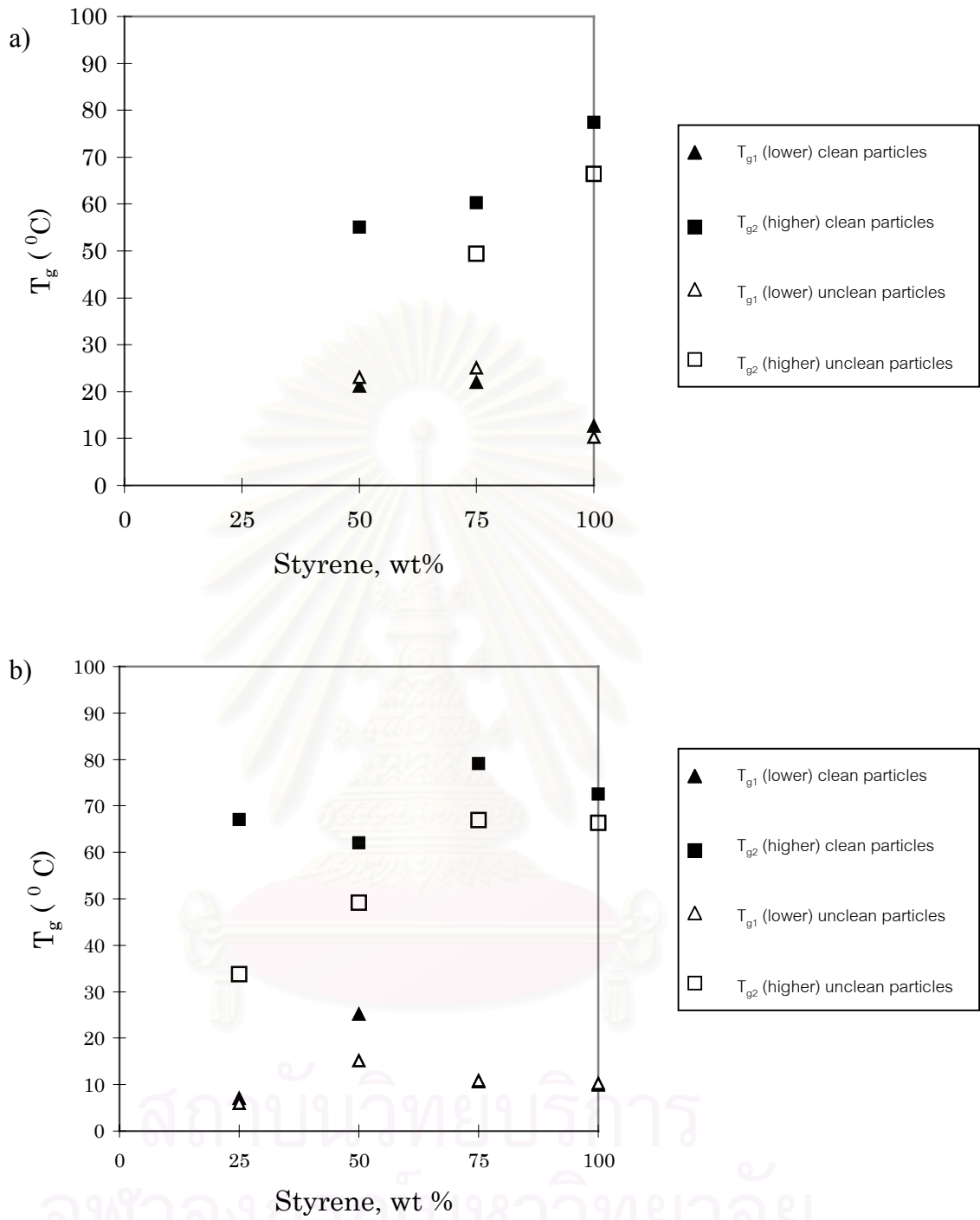


Figure 4.15 Relationship between T_g and styrene contents with different treatments:

a) Poly(St-co-MA) with DOP, and b) without DOP.

4.3.4 Effect of Monomer Composition on Molecular Weight of Polymer

The effect of monomer composition is shown in Figure 4.16. It can be observed that, in all cases, the different compositions led to a similar molecular weight. The effect of adding polystyrene (12.5 wt% of monomer) into various monomer compositions on molecular weight can be observed in Figure 4.17. The average molecular weight was decreased with the higher MA contents. On the other hand, it can be seen that the molecular weight was slightly increased with increasing the St-PSt concentration. The behavior could be explained as follows: as a consequence of the higher concentration of polystyrene, the average number of radicals per polymer particle was reduced; hence, the length of chain growth is somewhat reduced. Thus, the molecular weights were also reduced. As \overline{M}_n of PSt of 4200 and \overline{M}_w of 40000, the simple mixing with the low molecular weight PSt will result in the polymers of lower molecular weight.

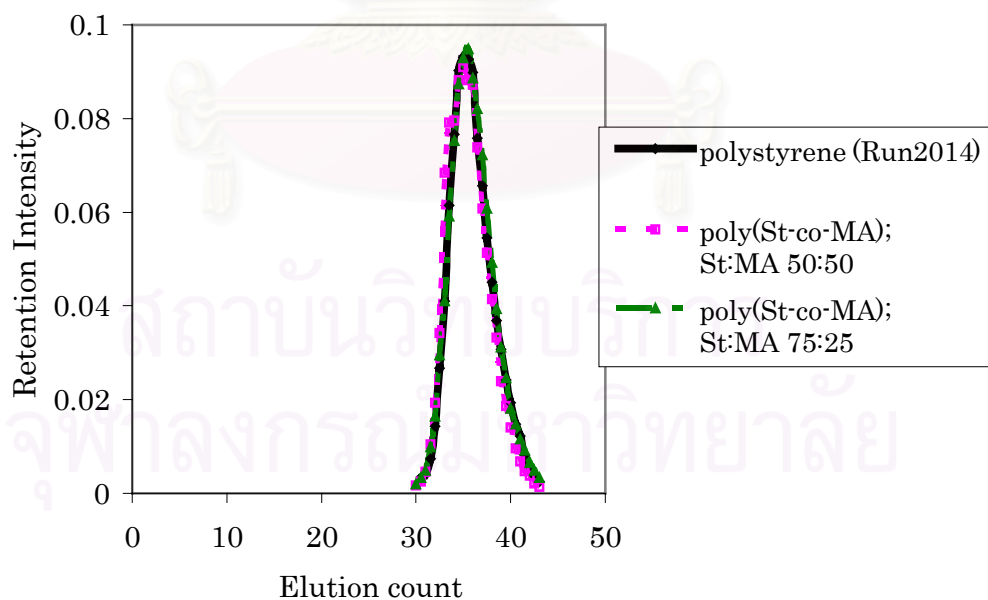


Figure 4.16 Normalized GPC chromatograms of poly(St-co-MA) particles showing the effects of monomer compositions.

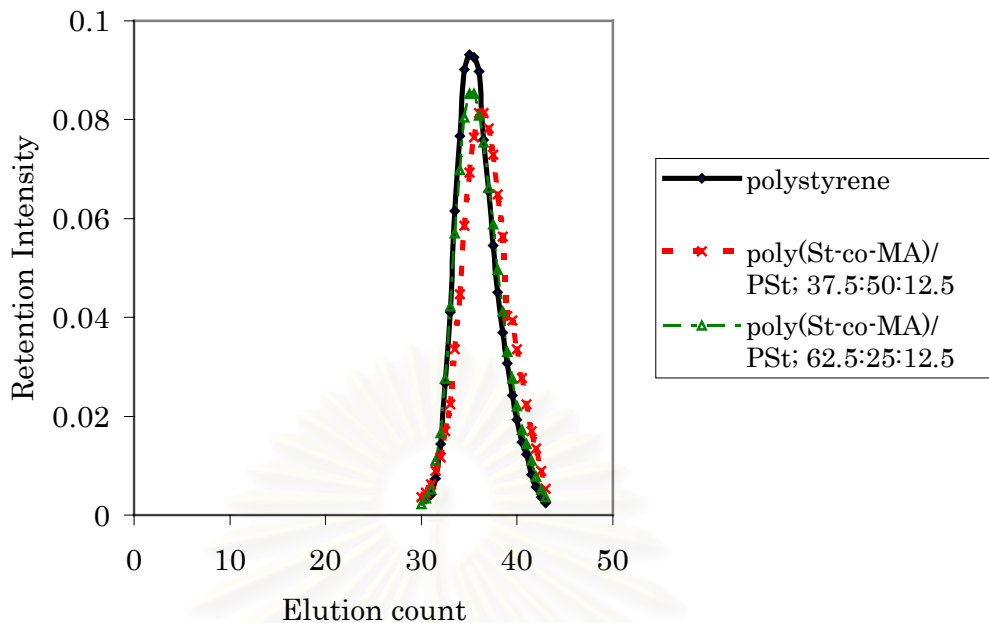


Figure 4.17 Normalized GPC chromatograms of poly(St-co-MA)/PSt particles showing the effects of monomer compositions.

4.3.5 Internal Morphology of Poly(St-co-MA)

The microtomed and stained polymer particles (Runs 2018 and 2019) reveal their internal morphology as shown in Figure 4.18. The particles were stained by RuO₄ vapor (Runs 2018 and 2019) to ensure an adequate contrast between PSt and PMA phases. The internal particle morphology was observed in various monomer compositions. The TEM photographs of poly(St-co-MA) with St:MA of 50:50 and 75:25 are shown in Figures 4.18a and 4.18b. On viewing inside of the particles, the minute white granules rich in MA were revealed. The granules were not found at the outermost submicron thickness or at the circumference of the particle. When a higher concentration of styrene was incorporated, the larger sizes of the minute white granules were produced as shown in Figure 4.18b.

When the droplets are formed, there is a time lapse before the subsequent suspension polymerization to take place. We observed separation of some droplets and suspend or disperse inside the large drops. Since the MA reactivity ratio is greater than that of styrene, MA monomers were consumed faster at the beginning of the polymerization to form MA rich copolymers which later grows to the small domains. The styrene-rich phase was subsequently produced which became later the matrix for the MA domains. The TEM photographs also suggested that some diffusion of MA-rich domains into the styrene-rich polymer matrix probably took place.

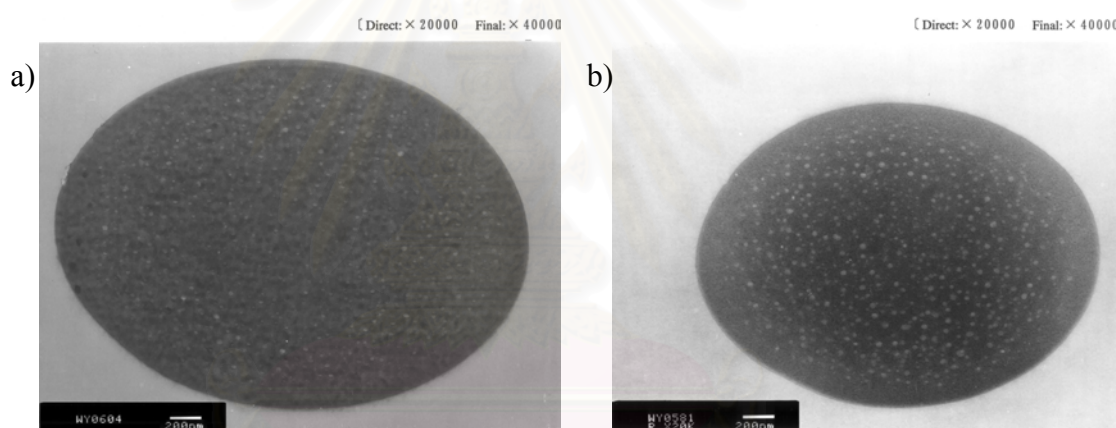


Figure 4.18 Microtomed and RuO₄-stained TEM photographs of poly(St-co-MA) particles: a) St:MA, 50:50 (Run 2018); and b) St:MA, 75:25 (Run 2019)

4.3.6 Poly(St-co-MA)/PSt Composite

In order to investigate the effect of the inert polymer chains dissolved in the monomer phase to the final particle morphology, polystyrene ($\overline{M}_n = 4200$, $\overline{M}_w = 40000$, and $\overline{M}_w/\overline{M}_n = 9.54$) was dissolved in the oil phase or the mixture of styrene and MA monomers, and the polymerization was then carried out as previously. The formulation along with the result for each run is shown in Table 4.5.

The poly(*St-co-MA*) particles were stained by osmium tetroxide (OsO_4) vapor. In 1966, Kato [112] discovered that OsO_4 was a powerful staining agent for polymer containing double bonds, such as various diene polymers. The staining is brought about by the high concentration of electrons in the osmium atom. Additionally, OsO_4 hardens diene elastomers and other polymers through a crosslinking reaction as shown in Figure 4.19.

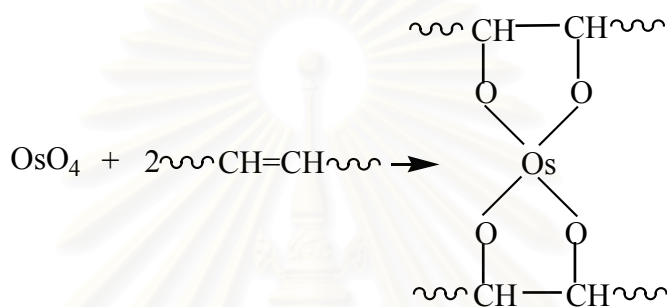


Figure 4.19 Demonstration of crosslinking reaction of polymer chains and OsO_4 [103]

Acrylic phase can also be stained with OsO_4 . For example, Schulze et al. [113] stained polymethacrylates in the presence of polyethylene (PE) to study the morphology of a number of materials. PSt has only aromatic double bonds and thus will not be stained with OsO_4 , but polyalkyl (meth)acrylate should have regular aliphatic double bonds so it could be stained easily with OsO_4 [114]. However, Vitali and Montani [115] pointed out that the low diffusion of OsO_4 often results in a poor contrast between the phases leading to the less precise determinations.

For poly(*St-co-MA*)/PSt particles, they show the normally obtained internal morphology. The darkly-stained granules were rich in PMA and grew inside because of the MA reactivity ratio is greater than that of styrene, MA monomers were

consumed faster at the beginning of the polymerization to form the small domains. The styrene-rich phase was subsequently produced, which became later the matrix for the MA domains. The compatibility between PSt and the newly-formed poly(St-co-MA) became less favorable due to the decreased fraction of styrene in the copolymer chains as shown in Figure 4.20a. Then, 5 wt% DOP based on monomer was added when the proportion of St:PSt is higher in Run 2025. It was found that the PSt contents were less compatible with PMA and provided a core-shell type, the phase separated domains of PMA remained in particles as shown in Figure 4.20c. One can see that the thin shell of PSt-hard phase is able to cover the soft phase of particles almost completely. The preferential staining leads to differences in contrast indicated by the dark-tiny granules of MA rich region in the inner part of the particles. The addition of DOP plasticizer, leads to difference in contrast of the dark gray-PMA and light gray-PSt (the lower contrast). Besides, the thin shell of hard-PSt was observed as shown in Figures 4.20b and 4.20d. Comparison with the copolymer of poly(St-co-MA) without the addition of PSt indicated the different types of morphology. As shown in Figures 4.21a to 4.21c, the core-shell type morphology was observed although the shell is difficult to recognize. Since the MA reactivity ratio is greater than that of styrene, MA monomer domains were generated faster at the beginning of the polymerization. Then, the styrene-rich phase was subsequently formed, which covered the MA-rich domains. For the St:MA ratio of 75:25, the phase separation is more obvious as shown in Figure 4.21b. DOP is in a limited extent compatible with St-rich or PSt phase and promotes those hydrophobic domains migrating to the surface (core/shell promotion). The addition of DOP revealed the more compatibility between the hard-St and soft-MA, the dark gray and light gray regions were observed. This implies that the addition of DOP may play a role of compatibilizer, and promote

the occurrence of phase behavior in polymer blends (Besides without the use of DOP as shown in Figures 4.18a and 4.18b, the salami-like morphologies were favored). It should be noted that, the sample Runs 2018 and 2022, and Runs 2019 and 2023, were synthesized by the same monomer component. The distilled St monomer was used in Runs 2022 and 2023 instead of the commercial St monomer without further treatment in Runs 2018 and 2019. It should be mentioned that all the surfaces of dried particles are smooth with tiny dimples as shown in Figure 4.10a (SEM photographs).

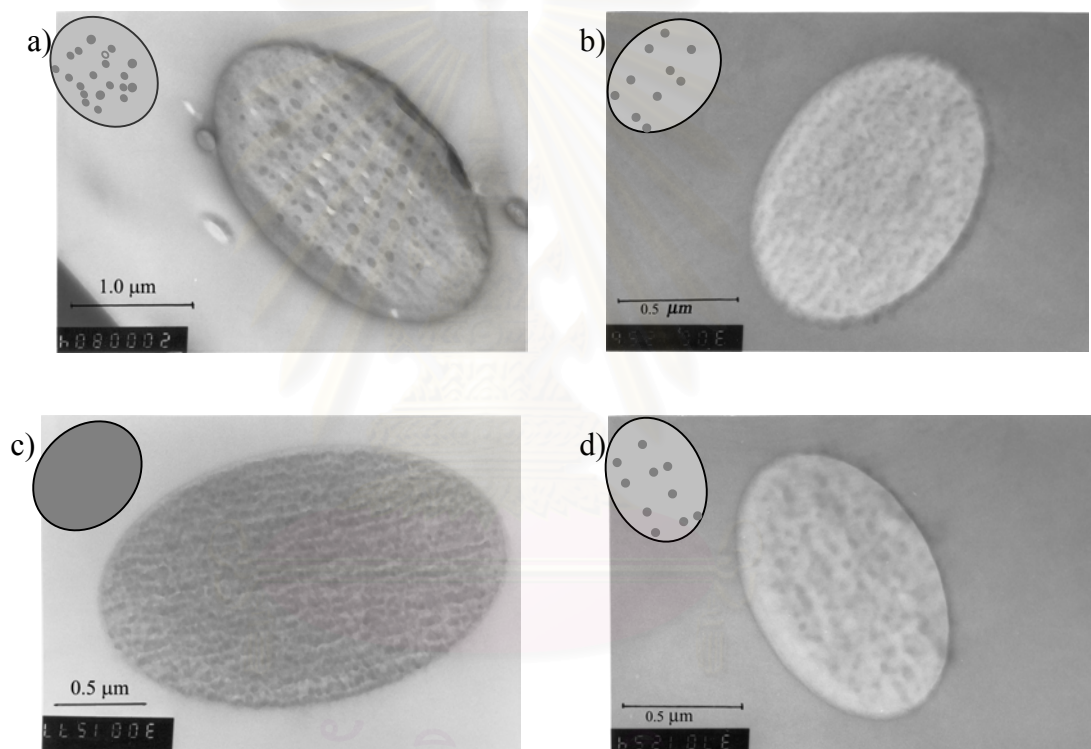


Figure 4.20 Microtomed and OsO₄-stained TEM photographs of poly(St-*co*-MA)/PSt composite polymer particles: a) St:MA:PSt, 37.5:50:12.5 without DOP (Run 2024); b) St:MA:PSt, 37.5:50:12.5 with DOP (Run 2029); c) St:MA:PSt, 62.5:25:12.5 without DOP (Run 2025); and d) St:MA:PSt, 62.5:25:12.5 with DOP (Run 2030)

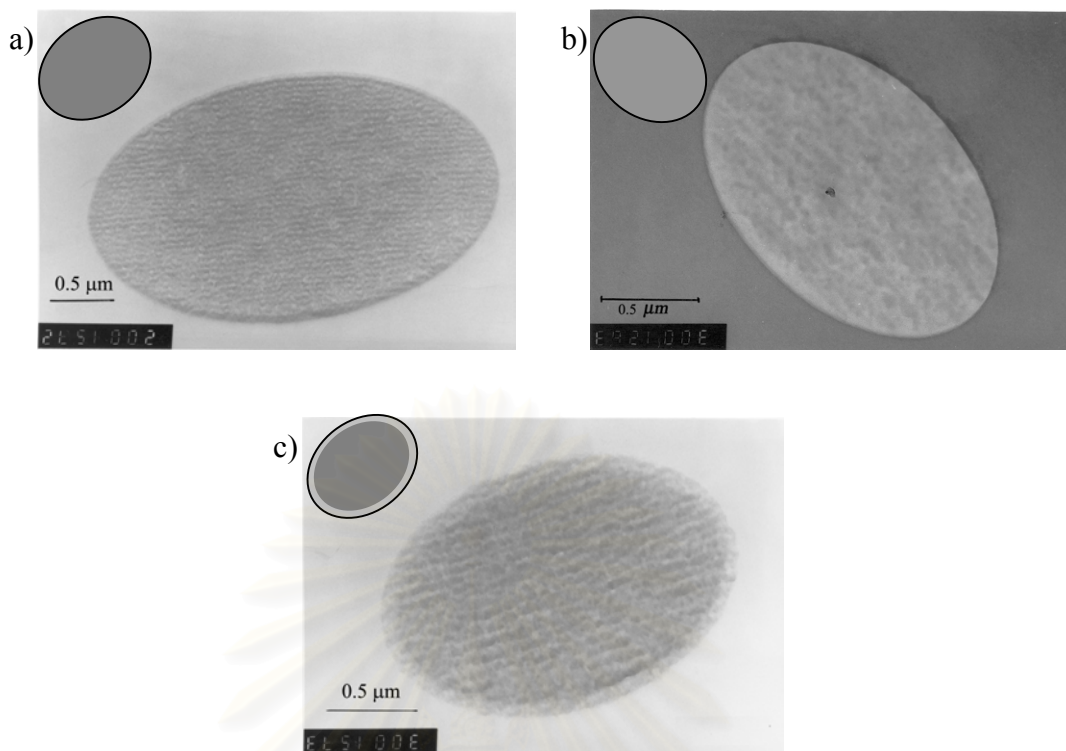


Figure 4.21 Microtomed and OsO₄-stained TEM photographs of poly(St-co-MA) copolymer particles: a) St:MA, 50:50 without DOP (Run 2022); b) St:MA, 50:50 with DOP (Run 2046); and c) St:MA, 75:25 without DOP (Run 2023).

4.3.7 Copolymer Composition by ¹H NMR

To predict the copolymer composition of poly(St-co-MA), the fraction of St:MA was calculated using the peak area of $-C_6H_5$ pendant group (styrene) at the chemical shift (δ) from 6.3 to 7.6 ppm and the peak area of $-OCH_3$ pendant group (MA) at the δ from 3.0 to 3.75 ppm. Based on the ¹H NMR spectra of the St-MA copolymers, the chemical shifts from the methine protons of the styrene units in the copolymers were observed in the region of 3.0 to 3.8 ppm, and the chemical shifts resulting from the methylene group in these copolymers are observed in the region 1.0 to 2.4 ppm. Equation 4.3 was used to calculate the molar fraction of styrene (F_{St}):

$$\text{Styrene (wt\% in copolymer)} = \frac{A_{\delta=7.6}(-\text{C}_6\text{H}_5)/5}{A_{\delta=7.6}(-\text{C}_6\text{H}_5)/5 + A_{\delta=3.0-3.751}(-\text{OCH}_3)/3} \quad (4.3)$$

where A represents the integrated area of the peak of the proton, which was calculated automatically by the apparatus. The ^1H NMR spectrum shows that the peaks used for the assignment were isolated from each other. Upon the addition of DOP, the $-\text{CH}-$ protons of the cyclic phthalic unit appeared as a set of two separate signals of the triplet at the δ from 7.2 to 7.8 ppm as shown in Figure 4.21 and Table 4.8.

Table 4.8 Calculated and experimental compositions in radical copolymerization of St and MA

| Run No. | Feed composition of St/MA (mol%) | Styrene in copolymer (mol%) calculated from Eq. 4.3 |
|---------|----------------------------------|--|
| 2022 | 45.3:54.7 | 66.0 |
| 2023 | 71.3:28.7 | 88.2 |

สถาบันวิทยบริการ
จุฬาลงกรณ์มหาวิทยาลัย

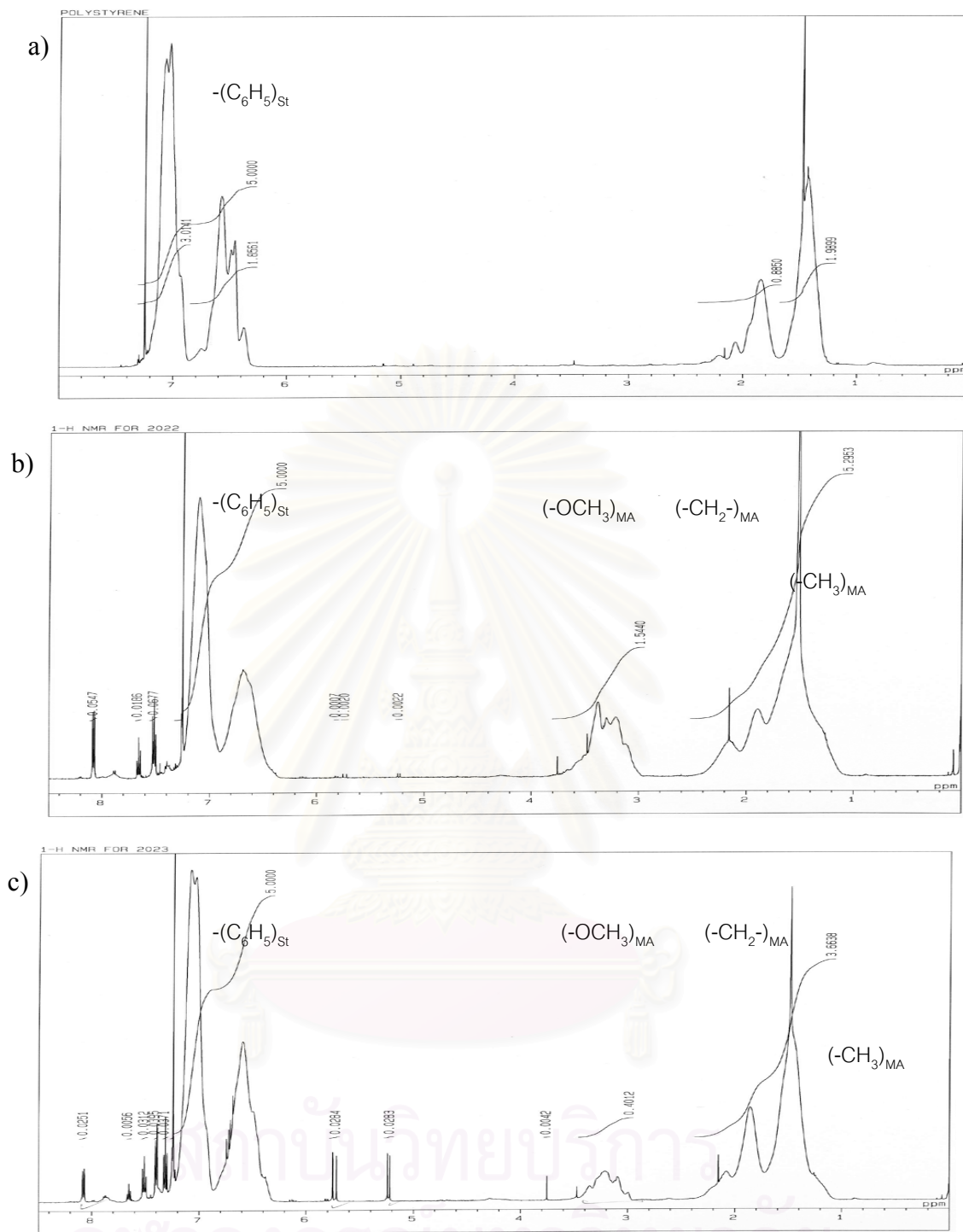


Figure 4.22 Typical 1H NMR spectra of St/MA copolymer in $CDCl_3$ at $40^\circ C$:
 a) polystyrene; b) poly(St-co-MA), St:MA of 50:50; and c) poly(St-co-MA), St:MA of 75:25

4.4 Synthesis of Poly(Styrene-*co*-BMA)

4.4.1 Effect of Initiator Type on Molecular Weight and Molecular Weight Distribution

When an oil soluble initiator such as ADVN was added in the dispersion phase, its minute solubility in the aqueous phase was anticipated. After the monomer droplets had been suspended in the continuous phase, the trace amount of monomer might possibly be partitioned in the aqueous phase. Inhibitor is present in the aqueous phase, which prevents the polymeric radicals to grow longer. Polymerization of the monomer in the run using ADVN could take place in the continuous phase to yield very low molecular weight and results in broad distribution polymers. The molecular weight and MWD of both initiators (ADVN and BPO) are shown in Figure 4.23. One can compare the resulting molecular weights and distributions with those polymerized in the run using BPO, a highly oil soluble initiator (Run 2058).

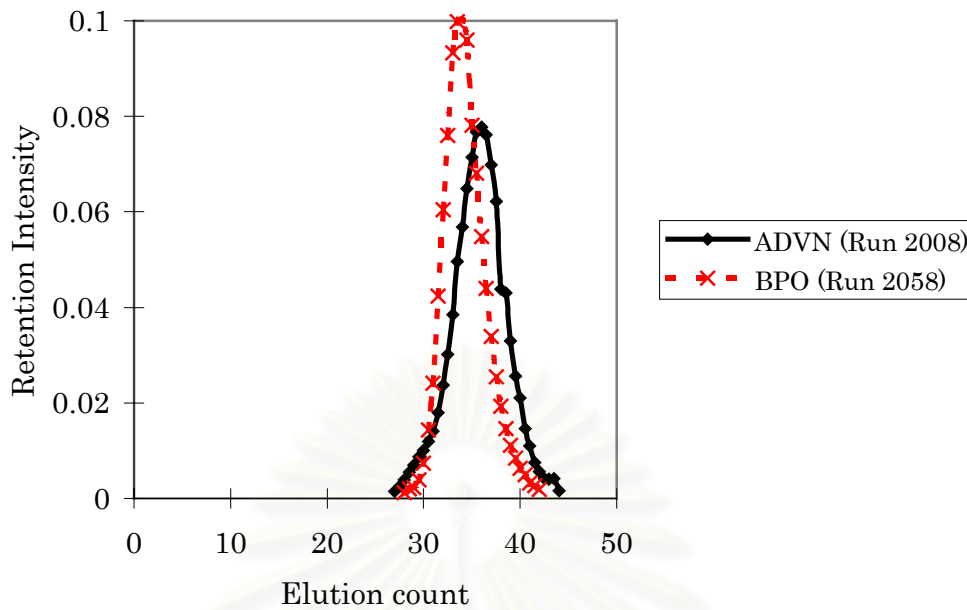


Figure 4.23 Normalized GPC chromatograms of poly (St-*co*-BMA) particles the ratio of St:BMA, 50:50 showing the effects of initiator type.

4.4.2 Effect of the Addition of Polystyrene on Properties of Poly(St-*co*-BMA) Copolymers

The SPG membrane pore size of 0.90 μm was used for the emulsification of St and BMA, with the results as shown in Table 4.9. The amount of the BMA phase was varied from 20 to 50 wt% of the monomer mixture in the presence of 5 wt% DOP based on the total monomer mixture. When the BMA phase is higher than 50 wt%, the particles become flattened, which is in agreement with our previous work [95,116]. The SEM photographs of the poly(St-*co*-BMA) particles are shown in Figure 4.24. Spherical particles having smooth surfaces were synthesized without a phase separation. Upon the addition of 12.5 wt% polystyrene (with $\overline{M}_n = 4200$, $\overline{M}_w = 40000$) into the St-BMA mixtures, the measured viscosity of the dispersion phase significantly increased. The number average molecular weight of the resulting copolymer was close to 5000 as shown in Table 4.9 (Runs 2051 and 2052). It can be

predicted that the added polystyrene functions as if it was a bulky molecule in the polymerization recipe, which diffuses rather slowly in the monomer mixture. Since it is of rather high molecular weight, polystyrene may retard the termination step between the radicals of St and BMA monomers. Therefore, the higher molecular weight polystyrene can be considered as a kind of molecular spacer to prevent the propagating radicals from adding more monomers. The most likely outcome for these short propagating radicals is to terminate, which ultimately results in a lower average molecular weight.

When methanol was added into the reaction mixture as a non-solvent, all the polymer components containing styrene units were precipitated to result in a mixture of poly(St-co-BMA) and polystyrene beads. This mixture of the plasticized poly(St-co-BMA) and polystyrene increased the glass transition temperatures of the particles. As shown by the second T_g of the clean particles in Runs 2051 and 2052, the addition of polystyrene in the reaction mixture does not significantly alter the efficiency of DOP in poly(St-co-BMA)/PSt.

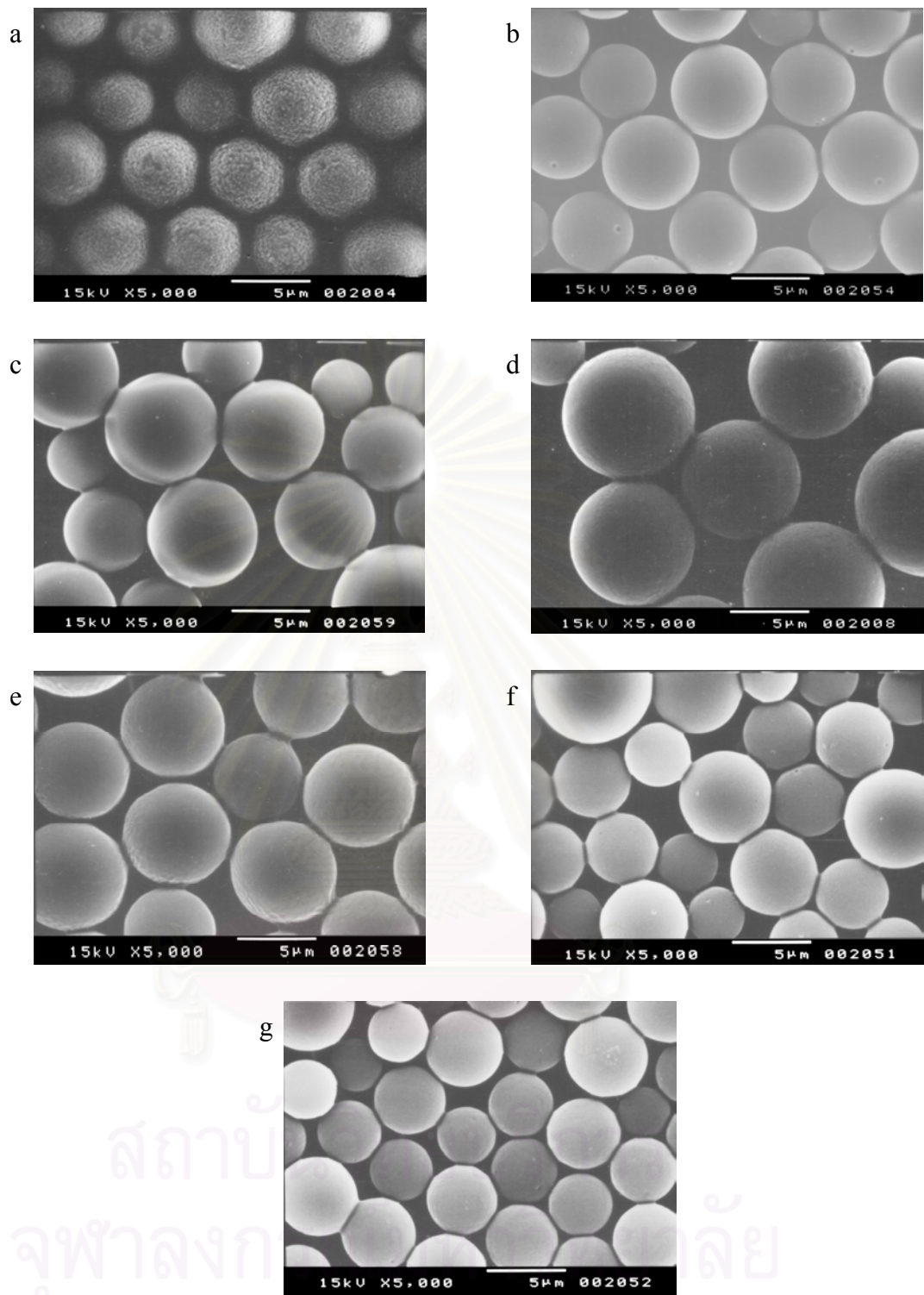


Figure 4.24 SEM photographs of poly(St-co-BMA) particles: a) St:BMA, 50:50; b) 75:25; c) 75:25, DOP 5 wt%; d) 50:50, DOP 5 wt% (ADVN as initiator); e) 50:50, DOP 5 wt% (BPO as initiator); f) St:BMA:PSt, 62.5:25:12.5; and g) St:BMA:PSt, 62.5: 25:12.5, DOP 5 wt%.

Table 4.9 Styrene and BMA copolymerization recipe and results

| Run No. | Composition | Monomer composition (wt.%) | Monomer conversion (%) | D _e (μm) | CV _e (%) | D _p (μm) | CV _p (%) | \overline{M}_n ×10 ⁻⁴ | \overline{M}_w ×10 ⁻⁴ | PDI | T _g (°C) clean | T _g (°C) unclean |
|-------------------|----------------------------|----------------------------|------------------------|---------------------|---------------------|---------------------|---------------------|------------------------------------|------------------------------------|------------------|---------------------------|-----------------------------|
| 2004 | P(St-co-BMA)/DOP | 50/50 | 66.4 | 7.4 | 9.6 | 5.9 | 12.8 | 2.7 | 20.6 | 7.5 ^b | 3.6/45.8 ^c | na |
| 2054 | P(St-co-BMA) | 75/25 | 70.1 | 7.5 | 12.1 | 6.3 | 13.0 | 1.3 | 5.6 | 4.2 | 13.0/62.2 ^c | 22.2/94.3 ^c |
| 2059 | P(St-co-BMA)/DOP | 75/25 | 83.1 | 10.4 | 17.9 | 7.3 | 22.0 | 2.7 | 6.1 | 2.2 | 22.5/47.3 ^c | 9.3 |
| 2008 ^a | P(St-co-BMA)/DOP | 50/50 | 71.8 | 8.4 | 21.6 | 3.8 | 13.1 | 1.5 | 5.2 | 4.0 | 12.2/43.8 ^c | -3.0 |
| 2058 | P(St-co-BMA)/DOP | 50/50 | 77.5 | 9.5 | 12.6 | 7.7 | 13.6 | 3.4 | 7.3 | 2.1 | 8.5/42.0 ^c | 2.4 |
| 2051 | P(St-co-BMA)/PSt | (62.5/25)/12.5 | 75.4 | 8.4 | 14.7 | 6.1 | 20.9 | 0.5 | 3.4 | 6.9 | 23.8/58.4 ^c | 17.2/65.7 ^c |
| 2052 | [P(St-co-BMA)/PSt]/ DOP | (62.5/25)/12.5 | 52.0 | 6.2 | 17.5 | 5.5 | 21.2 | 0.5 | 2.8 | 5.2 | 21.2/50.0 ^c | 17.3 |

^a SPG pore size 0.51 μm, otherwise are 0.90 μm. ^bBimodal curve, ^c Two separate T_g values were observed.

DOP was added 5 wt% of monomer.

Therefore, it is not necessary to include DOP in the composite particles of poly(St-co-BMA) when polystyrene is added before the polymerization. Our postulation on the plasticizing effect for glassy polymers is that it is not necessary to add conventional plasticizers like DOP, the polymers with lower molecular weights can also function as a plasticizer for the higher MW polymer instead.

The one possibility crew on particle morphology prediction can be proposed as shown in Figure 4.25, that two phases exist in monomer droplets, the one is the PSt phase swollen with some monomers, and the other is the monomer- rich phase. The initiator molecules are located in the monomer-rich phase in majority. One can state that the polymerization dominantly takes place in the monomer-rich phase, then the molecular weights of the copolymers formed are lower than the other runs without the addition of PSt.

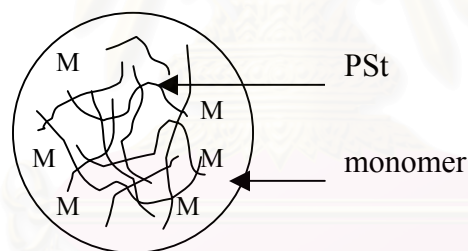


Figure 4.25 A schematic model for the phase separation of the poly(St-co-BMA)/PSt

The other possibility derived from the gel effect theory which refers to as the autoacceleration of the polymerization rate due to the decrease in the termination rate constant when polymeric radicals are present in a viscous media. At low conversions, the polymerization rate is described by conventional kinetics, the cumulative molecular weight averages do not change appreciably, and the molecular weight distribution conforms to the “Schulz-Flory most probable distribution” (Phase I) as shown in Figure 4.26. After a certain conversion, which appears to be

independent of initiator level at the same polymerization temperature, the well known gel effect is observed (Phase II). At still higher conversions the gel effect ceases. The polymerization rate is fast, but the cumulative molecular weight averages (except number-average molecular weight) start to level off or begin to decrease slightly (phase III).

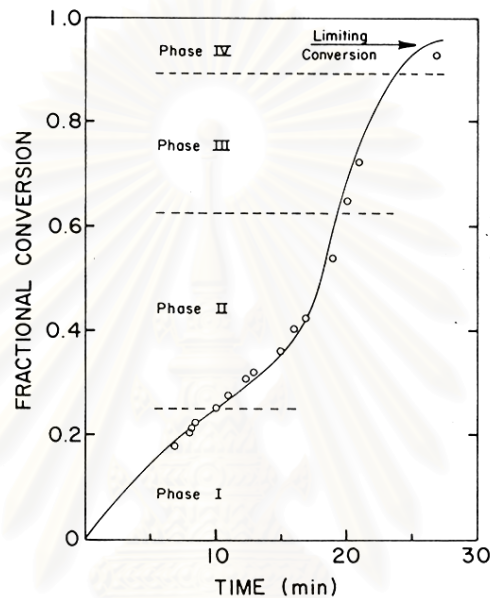


Figure 4.26 Conversion profile for methyl methacrylate polymerization depicting different phases of reaction. (o) data from Balke and Hamielec [117] at 90°C, and 0.3% AIBN, (—) model prediction [118].

The termination reaction is influenced by the viscosity of the reaction medium from zero conversion. Sundberg et al. [118-121] considered that the termination reaction is diffusion controlled and that the diffusivity of macroradicals depends on chain length. It is rather difficult to prove chain length dependence experimentally. The rate of termination reaction of homopolymerization is shown in Eq. 4.4.

$$R_t = k_t [R \bullet]^2 \quad (4.4)$$

where R_t is the rate of termination, and k_t is the rate constant of termination. Perhaps, the most important criticism of Hamielec's model [117] is that the limitation of the gel effect (i.e., the appearance of deceleration) is due to the decrease in k_p caused by diffusional restrictions of the monomer at low free volumes. There should be little of such behavior when the polymerization temperature is well above the glass transition temperature of the polymer.

These considerations lead to the conclusion that the polymerization behavior in phases II and III should only be a result of changes in the chain length dependence on the termination rate constant. Sundberg et al., [118-121] revealed that chain length is reached at which the termination rate constant stops decreasing as rapidly as it had before, and then stays constant or decreases at a less rapid rate. Based on the steady state, the $\overline{k_t}$ value approaching zero is not plausible because the termination reactions can still take place even when the polymer radical chain is completely immobile. Under this condition the very end of the chain will continue to translate in space with every propagation step and will eventually lead to termination. These comments lead to the conclusion that the overall termination behavior is made up of a chain length dependent (translational diffusion) portion and propagation step dependent portion. The latter is not related to chain length. When these dual mechanisms operate simultaneously, the overall termination rate constant should be expressed as Eq. 4.5

$$k_t(y) = (k_t)_{tr} + k_{tp} \quad (4.5)$$

where $k_t(y)$ is the rate constant of the termination step, $(kt)_{tr}$ is the rate constant of translational step, and k_{tp} is the rate constant of the propagation step.

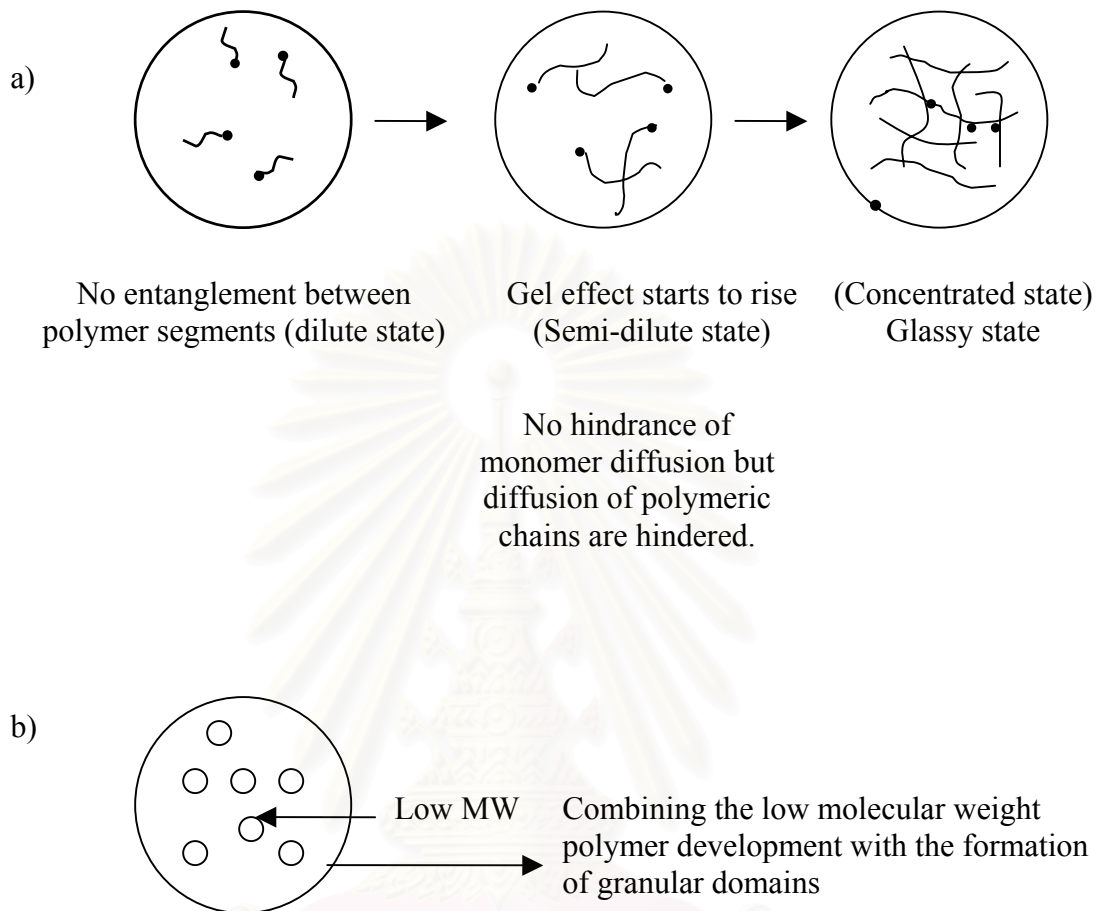


Figure 4.27 “Scaling model” demonstrated by Sundberg [118-121]: a) A schematic model for the path of gel effect; b) Illustration of morphological development

As described above, one can summarize that the mechanism of phase separation in composite particle was proposed based on the aforementioned thermodynamic effect and kinetic effect (behavior) as shown in Figure 4.27.

4.4.3 Effect of Polystyrene on Molecular Weight and Molecular Weight Distribution

The molecular weight of poly(St-co-BMA) was affected by the addition of polystyrene, which may behave like a bulky molecule at the beginning of the reaction. The low molecular weight copolymer was obtained with the unimodal molecular weight distribution as shown in Figure 4.28 in comparison with poly(St-co-BMA) without PSt added. Sundberg et al. [22] revealed that the development of the final morphology in polymer micro-particles involves the movement, or diffusion induced by some driving force to attained the phase-separated arrangement. The movement will certainly be related to the viscosity different between the phases. As described previously, polystyrene acts as a spacer, to retard the propagation ability of monomer molecules, while the distribution of polystyrene in the monomer droplets induces the higher viscosity. The polymerization loci in the presence of the viscous materials like polystyrene in the present case limited the movement of polymer molecules, it enhanced the formation of the lower molecular weight polymer and causing phase separations at a high viscosity domains at which the viscosity is controlled by the ratio of poly(St-co-BMA) produced/PSt added.

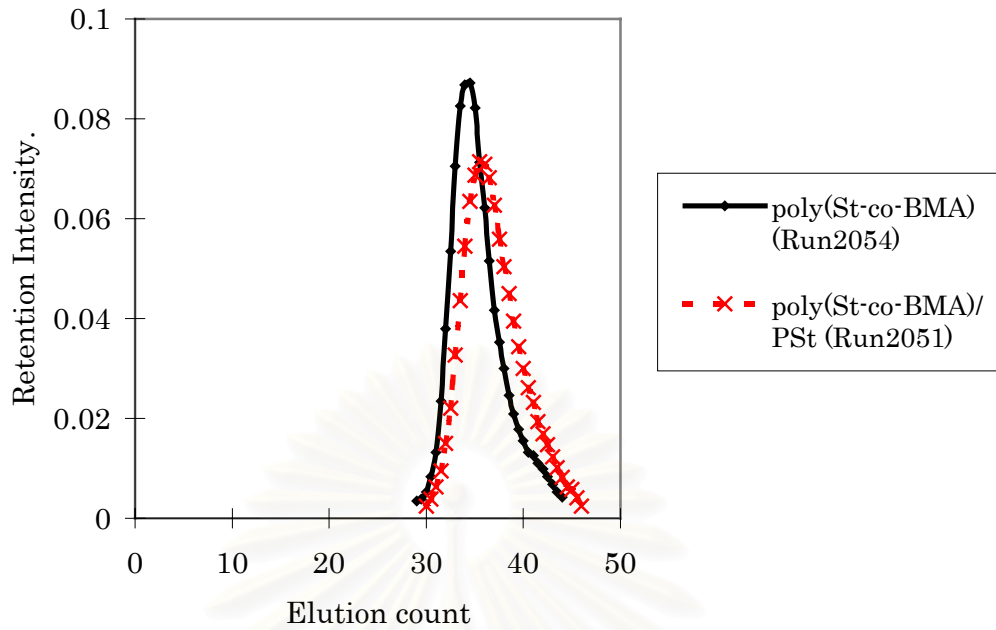


Figure 4.28 Normalized GPC chromatograms of poly(St-co-BMA) and poly(St-co-BMA)/PSt.

4.4.4 Poly(St-co-BMA)/PSt Composite

Similarly, the effect of the inert polymer chains (PSt) dissolved in the monomer phase on the final particle morphology was investigated. Polystyrene ($\overline{M}_n = 4200$, $\overline{M}_w = 40000$, and $\overline{M}_w/\overline{M}_n = 9.54$) was dissolved in the oil phase of the mixture of styrene and BMA monomers, and the polymerization was carried out similarly to poly(St-co-MA)/PSt system as described previously in Section 4.3.6. The poly(St-co-BMA)/PSt composites were selected for the investigation since the BMA monomer gave lower T_g . The formulations and results for each run are shown earlier in Table 4.9. It is known that the OsO_4 vapor stains PBMA better than PSt. Most of the particles look ellipsoidal because of the compressive stress deformation by microtoming. The darkly stained domains of the PBMA core grew inside and embraced with the PSt shell as a core/shell type polymer shown in Figure 4.29a-2,

4.29a-4. In contrast, the particle in Figure 4.29a-3 become more homogeneous without showing much different contrasts of the stained areas. Thermodynamic considerations [22,25] were applied to the morphology of composite latex particles, which indicated that there is a more polar PBMA shell surrounding the hydrophobic PSt core. It yields a minimum interfacial tension of each phase (the term of $\sum \gamma_{12} A_{12}$ in Eq. 2.16), which controls primarily the arrangement of the polymer phases in latex particles. According to the thermodynamic theory that the morphology of the lowest change of Gibb's free energy (ΔG) will be dominant, this suggests that the PBMA is concentrated in the shell region. When DOP was added in Run 2052, it was found that the PSt gained more compatibility between them by converting the small dispersed domains to become a large matrix, which resulted in a more perfect core-shell type. However, the phase separated domains of PSt still remained in the particles as shown in Figure 4.29b, especially in the copolymer containing 5 wt% DOP as shown in Figure 4.29b-3. Upon the addition of DOP, the copolymer particles show both core-shell with the smoothly interface between the stained-PBMA phase and unstained-PSt, and the homogeneous type. According to Table 4.7, the BMA reactivity ratio is relatively similar to that of the styrene ($r_{St} = 0.52$, $r_{BMA} = 0.47$). However, the St-PSt fraction in the copolymer mixture is the higher than BMA monomer. At any circumstance, the PSt portions were generated faster at the beginning of the polymerization as the core polymer. The BMA-rich phase was formed, which became later the shell to envelop the core-St structure. For comparison with poly(St-co-BMA) particle at the St-to-BMA ratio of 75:25, the TEM photographs in Figures 4.30a and 4.30b shows the particles without any phase separation when St to BMA composition was set higher.

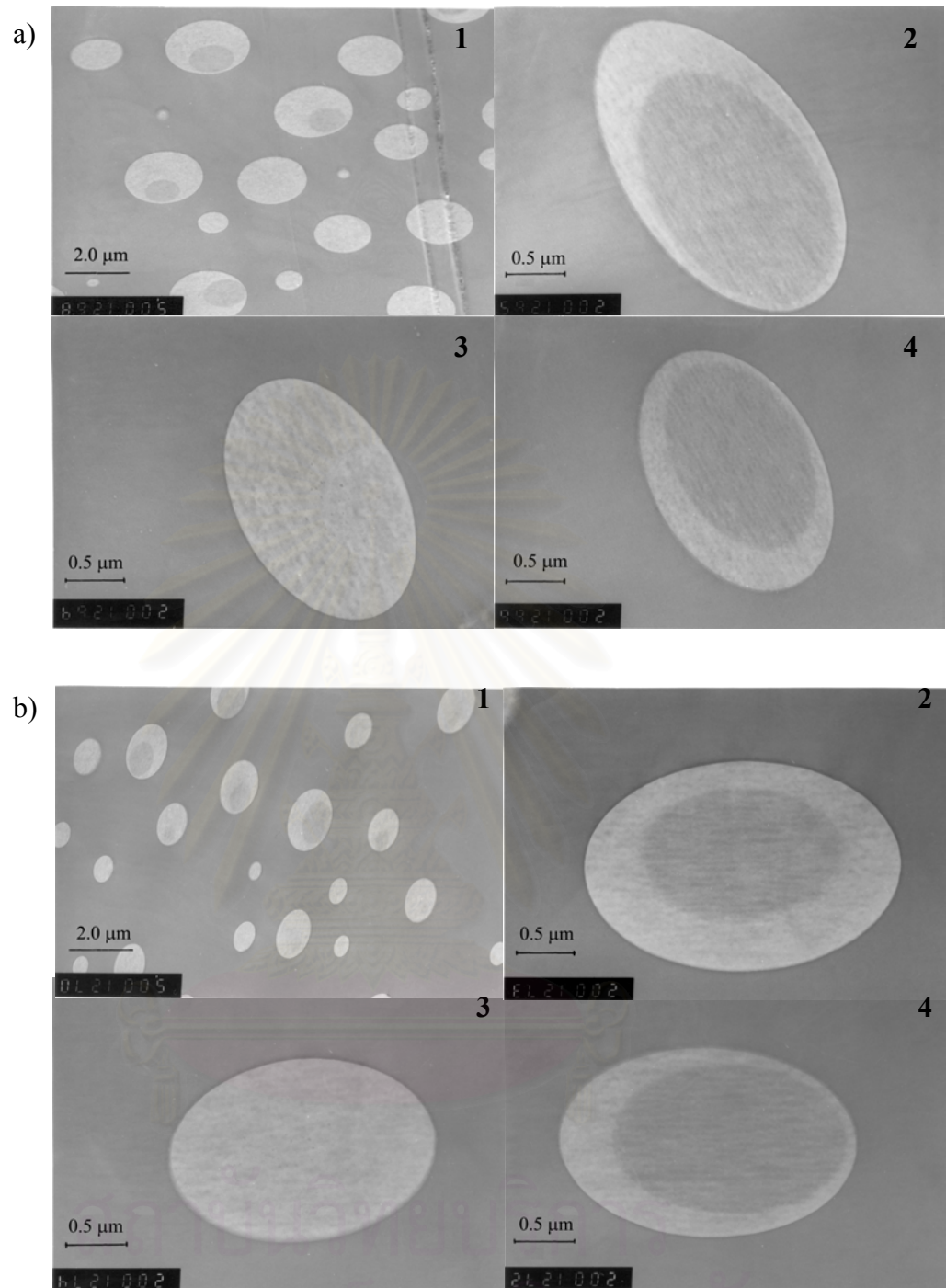


Figure 4.29 Microtomed and OsO_4 -stained TEM photographs of poly(St-co-BMA)/PSt composite particles: a) St:BMA:PSt, 62.5:25:12.5 without DOP (Run 2051); and b) St:BMA:PSt, 62.5:25:12.5 with DOP (Run 2052).

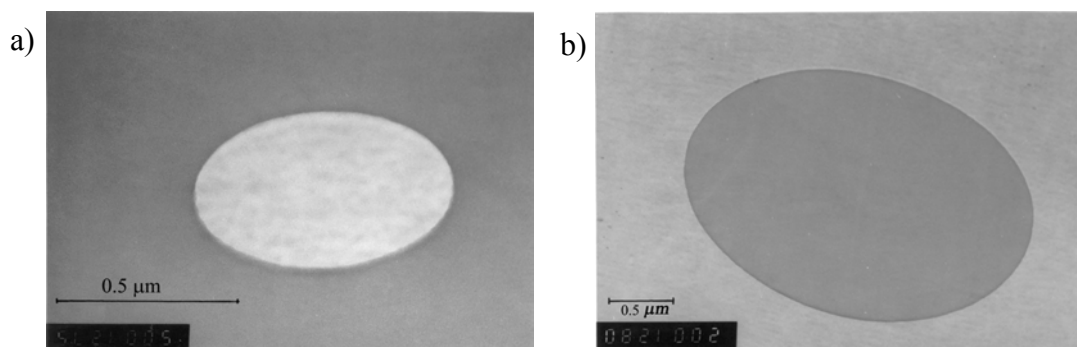


Figure 4.30 Microtomed and OsO_4 -stained TEM photographs of poly(*St-co-BMA*) copolymer particles: *St*:*BMA*, 75:25 (Run 2054); and b) *St*:*BMA*, 75:25 with DOP 5 wt% of monomer (Run 2059).

4.4.5 Glass Transition Temperature of Poly(*St-co-BMA*)

A single transition was revealed in the unclean poly(*St-co-BMA*) copolymer as shown earlier in Table 4.9. The presence of DOP in the copolymer increases the free volume of the hard phase. Because both DOP and BMA contain the similar ester functional group, the DOP can be compatible with the BMA soft domain. In each domain, the DOP molecular chains lubricate the *St* backbone, resulting in a low single T_g in both poly(*St-co-BMA*)/PSt and poly(*St-co-BMA*) copolymers. For the clean polymer, the two separate T_g values were observed. This result can be explained as that the compatibility of DOP plasticizer in the copolymer depends largely on the physical interaction between the copolymer and the plasticizer. After the solvent washing, DOP could remain partially in the polymer particles, if this interaction is strongly enough.

4.4.6 Effect of Stabilizer Concentration on Molecular Weight and Molecular Weight Distribution

A different concentration of the stabilizer, PVA-217, was studied in order to find the optimum stabilizer to stabilize the monomer droplets in an aqueous phase. The preparation recipe and experimental results are shown in Table 4.9. The stabilizer is absorbed on the monomer droplet surface. The large concentration of PVA stabilizer will thus prevent the monomer droplets to dissolve into the aqueous phase. As shown in Figure 4.31, the bimodal MWD curve was revealed when the ADVN was used as an initiator described previously in Section 4.4.4. The concentration of the PVA stabilizer of 0.65 wt% was not high enough to retain the droplet stability, then the polymerization will take place by both suspension and emulsion mechanisms. Depending on its solubility, the monomer molecules can slightly dissolve in the aqueous phase. Therefore, the formation of new particles in the aqueous phase is possible to take place. As shown in Figure 4.24a, the secondary particles on the polymer particle surface were found when lesser concentration of the stabilizer was used.

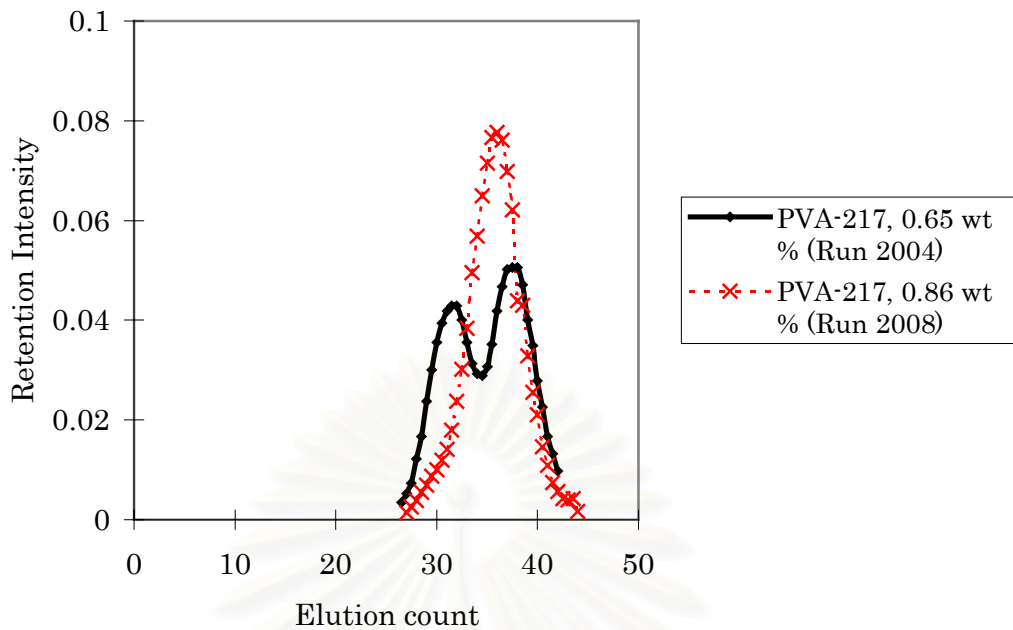


Figure 4.31 Normalized GPC chromatograms of poly(St-*co*-BMA) with the ratio of St:BMA, 50:50 showing the effects of PVA-217 concentrations.

4.5 Synthesis of poly(Styrene-*co*-BA)

St-butylacrylate (BA) emulsion copolymers have received considerable attention in the past few years due to their successful applications in industry [122]. The flexibility of obtaining a large number of polymer materials is usually controlled through the variation of the copolymer composition and the polymerization process. Owing to the differences in the physicochemical properties of monomers (polarity, water solubility) and of the corresponding polymers (T_g , solubility parameters), this copolymerization system is quite interesting to industry and has been extensively studied [123,124]. Kinetic study showed that the reactivity ratios determined in batch emulsion polymerization are close to those obtained in bulk or solution polymerization [125]; some differences exist in comparison with a semicontinuous condition. In addition, the formation of particles is significantly dominated by a

homogeneous nucleation mechanism due to the relatively higher water solubility of BA (1.2 g cm^{-3} at 70°C , while water solubility of St 0.3 g cm^{-3} at 70°C) [123], except when the emulsifier concentration exceeds its critical micelle concentration.

4.5.1 Effect of DOP on Properties of Poly(St-co-BA) Copolymer

The SPG membrane pore size of $0.90 \text{ }\mu\text{m}$ was used for the emulsification of the St and BA monomers. The results are shown in Table 4.10 and the SEM photographs of polymer particles in Figure 4.32. The presence of the soft BA phase in the copolymer synergistically enhances the plasticizing effect of DOP. Since BA itself behaves like a plasticizing monomer, the expected single glass transition temperature was found in poly(St-co-BA) particles for both clean and unclean samples (Run 2047). However, when PSt was added into the St-BA monomer mixture, the synthesized poly(St-co-BA)/PSt (Run 2050) gave a single T_g value in the unclean particles. For the clean particles, two separate T_g values were found. Likewise, a low number average molecular weight was also found, as described in Section 4.4.2 for poly(St-co-BMA) copolymers. For possible explanation of difference in T_g when PSt was added in comparison with the poly(St-co-BMA) system. One can be mentioned that, the side chain of BA is the key variable influencing the glass transition temperature since it is more flexible than that of BMA-side chain.

Table 4.10 Recipe and results for styrene and butyl acrylate copolymerization

| Run No. | Composition | Monomer composition (wt%) | Monomer conversion (%) | D _e (μm) | CV _e (%) | D _p (μm) | CV _p (%) | \overline{M}_n ×10 ⁻⁴ | \overline{M}_w ×10 ⁻⁴ | PDI | T _g (°C) clean | T _g (°C) unclean |
|---------|-------------------------|---------------------------|------------------------|---------------------|---------------------|---------------------|---------------------|------------------------------------|------------------------------------|-----|---------------------------|-----------------------------|
| 2048 | P(St-co-BA) | 75/25 | 71.3 | 8.7 | 13.9 | 6.2 | 15.8 | 2.6 | 6.2 | 2.4 | 22.7/58 ^a | 17.4/51.6 ^a |
| 2047 | P(St-co-BA)/DOP | 75/25 | 65.1 | 8.1 | 15.1 | 6.5 | 16.3 | 2.1 | 4.9 | 2.3 | 40.2 | 16.8 |
| 2049 | P(St-co-BA)/PSt | (62.5/25)/12.5 | 86.0 | 7.6 | 13.5 | 5.3 | 17.4 | 0.7 | 3.9 | 5.4 | 17.2/55 ^a | 18.8/52.0 ^a |
| 2050 | P(St-co-BA)/PSt/ DOP | (62.5/25)/12.5 | 67.9 | 6.8 | 21.7 | 5.2 | 23.3 | 0.6 | 3.7 | 5.9 | 22.2/53.3 ^a | 19.7 |

SPG pore size 0.90 μm

^aTwo separate T_g values were observed, otherwise a single T_g.

DOP concentration of 5 wt% was based on the monomer concentration.

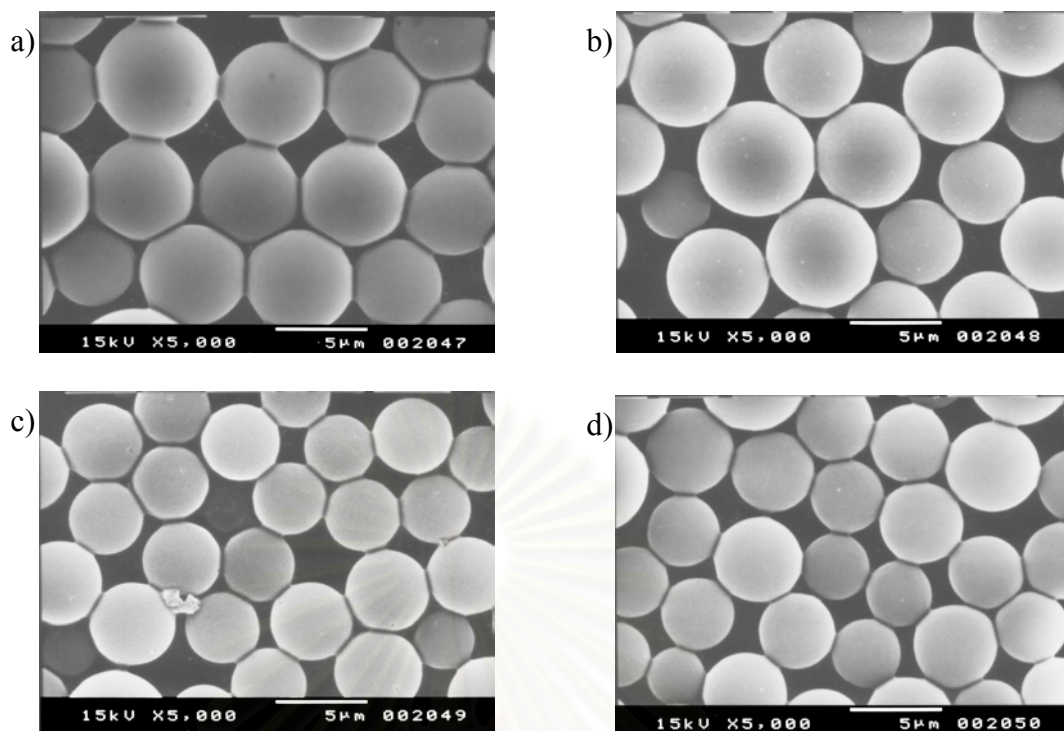


Figure 4.32 SEM photographs of poly(St-co-BA) and poly(St-co-BA)/PSt particles: a) St:BA, 75:25; b) St:BA, 75:25, DOP 5 wt%; c) St:BA:PSt, 62.5:25:12.5; and d) St:BA:PSt, 62.5:25:12.5, DOP 5 wt%.

4.5.2 Effect of Polystyrene Bulky Molecule on Molecular Weight and Molecular Weight Distribution of Poly(St-co-BA)

The addition of polystyrene as bulky molecule affected the molecular weight of polymer. The molecular weight distribution curves of the copolymer and the copolymer including polystyrene were shifted to the lower molecular weight as shown in Figure 4.33. Meanwhile, the presence of low molecular weight was observed as the results of increasing viscosity of initial dispersion phase. Since, the bulky molecule of PSt retarded the propagation radicals of propagation step, the low molecular weight was yielded. Following the previous discussion, the PSt domains gained viscosity to the extent that the propagation of monomer was greatly hindered.

Although the termination rate was also retarded the resulting polymers were short-chained.

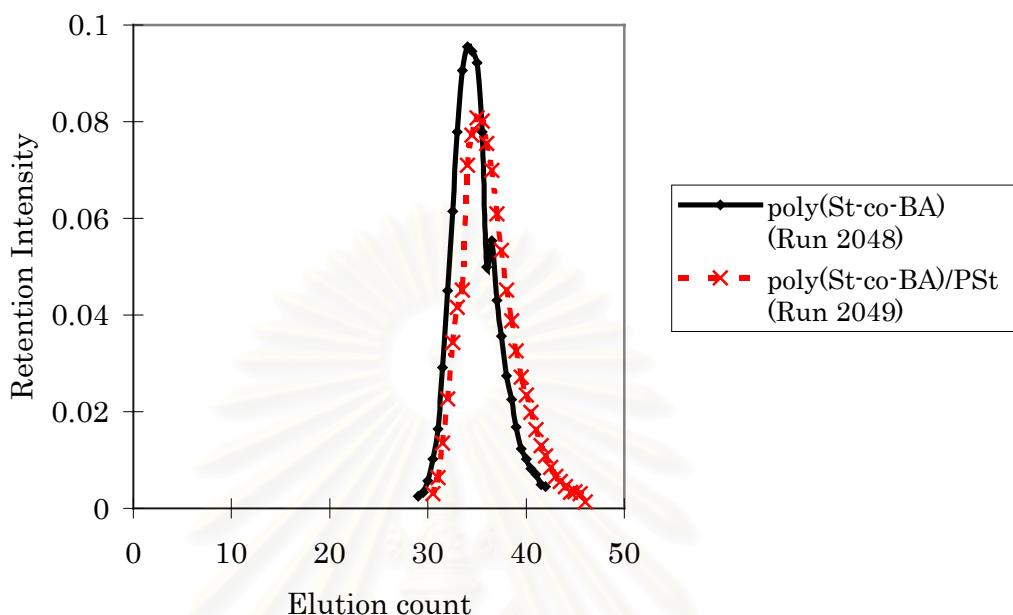


Figure 4.33 Normalized GPC chromatograms of poly(St-co-BA) and poly(St-co-BA)/PSt

4.5.3 Internal Morphology of Poly(St-co-BA)/PSt Composites

On the previous discussion, polyacrylates were stained preferentially to PSt. The cross-section of copolymer composite revealed that the lightly stained PSt granules were distributed over the whole area of the particle. Another phase separation of a salami-like morphology was observed. A marked composition drift in the copolymer was observed as the reactivity ratios between St and BA monomers are largely different. From Table 4.7, styrene and BA have the reactivity ratios of 0.84 and 0.18 [109], respectively; hence the monomer pair then can form a random copolymer because of the r_1r_2 value of 0.154. St monomer molecules were consumed faster at the beginning of the polymerization. Then, the BA-rich phase was subsequently produced, which surrounded later the core-St domains. In comparison

with poly(St-*co*-MA)/PSt as described in Section 4.3.6, the St-BA copolymer has an inverted morphology of the St-MA copolymer. Moreover, the BA-rich shell morphology was also observed as shown in Figures 4.34a and 4.34b. Because St is more reactive than BA [109] ($r_{BA} = 0.18$, $r_{St} = 0.84$), The resulting particle morphology indicated that the largely different reactivity ratio is a key reason to govern the particular morphologies of the copolymer particles formed from the monomer pair.

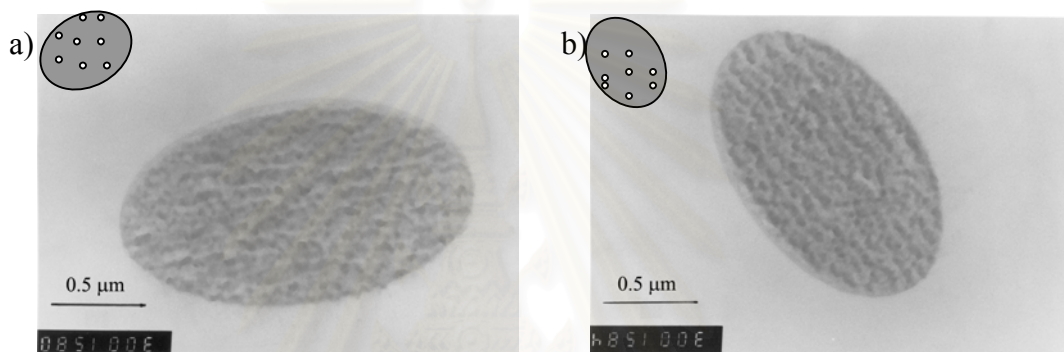


Figure 4.34 Microtomed and OsO₄-stained TEM photographs of poly(St-*co*-BA)/PSt composite particles: a) St:BA:PSt, 62.5:25:12.5 without DOP (Run 2049); and b) St:BA:PSt, 62.5:25:12.5 with DOP (Run 2050).

4.6 Synthesis of Poly(MMA-*co*-MA)

The synthesis of poly(MMA-*co*-MA) was carried out using MMA as a rigid component. The experiments were scheduled by the similar methods to that for poly(St-*co*-MA). The copolymers incorporated with or without the DOP plasticizer were obtained. The effects of the monomer composition, stabilizer, and initiator were carried out and described as follows:

4.6.1 Effect of the Stabilizer Type on Molecular Weight and Morphology of the Copolymer

The PVA-217 or PVP K-30 stabilizer was added to stabilize the monomer droplets. Since MMA and MA are slightly soluble in water, it was revealed that the smaller monomer droplets were found when the monomer droplet was permeated one by one through the membrane. The effects of stabilizer type on molecular weight and morphology are shown in Table 4.11. Figures 4.35 and 4.36 show the external morphology investigated by SEM. The smooth surface of the spherical particles was obtained in all copolymer compositions. However, the particle surface was soft and easily damaged by electron beams during the investigation. It was found that an increase in PVP K-30 concentration to 1.1 wt% of the monomer led to the formation of small dimples on the particle surface as shown in Figure 4.34e. This may be caused from the interaction between surfactant and monomer droplets. Typically, the dispersion of PVP K-30 is non-electrolyte type, which is soluble in water. PVP was thus used as the steric stabilizer. The surface of resultant polymer particles could anchor with PVP. According to the particle formation mechanism proposed by Tseng et al. [126], PVP molecules were absorbed by the aggregates of growing polymer chains and finally anchored on the mature particles, in order to stabilize the dispersion of hydrophobic particles in the polar medium. The anchored PVP resulting from possible adsorbing or grafting could not be washed out; the hydrophobicity of the particle surface was thus probably reduced by the presence of this hydrophilic PVP. However, Wu et al. [127] revealed that these anchored PVPs could be partially released from the particle during the process of chemical modification on the particle surface.

Table 4.11 Recipe and results of methyl methacrylate and methyl acrylate in various stabilizer types

| Run No. | Composition | Monomer composition (wt%) | Monomer conversion (%) | D _e (μm) | CV _e (%) | D _p (μm) | CV _p (%) | \bar{M}_n ×10 ⁻⁴ | \bar{M}_w ×10 ⁻⁴ | PDI | T _g (°C) clean | T _g (°C) unclean |
|---------|--|---------------------------|------------------------|---------------------|---------------------|---------------------|---------------------|-------------------------------|-------------------------------|-------------------|---------------------------|-----------------------------|
| 2010 | PMMA | 100 | 85.6 | 6.9 | 25.9 | Coag | Coag | 3.7 | 13.0 | 3.5 | 14.0 | 14.0 |
| 2040 | P(MMA- <i>co</i> -MA), PVA 0.54 wt% | 75/25 | 76.5 | 6.7 | 27.6 | 5.2 | 12.6 ^a | 3.0 | 15.2 | 5.1 | 44.1 | 27.8 |
| 2035 | P(MMA- <i>co</i> -MA), PVA 1.1 wt% | 50/50 | 79.9 | 5.6 | 22.8 | 5.4 | 14.5 ^a | 4.0 | 52.3 | 13.2 ^b | 29.5 | 25.3 |
| 2034 | P(MMA- <i>co</i> -MA), PVA 1.1 wt% | 75/25 | 57.1 | 4.6 | 13.6 | 4.7 | 18.7 | 3.3 | 22.1 | 6.7 | 38.0 | 29.2 |
| 2042 | P(MMA- <i>co</i> -MA), PVP 1.1 wt% | 50/50 | 18.5 | 4.4 | 18.5 | 3.9 | 26.4 ^a | 2.6 | 26.5 | 10.2 | 22.9 | 43.2 |
| 2041 | P(MMA- <i>co</i> -MA), PVP 1.1 wt% | 75/25 | 13.0 | 4.1 | 16.9 | 3.9 | 12.1 ^a | 1.8 | 11.4 | 6.3 | 38.8 | 24.3 |

^a Coagulum was observed. ^b Bimodal curve, otherwise are unimodal.

\bar{M}_w of PVP K-30 = 40,000

DOP concentration of 5 wt% was based on the monomer concentration.

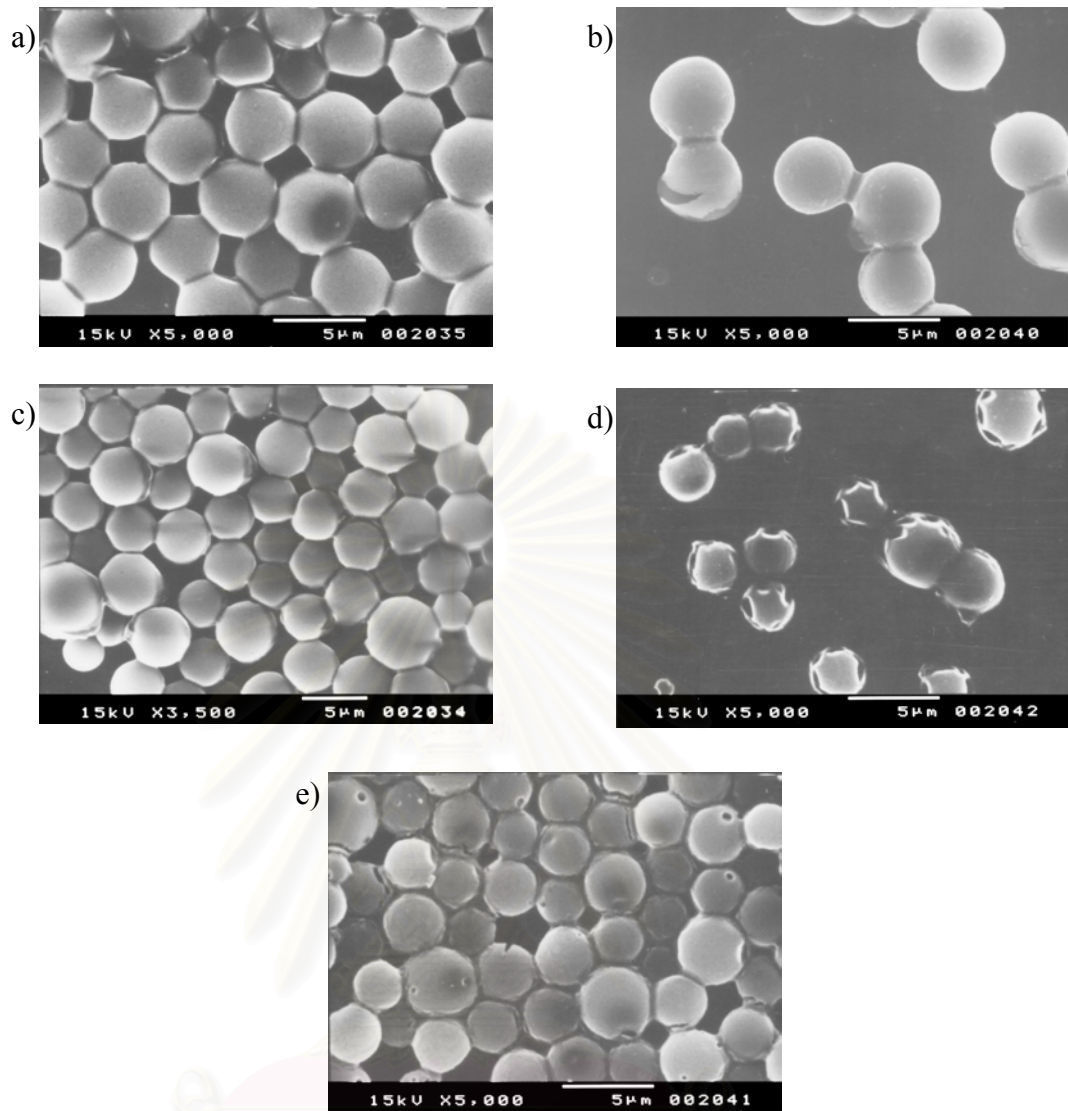


Figure 4.35 SEM photographs of poly(MMA-*co*-MA): a) poly(MMA-*co*-MA), MMA:MA 50:50, PVA-217:1.1 wt%; b) poly(MMA-*co*-MA), MMA:MA, 75:25, PVA-217: 0.54 wt%; c) poly(MMA-*co*-MA), MMA:MA 75:25, PVA-217:1.1 wt%; d) poly(MMA-*co*-MA), MMA:MA 50:50, PVP K-30:1.1 wt%; and e) poly(MMA-*co*-MA), MMA:MA, 75:25, PVP K-30:1.1 wt%.

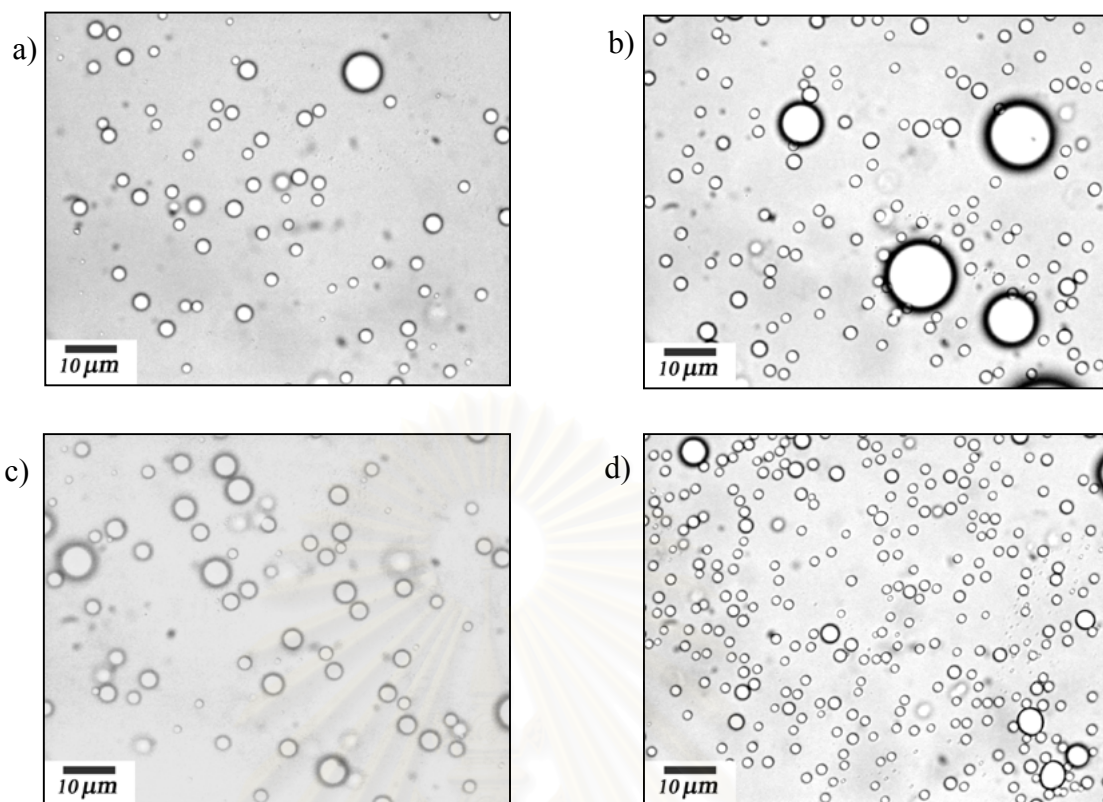


Figure 4.36 Optical micrographs of poly(MMA-*co*-MA): a) poly(MMA-*co*-MA), MMA:MA 50:50, PVA-217 (Run 2035); b) poly(MMA-*co*-MA), MMA:MA of 50:50, PVP K-30 (Run 2042); c) poly(MMA-*co*-MA), MMA:MA of 75:25, PVA-217 (Run 2034); and d) poly(MMA-*co*-MA), MMA:MA of 75:25, PVP K-30 (Run 2041).

The slight effect of the emulsifier concentration on the average molecular weight can be observed in Figure 4.37. The emulsifiers were added at 1.1 wt% of the monomer concentration. The bimodal molecular weight distribution curve was revealed in case of PVA. However, the MWD was shifted to the unimodal molecular weight when the copolymer was prepared from MMA 75 wt% of monomer. A possible explanation, the solubility of monomers in water was decreased with the higher amount of MMA (MMA:MA ratios of 75:25). The polymerization process will more dominantly proceed by suspension polymerization than that of emulsion polymerization. The stabilizer concentration also affected average molecular

weight of the polymer. As shown in Figure 4.37, the broad molecular weight distribution was found with increasing PVA concentration.

4.6.2 Effect of Stabilizer on Monomer Droplet Size, Droplet Size Distribution, Polymer Particle Size and Particle Size Distribution

In an emulsification procedure, nitrogen pressure was precisely controlled in order to permeate the dispersion phase via a membrane at the constant rate. After the emulsification was over, the monomer droplets of MMA-MA ratio of 50:50 were suspended in the aqueous phase. When PVA was used as a stabilizer, more stable droplets were observed as shown in Figure 4.36a in comparison with the run using PVP in Figure 4.36b. However, after the ratio of MMA was increased to 75 wt% of monomers, the narrower droplet size distribution was observed with a small percentage CV as the amount of smaller droplets also decreased as shown in Figure 4.36c and 4.36d. In Figure 4.39a, the broad PSDs were observed both in the experiments using PVA (Run 2035) and PVP (Run 2042). In comparison with Figure 4.39b, the particle size distribution becomes narrower when the concentration of MMA was increased. The copolymer with PVP as a stabilizer revealed a narrower PSD than that of PVA. However, this may be an effect of the monomer ratio, since the narrower PSD was observed with the higher amount of MMA. Unfortunately, even PVP gave the better PSD results than PVA, the polymer conversion was found lower at 18.5% and 13% for MMA:MA ratios of 50:50 and 75:25, respectively. As shown in Figure 4.37, a substantial amount of coagulum was achieved. Then, the yield of the resulting particles is very low. Precisely, the stabilizer PVP has a less efficiency to promote the interfacial tension between the monomer phase and water phase. Because MMA and MA are partially water-soluble, they can dissolve in water

better (the solubility in water of MMA is 16 g dm^{-3} , and MA is 52 g dm^{-3} at 293 K) [109,110]. Then, PVP will not be used for the future experiments of MMA-MA.

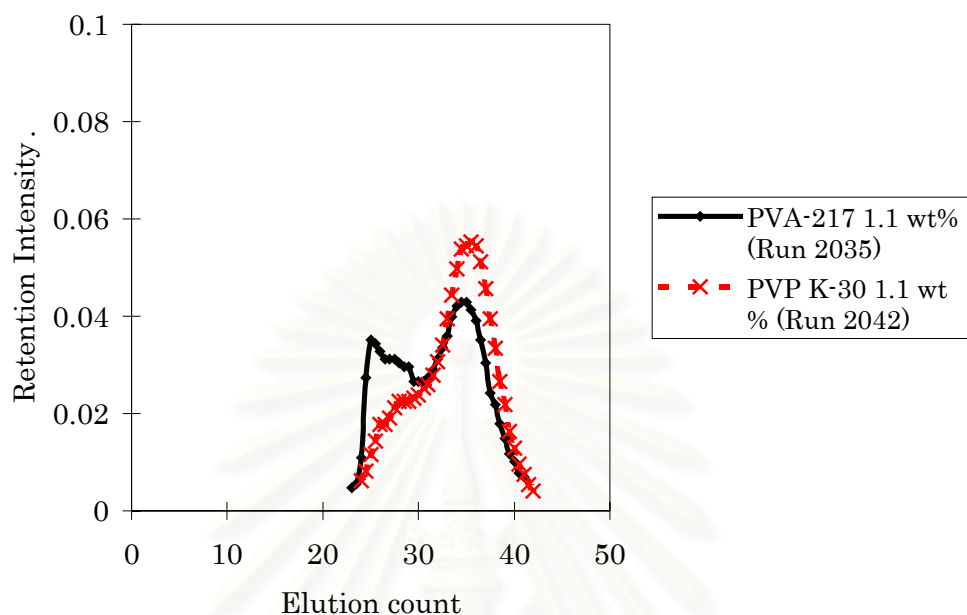


Figure 4.37 Normalized GPC chromatograms of poly(MMA-*co*-MA) at the ratio of MMA:MA is 50:50 showing the effect of stabilizer type.

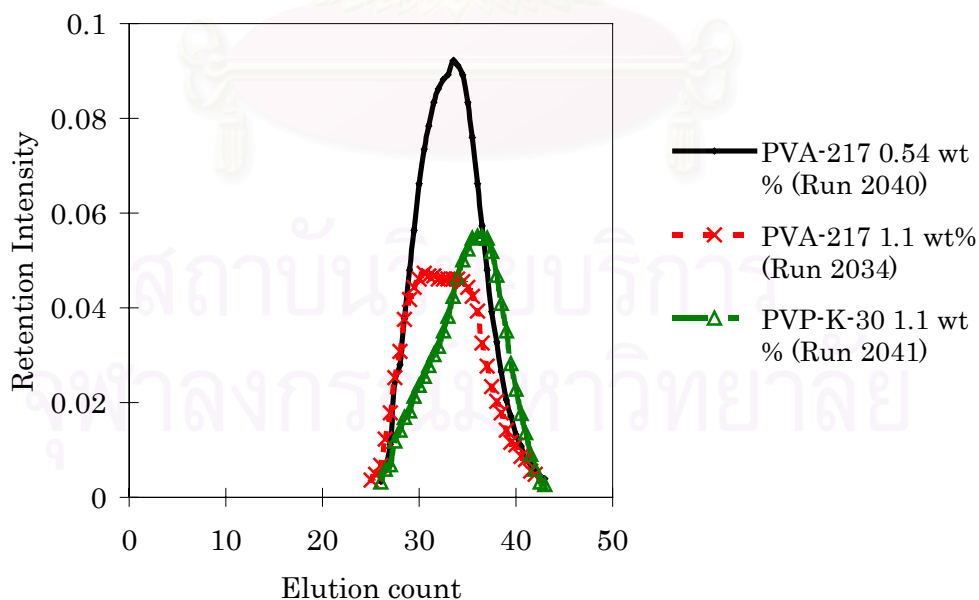


Figure 4.38 Normalized GPC chromatograms of poly(MMA-*co*-MA) at the ratio of MMA:MA is 75:25 showing the effect of stabilizer type.

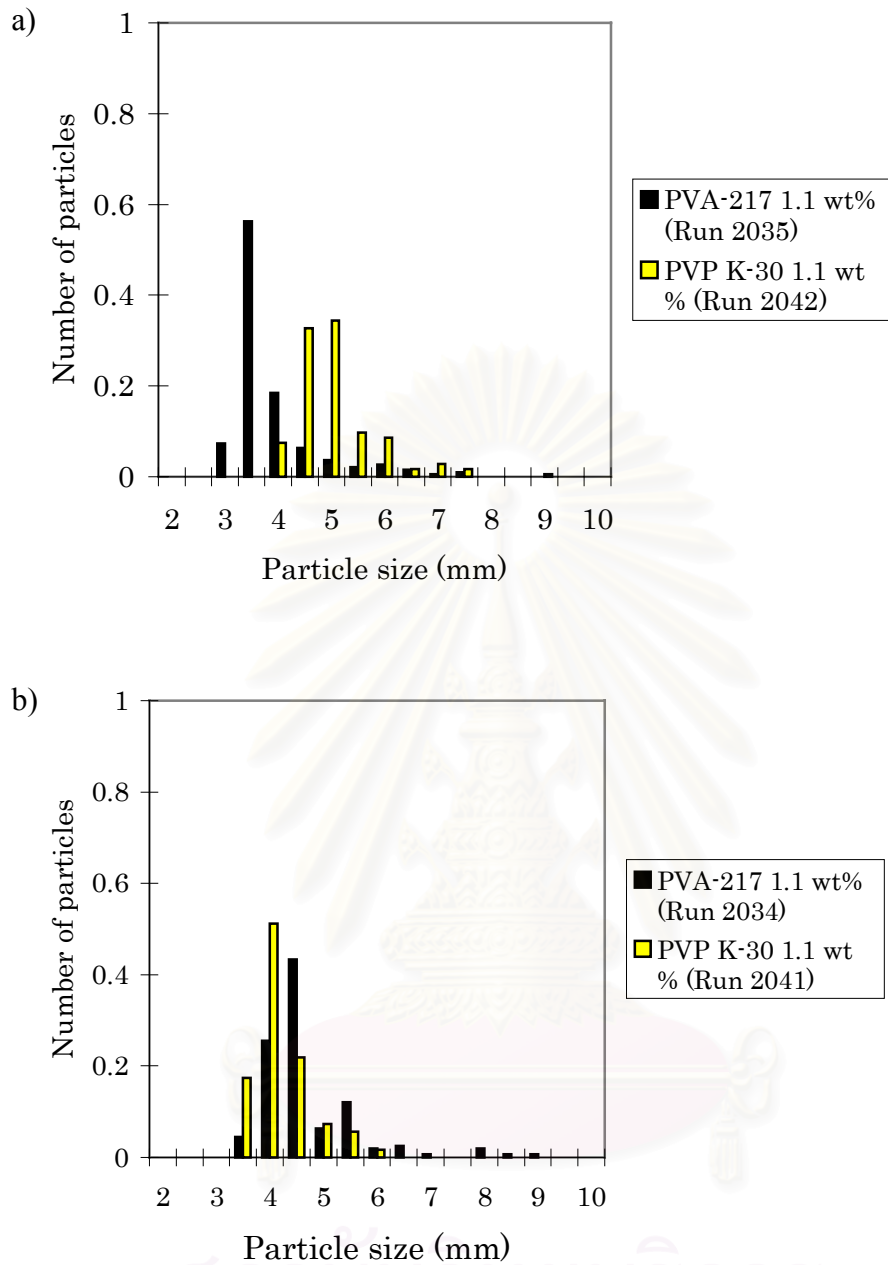


Figure 4.39 Comparison of particle size distribution of poly(MMA-co-MA) with different stabilizer types by the SPG membrane pore size of 0.90 μm , the ratio of MMA:MA is a) 50:50; and b) 75:25.

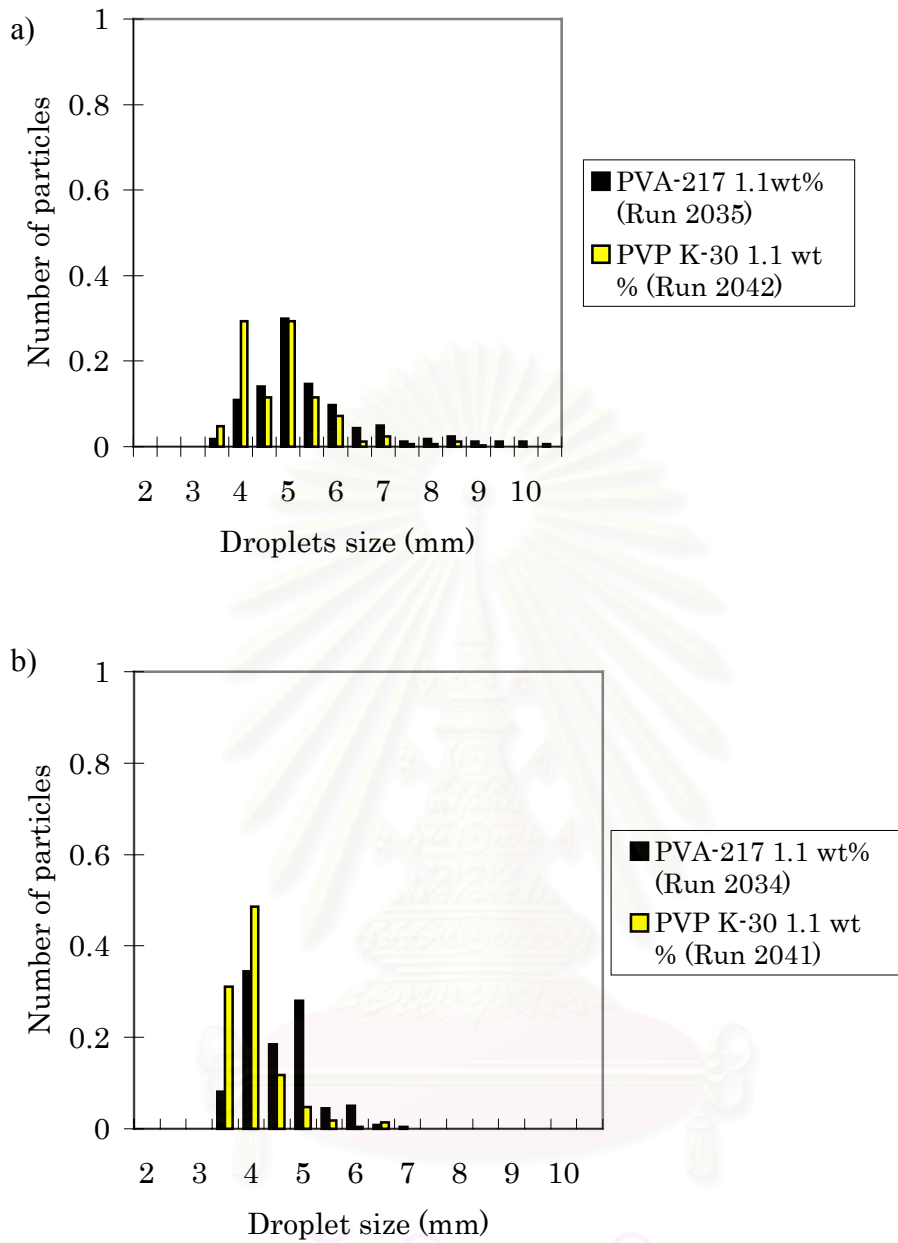


Figure 4.40 Comparison of droplet size distribution of poly(MMA-co-MA) with different types of stabilizer by the SPG membrane pore size of 0.90 μm : a) the ratio of MMA:MA of 50:50, and b) the ratio of MMA:MA of 75:25.

4.6.3 Monomer Composition on Average Molecular Weight, Molecular Weight Distribution, and Glass Transition Temperature

The effect of monomer composition on molecular weight is shown in Table 4.6 and Figure 4.41. The copolymers were synthesized using various monomer compositions. To compare the four recipes on polymer morphology, the SEM photographs are presented in Figures 4.11a to 4.11d (Runs 2010, 2032, 2033, and 2045, respectively). Since the air pressure was applied for each run at different ranges, the applied pressure certainly affected the droplet size and particle size distribution. The mixed MMA/MA was more hydrophilic than the mixed St/MA. The mixed MMA/MA monomer could easily wet the membrane pores and disturbed permeation of the monomer droplets as described earlier in Section 4.1. As shown in Table 4.6, the broad droplet size distribution of the monomers is observed in all monomer compositions, and at the MMA/MA of 25:75 yields the broadest size distribution. Besides, the coagulum and lower monomer conversions were observed. Unfortunately, PMMA particles in Run 2010 were coagulated, therefore the particle size could not be determined. This behavior was resulted from the properties of PMMA. The partially water-soluble PMMA was surrounded by water molecules in the aqueous phase, because of the relative hydrophilic PMMA chains. The particles could absorb some water during the polymerization, which behaves like a plasticizer for the chains. During the drying period, the moisture is released and leaves microvoids in the particles [110]. Therefore, the volume of polymer particle was increased resulting in the larger particle diameter.

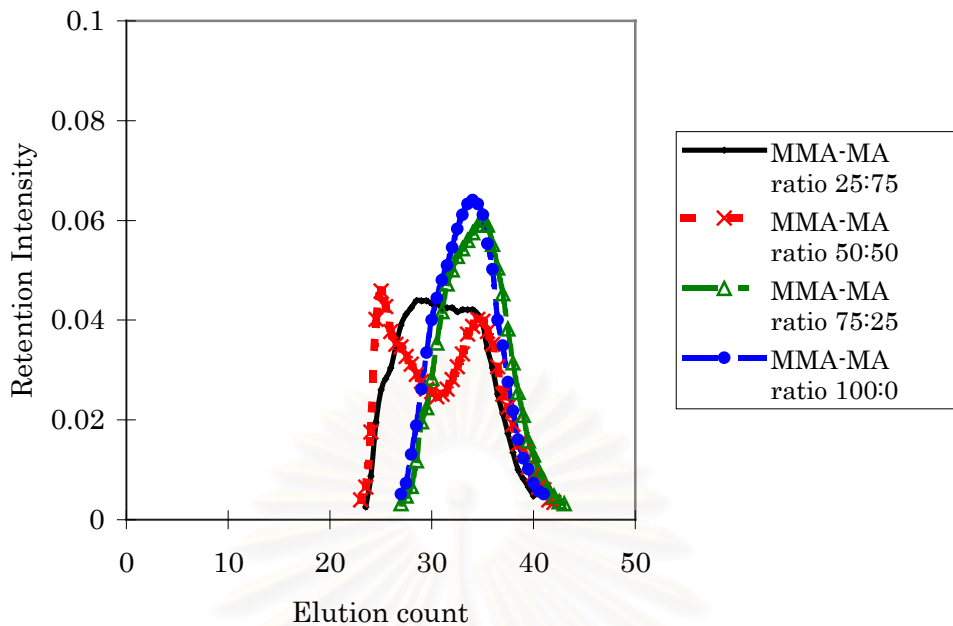


Figure 4.41 Normalized GPC chromatograms of poly(MMA-*co*-MA) particles showing the effects of monomer compositions.

The T_g s of PMMA were found lower at 14°C for both clean and unclean particles, compared to the normal T_g of PMMA are almost 100°C [109,110]. The T_g for both clean and unclean copolymer samples revealed the similar low values and was located between the T_g s of the PMMA and PMA. Addition of DOP 5 wt% of monomer plasticized the PMMA stiff chains and increased the chain mobility of the polymer. However, the experimental T_g value is extremely low in comparison with the other copolymer ratio as shown in Figure 4.42. The formation of coagulum during the polymerization may cause the erratum on the glass transition temperature by DSC technique. Probably, the PMMA coagulum still contained moisture unreacted monomer or methanol. All these act as plasticizer to lower T_g s. The DOP plasticizing effect which is more enhanced in the acrylate-acrylate copolymers, while the DOP

also strongly effected the T_g of poly(MMA-*co*-MA) at all compositions by reducing T_g values.

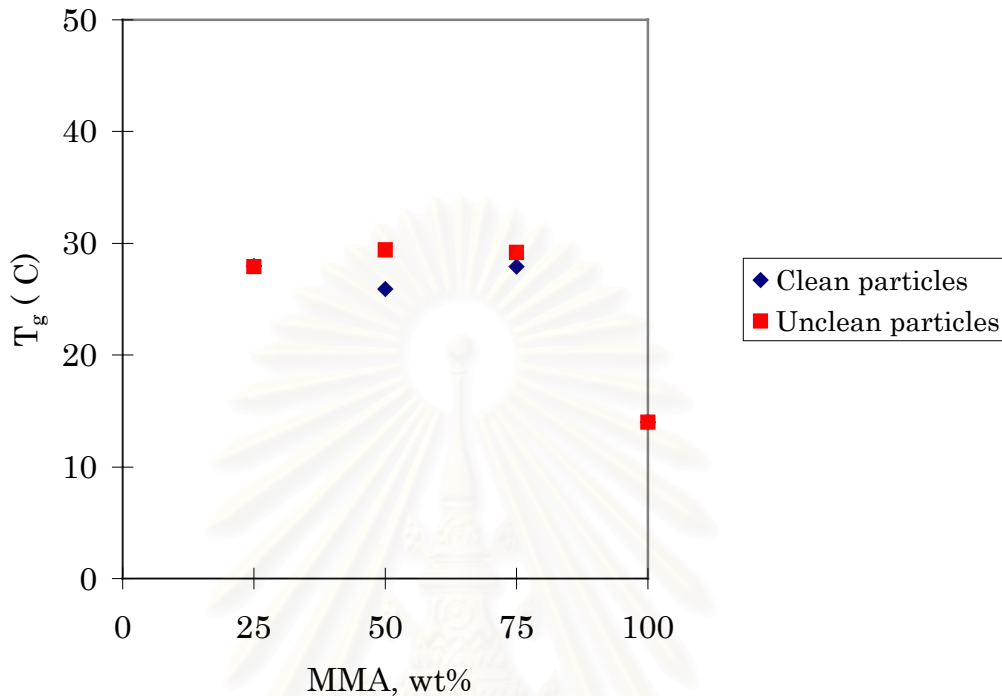


Figure 4.42 Glass transition temperatures of poly(MMA-*co*-MA) at various monomer compositions (DOP including 5 wt% by weight of the mixed monomer)

4.6.4 Effect of Initiator Concentration on Polymer Morphology

As shown in Figure 4.43, the smooth surfaces were observed for all experiments. Viewing more closer to the particle surfaces and the polymer latex, no generation of secondary particles was observed using different concentrations of the initiator. Polymerization using the ADVN initiator was thus justified because ADVN has a fast decomposition rate with a half-life 58 min [128,116]. However, the different average molecular weights of polymers were observed as shown in Table 4.12 and Figure 4.44. The average molecular weight was shifted to a broad molecular weight distribution. When increasing the initiator concentration, the lower number-average

molecular weight (\overline{M}_n) was achieved. This indicates the fast decomposition rate of the initiator to give a large number of oligomers, which would tend to propagate and form particle nuclei of various chain lengths, and mostly short chains. The propagation rate was probably faster than the rate of stabilizer to be adsorbed onto the droplets and stabilize them. Then, a broad particle size distribution having a similar average-particle size was achieved, as shown in Figure 4.45c.

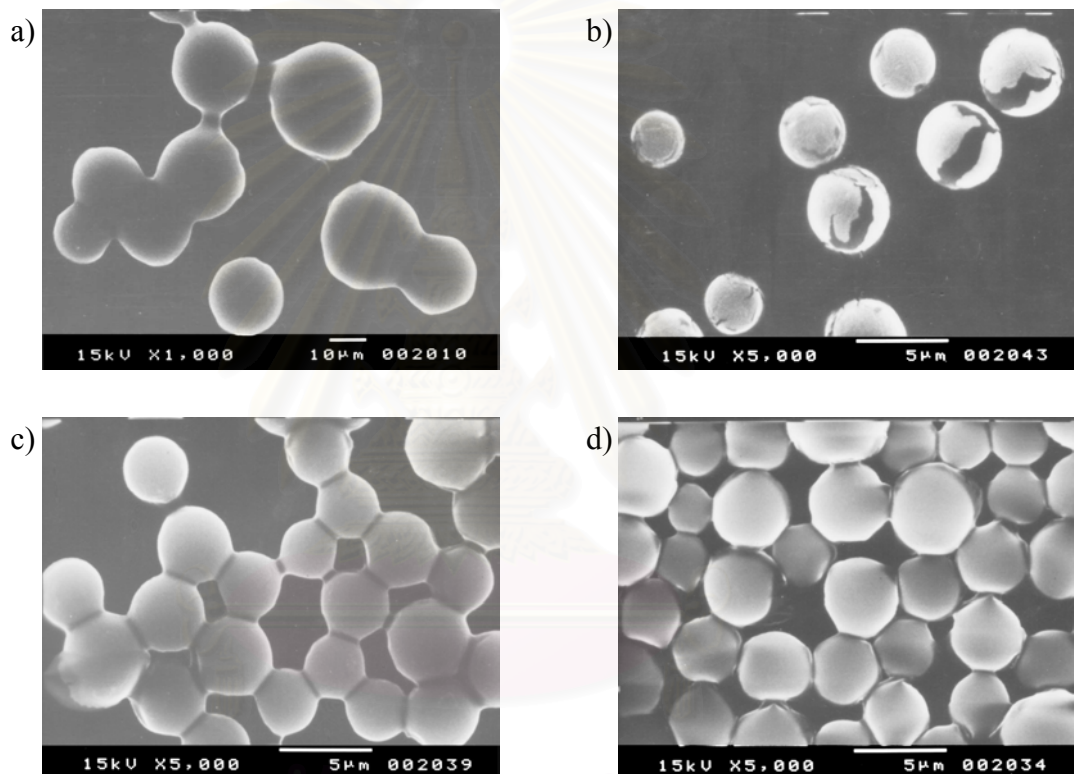


Figure 4.43 SEM photographs of poly(MMA-co-MA) for a) PMMA, ADVN 5 wt%; b) poly(MMA-co-MA), MMA:MA 75:25, ADVN 0.62 wt%; c) poly(MMA-co-MA), MMA:MA 75:25, ADVN 1.25 wt%; and d) poly(MMA-co-MA), MMA:MA 75:25, ADVN 2.50 wt%

Table 4.12 Recipe and results of methyl methacrylate and methyl acrylate copolymerization using various amounts of initiator

| Run No. | Composition | Monomer composition (wt%) | Monomer conversion (%) | D_e (μm) | CV_e (%) | D_p (μm) | CV_p (%) | \overline{M}_n $\times 10^{-4}$ | \overline{M}_w $\times 10^{-4}$ | PDI | T_g ($^{\circ}\text{C}$) clean | T_g ($^{\circ}\text{C}$) unclean |
|---------|--|---------------------------|------------------------|-------------------------|------------|-------------------------|---------------------------|-----------------------------------|-----------------------------------|-----|------------------------------------|--------------------------------------|
| 2010 | PMMA | 100 | 85.6 | 6.9 | 25.9 | Coag ^a | Coag ^a | 3.7 | 13.0 | 3.5 | 14.0 | 14.0 |
| 2043 | P(MMA- <i>co</i> -MA), ADV N 0.62 wt% | 75/25 | 34.6 | 5.0 | 14.3 | 5.3 | 11.8 | 5.3 | 28.0 | 5.3 | 30.8 | 25.5 |
| 2039 | P(MMA- <i>co</i> -MA), ADV N 1.25wt% | 75/25 | 63.9 | 4.8 | 32.9 | 4.7 | 14.6 Coag ^a | 4.8 | 23.9 | 5.0 | 42.9 | 24.3 |
| 2034 | P(MMA- <i>co</i> -MA), ADV N 2.50 wt% | 75/25 | 57.1 | 4.6 | 13.6 | 4.7 | 18.7 | 3.3 | 22.1 | 6.7 | 38.0 | 29.2 |

^a Coagulum was formed.

DOP was added 5 wt% for each experiment.

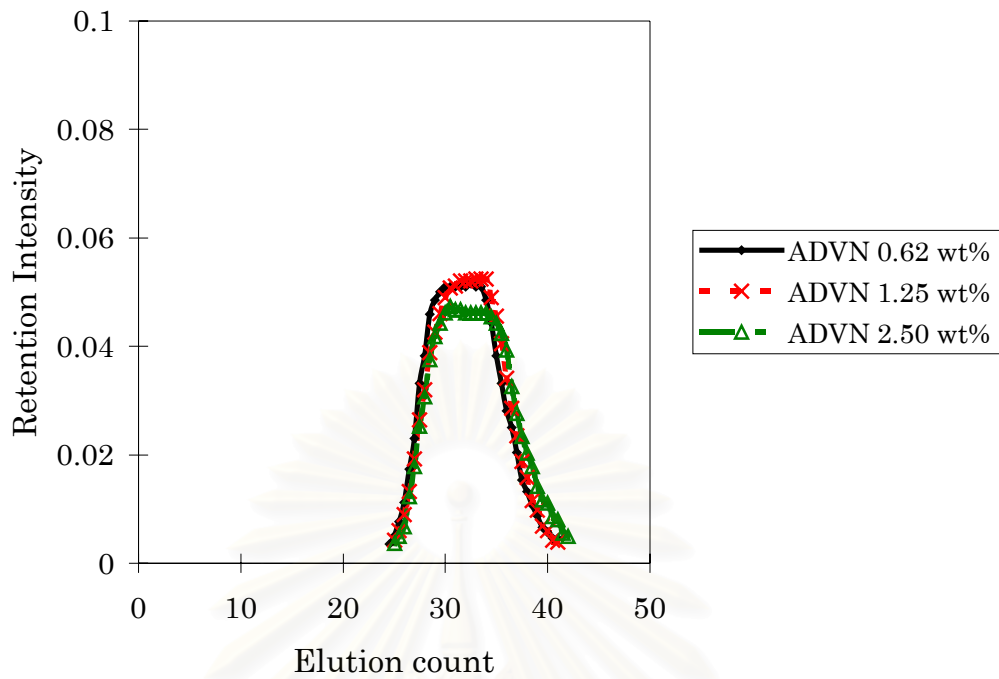


Figure 4.44 Normalized GPC chromatograms of poly(MMA-*co*-MA) particles showing the effects of ADVN concentrations.

สถาบันวิทยบริการ
จุฬาลงกรณ์มหาวิทยาลัย

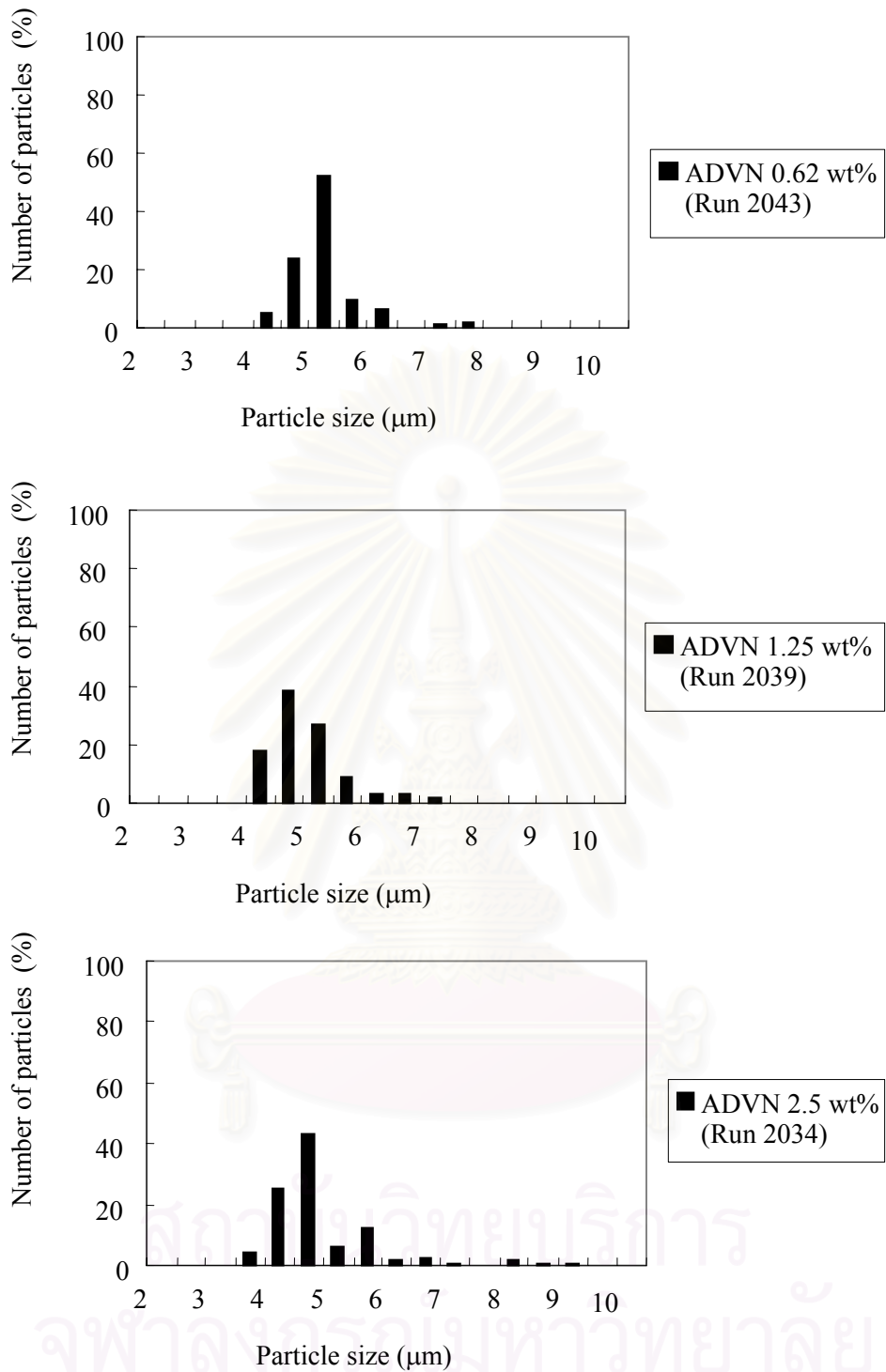


Figure 4.45 Particle size distribution of poly(MMA-co-MA) with different amounts of initiator

4.6.5 Synthesis of Poly(MMA-co-MA) with Various Additives

The polymerization recipe and experimental results are summarized in Table 4.13. The crosslinking agent, ethyleneglycol dimethacrylate (EGDMA) required to give fairly monodisperse crosslinked particles was added by 2 wt% of monomer into the oil phase (Runs 2036 and 2037). The addition of crosslinking agent was expected to increase the particle hardness and stabilize the shape. The reaction of EGDMA formed the nuclei of crosslinked copolymer, which became insoluble in water. However, an apparent phase separation was observed as shown in Figure 4.46d when the second additive, hexadecane (HD) was added by 1.25 wt% of the monomer mixture. The non-spherical particles with a head (snowman-like) were observed. This was induced by the incompatibility between hydrophobic HD and slightly hydrophilic monomer mixture of MMA-MA. Hexadecane played a role of hydrophobic additive in an emulsification, which stabilized the emulsion droplets, the solubility of HD in water is $3.6 \times 10^{-5} \text{ g dm}^{-3}$. It was isolated in the MMA-MA-rich phase (MMA is favored) [71,95,116,]. In monomer droplets, HD remains well-mixed with MMA-MA. As the polymerization progresses, HD starts to separate from copolymer-monomer mixture and gradually assembles to form several isolated domains. These domains move to the surface because of the light density. When the hydrophobic plasticizer like DOP was added at 5 wt% of monomer. DOP affects mostly and probably at the boundary between the oil phase and the continuous phase like HD does. Therefore, DOP can yield the stable emulsion droplets by promoting the interfacial tension between the monomer-phase and the water-phase and also increase the surface area.

Besides, in the absence of HD in the synthesis of the crosslinked MMA-MA copolymer (Run 2037), the spherical polymer particles were observed without any phase separation. One can assume that, the EGDMA crosslinker

promotes a good compatibility with the MMA-MA pairs due to the similar chemical structure of acrylate. Comparison with the addition of HD in non-crosslinked poly(MMA-*co*-MA) containing DOP at 5 wt%, they gave all the better results on monomer conversion (>80%; Run 2038), and no phase separation could be observed from the SEM photographs. No sign of coagulum was observed. HD-containing copolymer could also yield the smooth particle surface as shown in Figure 4.46d. In doubt, we do not realized its role whether HD is located close to the droplet interface or mixed homogeneously within each droplet. Fortunately, the copolymer revealed two separated T_g s for both the clean and unclean particles. Thus, a long chain alkane of HD should only exhibit hydrophobicity on the monomer surface as well as provide the similar property to any molecules inside the monomer droplets. The role of HD is to provide hydrophobicity to the relatively hydrophilic MMA-MA mixture and protect the SPG membrane from being wetted by the hydrophilic mixed-monomer dispersion.



สถาบันวิทยบริการ
จุฬาลงกรณ์มหาวิทยาลัย

Table 4.13 Recipe and results for methyl methacrylate and methyl acrylate using various additives

| Run No. | Composition | Monomer composition (wt%) | Monomer conversion (%) | D_e (μm) | CV_e (%) | D_p (μm) | CV_p (%) | $\overline{M}_n \times 10^{-4}$ | $\overline{M}_w \times 10^{-4}$ | PDI | T_g ($^{\circ}\text{C}$) clean | T_g ($^{\circ}\text{C}$) unclean |
|---------|------------------------------------|---------------------------|------------------------|-------------------------|------------|-------------------------|-------------------|---------------------------------|---------------------------------|-------------------|------------------------------------|--------------------------------------|
| 2010 | PMMA | 100 | 85.6 | 6.9 | 25.9 | Coag ^a | Coag ^a | 3.7 | 13.0 | 3.5 | 14.0 | 14.0 |
| 2035 | P(MMA- <i>co</i> -MA) | 50/50 | 79.9 | 5.6 | 22.8 | 5.4 | 14.5 ^a | 4.0 | 52.3 | 13.2 ^b | 29.5 | 25.3 |
| 2034 | P(MMA- <i>co</i> -MA) | 75/25 | 57.1 | 4.6 | 13.6 | 4.7 | 18.7 | 3.3 | 22.1 | 6.7 | 38.0 | 29.2 |
| 2036 | P(MMA- <i>co</i> -MA)/ EGDMA/HD | 50/50 EGDMA 2 wt% | 71.3 | 4.6 | 14.1 | 5.1 | 13.7 | na | na | na | 43.6 | 25.0 |
| 2037 | P(MMA- <i>co</i> -MA)/ EGDMA | 75/25 EGDMA 2 wt% | 61.2 | 7.4 | 18.3 | 7.3 | 14.1 | na | na | na | 32.4 | 23.9/105.1 |
| 2038 | P(MMA- <i>co</i> -MA)/ HD | 75/25 | 82.3 | 5.2 | 16.8 | 7.1 | 15.5 | 2.7 | 16.4 | 6.1 | 13.0/49.0 | 12.4/28.9 |

^a Coagulated particles were partially observed. ^b Bimodal curve, otherwise are unimodal.

5 wt% DOP was added for each experiment.

HD = hexadecane was added 1.25 wt% of monomer.

na = not available; no soluble fraction

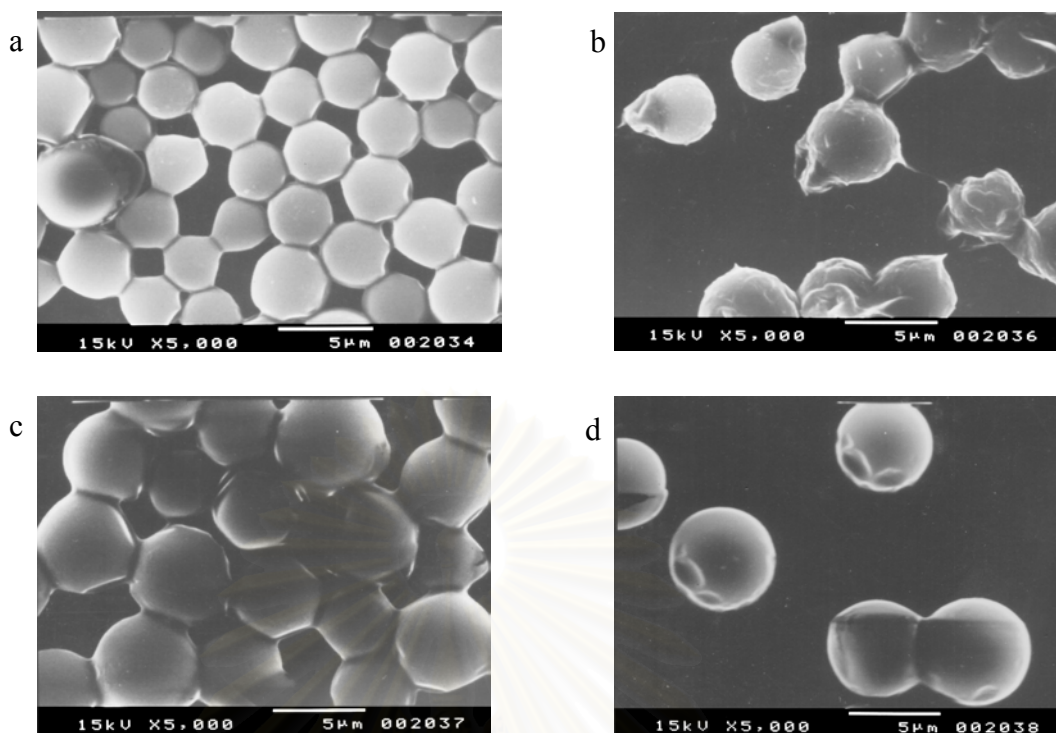


Figure 4.46 SEM photographs of poly(MMA-*co*-MA): a) poly(MMA-*co*-MA), MMA:MA of 75:25; b) poly(MMA-*co*-MA)/EGDMA/HD, MMA:MA of 50:50; c) poly(MMA-*co*-MA)/EGDMA, MMA:MA of 75:25; and d) poly(MMA-*co*-MA)/HD, MMA:MA of 75:25, DOP was added at 5 wt% of the monomer in each experiment.

4.7 Synthesis of Poly(MMA-*co*-BA) and Poly(MMA-*co*-BMA) Particles

The monomer mixtures of MMA-BA or MMA-BMA were polymerized in order to control the polymer T_g . We anticipated that the lower T_g monomers such as BMA and BA could function as an internal plasticizer, which was in-situ copolymerized with MMA monomer. The T_g values for all recipes were in the lower and higher regions shown in Table 4.14. However, the DSC measurement may be found inadequate since the polymer latex was partially separated into soft and hard layers in all experiments. After the latex was dried, the soft layer gave a yellowish color and was sticky compared with a powdery-like hard layer. In a series of

experiments using different initiator types, the composition of MMA-BA was fixed at MMA:BA ratio of 75:25 wt%. The external morphologies of polymers were found different as shown in Figures 4.47a and 4.47b. The smooth and softened surface was observed with close sticking of each particle. When BPO was used as the initiator in Run 2053, the secondary particles were observed in the latex and a fraction of which was attached on the particle surface (Figure 4.47b). Normally, the slow-decomposing initiator BPO with a half-life of 1049 min [128] gives a better stability of emulsion droplets in the aqueous phase than the fast-decomposing initiator, ADVN. However, the pathway of secondary nucleation may occur during the preparation of monomer droplets, since the SPG emulsification step for Run 2053 needed 20 h to complete in comparison with that of 2 h (Run 2055). The resulting external morphology in the latex obtained was viewed and found, the particles size was in a range of hundred nanometers as shown in Figure 4.47b. This finding is a good evidence to support the statement that the emulsion polymerization was initiated rather than the suspension polymerization. However, the lower average-molecular weight suggested that the polymerization took place by the suspension polymerization than emulsion polymerization.

สถาบันวิทยบริการ
จุฬาลงกรณ์มหาวิทยาลัย

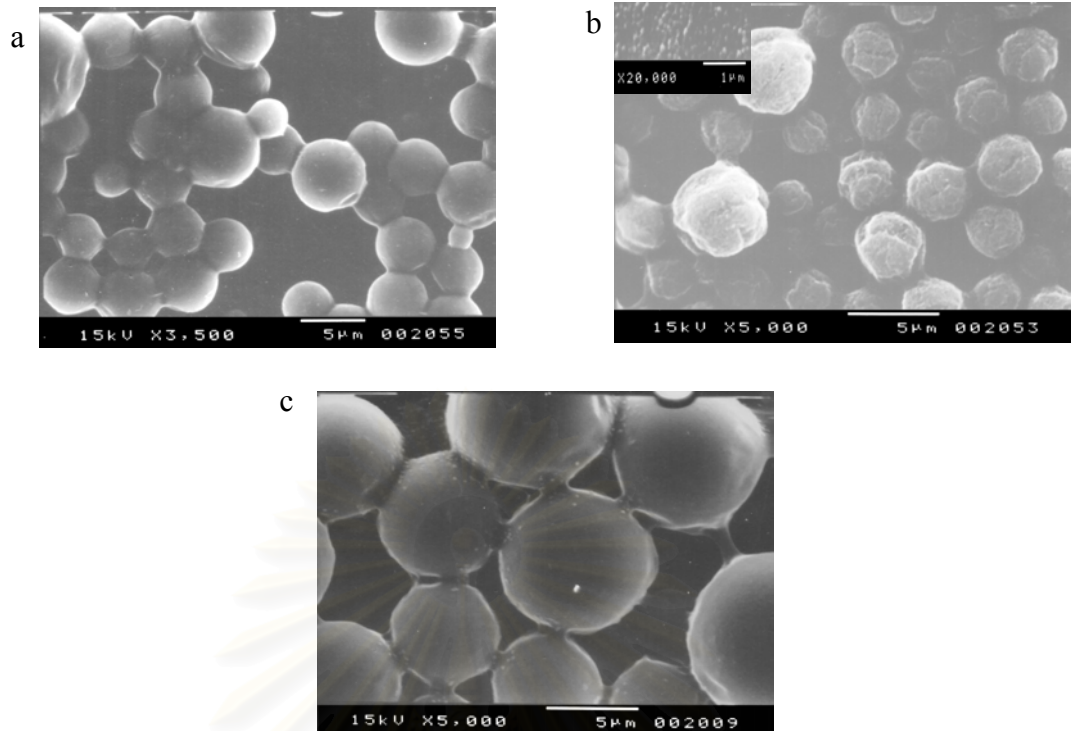


Figure 4.47 SEM photographs of a) poly(MMA-*co*-BA), MMA:BA of 75:25; ADVN initiator; b) poly(MMA-*co*-BA), MMA:BA of 75:25, BPO as initiator; c) poly(MMA-*co*-BMA), MMA:BMA of 50:50; BPO initiator.

Table 4.14 Recipe and results of methyl methacrylate and butyl acrylate, methyl methacrylate and butyl methacrylate copolymerization

| Run No. | Composition | Monomer composition (wt.%) | Monomer conversion (%) | D_e (μm) | CV_e (%) | D_p (μm) | CV_p (%) | $\overline{M}_n \times 10^{-4}$ | $\overline{M}_w \times 10^{-4}$ | PDI | T_g ($^{\circ}\text{C}$) clean | T_g ($^{\circ}\text{C}$) unclean |
|---------|---|----------------------------|------------------------|-------------------------|------------|-------------------------|------------|---------------------------------|---------------------------------|-----|------------------------------------|--------------------------------------|
| 2055 | P(MMA- <i>co</i> -BA), ADV N 2.5 wt% | 75/25 | 80.4 | 6.6 | 15.7 | 5.8 | 16.8 | 4.0 | 12.4 | 3.1 | 7.5/50.2 ^a | 13.5/44.3 ^a |
| 2053 | P(MMA- <i>co</i> -BA), BPO 2.5 wt% | 75/25 | 35.1 | 6.1 | 14.2 | 4.7 | 16.4 | 2.2 | 7.9 | 3.6 | 40.4 | 20.5/44.4/88.0 ^b |
| 2009 | P(MMA- <i>co</i> -BMA), BPO 2.5 wt% | 50/50 | 96.7 | 8.2 | 17.3 | 7.3 | 19.4 | 4.0 | 13.0 | 3.2 | 5.7 | na |

^a Two separate T_g values were observed. ^b Three separate T_g values were observed, otherwise was single T_g

na = not available

SPG membrane pore size 0.90 μm

4.8 Film Formation and Characterization

4.8.1 Polystyrene Cast Film

One layer of the styrene latex (Figure 4.48a, Run 2013) was cast on the glass substrate without further treatment. Then, the film was gradually dried under vacuum at room temperature for 48 h. Upon viewing the styrenic latex of Run 2013 by optical microscopy, it was found a randomly-packed array of the particles, while the film representing both transparent and opaque portions was observed. This may be because the polymerization routes for both suspension and emulsion polymerizations took place. Besides, the additional and possible cause was resulted from the low solid content in the polymer latex (ca. 6.7% solid). The SEM photograph shows that the small particles in a size range of 0.1 μm laid on the surface of substrate formed the transparent film, while the larger particles from the suspension polymerization became an opaque film. As described in Section 4.1.2, even though the external morphology of polymer particles was not affected by the inhibitor type, chemical structure of inhibitor controlled the optical appearance of polymer latex. It was found that the coalescence film cast from polystyrene with NaNO_2 as an inhibitor revealed the distribution of polymer particles in a size range of smaller than 5 μm embedded on the polymer film as the nanometer particles as shown in Figure 4.48a.

The particles of suspension polymerization becoming the opaque film as shown in Figures 4.48b to 4.48d, as a densely packed array of particles indicated that each particle contact each other to form a continuous boundary. However, the voids were present, particularly on the samples with a rather broad particle size distribution (Run 2016, CV = 16.1%) than that of the fairly uniform particle size distribution (Run 2014, CV = 11.2%).

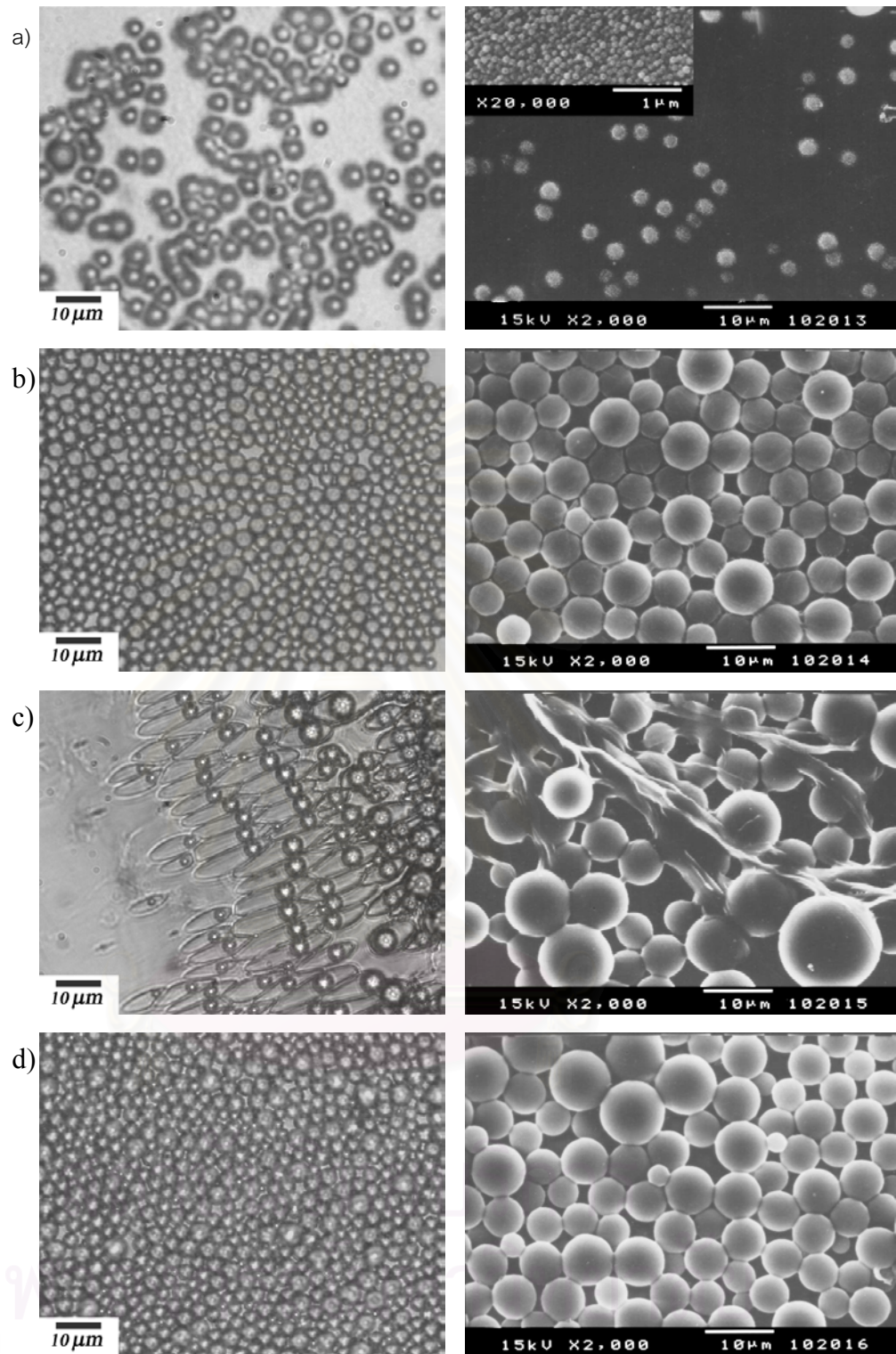


Figure 4.48 OM and SEM photographs of polystyrene film cast on the glass substrate: a) Run 2013 (a magnified image of secondary particles in the left corner); b) Run 2014; and c) Run 2015; and d) Run 2016 (Preparative conditions are in Tables 4.1 and 4.3).

4.8.2 Poly(St-co-MA) Cast Film

When T_g s of particles are much lower than the hard sphere of polystyrene, the densest packing of latex particles was obtained as shown in Figures 4.49a and 4.49b. The boundaries of a latex particle in a packed array was filled and closed by the lower glass transition of poly(St-co-MA). However, the particle size distribution of polymer particles was significantly important, since MA is more hydrophilic. The more differences in particle size, the greater the disorder of the coalescence particles.

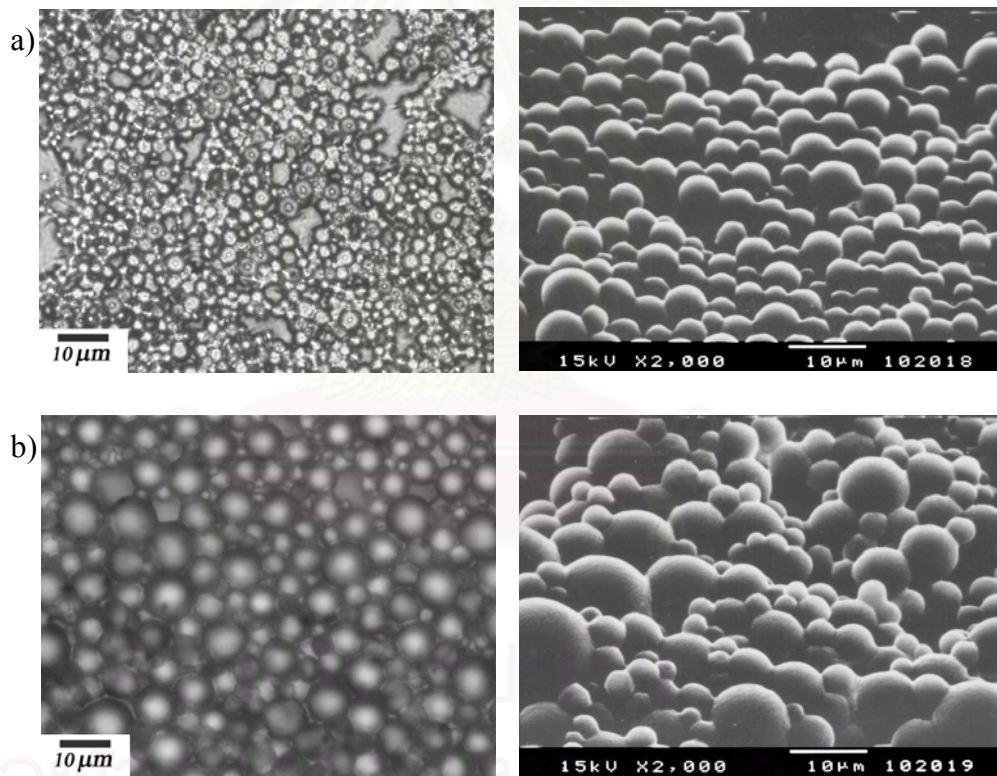


Figure 4.49 OM (left) and SEM photographs (right) taken at angle of 40° of poly(St-co-MA) particles: a) St:MA 50:50 (Run 2018); and b) St:MA 75:25 (Run 2019), SPG pore size of $0.51 \mu\text{m}$

So far, the membrane emulsification technique in a single-stage emulsion preparation step was limited to the more hydrophilic nature of dispersion phase. The pressure for monomer protrusion through the membrane pore was found unstable and jet stream-like monomer droplets formation occurred. Then, the fairly broad monomer droplets and polymer particles size distributions were obtained. As for the addition of PSt in the dispersion phase, the viscosity of the dispersion could be adjusted. As shown in Figures 4.50a and 4.50b, the film of copolymer was revealed a monolayer packed array. The fairly uniform poly(St-co-MA)/PSt was obtained.

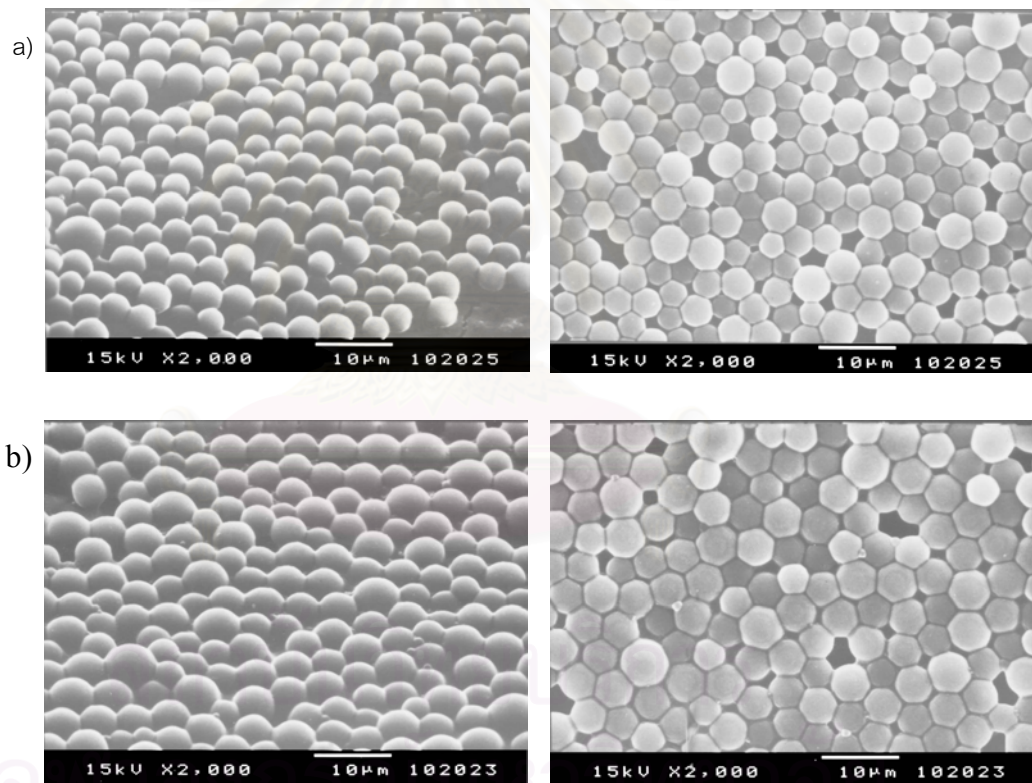


Figure 4.50 SEM photographs (left taken at an angle 40°), a) poly(St-co-MA)/PSt, St:MA:PSt 62.5:25:12.5 (Run 2025); b) poly(St-co-MA), St:MA 75:25 (Run 2023); SPG pore size of $0.90 \mu\text{m}$

A common way to manipulate the T_g of a polymer latex is by the addition of plasticizer or the use of low T_g polymer i.e. butyl methacrylate or butyl acrylate. The measured T_g s of the poly(St-co-BMA)/PSt are at about 17 and 66°C, for poly(St-co-BA)/PSt at 19 and 52°C, and poly(St-co-BA)/PSt with DOP 5 wt% at about 20°C. In the PSt-rich phase and PBA-or PBMA-rich phase, the higher T_g were supposed to be the T_g of the hard polymer phase. However, the external morphology of the polymer particles did not allow us to distinguish the differences of the deformation pattern. The dodecahedral structure of both films were found. All polymer samples appeared very similarly as the close-packed layer shown in Figures 4.51a to 4.51c.



สถาบันวิทยบริการ
จุฬาลงกรณ์มหาวิทยาลัย

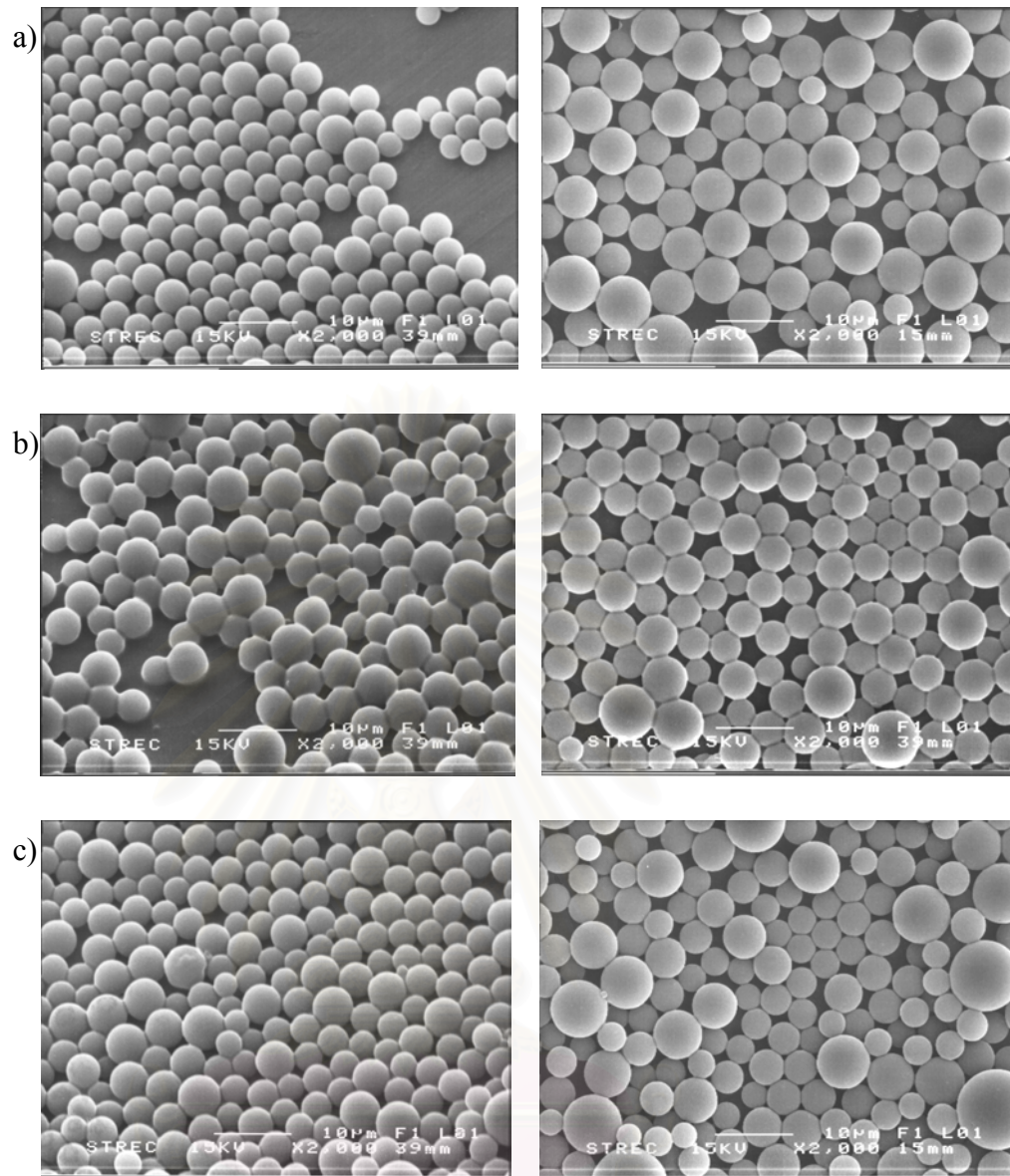


Figure 4.51 SEM photographs (left taken at angle of 30°), a) poly(St-co-BMA)/PSt (Run 2051); b) poly(St-co-BA)/PSt, (Run 2049); and c) poly(St-co-BA)/PSt/DOP, (Run 2050)

4.8.3 Structure of Film Surfaces Studied by Atomic Force Microscopy

AFM is a powerful technique for surface characterization, which is now well-established for latex film studies [1,129-132]. It can resolve objects on a micro-scale to nano-scale, thus enabling one to study fine details of the surface structure. According to the experimental set-up and measurement mentioned in Chapter 3, all the images were obtained in the contact mode, which showed only the topology of the surface in a three-dimensional image, but does not provide information about the chemical species involved. However, it is possible to make phase assignments of the film based on the difference in the glass transition temperature of the components if the phase separation occurred.

Table 4.15 Summary of AFM Observations

| | Run 2025 |
|---|----------|
| Average particle height; (R_z), (μm) | 1.96 |
| Surface roughness (R_a), (μm) | 0.365 |
| Surface area (μm^2) (100% = flat) | 0.143 |

The $10 \mu\text{m} \times 10 \mu\text{m}$ image area (z -range = $5 \mu\text{m}$) was chosen to show the best resolution of the copolymer spheres if possible. Peak and valley analysis was the measurement technique chosen for quantifying the size of the microspheres by defining the lateral spacing and the slope of the features. As opposed to the other analysis techniques that focused primarily on the z height component of the sample topography, the peak and valley analysis allow to predict the behavior of microspheres formed on the glass substrate as shown in Figure 4.52 and Table 4.15.

However, the results obtained by AFM was found limitation as its technique depended on greatly the polydispersity of polymer particles size. The peak-to-valley distance was to great for the limit of the measurement allowed. Therefore, the AFM analysis for polymer cast films cannot be investigated because no significant scientific data were obtained for further analysis. Image analysis of the polymer cast film by OM and SEM gave some useful information instead.

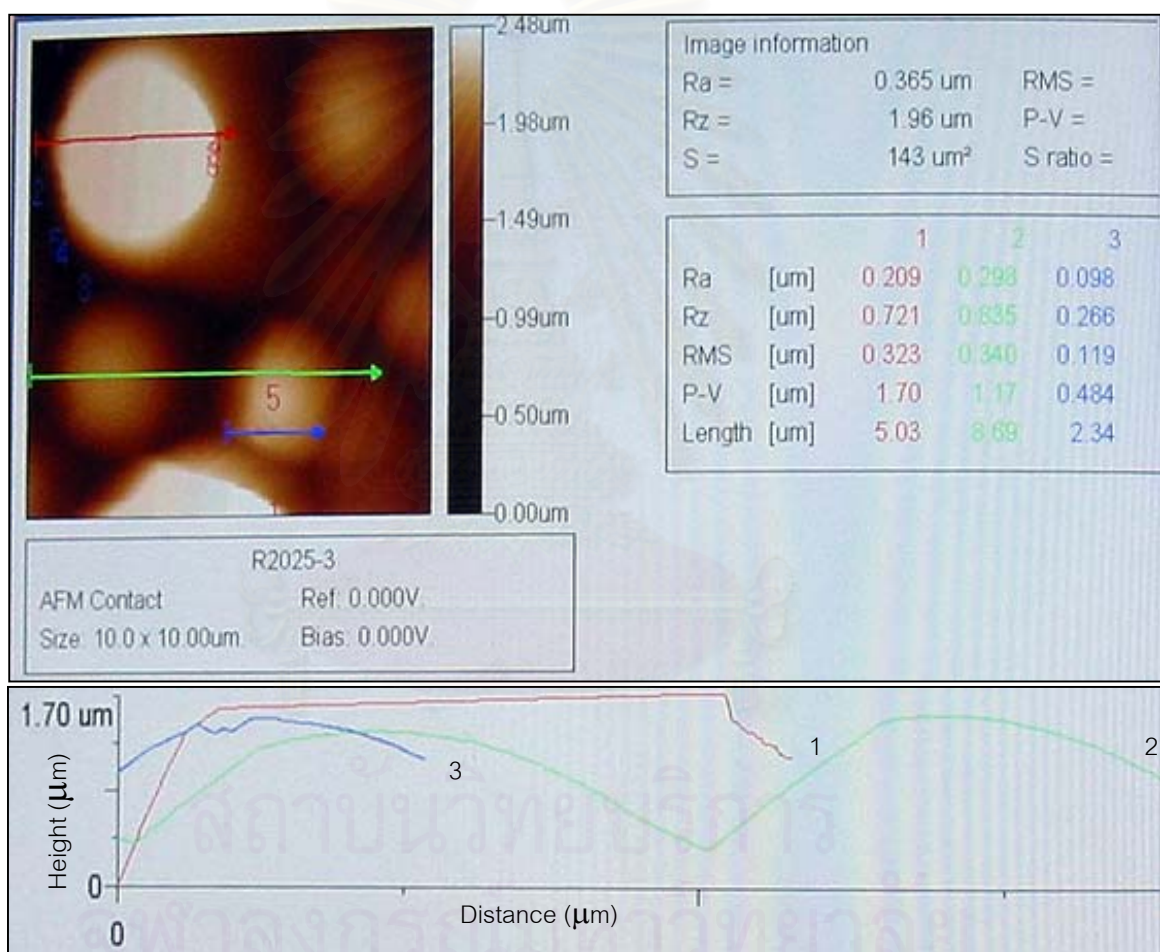


Figure 4.52 AFM image ($2.5 \mu\text{m} \times 2.5 \mu\text{m}$; z-range $5 \mu\text{m}$) recorded in air for poly(St-co-MA)/PSt, St:MA:PSt 62.5:25:12.5 (Run 2025).

CHAPTER 5

CONCLUSION

In this thesis, the application of membrane emulsification for synthesizing the copolymers in uniform droplets was investigated. The SPG emulsification and subsequent suspension polymerization were employed for the preparation of two-phase styrene-acrylate copolymer particles incorporating dioctyl phthalate (DOP) plasticizer. The influence of DOP on the styrene-acrylate polymerization was studied. It was found that both suspension and emulsion polymerizations took place, but the former controlled the polymerization course. Secondary nucleation generation and its deposition in the parent particles increased, when the pore size of SPG membrane decreased and the long emulsification time of the dispersed phase. A water-soluble inhibitor, NaNO_2 , was used to suppress the secondary nucleation, which was found more effective and no staining was needed when compared with hydroquinone or *p*-phenyldiamine (PDA).

The effects of DOP plasticizer on the critical pressure of emulsification, size distribution of monomer droplets, glass transition temperature of the copolymer, and morphologies of the particles were investigated. The DOP molecules were well mixed with the monomers in the initial stage of emulsification. Dependence of glass transition temperature on DOP was found significantly because it decreased the polymer glass transition temperature. The contribution of DOP to the polystyrene-based particles by significantly enhancing the mobility of the styrene backbone, which decreased T_g values of the copolymers.

Fairly uniform poly(St-*co*-MA) composite microspheres by SPG emulsification technique were carried out. The morphology of the composite particles could be controlled by adding DOP or varying the PSt/PMA ratio. When PSt was added, the core-shell morphology as microdomains was obtained in the absence of DOP. The slightly non-polar DOP preferentially plasticized the matrix phase of both the hard PSt and soft (meth)acrylate phases. Regardless of the monomer concentration ratios, the spherical polymer particles were resulted in the size ranging from 3 to 7 μm . Upon washing the polymer particles with methanol, DOP in the polymers was washed out, and two separate T_g peaks were observed. Micro-phase separation was found when the monomer droplets were formed at a later stage in the emulsification process. Small particles were then produced to give a broad molecular weight distribution.

A computer program based on the Skeist's equation was used to simulate the composition drift in copolymerization systems (St-MA, and MMA-MA). All the comonomer pairs understudy exhibited the composition drift during the copolymerization due to their large difference in monomer reactivity ratios, which was realized by the T_g values of the copolymers. In comparison, poly(MMA-*co*-MA) was synthesized by the same experimental method as for the poly(St-*co*-MA). The smooth and even spherical surface particles were obtained. The particles were soft and easily deformed by the electron beam. Poly(MMA-*co*-MA) revealed that they were well compatibilized with DOP, as shown by a single T_g value with a sharp transition found in both clean and unclean particles. Because of both DOP and acrylate polymer comprising a similar functional group (an ester), the physical interaction between them was significantly enhanced, which provided more compatible behavior. When the low T_g polymers are carefully produced, the polymer particles can be used for

surface coating applications without the inclusion of plasticizers, because film flexibility and low glass transition temperatures can be obtained directly from the inherent properties of the selected monomers and their corresponding copolymer. In addition, when including the moderately high molecular weight polystyrene in the monomer solution, or adding DOP as a plasticizer for the copolymer, properties and glass transition temperature of the DOP plasticized polymer are not so significantly different from the neat polymer.

The composite particles of poly(St-*co*-MA)/PSt were studied by varying the St/PSt ratio or DOP amount. The addition of PSt induced a high viscosity of the dispersion phase. The molecular weight slightly increased with increasing St/PSt concentration. The multiple phase separation of the St-rich phase and PMA domains observed by TEM, was caused by the composition drift because the MA reactivity ratio is greater than that of St. The addition of DOP revealed the more compatibility between the hard-St and soft-MA moieties than that without DOP.

The synthesis of poly(St-*co*-BMA) was carried out. The addition of 5 wt% of DOP based on the monomer concentration affected T_g of the copolymer. In the presence of DOP, the unclean particles gave a single T_g . The DOP could be washed out from the particles by methanol. Besides, the PBMA could also function as an internal plasticizer within its copolymer. The addition of PSt before polymerization produced the smooth surface of particles. A core-shell type polymer resulting from the phase separation between PSt and PBMA was found by TEM technique in which the PSt shell embraced the hydrophobic PBMA core.

Thermal behavior of poly(St-*co*-BA) revealed that BA itself also behaves like a plasticizing monomer as indicated by the single glass transition temperature found in all compositions of poly(St-*co*-BA) particles for both clean and unclean

samples. However, when PSt was dissolved in the St-BA monomer mixture, the poly(St-*co*-BA)/PSt only gave a single T_g value in the unclean particles. For the clean particles, two separate T_g values were found. The TEM photographs of the cross-section of the copolymer composite revealed that the lightly stained PSt granules were spread over the whole area of the particle. Another type of the phase separation of a salami-like morphology was also observed. The reactivity ratio was claimed to be the main factor, which induced the phase separation because the St monomer molecules were consumed faster at the beginning of the polymerization.

In conclusion, the influence of DOP on the glass transition temperature of copolymer was revealed. The copolymers with the lower glass transition temperature were obtained. The copolymer comprising the low T_g values of alkyl methacrylate monomers of MA, BMA and BA were successfully prepared. T_g values of the synthesized copolymers were in a good agreement with the calculated values based on Fox's equation. Effects of the DOP plasticizer on glass transition temperatures of poly(St-*co*-MA), poly(St-*co*-BMA), and poly(St-*co*-BA) particles demonstrate that the incompatibility between DOP and high T_g of PSt may provide a phase separation resulting in two separate T_g values. The different values of lower T_g and higher T_g of the copolymer were found as the following sequence:



Utmost interesting point is found as that poly(St-*co*-BA) incorporating DOP exhibited only one T_g value. It indirectly implies that both internal and external plasticizers are compatible with each other.

For the preparation of poly(MMA-*co*-MA), two different stabilizers were used. Since the MMA and MA are both slightly water-soluble, the selection of a suitable stabilizer type between PVP K-30 and PVA-217 is important. When PVA

was used as a stabilizer, more stable droplets of MMA/MA monomer were observed in comparison with the experiments using the PVP stabilizer because the mixture of MMA/MA was more hydrophilic than the mixture of St/MA. The former could then easily wet the membrane pores and disturbed permeation of the monomer droplets to result in the broad droplet size distribution of monomer droplets in all monomer compositions, producing the broadest size distribution in the MMA-to-MA ratio of 25:75. Besides, coagulation and lower monomer conversion occurred. The PMMA-MA particles could absorb some water during the polymerization because of the relatively hydrophilic copolymer chains. The water therein behaves like a plasticizer for the chains. During the drying period, the moisture was released and micro-voids were produced in the particles. T_g s of PMMA were found lower at 14°C for both clean and unclean particles, which was far away from their normal T_g of 100°C. T_g s for both clean and unclean copolymer samples were similar and closed to T_g of PMA. DOP added in this polymer was not effective as reflected in T_g values because the PMA polymer can plasticize the PMMA moiety.

Suggestions for Future Work

To make full utilization of this membrane technology in producing the hydrophilic copolymers like our present case of PMMA/PMA, the following steps should be performed.

1. Treatment of membrane surface to become hydrophobic or change the type of membrane
2. Adjusting the proper ratio of the composite hydrophilic monomer
3. Application of the two-step swelling emulsification for the preparation of fairly uniform polymer particles.

REFERENCES

1. Ton-That, C.; Shard, A.G.; Taere, D.O.H.; Bradly, R.H. APS and AFM surface studies of solvent-cast PS/PMMA blends. Polymer 42 (2001), 1121-1129.
2. Hill, A.J.; Tant, M.R.; McGill, R.L.; Shang, P.P.; Stockl, R.R.; Murray, D.L.; Cloyd, J.D. Free volume distribution during consolidation and coalescence of latex films. J. Coatings Tech. 73, (913) (2001), 115-124.
3. Webster, C. The development of a reduced coalescent latex binder system using the core shell technique. Surface Coatings Australia 35, (5) (1996), 24-27.
4. Strauss, J. A versatile all acrylic binder; environmentally friendly interior and exterior broadwall paints. Surface Coatings Australia 37, (6) (2000), 10-19.
5. Kobmann, H.; Schwartz, M. Acrylic and acrylic styrene copolymer dispersions modern binders for emulsion paints. Surface Coatings Australia 36, (12) (1999), 14-18.
6. Hatate, Y.; Ohta, H.; Uemura, Y.; Ijichi, K.; Yoshizawa, H. Preparation of monodispersed polymeric microspheres for toner particles by the Shirasu porous glass membrane emulsification technique. J. Appl. Polym. Sci. 64 (1997), 1107-1113.
7. Omi, S.; Kaneko, K.; Nakayama, A.; Katami, K.; Taguchi, T.; Iso, M.; Nagai, M.; G. Ma, G.H. Application of porous microspheres prepared by SPG emulsification as immobilizing carriers of glucoamylase (GluA). J. Appl. Polym. Sci. 65 (1997), 2655-2664.
8. Kandori, K.; Kishi, K.; Ishikawa, T. Preparation of uniform silica hydrogel particles by SPG filter emulsification method. Colloids Surf. 62 (1992), 259-262.

9. Nakashima, T.; Shimizu, M.; Kukizaki, M. Key Eng. Mater. 61-62 (1991), 513.
10. Lee, H.J.; Kim, J.H. Preparation of the large size polybutadiene latexes by membrane emulsification process. Membrane J. 6, (2) (1996), 166-172.
11. Kandori, K.; Kishi, K.; Ishikawa, T. Preparation of monodispersed W/O emulsions by Shirasu-porous-glass filter emulsification technique. Colloids Surf. 55 (1991), 73- 78.
12. Baba, Y.; Nakamura, S.; Fujimoto, K.; Ohe, K.; Shimizu, M.; Nakashima, T. Preparation of monodispersed chitosan microspheres using SPG membrane emulsification and its application as drug carriers.
Webpage: http://www.cape.canterbury.ac.nz/apcche_Proceedings/APCCHE/data/434rev.pdf; Dated 2003
13. Omi, S.; Katami, K.; Yamamoto, A.; Iso, M. Synthesis of polymeric microspheres employing SPG emulsification technique J. Appl. Polym. Sci. 51 (1994), 1-11.
14. Omi, S.; Katami, K.; Taguchi, T.; Kaneko, K.; Iso, M. Synthesis of uniform PMMA microspheres employing modified SPG (Shirasu porous glass) emulsification technique. J. Appl. Polym. Sci. 57 (1995), 1013-1024.
15. Omi, S.; Katami, K.; Taguchi, T.; Nagai, M.; Ma, G.H. Synthesis of 100 μm uniform porous spheres by SPG emulsification with subsequent swelling of the droplets. J. Appl. Polym. Sci. 63 (1997), 931-942.
16. Hatate, Y.; Uemura, Y.; Ijichi, K.; Kato, Y.; Hano, T.; Baba, Y.; Kawano, Y. Preparation of GPC packed polymer beads by a SPG membrane emulsification. J. Chem. Eng. Jpn. 28, (6) (1995), 656-659.
17. Miller, C.M.; Sudol, E.D.; Silebi, C.A.; El-Aasser, M.S. Miniemulsion polymerization of styrene: Evolution of the particle size distribution. J. Polym. Sci. A Polym Chem. 33 (1995), 1391-1408.

18. Omi, S.; Katami, K.; Taguchi, T.; Kaneko, K.; Iso, M. Synthesis and application of porous SPG (Shirasu porous glass) microspheres. Macromol. Symp. 92 (1995), 309-320.
19. Okubo, M.; Lu, Y. Production of core-shell composite polymer particles utilizing the stepwise heterocoagulation method. Colloids and Surf. A: Physicochem. Eng. Aspects 109 (1996), 49-53.
20. Lee, D.I. Morphology of two-stage latex particles: Polystyrene and styrene-butadiene copolymer pair systems; in "Emulsion polymer and emulsion polymerization", Edited by Bassett, D.R.; and Hamielec, A.E. 180th ACS National Meeting, August 25-29, 1980, Las Vegas, Nevada, pp. 405-414.
21. Sundberg, D.C.; and Eliasson, J.D. The prediction of particle size and molecular weight distributions in emulsion polymerization; in "Polymer colloids", Proceeding of the American Society Symposium on Polymer Colloids Sept 13-18, edited by Fitch, R.M. Chicago, Illinois, 1970. pp 153-161.
22. Sundberg, D.C.; Casassa, A.P.; Pantazopoulos, J.; Muscato, M.R.; Kronberg, B.; Berg, J. Morphology development of polymeric microparticles in aqueous dispersions. I. Thermodynamic considerations. J. Appl. Polym. Sci. 41 (1990), 1425-1442.
23. Muscato, M.R.; Sundberg, D.C. A note on the morphology of composite polymer particles. J. Polym Sci B: Polym Physics 29 (1991), 1021-1024.
24. Lee, S.; and Rudin, A. in "Control of Core-Shell Latex Morphology" Edited by Daniels, E.S.; Sudol, E.D.; El-Aasser, M.S. ACS Symposium Series 492, American Chemical Society, Washington D.C., 1992, pp. 234-254.

25. Chen, Y.C.; Dimonie, V.; El-Aasser, M.S. Interfacial phenomena controlling particle morphology of composite latexes. J. Appl. Polym. Sci. 42 (1991), 1049-1063.
26. Sundberg, E.J.; and Sundberg, D.C. Morphology development for three-component emulsion polymerization: Theory and experiments. J. Appl. Polym. Sci. 47 (1993), 1277-1298.
27. Shen, S.; El-Aasser, M.S.; Dimonie, V.; Vanderhoff, J.W.; Sudol, E.D. Preparation and morphological characterization of microscopic composite particles. J. Polym. Sci. A: Polym. Chem. 29 (1991), 857-867.
28. Winzor, C.L.; and Sundberg, D.C. Conversion dependent morphology predictions for composite emulsion polymers: 1. Synthetic lattices. Polymer 33, (18) (1992), 3797-3810.
29. Winzor, C.L.; and Sundberg, D.C. Conversion dependent morphology predictions for composite emulsion polymers: 2. Artificial lattices. Polymer 33, (20) (1992), 4269-4279.
30. Kirsch, S.; Pfau, A.; Stubbs, J.; Sundberg, D.C. Control of particle morphology and film structures of cooxylated poly(n-butyl acrylate)/ poly(methyl methacrylate) composite latex particles. Colloids Surf. A: Physicochem. Eng. Aspects 183-185 (2001), 725-734.
31. Ugelstad, J.; Mfutakamba, H.R.; Mørk, P.C.; Ellingsen, T.; Berge, A.; Schmid, R.; Holm, L.; Jorgedal, A.; Hansen, F.K.; Nustad, K. Preparation and application of monodisperse polymer particles. J. Polym. Sci. Polym. Symp. 72 (1985), 225-240.
32. Ugelstad, J.; Berge, A.; Ellingsen, T.; Helgee, B. Preparation of magnetic polymer particles. PCT Int. Appl. 83, (3) (1983), 920.

33. Rembaum, A.; Yen, R.S.K.; Kempner, D.H.; Ugelstad, J. Cell labeling and magnetic separation by immuno-reagents based on polyacrolein microspheres. J. Immunol. Methods 52 (1982), 341.
34. Ugelstad, J.; Kaggerud, K.H.; Hansen, F.K.; Berge, A. Absorption of low molecular weight compounds in aqueous dispersions of polymer-oligomer particles, 2a. A two step swelling process of polymer particles giving an enormous increase in absorption capacity. Makromol. Chem. 180 (1979), 737-744.
35. Ugelstad, J.; Mørk, P.C.; Mfutakamba, H.R.; Soleimany, E.; Nordhuus, I.; Schmid, R.; Berge, A.; Ellingsen, T.; Aune, O.; Nustad, K. in Science and Technology of Polym. Colloids, Vol. I, Poehlein, G.W.; Ottewill, R.H.; Goodwin, J.W. Eds., NATO ASI, Series E., Appl. Sci., No. 67, Nijhoff, Boston, 1983
36. Ugelstad, J.; Soderberg, L.; Berge, A.; Bergstrom, J. Monodisperse polymer particles - A step forward for chromatography. Nature 303 (May 5) (1983), 95-96.
37. Wilson, Webpage. <http://www.ameliaww.com/fpin/phthalates.htm>; Dated 1995
38. Darby, J.; Sears, R.; Kern, J. Theory of Solvation and Plasticization; Encyclopedia of PVC, Volume 1. Chapter 10, Edited by Nass, L.J. New York: Marcel Dekker, 1976, pp. 386-503.
39. Krauskopf, L.G. Plasticizer; Encyclopedia of PVC, Volume 1. Chapter 11, Edited by Nass, L.J. New York: Marcel Dekker, 1976, pp. 505-592.
40. Sears, J.K.; Darby, J.R. in "The Encyclopedia of Plasticizers". New York: John Wiley & Sons, 1982.
41. O'Brien, J. Plasticizer in "Modern Plastics Encyclopedia", 1986-1987., McGraw Hill, 1986, pp. 166-168.

42. Resistance of Plastic Films to Extraction by Chemicals. ASTM D-1239.
43. Couchman, P.R. Compositional variation of glass-transition temperatures. 2.
Application of the thermodynamic theory to compatible polymer blends.
Macromolecules 11, (6) (1978), 1156-1161.
44. Couchman, P.R. Compositional variation of glass-transition temperatures. 7.
Copolymer. Macromolecules 15 (1982), 770-773.
45. Fox, T.G. Bull. Am. Phys. Soc. 1 (1956), 123.
46. Lee, W.A.; and Rutherford, R.A. "The Glass transition temperatures of polymer,"
in J. Brandrup and E.H. Immergut, Eds., Polymer Handbook. 2nd ed., Wiley,
New York, 1995, pp. III/139-192.
47. Lesko, P.M.; and Sperry, P.R. "Acrylic and Styrene-Acrylic Polymers," in P.A.
Lowell and M.S. El-Aasser, Emulsion Polymerization and Emulsion
Polymers, Eds., Wiley, New York, 1997, pp. 622-623.
48. Flory, P.J. Principles of Polymer Chemistry, Cornell University Press, New York,
USA. 1953.
49. Brandup, J.; Immergut, E.H.; Gruke, E.A. in "Polymer Handbook", 4th Edition,
Wiley, New York, 1999, pp. VII /675-711.
50. Schröder, V.; and Schubert, H. Production of emulsions using microporous,
ceramic membrane. Colloids and Surf. A: Physicochem. Eng. Aspects 152
(1999), 103-109.
51. Nakashima, T.; Shimizu, M.; Kukizaki, M. in "Membrane emulsification
operation manual", 1st Edition, Dept. of Chemistry, Industrial Research
Institute of Miyazaki Prefecture, Miyazaki, Japan, 1991
52. Nakashima, T.; and Shimizu, M. Ceramics 21 (1986), 408.

53. Tsuno, T. Alkyl-containing porous resin process for its preparation and its use.
United States Patent No. 5880240, Mar.9, 1999, pp. 1-22.
54. SPG Technology Co., Ltd, Applications of SPG membrane, Webpage:
http://www.mnet.ne.jp/~spg/00_e/spgtec/index.html; Dated 2002
55. Takagi, R.; Nakagaki, M. Membrane charge of microporous glass membrane determined by the membrane potential methods and its pore size dependency.
J. Membrane Sci. 111 (1996), 19-26.
56. Yasuno, M.; Nakajima, M.; Iwamoto, S.; Maruyama, T.; Sugiura, S.; Kobayashi, I; Shono, A.; Satoh, K. Visualization and characterization of SPG membrane emulsification. J. Membrane Sci. 210 (2002), 29-37.
57. Schröder, V.; Behrend, O.; Schubert, H. Effect of dynamic interfacial tension on the emulsification process using microporous, ceramic membranes J. Colloids Interfaces Sci. 202 (1998), 334-340.
58. Joscelyne, S.M.; Trägårdh, G. Membrane emulsification- a literature review. J. Membrane Sci. 169 (2000), 107-117.
59. Mine, Y.; Shimizu, M.; Nakashima, T. Preparation and stabilization of simple and multiple emulsions using a microporous glass membrane. Colloids Surf. B: Biointerfaces 6 (1996), 261-268.
60. Christov, N.C.; Ganchev, D.N.; Vassileva, N.D.; Denkov, N.D.; Danov, K.D.; Kralchevsky, P.A. Capillary mechanisms in membrane emulsification: oil-in-water emulsions stabilized by Tween 20 and milk proteins. Webpage:
<http://www.lcpe.unisofia.bg/publications/2002/pdf/2002-03-PK.pdf>; Dated 2001

61. Kandori, K.; Kishi, K.; Ishikawa, T. Formation mechanisms of monodispersed W/O emulsions by SPG filter emulsification method. Colloids Surf. 61 (1991), 269-279.
62. Kandori, K.; Kishi, K.; Ishikawa, T. Preparation of monodispersed W/O emulsions by Shirasu-porous-glass filter emulsification technique. Colloids Surf. 55 (1991), 73-78.
63. Higashi, S.; Tabata, N.; Kondo, K.; Maeda, Y.; Shimizu, M.; Nakashima, T.; Setoguchi, T. Size of lipid microdroplets effects results of hepatic arterial chemotherapy with an anticancer agent in water-in-oil-in-water emulsion to hepatocellular carcinoma. J Pharmacol Exp Ther. 289 (1999), 816-819.
64. Vladisavljevic, G.T.; and Schubert, H. Preparation and analysis of oil-in-water emulsions with a narrow droplet size distribution using Shirasu-porous-glass (SPG) membranes. Desalination 144 (2002), 167-172.
65. Yuyama, H.; Watanabe, T.; Ma, G.H.; Nagai, M.; Omi, S. Preparation and analysis of uniform emulsion droplets using SPG membrane emulsification technique. Colloids Surfaces A: Physicochem. Eng. Aspects 168 (2000), 159-174.
66. Eckersley, S.T.; Rudin, A. Mechanism of film formation from polymer latexes. J. Coating Tech. 62, (780) (1990), 89-100.
67. Jensen, D.P.; Morgan, L.W. Particle size as it relates to the minimum film formation temperature of latices. J. Appl. Polym. Sci. 42 (1991), 2845-2849.
68. Wirth, T.; Pfoehler, P. The film formation and properties of polymer dispersion. Surf. Coating Australia. 33, (5) (1995), 14-22.

69. Du Chesne, A.; Bojkova, A.; Stöckelmann, E.; Krieger, S.; Heldmann, C.
Determination the compacting of latex films upon drying by interference measurements-an approach for the investigation of film formation. Acta Polym. 49 (1998), 346-355.
70. Routh, A.F.; Russel, W.B.; Tang, J.; El-Aasser, M.S. Process model for latex film formation: Optical clarity fronts. J. Coatings Tech. 73, (916) (2001), 41-48.
71. Landfester, K.; Bechthold, N.; Forster, S.; Antonietti, M. Evidence for the preservation of the particle identity in miniemulsion polymerization. Macromol. Rapid Commun. 20 (1999), 81-84.
72. Meincken. M.; Sanderson, R.D. Determination of the influence of polymer structure and particle size on the film formation process of polymers by atomic force microscopy. Polymer 43 (2002), 4947-4955.
73. Feng, J.; Winnik, M.; Shivers, R.; Clubb, B. Polymer blend latex films: Morphology and transparency. Macromolecules 28 (1995), 7671-7682.
74. Winnik, M.A.; Wang, Y.; Haley, F. Latex film formation at the molecular level: The effect of coalescing aids on polymer diffusion. J. Coatings Tech. 64, (811) (1992), 51.
75. Hoy, K.L. Estimating the effectiveness of latex coalescing aids, J. Paint Tech. 45, (579) (1973), 51-56.
76. Shiomori, K.; Hayashi, T.; Baba, Y.; Kawano, Y.; Hano, T. Hydrolysis rates of olive oil by lipase in a monodispersed O/W emulsion system using membrane emulsification. J. Fermentation Bioengineering 80, (6) (1995), 552-558.

77. Hosoya, K.; Ohta, H.; Yoshizako, K.; Kimata, K.; Ikegami, T.; Tanaka, N. Preparation of uniformly for small-scale high-performance liquid chromatography and/or capillary electrochromatography. J. Chromatography A 853 (1999), 11-20.
78. Ha, Y.K.; Song, H.S.; Lee, H.J.; Kim, J.H. Preparation of core particles for toner application by membrane emulsification. Colloids Surf. A: Physicochem. Eng. Aspects 162 (1999), 289-293.
79. Supsakulchai, S.; Ma, G.H. Nagai, M.; Omi, S. Microencapsulation of fine titanium dioxide powder from (S/O)/W emulsion with subsequent solvent evaporation. ACS symposium series 801: Polymer Colloids Science and Technology of Latex Systems, Editors Daniel, E.S.; Sudol, E.D.; El-Aasser, M.S., American Chemical Society, Washington DC, 2002, pp. 260-275.
80. Supsakulchai, S.; Ma, G.H. Nagai, M.; Omi, S. Uniform titanium dioxide (TiO₂) microcapsules prepared by glass membrane emulsification with subsequent solvent evaporation. J. Microencapsulation. 19, (4) (2002), 425-449.
81. You, J.O.; Park, S.B.; Park, H.Y.; Haam, S.; Chung, C.H.; Kim, W.S. Preparation of regular size Ca-alginate microspheres using membrane emulsification method. J. Microencapsulation. 18, (4) (2001), 521-532.
82. El-Mahdy, M.; Ibrahim, E.S.; Safwat, S.; El-Sayed, A.; Ohshima, H.; Makino, K.; Muramatsu, N.; Kondo, T. Effects of preparation conditions on the monodispersity of albumin microspheres. J. Microencapsulation. 15, (5) (1998), 661-673.
83. Nakajima, M.; Kikuchi, Y.; Kawakatsu, T. Method and device for producing emulsions. United States Patent, No. 6155710, Dec. 5 (2000), 1-7.

84. Sugiura, S.; Nakajima, M.; Tong, J.; Nabetani, H.; Seki, M. Preparation of monodispersed solid lipid microspheres using a microchannel emulsification technique. J. Colloid Interface Sci. 227 (2000), 95-103.
85. Nakajima, M. Novel microchannel system for monodispersed microspheres. RIKEN Review: Focused on Science and Technology in Micro/Nano Scale 36 (2001), 21-23.
86. Liu, X.; Nakajima, M.; Nabetani, H.; Xu, Q.Y.; Ichikawa, S.; Sano, Y. Stability characteristics of dispersed oil droplets prepared by the microchannel emulsification method. J. Colloid Interface Sci. 233 (2001), 23-30.
87. Nisisako, T.; Torii, T.; Higuchi, T. Rapid preparation of monodispersed droplets with confluent laminar flows: Webpages: http://droptech.pe.u-tokyo.ac.jp/pub_pdf/nisisako/MEMS2003_Tp25.pdf; Dated 2003
88. Partch, R.E.; Matijevic, E.; Hodgson, A.W.; Aiken, B.E. Preparation of polymer colloids by chemical reactions in Aerosols. I. Poly(p-tertiarybutylstyrene). J. Polym. Sci., Polym. Chem. Ed. 21 (1983), 961-967.
89. Panagiotou, T.; and Levendis, Y.A. Generation of spherical and monodisperse particles of poly(styrene) and poly(methyl methacrylate) by atomization of monomers and dissolved polymer precursors. J. Appl. Polym. Sci. 43 (1991), 1549-1558.
90. Tawonsree, S.; Omi, S.; Kiatkamjornwong, S. Control of various morphological changes of poly(meth)acrylate microspheres and their swelling degrees by SPG emulsification. J. Polym. Sci. A: Polym. Chem. 38 (2000), 4038-4056.

91. Ma, G.H. Mechanism of formation of monodisperse polystyrene hollow particles prepared by membrane emulsification technique. Effect of hexadecane amount on the formation of hollow particles. Macromol. Symp. 179 (2002), 223-240.
92. Ma, G.H.; Omi, S.; Dimonie, V.L.; Sudol, E.D.; El-Aasser, M.S. Study of the preparation and mechanism of formation of hollow monodisperse polystyrene microspheres by SPG (Shirasu Porous Glass) emulsification technique. J. Appl. Polym. Sci. 85 (2002), 1530-1543.
93. Ma, G.H.; Su, Z.G.; Omi, S.; Sundberg, D.; Stubbs, J. Microencapsulation of oil with poly(styrene-N,N-dimethylaminoethyl methacrylate) by SPG emulsification technique: effects of conversion and composition of oil phase. J. Colloid Interface Sci. 266 (2003), 282-294.
94. Kiatkamjornwong, S.; Nuisin, R.; Ma, G.H.; Omi, S. Synthesis of styrenic toner particles by SPG emulsification technique. Chinese J. Polym. Sci. 18, (4) (2000), 309.
95. Nuisin, R.; Ma, G.H.; Omi, S.; Kiatkamjornwong, S. Dependence of morphological changes of polymer particles on hydrophobic/hydrophilic additives. J. Appl. Polym. Sci. 77 (2000), 1013-1028.
96. Omi, S.; Senba, T.; Nagai, M.; Ma, G.H. Morphology development of 10- μ m scale polymer particles prepared by SPG emulsification and suspension polymerization. J. Appl. Polym. Sci. 79 (2001), 2200-2220.
97. Ma, G.H.; Nagai, M.; Omi, S. Study on preparation and morphology of uniform artificial polystyrene-poly(methyl methacrylate) composite microspheres by employing the SPG (Shirasu Porous Glass) membrane emulsification technique. J. Colloids Interface Sci. 214 (1999), 264-282.

98. Tokarev, V.S.; Voronov, S.A.; Adler, H.P.; Datzuk, V.V.; Pich, A.Z.; Shevchuk, O.M.; Myahkostupov, M.V. Application of peroxide macroinitiators in core-shell technology for coating improvements. Macromol. Symp. 187 (2002), 155-164.
99. Ma, A.; Sauer, J.A.; Hara, M. Influence of plasticizers on poly(methyl methacrylate) ionomers. Polymer 38, (17) (1997), 4425-4431.
100. Lin, S.Y.; Chen, K.S.; Chu, L.R. Organic esters of plasticizers affecting the water absorption, adhesive property, glass transition temperature and plasticizer permanence of Eudragit acrylic films. J. Controlled Release. 68 (2000), 343-350.
101. Shieh, Y.T.; Liu, C.M. Influences of contents and molecular weights of LDPE on DOP plasticization of PVC. J. Appl. Polym. Sci. 83 (2002), 2548-2555.
102. Kovačić, T.; and Mrklič, Ž. The kinetic parameters for the evaporation of plasticizers from plasticized poly(vinyl chloride). Thermochimica 381 (2002), 49-60.
103. Webpage: http://invsee.asu.edu/srinivas/pdf/AFM_of_Polystyrene.pdf; Dated 2003
104. Zhlong, Q.; Innis, D.; Kjoller, K.; Elings, V.B. Surf. Sci. 290 (1993) L688
105. Magonov, S.N.; Elings, V.; Whangbo, M.H. Surf. Sci. 375 (1997) L385.
106. Lemoine, P.; McLaughlin, J. Nanomechanical measurements on polymers using contact mode AFM. Surface Topography Applications Rev. A 2/98, 16 (1998). Webpage: <http://www.eetasia.com/articles/2001Sep/2001Sep12ICTAN9.PDF>; Dated 2001

107. Sudol, E.D.; El-Aasser, M.S.; Vanderhoff, J.W. Kinetics of successive seeding of monodisperse polystyrene latexes. II. Azo initiators with and without inhibitors. J. Polym. Sci. A: Polym. Chem. 24 (1986), 3515-3527.
108. Omi, S. Private Communication December 5 (1998).
109. Brandup, J.; Immergut, E.H.; Gruke, E.A. in "Polymer Handbook", 4th Edition. New York: John Wiley, 1999; Sec. II, pp. 182-216.
110. Odian, G. in "Principles of Polymerization", 3rd ed. Singapore, John Wiley, 1991, pp. 460-466.
111. Zhao, Y.; and Urban, M.W. Novel STY/nBA/GMA and STY/nBA/MAA core-shell latex blends: Film formation, particle morphology, and cross-linking. 2). A spectroscopic study. Macromolecules 33 (2000), 8426-8434.
112. Kato, K. Polym. Lett. 35 (1966), 4.
113. Schulze, U.; Pompe, G.; Meyer, E.; Janke, A.; Pionteck, J.; Fiedlerová, A.; Borsig, E. IPN-like systems based on polyethylene and methacrylates. Polymer 36 (1995), 3393-3398.
114. Graber, C. SPI Co. Ltd., Private communication, December 2003.
115. Vitali, R.; and Montani, E. Ruthenium tetroxide as a staining agent for unsaturated and saturated polymers. Polymer 21 (1980), 1220-1222.
116. Nuisin, R. Synthesis of Super-fine particles of poly(styrene-co-methyl methacrylate) by SPG emulsion polymerization. Masters Thesis, Chulalongkorn University, 1999
117. Balke, S. T.; Hamielec, A. E. Bulk polymerization of methyl methacrylate. J. Appl. Polym. Sci., 17, (3) (1973), 905-949.
118. Soh, S.K.; Sundberg, D.C. Diffusion-controlled vinyl polymerization. I. The gel effect. J. Polym. Sci. Polym. Chem. Ed. 20 (1982), 1299-1313.

119. Soh, S.K.; Sundberg, D.C. Diffusion-controlled vinyl polymerization. II. Limitations on the gel effect. J. Polym. Sci. Polym. Chem. Ed. 20 (1982), 1315-1329.
120. Soh, S.K.; Sundberg, D.C. Diffusion-controlled vinyl polymerization. III. The volume parameters and diffusion-controlled propagation. J. Polym. Sci. Polym. Chem. Ed. 20 (1982), 1231-1344.
121. Soh, S.K.; Sundberg, D.C. Diffusion-controlled vinyl polymerization. IV. Comparison of theory and experiment. J. Polym. Sci. Polym. Chem. Ed. 20 (1982), 1345-1371.
122. Yang, H.J.; Yang, C.H. Statistical Experimental strategies approach to emulsion copolymerization of styrene and *n*-butyl acrylate. J. Appl. Polym. Sci. 69 (1998), 551-563.
123. Cruz-Rivera, A.; Rios-Guerrero, L.; Monnet, C.; Schlund, B.; Guillot, J.; Pichot, C. Structure-property relationships in styrene-butyl acrylate emulsion copolymers: 1. Preparation and characterization of latexes. Polymer 30, (10) (1989), 1872-1882.
124. Schlund, B.; Guillot, J.; Pichot, C.; Cruz, A. Structure-property relationships in styrene-butyl acrylate emulsion copolymers: 2. Viscoelastic properties of latex films-experimental results and simulation. Polymer 30, (10) (1989), 1883-1893.
125. Xu, X.; Ge, X.; Zhang, Z.; Zhang, M. Copolymerization of styrene with acrylates in emulsion and microemulsion. Polymer 39, (22) (1998), 5321-5325.

126. Tseng, C.M.; Lu, Y.Y.; El-Aasser, M.S.; Vanderhoff, J.W. Uniform polymer particles by dispersion polymerization in alcohol. J. Polym. Sci. A: Polym. Chem. 24 (1986), 295.
127. Wu, C.W.; Lee, J.G.; Lee, W.C. Biotechnol. Appl. Biochem. 27 (1998), 225.
128. Nomura, N.; Yamada, A.; Fujita, S.; Sugimoto, A.; Ikoma, J.; Fujita, K. Kinetics and mechanism of emulsion polymerization initiated by oil-soluble initiators. II. Kinetic behavior of styrene emulsion polymerization initiated by 2,2'-azoisobutyronitrile. J. Polym. Sci. A. Polym. Chem. 29 (1991), 987-994.
129. Vorobyova, O.; Winnik, M.A. Morphology of poly(2-ethylhexyl methacrylate): poly(butyl methacrylate) latex blend films. Macromolecules 34 (2001), 2298-2314.
130. Jandt, K.D.; Finke, M.; Cacciafesta, P. Aspects of the physical chemistry of polymers, biomaterials and mineralised tissues investigated with atomic force microscopy (AFM). Colloids Surf. B: Biointerfaces 19 (2000), 301-314.
131. Steward, P.A.; Hearn, J.; Wilkinson, M.C. An overview of polymer latex film formation and properties. Adv. Colloid Interface Sci. 86 (2000), 195-267.
132. Tamai, T.; Pinenq, P.; Winnik, M.A. Effect of cross-linking on polymer diffusion in poly(butyl methacrylate-co-butyl acrylate) latex films. Macromolecules 32 (1999), 6102-6110.
133. Omi, S. Private communication, October 2002.

Skeist equation:

$$\frac{dZ_A}{dx} = -\frac{y_A - Z_A}{1-x} \quad (\text{A-1})$$

Lewis-Mayo equation:

$$y_A = \frac{(r_A Z_A + Z_B) Z_A}{(r_A Z_A + Z_B) Z_A + (Z_A + r_B Z_B) Z_B}, \quad Z_B = 1 - Z_A \quad (\text{A-2})$$

From the material balance of monomer A:

$$Y_A = \frac{Z_{A0} - Z_A(1-x)}{x} \quad (\text{A-3})$$

r_A, r_B = reactivity ratio of monomer A and B. From Eq. A-2, y_A is solely dependent on Z_A and Eq. A-1 can be numerically integrated by employing the modified Euler method.

The increment of integration, Δx , is set as 0.001. The initial condition is as follows.

$$x=0, \quad Z_A=Z_{A0} \quad (\text{A-4})$$

The calculated results for the copolymerizations Styrene-MA and MMA-MA are summarized in Table A-1 to A-6. Notice that the shift of the instantaneous copolymer composition against the total monomer composition directly corresponds to the composition distribution.

APPENDIX

FUNDAMENTAL EQUATIONS FOR OBTAINING RELATIONSHIPS BETWEEN Z_A , Y_A , y_A AND X

For the purpose of calculating composition drift in the copolymerization for predicting the tendency of morphology development, a computer program [133] was developed based on the terminal model and the assumption that the polymerization in the droplets proceeded as homogeneous phase process. The model can essentially predict the course of composition drift in homogeneous phase copolymerization by applying the Skeist equation (Eq. A-1) and the equation derived from the Lewis-Mayo theory (Eq. A-2). Eq. A-3 can be obtained from simple material balance of monomer A.

The basic assumptions are that:

1. The composition of the copolymers can be described with the terminal model.
2. The partition of moderately water-soluble monomers, MMA and MA, in the aqueous phase can be neglected from the assumption that a majority of unreacted monomers are distributed in the droplets.

where Y_A = cumulative composition of monomer A in copolymer.

y_A = instantaneous composition of monomer A in copolymer.

z_A = composition of monomer A remained in unreacted monomer.

All these quantities are expressed in mole fraction.

x = overall conversion of monomer.

Skeist equation:

$$\frac{dZ_A}{dx} = -\frac{y_A - Z_A}{1 - x} \quad (\text{A-1})$$

Lewis-Mayo equation:

$$y_A = \frac{(r_A Z_A + Z_B)Z_A}{(r_A Z_A + Z_B)Z_A + (Z_A + r_B Z_B)Z_B}, Z_B = 1 - Z_A \quad (\text{A-2})$$

From the material balance of monomer A:

$$Y_A = \frac{Z_{A0} - Z_A(1 - x)}{x} \quad (\text{A-3})$$

r_A, r_B = reactivity ratio of monomer A and B. From Eq. A-2, y_A is solely dependent on Z_A and Eq. A-1 can be numerically integrated by employing the modified Euler method. The increment of integration, Δx , is set as 0.001. The initial condition is as follows.

$$x=0, Z_A=Z_{A0} \quad (\text{A-4})$$

The calculated results for the copolymerizations Styrene-MA and MMA-MA are summarized in Table A-1 to A-6. Notice that the shift of the instantaneous copolymer composition against the total monomer composition directly corresponds to the composition distribution.

Table A-1 Calculated cumulative composition of styrene in poly(St-co-MA); **YA** vs **x**Monomer 1 = Styrene $r_{St} = 0.192$ Monomer 2 = MA $r_{MA} = 0.800$

| x | zA0 | 0.453 | 0.713 | 0.2 | 0.4 | 0.5 | 0.8 | 0.9 | 0.95 |
|-------|--------|--------|--------|--------|--------|--------|--------|--------|--------|
| | 0 | 0.3709 | 0.5277 | 0.1997 | 0.3389 | 0.3984 | 0.5957 | 0.7147 | 0.8169 |
| 0.025 | 0.3715 | 0.5293 | 0.1997 | 0.3394 | 0.3991 | 0.598 | 0.7185 | 0.8212 | |
| 0.05 | 0.3723 | 0.5313 | 0.1997 | 0.34 | 0.4001 | 0.6009 | 0.7228 | 0.8259 | |
| 0.1 | 0.3735 | 0.5347 | 0.1997 | 0.341 | 0.4016 | 0.6058 | 0.7309 | 0.8347 | |
| 0.2 | 0.3762 | 0.5422 | 0.1997 | 0.3431 | 0.4049 | 0.617 | 0.7488 | 0.853 | |
| 0.3 | 0.3794 | 0.5511 | 0.1997 | 0.3455 | 0.4088 | 0.6305 | 0.7691 | 0.8714 | |
| 0.4 | 0.3829 | 0.5618 | 0.1998 | 0.3482 | 0.4131 | 0.6467 | 0.7914 | 0.8888 | |
| 0.5 | 0.3871 | 0.5748 | 0.1998 | 0.3514 | 0.4182 | 0.6666 | 0.8148 | 0.9045 | |
| 0.6 | 0.392 | 0.5916 | 0.1998 | 0.3551 | 0.4243 | 0.6912 | 0.8376 | 0.9179 | |
| 0.7 | 0.398 | 0.6142 | 0.1998 | 0.3596 | 0.4319 | 0.7203 | 0.858 | 0.9288 | |
| 0.8 | 0.4059 | 0.6453 | 0.1999 | 0.3654 | 0.4421 | 0.7507 | 0.8751 | 0.9375 | |
| 0.9 | 0.418 | 0.6812 | 0.1999 | 0.3741 | 0.4588 | 0.7778 | 0.8889 | 0.9444 | |
| 0.95 | 0.4292 | 0.6979 | 0.1999 | 0.3813 | 0.475 | 0.7895 | 0.8947 | 0.9474 | |
| 0.975 | 0.4393 | 0.7056 | 0.2 | 0.3873 | 0.4872 | 0.7942 | 0.8974 | 0.9487 | |
| 1 | 0.453 | 0.713 | 0.2 | 0.4 | 0.5 | 0.8 | 0.9 | 0.95 | |

YA = cumulative composition of styrene in copolymer.**yA** = composition of styrene in unreacted monomer.**zA** = instantaneous composition of styrene in copolymer.**x** = monomer in feed

Table A-2 Calculated styrene fraction in unreacted monomers. For poly(St-co-MA);**zA vs x**

| zA0 \ x | 0.453 | 0.713 | 0.2 | 0.4 | 0.5 | 0.8 | 0.9 | 0.95 |
|---------|--------|--------|--------|--------|--------|--------|--------|--------|
| 0 | 0.453 | 0.713 | 0.2 | 0.4 | 0.5 | 0.8 | 0.9 | 0.95 |
| 0.025 | 0.4551 | 0.7177 | 0.2 | 0.4016 | 0.5026 | 0.8052 | 0.9047 | 0.9533 |
| 0.05 | 0.4572 | 0.7226 | 0.2 | 0.4032 | 0.5053 | 0.8105 | 0.9093 | 0.9565 |
| 0.1 | 0.4618 | 0.7328 | 0.2 | 0.4066 | 0.5109 | 0.8216 | 0.9188 | 0.9628 |
| 0.2 | 0.4722 | 0.7557 | 0.2001 | 0.4142 | 0.5238 | 0.8457 | 0.9378 | 0.9742 |
| 0.3 | 0.4846 | 0.7824 | 0.2001 | 0.4234 | 0.5391 | 0.8726 | 0.9561 | 0.9837 |
| 0.4 | 0.4997 | 0.8138 | 0.2002 | 0.4345 | 0.5579 | 0.9022 | 0.9724 | 0.9908 |
| 0.5 | 0.5189 | 0.8512 | 0.2002 | 0.4486 | 0.5818 | 0.9334 | 0.9852 | 0.9955 |
| 0.6 | 0.5446 | 0.8951 | 0.2003 | 0.4674 | 0.6136 | 0.9631 | 0.9937 | 0.9982 |
| 0.7 | 0.5814 | 0.9435 | 0.2004 | 0.4943 | 0.659 | 0.9859 | 0.998 | 0.9995 |
| 0.8 | 0.6413 | 0.9838 | 0.2006 | 0.5382 | 0.7316 | 0.9971 | 0.9996 | 0.9999 |
| 0.9 | 0.7667 | 0.999 | 0.2009 | 0.6328 | 0.8711 | 0.9998 | 1 | 1 |
| 0.95 | 0.9054 | 0.9999 | 0.2012 | 0.7562 | 0.9751 | 1 | 1 | 1 |
| 0.975 | 0.9867 | 1 | 0.2016 | 0.8957 | 0.9982 | 1 | 1 | 1 |

สถาบันวิทยบริการ
จุฬาลงกรณ์มหาวิทยาลัย

Table A-3 Instantaneous composition of styrene in the copolymer poly(St-co-MA);**y_A vs x.**

| $x \backslash z_{A0}$ | 0.453 | 0.713 | 0.2 | 0.4 | 0.5 | 0.8 | 0.9 | 0.95 |
|-----------------------|--------|--------|--------|--------|--------|--------|--------|--------|
| 0 | 0.3709 | 0.5277 | 0.1997 | 0.3389 | 0.3984 | 0.5957 | 0.7147 | 0.8169 |
| 0.025 | 0.3721 | 0.531 | 0.1997 | 0.3399 | 0.3999 | 0.6004 | 0.7224 | 0.8256 |
| 0.05 | 0.3734 | 0.5344 | 0.1997 | 0.3409 | 0.4014 | 0.6054 | 0.7304 | 0.8345 |
| 0.1 | 0.3761 | 0.5417 | 0.1997 | 0.343 | 0.4047 | 0.6162 | 0.7477 | 0.8528 |
| 0.2 | 0.3822 | 0.5588 | 0.1998 | 0.3476 | 0.4122 | 0.6417 | 0.7872 | 0.89 |
| 0.3 | 0.3894 | 0.5803 | 0.1998 | 0.3532 | 0.421 | 0.6746 | 0.8333 | 0.9255 |
| 0.4 | 0.3982 | 0.6086 | 0.1998 | 0.3599 | 0.4319 | 0.7183 | 0.8836 | 0.9556 |
| 0.5 | 0.4094 | 0.648 | 0.1999 | 0.3683 | 0.4458 | 0.7773 | 0.9317 | 0.9774 |
| 0.6 | 0.4242 | 0.707 | 0.1999 | 0.3794 | 0.4646 | 0.8538 | 0.9687 | 0.9907 |
| 0.7 | 0.4456 | 0.8004 | 0.2 | 0.3951 | 0.4923 | 0.9343 | 0.9899 | 0.9972 |
| 0.8 | 0.4813 | 0.9258 | 0.2002 | 0.4205 | 0.5408 | 0.9853 | 0.9981 | 0.9995 |
| 0.9 | 0.5674 | 0.9946 | 0.2004 | 0.4762 | 0.6726 | 0.9992 | 0.9999 | 1 |
| 0.95 | 0.7237 | 0.9997 | 0.2007 | 0.5591 | 0.8931 | 1 | 1 | 1 |
| 0.975 | 0.9378 | 1 | 0.201 | 0.7079 | 0.991 | 1 | 1 | 1 |

สถาบันวิทยบริการ
จุฬาลงกรณ์มหาวิทยาลัย

Table A-4 Calculated cumulative composition of MMA in poly(MMA-*co*-MA);

YA vs x.

Monomer 1 = MMA $r_{MMA} = 2.150$

Monomer 2 = MA $r_{MA} = 0.400$

| z_{A0} | 0.462 | 0.721 | 0.2 | 0.4 | 0.5 | 0.8 | 0.9 | 0.95 |
|----------|--------|--------|--------|--------|--------|--------|--------|--------|
| x | | | | | | | | |
| 0 | 0.6601 | 0.8502 | 0.3716 | 0.6033 | 0.6923 | 0.8972 | 0.9512 | 0.9762 |
| 0.025 | 0.6579 | 0.8492 | 0.3686 | 0.6008 | 0.6903 | 0.8965 | 0.9509 | 0.976 |
| 0.05 | 0.6553 | 0.8479 | 0.3651 | 0.5979 | 0.6879 | 0.8956 | 0.9504 | 0.9758 |
| 0.1 | 0.6508 | 0.8459 | 0.3589 | 0.5929 | 0.6838 | 0.8942 | 0.9497 | 0.9755 |
| 0.2 | 0.6409 | 0.8413 | 0.3457 | 0.5818 | 0.6747 | 0.891 | 0.9483 | 0.9748 |
| 0.3 | 0.6297 | 0.8359 | 0.3314 | 0.5692 | 0.6643 | 0.8873 | 0.9465 | 0.9739 |
| 0.4 | 0.6169 | 0.8298 | 0.316 | 0.555 | 0.6525 | 0.8831 | 0.9445 | 0.9729 |
| 0.5 | 0.6022 | 0.8225 | 0.2994 | 0.5388 | 0.6388 | 0.8781 | 0.9421 | 0.9718 |
| 0.6 | 0.5849 | 0.8139 | 0.2815 | 0.5201 | 0.6226 | 0.872 | 0.9392 | 0.9704 |
| 0.7 | 0.5642 | 0.803 | 0.2624 | 0.4981 | 0.603 | 0.8645 | 0.9356 | 0.9686 |
| 0.8 | 0.5385 | 0.7884 | 0.242 | 0.4715 | 0.5783 | 0.8543 | 0.9307 | 0.9662 |
| 0.9 | 0.5052 | 0.7666 | 0.2209 | 0.4389 | 0.5453 | 0.8386 | 0.9231 | 0.9625 |
| 0.95 | 0.4847 | 0.7493 | 0.2103 | 0.42 | 0.5243 | 0.8257 | 0.9167 | 0.9594 |
| 0.975 | 0.4736 | 0.7372 | 0.2051 | 0.4101 | 0.5124 | 0.8158 | 0.9115 | 0.9568 |
| 1 | 0.462 | 0.721 | 0.2 | 0.4 | 0.5 | 0.8 | 0.9 | 0.95 |

YA = cumulative composition of MMA in copolymer.

yA = composition of MMA in unreacted monomer.

zA = instantaneous composition of MMA in copolymer.

x = monomer in feed

Table A-5 Calculated MMA fraction in unreacted monomer; for poly(MMA-co-MA);

zA vs x.

| zA0 \ x | 0.462 | 0.721 | 0.2 | 0.4 | 0.5 | 0.8 | 0.9 | 0.95 |
|---------|--------|--------|--------|--------|--------|--------|--------|--------|
| 0 | 0.462 | 0.721 | 0.2 | 0.4 | 0.5 | 0.8 | 0.9 | 0.95 |
| 0.025 | 0.457 | 0.7177 | 0.1957 | 0.3949 | 0.4951 | 0.7975 | 0.8987 | 0.9493 |
| 0.05 | 0.4518 | 0.7143 | 0.1913 | 0.3896 | 0.4901 | 0.795 | 0.8973 | 0.9486 |
| 0.1 | 0.441 | 0.7071 | 0.1823 | 0.3786 | 0.4796 | 0.7895 | 0.8945 | 0.9472 |
| 0.2 | 0.4173 | 0.6909 | 0.1636 | 0.3546 | 0.4563 | 0.7772 | 0.8879 | 0.9438 |
| 0.3 | 0.3901 | 0.6717 | 0.1431 | 0.3275 | 0.4296 | 0.7626 | 0.8801 | 0.9398 |
| 0.4 | 0.3587 | 0.6485 | 0.1227 | 0.2967 | 0.3984 | 0.7446 | 0.8703 | 0.9347 |
| 0.5 | 0.3218 | 0.6195 | 0.1006 | 0.2612 | 0.3612 | 0.7219 | 0.8579 | 0.9282 |
| 0.6 | 0.2776 | 0.5817 | 0.0777 | 0.2198 | 0.3161 | 0.6919 | 0.8411 | 0.9194 |
| 0.7 | 0.2235 | 0.5298 | 0.0545 | 0.1711 | 0.2596 | 0.6496 | 0.8169 | 0.9066 |
| 0.8 | 0.1561 | 0.4513 | 0.0319 | 0.1139 | 0.1869 | 0.5829 | 0.7771 | 0.8851 |
| 0.9 | 0.0733 | 0.3109 | 0.012 | 0.0498 | 0.0921 | 0.4526 | 0.6917 | 0.8372 |
| 0.95 | 0.0298 | 0.1826 | 0.0043 | 0.0194 | 0.0388 | 0.3123 | 0.5825 | 0.7716 |
| 0.975 | 0.0112 | 0.0894 | 0.0016 | 0.0071 | 0.0148 | 0.1837 | 0.452 | 0.6844 |

สถาบันวิทยบริการ
จุฬาลงกรณ์มหาวิทยาลัย

Table A-6 Calculated instantaneous composition of MMA in poly(MMA-co-MA);**y_A vs x.**

| z_{A0} | 0.462 | 0.721 | 0.2 | 0.4 | 0.5 | 0.8 | 0.9 | 0.95 | |
|----------|--------|--------|--------|--------|--------|--------|--------|--------|--------|
| x | 0 | 0.6601 | 0.8502 | 0.3716 | 0.6033 | 0.6923 | 0.8972 | 0.9512 | 0.9762 |
| 0.025 | 0.6557 | 0.8482 | 0.3655 | 0.5983 | 0.6883 | 0.8958 | 0.9505 | 0.9759 | |
| 0.05 | 0.6511 | 0.8461 | 0.3592 | 0.5932 | 0.6841 | 0.8943 | 0.9498 | 0.9755 | |
| 0.1 | 0.6415 | 0.8415 | 0.3462 | 0.5823 | 0.6752 | 0.8912 | 0.9483 | 0.9748 | |
| 0.2 | 0.6197 | 0.8312 | 0.3181 | 0.5579 | 0.6551 | 0.8841 | 0.945 | 0.9732 | |
| 0.3 | 0.5938 | 0.8187 | 0.2868 | 0.5292 | 0.6311 | 0.8755 | 0.9409 | 0.9712 | |
| 0.4 | 0.5622 | 0.8032 | 0.252 | 0.4946 | 0.6017 | 0.8647 | 0.9358 | 0.9687 | |
| 0.5 | 0.9291 | 0.7832 | 0.2133 | 0.4523 | 0.5648 | 0.8508 | 0.9291 | 0.9655 | |
| 0.6 | 0.4722 | 0.756 | 0.1705 | 0.3989 | 0.5166 | 0.8319 | 0.9291 | 0.9611 | |
| 0.7 | 0.4038 | 0.7163 | 0.1239 | 0.3295 | 0.4503 | 0.8039 | 0.9067 | 0.9545 | |
| 0.8 | 0.3065 | 0.6506 | 0.0753 | 0.2369 | 0.3529 | 0.7569 | 0.884 | 0.9435 | |
| 0.9 | 0.1618 | 0.5109 | 0.0293 | 0.1142 | 0.1978 | 0.6518 | 0.8317 | 0.9179 | |
| 0.95 | 0.0707 | 0.3466 | 0.0108 | 0.0468 | 0.0905 | 0.5123 | 0.7566 | 0.8808 | |
| 0.975 | 0.0274 | 0.1927 | 0.0039 | 0.0179 | 0.036 | 0.3481 | 0.6513 | 0.827 | |

สถาบันวิทยบริการ
จุฬาลงกรณ์มหาวิทยาลัย

VITA

Miss Roongkan Nuisin was born on October 26, 1974 in Chiang Rai, Thailand. She received her B.Sc. degree in Chemistry from the Faculty of Science, Chiang Mai University in 1996. Her Master degree in Polymer Science was received from the Faculty of Science, Chulalongkorn University in 1999. During her masters degree study (1998), she was granted a fellowship from the King Prajadhipok and Queen Rambhai Barni Memorial foundation; and AIEJ Short-term Student Exchange Promotion Program to the Graduate School of Bio-Applications and Systems Engineering (BASE), Tokyo University of Agriculture and Technology. She has been a Ph.D. candidate in Materials Science, Faculty of Science, Chulalongkorn University since 2000. She was granted a fellowship from the Thailand Research Fund (The Golden Jubilee Scholarship) through grant no. PHD/0041/2543 and Graduate School of BASE, Tokyo University of Agriculture and Technology.

สถาบันวิทยบริการ
จุฬาลงกรณ์มหาวิทยาลัย

Synthesis and Property Behavior of Dioctyl Phthalate Plasticized Styrene–Acrylate Particles by Shirasu Porous Glass Emulsification and Subsequent Suspension Copolymerization

Roongkan Nuisin,¹ Shinzo Omi,² Suda Kiatkamjornwong³

¹Department of Materials Science, Faculty of Science, Chulalongkorn University, Bangkok 10330, Thailand

²Graduate School of Bio-Applications and Systems Engineering, Tokyo University of Agriculture and Technology, Tokyo 184-8588, Japan

³Department of Imaging and Printing Technology, Faculty of Science, Chulalongkorn University, Bangkok 10330, Thailand

Received 20 November 2002; accepted 17 March 2003

ABSTRACT: Two-phase model styrene–acrylate copolymers were synthesized with a soft phase consisting of methyl acrylate, butyl acrylate, and butyl methacrylate. Besides the styrenic copolymers, copolymers containing a hard phase of methyl methacrylate and methyl acrylate were also synthesized. Comonomer droplets with a narrow size distribution and fair uniformity were prepared using an SPG (Shirasu porous glass) membrane having pore size of 0.90 μm . After the single-step SPG emulsion, the emulsion droplets were composed mainly of monomers, hydrophobic additives, and an oil-soluble initiator, suspended in the aqueous phase containing a stabilizer and inhibitor. These were then transferred to a reactor, and subsequent suspension polymerization was carried out. Uniform copolymer particles with a mean diameter ranging from 3 to 7 μm , depending on the recipe, with a narrow particle size distribution and a coefficient of variation of about 10% were achieved.

Based on the glass-transition temperatures, as measured by differential scanning calorimetry, the resulting copolymer particles containing a soft phase of acrylate were better compatibilized with a hard phase of methyl methacrylate than with styrene with dioctyl phthalate (DOP) addition. Glass-transition temperatures of poly(MMA-co-MA) particles were strongly affected by the composition drift in the copolymer caused by their substantial difference in reactivity ratios. Incorporation of DOP in the copolymer particles does not significantly affect the glass-transition temperature of MMA- or MA-containing copolymer particles, but it does affect the St-containing copolymer and particle morphology of the copolymers. © 2003 Wiley Periodicals, Inc. *J Appl Polym Sci* 90: 3037–3050, 2003

Key words: suspension copolymerization; glass-transition; polystyrene; plasticizers; Shirasu porous glass (SPG)

INTRODUCTION

Polymer latices are the essential materials of the surface coatings industry. A large proportion of the commercially produced latex polymer has typically been used by being cast into films or acting as binders. Recent concerns for the environmental and safety effects have emerged from highly volatile organic compounds used in the traditional coating industry. The growing demand for waterborne coatings thus requires a substitution for solvent-based coatings. Properties of polymer films are affected by polymer type and its nature and film-preparation conditions. A co-

alescing agent is required to enable the latex particles to attract each other to form a continuous film. A core-shell polymer can be used to reduce the need for a coalescing solvent.^{1,2}

Control of the latex particle morphology is important for many applications. Particle morphology is controlled by many factors, including the polymerization method, hydrophilicity of monomers and polymers, the particle viscosity,³ the degree of grafting between the polymers,^{4,5} and initiator properties and the mode of monomer addition.^{6–9} Such heterogeneity could provide uniquely tailored properties, for example, dispersion of a soft, lower glass-transition temperature (T_g) latex, or a soft particle core entrapped in a matrix of a harder polymer shell, which can prevent cracks in the film as an impact modifier.^{10–14}

Landfester et al.¹ investigated the polybutylacrylate (PBA)/poly(methyl methacrylate) (PMMA) system and found that the interface depends on different synthesis conditions and the size of the particles. The

Correspondence to: S. Kiatkamjornwong (ksuda@chula.ac.th).

Contract grant sponsor: Thailand Research Fund; contract grant number: 2.M.CU/42/E.1.

Contract grant sponsor: BASE, Tokyo University of Agriculture and Technology.

core-shell latices are composed of the PBA soft core at room temperature and the rigid shell of PMMA. The T_g of PBA of -45°C is of course well below room temperature. PBA/PMMA (66:34) copolymer, or pure PBA (soft phase) as a seed in a two-stage emulsion polymerization with MMA (hard phase), was prepared by Kirsch et al.² The soft-to-hard phase ratio was varied over a wide range, and the influence of crosslinking the second-stage material was investigated.¹⁴ The influence of the content and molecular weight of low-density polyethylene (LDPE) on dioctyl phthalate (DOP) plasticization in poly(vinyl chloride) (PVC) was studied. The plasticizing effects of DOP on the PVC plastisol were found to decrease with increasing LDPE content and LDPE molecular weight.¹⁵ Uniform poly(styrene-co-MMA) [poly(St-co-MMA)] microspheres were prepared using the SPG (Shirasu porous glass) emulsification technique. The additives containing ester groups in the emulsion droplets demonstrated that the compatibility between the hydrophobic additive and the monomer was responsible for the varied morphologies of the particles.¹⁵

In the present study, the SPG emulsification technique and subsequent suspension polymerization were used in synthesis of poly(St-co-MA) and poly(MMA-co-MA), and poly(St-co-BMA) in the presence of DOP. The effect of the added DOP plasticizer on the copolymer morphology, glass-transition temperature, molecular weight, and particle size were studied.

EXPERIMENTAL

Materials

Styrene (Wako Pure Chemicals, Osaka, Japan) was reagent grade and stored at -10°C before use. Styrene monomer was distilled before use for Runs 2022–2052. Methyl methacrylate, methyl acrylate, butyl acrylate, and butyl methacrylate (Wako Pure Chemicals) were reagent grade and distilled to remove inhibitors before use. Polystyrene having a number-average molecular weight (M_n) of 4200, a weight-average molecular weight (M_w) of 40,000, and M_w/M_n [or polydispersity index (PDI)] of 9.54 was produced in-house. Dioctyl phthalate (DOP, GC grade, Wako Pure Chemicals) was used as a plasticizer. N,N' -Azobisisobaleronitrile (ADV N, V65; Wako Pure Chemicals) and benzoyl peroxide (BPO; Kishida, Osaka, Japan) were used as initiators. Sodium dodecyl sulfate (SLS, biochemical grade; Merck, Darmstadt, Germany) and poly(vinyl alcohol) (PVA) having a degree of polymerization of 1700 and 88.5% saponification (Kuraray, Osaka, Japan) were used as the surfactant and stabilizer, respectively. Sodium nitrite (NaNO_2 , reagent grade; Chameleon Chemicals, Osaka, Japan) and *p*-phenylenediamine (reagent grade; Chameleon Chemicals) were

TABLE I
Standard Recipe for the SPG Emulsification

| Component | Weight (g) |
|--|--------------------------------------|
| Continuous phase | |
| PVA-217 | 2.00, ^a 3.00 ^b |
| SLS | 0.10 |
| Na_2SO_4 | 0.10 |
| Inhibitor (NaNO_2 , PDA) | 0.04 |
| Water | 230 |
| Dispersion phase | |
| Initiator (BPO, ADVN) | 0.04 |
| Total monomer content (St, MMA, MA, BA, BMA) | 16.0 |
| DOP | 0.8 |

^a SPG membrane pore size 0.51 μm .

^b SPG membrane pore size 0.90 μm .

used as inhibitors. Sodium sulfate (Na_2SO_4 , commercial grade; Kokusan Chemical Works, Tokyo, Japan) was used as electrolyte. Methyl alcohol (commercial grade; Wako Pure Chemicals) was used as a solvent and nonsolvent for the copolymers.

Emulsification procedure

An SPG membrane with a pore size of 0.51 or 0.90 μm (Ise Chemicals, Japan) was used for the emulsification. The preparative conditions for a one-step emulsification and experimental results are shown in Table I. Air pressure was used to permeate the dispersion phase from the SPG membrane. The pressure in a range of 1.28–1.45 kgf cm^{-2} for the 0.51- μm membrane and 0.30–0.70 kgf cm^{-2} for the 0.90- μm membrane were used. The dispersion phase containing a mixture of the monomers, DOP, and BPO (or ADVN) initiator was prepared. In a continuous phase, the PVA stabilizer, SDS surfactant, Na_2SO_4 electrolyte, and NaNO_2 inhibitor were dissolved. To prevent creaming of the droplets, the continuous phase was gently stirred at 300 rpm with a magnetic bar.

Polymerization

The emulsion obtained was transferred to a three-neck glass vessel with a capacity of 300 cm^3 connected with a semicircular anchor-type blade made of PTFE for agitation, a Dimroth condenser, and a nitrogen inlet nozzle. Nitrogen gas was gently bubbled into the emulsion for 1 h; the nozzle was lifted above the emulsion level. The temperature was increased to reach 75°C , and the emulsion was polymerized for 24 h under nitrogen atmosphere by suspension polymerization.

Characterization

Conversion of monomers

Percentage conversion of the monomer was monitored by a gravimetric method. Methyl alcohol was

TABLE II
Polymerization Recipe and Experimental Results for Styrene (SPG pore size 0.51 μm)^a

| Run no. | Composition | Monomer composition (wt %) | Monomer conversion (%) | D_e (μm) | CV_e (%) | D_p (μm) | CV_p (%) | \bar{M}_n ($\times 10^{-4}$) | \bar{M}_w ($\times 10^{-4}$) | PDI | T_g ($^{\circ}\text{C}$) | |
|---------|--|----------------------------|------------------------|-------------------------|------------|-------------------------|------------|----------------------------------|----------------------------------|------------------|------------------------------|------------------------|
| | | | | | | | | | | | Clean | Unclean |
| 2013 | PSt/DOP 2.5 wt % ADV, NaNO_2 | 100 | 86.6 | 4.1 | 8.3 | 2.9 | 10.3 | 4.1 | 33.7 | 8.1 ^b | 18.1/71.0 ^c | 6.4/86.0 ^c |
| 2012 | PSt/DOP 5 wt % ADV, NaNO_2 | 100 | 74.6 | 8.8 | 18.4 | 7.3 | 18.5 | 1.8 | 8.2 | 4.6 | 3.1/48.2 ^c | 1.0/43.1 ^c |
| 2014 | PSt/DOP 5 wt % BPO, NaNO_2 | 100 | 76.5 | 6.3 | 15.2 | 5.9 | 11.2 | 1.7 | 3.9 | 2.3 | 12.7/77.4 ^c | 6.0/43.4 ^c |
| 2016 | PSt/DOP 5 wt % ADV, PDA | 100 | 76.0 | 7.1 | 15.9 | 5.8 | 16.1 | 1.7 | 7.5 | 4.5 | 6.3/65.9 ^c | 11.7/54.8 ^c |

^a D_e and D_p are diameters of emulsion droplets and polymer particles, respectively. CV_e and CV_p are coefficients of variation for emulsion droplets and polymer particles, respectively. \bar{M}_n and \bar{M}_w are the number-averaged molecular weight and weight-average molecular weight, respectively. PDI, polydispersity index.

^b Bimodal peak.

^c Two separate T_g values were observed.

added to precipitate the polymer. Polymer particles were separated by centrifugation at 2000 rpm and washed repeatedly with methyl alcohol two to three times. The polymer particles were dried under vacuum at room temperature for 48 h, after which they were weighed.

Surface morphology

The external morphology of polymer particles was observed by scanning electron microscopy (JEOL, Model JSM-5310, Japan). The specimens were prepared by diluting the polymer latex, from which the diluted suspension was dropped onto an aluminum stub surface and coated with a thin layer of gold under

reduced pressure ($<10^{-2}$ Pa) using a fine coater (JEOL, Model JFC-1200). The magnification was set at $\times 2000$ in the SEM micrographs taken for the determination of the average polymer particle size and coefficient of variation (CV).

Size and size distribution of emulsion droplets and polymer particles

Monomer droplets before polymerization were observed by optical microscopy (Olympus BHC optical microscope). Diameters of about 150 monomer droplets were measured to calculate an average diameter and a size distribution. The polymer particle sizes were measured by SEM techniques.

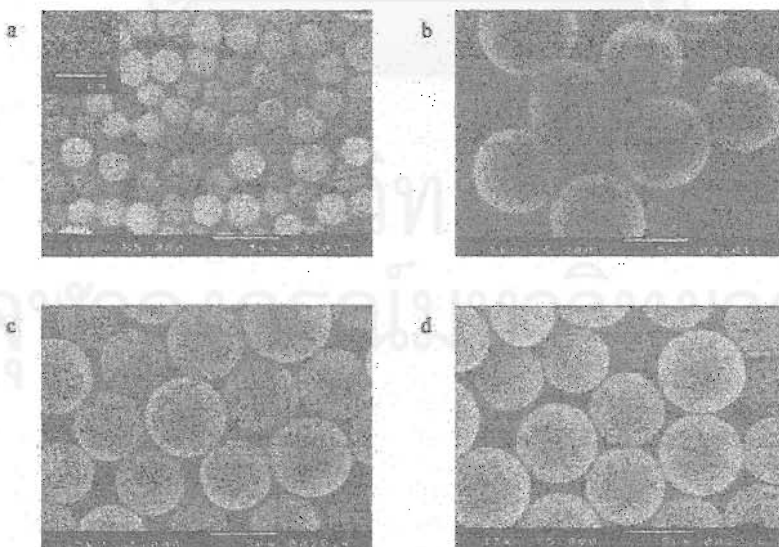


Figure 1 SEM micrographs of polystyrene incorporated with DOP: (a) DOP 2.5 wt % (Run 2013); (b) DOP 5 wt % (Run 2012, ADVN as initiator); (c) DOP 5 wt % (Run 2014, BPO as initiator); (d) DOP 5 wt % (Run 2016, ADVN as initiator and PDA as inhibitor).

TABLE III
Recipe and Experimental Results of Styrene and Methyl Acrylate Copolymerization

| Run no. | Composition | Monomer composition (wt %) | Monomer conversion (%) | D_c (μm) | CV _c (%) | D_p (μm) | CV _p (%) | \bar{M}_n ($\times 10^{-4}$) | \bar{M}_w ($\times 10^{-4}$) | PDI | T_g ($^{\circ}\text{C}$) | |
|-------------------|-----------------------|----------------------------|------------------------|-------------------------|---------------------|-------------------------|---------------------|----------------------------------|----------------------------------|-----|------------------------------|------------------------|
| | | | | | | | | | | | Clean | Unclean |
| 2016 ^a | PSt/DOP | 100 | 76.0 | 7.1 | 25.9 | 5.8 | 16.1 | 1.7 | 7.5 | 4.5 | 6.3/65.9 ^b | 11.7/54.8 ^b |
| 2022 | P(St-co-MA) | 50/50 | 93.0 | 8.4 | 21.6 | 3.8 | 13.1 ^c | 2.0 | 4.4 | 2.2 | 23.2/65.4 ^b | 17.5/37.9 ^b |
| 2023 | P(St-co-MA) | 75/25 | 89.7 | 5.8 | 10.0 | 4.8 | 10.8 | 1.6 | 3.9 | 2.4 | 11.2/78.2 ^b | 11.0/47.5 ^b |
| 2046 | P(St-co-MA)/DOP | 52/48 | 17.4 | 6.5 | 15.3 | 5.8 | 16.5 | 0.4 | 1.6 | 4.5 | 21.1/55.1 ^b | 23.1 |
| 2028 | P(St-co-MA)/DOP | 75/25 | 52.2 | 7.1 | 16.1 | 5.9 | 19.7 | 1.6 | 3.6 | 2.3 | 24.9/58.3 ^b | 27.9 |
| 2024 | P(St-co-MA)/PSt | 37.5/50/12.5 | 89.8 | 7.8 | 21.1 | 5.2 | 15.8 | 1.3 | 3.8 | 2.8 | 26.7/72.2 ^b | 25.4/50.4 ^b |
| 2025 | P(St-co-MA)/PSt | 62.5/25/12.5 | 69.6 | 6.1 | 10.4 | 4.4 | 14.3 | 1.5 | 3.2 | 2.2 | 31.7/53.9 ^b | 20.9/49.9 ^b |
| 2029 | [P(St-co-MA)/PSt]/DOP | 37.5/50/12.5 | 38.9 | 7.0 | 16.1 | 5.0 | 18.3 | 1.2 | 3.2 | 2.8 | 22.2/50.1 ^b | 22.9/44.2 ^b |
| 2030 | [P(St-co-MA)/PSt]/DOP | 62.5/25/12.5 | 67.5 | 5.9 | 10.1 | 4.1 | 13.8 | 1.5 | 3.9 | 2.6 | 15.0/51.7 ^b | 14.6/46.9 ^b |

^a SPG membrane pore size 0.51 μm ; otherwise, 0.90 μm .

^b Two separate T_g values were observed.

^c Coagulated particles were partially observed.

On average, the diameters of 200 polymer particles were determined from SEM micrographs. Through the evaluation of the OM and SEM micrographs, the number-averaged diameters of the emulsion droplets (D_e) and polymer particles (D_p) were calculated according to eq. (1). In addition, the standard deviation (σ) and CV were calculated using the formulas expressed in eqs. (2) and (3). Here

$$D_n = \frac{\sum_{i=1}^n n_i D_i}{\sum_{i=1}^n n_i} \quad (1)$$

where n_i is the number of particles at diameters D_i , and D_n corresponds to the exact mean diameter of the population. The standard deviation σ is determined from the measured particle diameters in the following equation:

$$\sigma = \left[\frac{1}{n-1} \sum_{i=1}^n (D_i - D_n)^2 \right]^{1/2} \quad (2)$$

where i refers here to an individual particle.

The particle size distribution is reflected in the standard deviation. The breadth of the particle size distribution is proportional to the standard deviation of the particle diameters using the CV as follows:

$$\text{CV} (\%) = (\sigma/D_n) \times 100 \quad (3)$$

Internal morphology of the particles

The polymer particles of Runs 2018 and 2019 prepared from St:MA contents of 50:50 and 75:25, respectively, with incorporation of 5% DOP were subjected to TEM observation (JEOL, Model JEM 1010). The samples were microtomed and stained with RuO₄ and viewed at $\times 20,000$ magnification.

Molecular weights and distribution

Gel permeation chromatography (GPC) was used for the examination of average molecular weights and the molecular weight distribution. The GPC chromatograms were obtained using Tosoh gel permeation chromatography (Model HLCH820 Chromato column; Tosoh, Tokyo, Japan) at the oven temperature of 40 $^{\circ}\text{C}$, and the injection temperature at 35 $^{\circ}\text{C}$. Pressure was applied to samples at 16 kgf cm⁻² and reference was at 12 kgf cm⁻². There are two types of GPC columns for sample analysis. The first column (Model GRCX4) and the second column (Model GMMXL) were both packed with mixed gels of

TABLE IV
Recipe and Experimental Results for Methyl Methacrylate and Methyl Acrylate Copolymerization^a

| Run no. | Composition | Monomer composition (wt %) | Monomer conversion (%) | D_e (μm) | CV_e (%) | D_p (μm) | CV_p (%) | \overline{M}_n ($\times 10^{-4}$) | \overline{M}_w ($\times 10^{-4}$) | PDI | T_g ($^{\circ}\text{C}$) | |
|---------|------------------|----------------------------|------------------------|-------------------------|------------|-------------------------|-------------------|---------------------------------------|---------------------------------------|-------------------|------------------------------|---------|
| | | | | | | | | | | | Clean | Unclean |
| 2010 | PMMA/DOP | 100 | 85.6 | 6.9 | 25.9 | Coag ^b | Coag ^b | 3.7 | 13.0 | 3.5 | 14.0 | 14.0 |
| 2033 | P(MMA-co-MA) | 50/50 | 73.7 | 7.0 | 39.7 | 5.4 | 26.6 | 3.9 | 62.6 | 16.0 ^c | 25.9 | 29.4 |
| 2032 | P(MMA-co-MA) | 75/25 | 68.1 | 4.5 | 22.7 | 5.5 | 18.8 | 2.3 | 10.2 | 4.5 | 27.9 | 29.2 |
| 2035 | P(MMA-co-MA)/DOP | 50/50 | 79.9 | 5.6 | 22.8 | 5.4 | 14.5 ^b | 4.0 | 52.3 | 13.2 ^c | 29.5 | 25.3 |
| 2034 | P(MMA-co-MA)/DOP | 75/25 | 57.1 | 4.6 | 13.6 | 4.7 | 18.7 | 3.3 | 22.1 | 6.7 | 38.0 | 29.2 |

^a SPG membrane pore size 0.9 μm .

^b Coagulated particles were partially observed.

^c Bimodal curve.

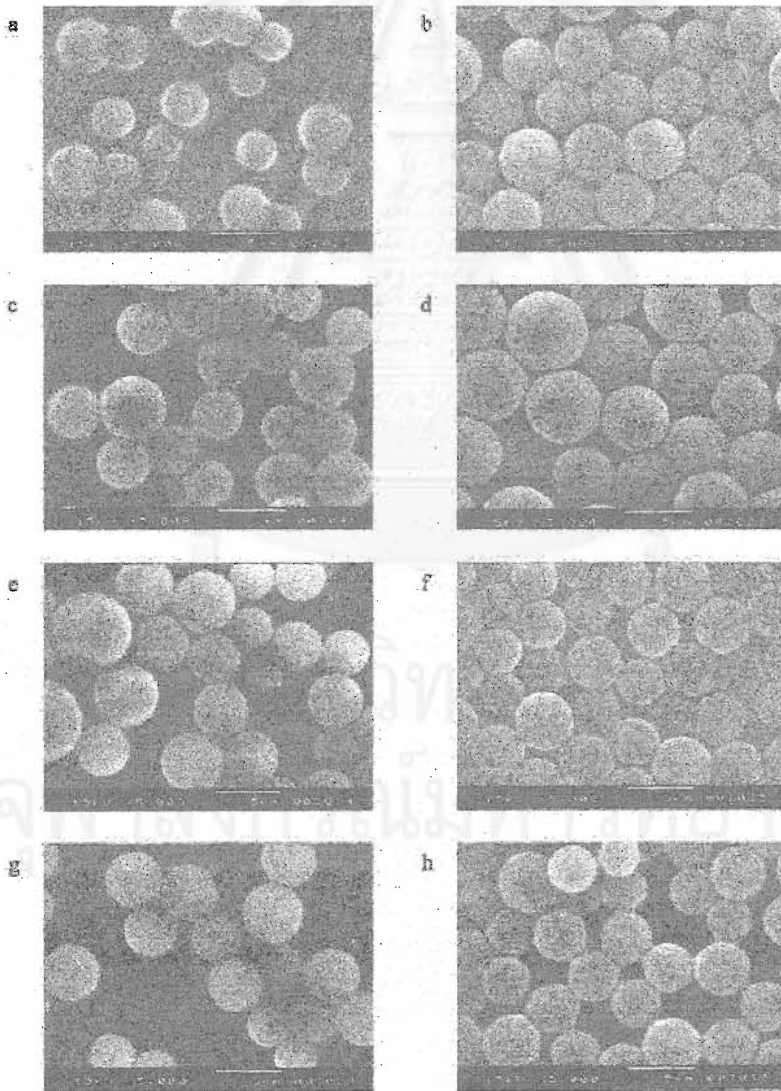


Figure 2 SEM micrographs of poly(St-co-MA): (a) St : MA = 50 : 50; (b) St : MA = 75 : 25; (c) St : MA = 52 : 48 with DOP; (d) St : MA = 75 : 25 with DOP; (e) St : MA : PSt = 37.5 : 50 : 12.5; (f) St : MA : PSt = 62.5 : 25 : 12.5; (g) St : MA : PSt = 37.5 : 50 : 12.5 with DOP; (h) St : MA : PSt = 62.5 : 25 : 12.5 with DOP.

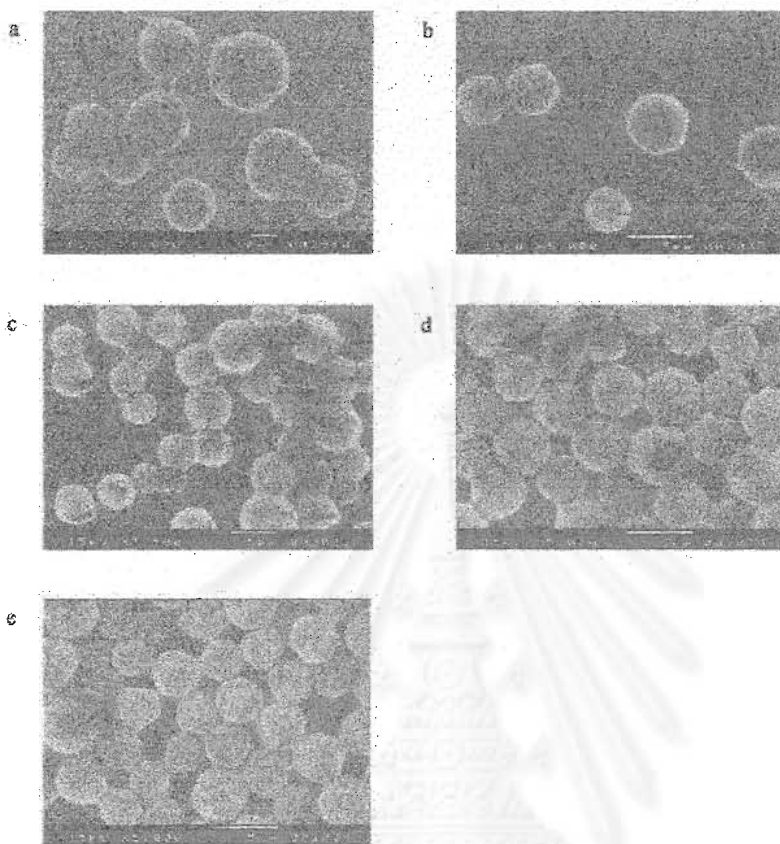


Figure 3 SEM micrographs of poly(MMA-*co*-MA): (a) PMMA-DOP; (b) poly(MMA-*co*-MA), MMA : MA = 50 : 50; (c) poly(MMA-*co*-MA), MMA : MA = 75 : 25; (d) poly(MMA-*co*-MA)-DOP, MMA : MA = 50 : 50; (e) poly(MMA-*co*-MA)-DOP, MMA : MA = 75 : 25.

poly(divinylbenzene-*co*-styrene). Likewise, the reference column (Model GMMXL) was also packed with mixed gels of poly(divinylbenzene-*co*-styrene). Tetrahydrofuran (THF, Wako Pure Chemicals) was used as solvent and eluent. For analysis, 1 mg of dried polymer sample was dissolved into 2 cm³ of THF to obtain an approximate concentration of 0.1 wt %. Then the polymer solution, filtered with 0.2 μm PTFE membrane (Advantec, Tokyo, Japan), was injected into the columns at a flow rate of 0.5 cm³ min⁻¹. The chromatogram was detected by a refractive index detector.

Glass-transition temperature

Measurements of glass-transition temperature (T_g) were performed using a differential scanning calorimeter (DSC, Model 3100; MAC Science). The sample was prepared by two methods, unclean and clean. For the first method, the polymer latex was dried under vacuum at ambient temperature for 120 h without further cleaning. For the second method, the polymer latex was washed repeatedly with methanol to remove all the surfactant and stabilizer. Then the precipitate

latex was dried under vacuum at ambient temperature for 48 h. A sample (5–10 mg) from each preparation method was placed in the aluminum pan and put on the sensor at room temperature along with an empty pan as a reference to adjust the output balance. Measurement of the sample was performed at a heating rate of 10°C min⁻¹. The range of temperatures scanned was from -30 to 130°C.

RESULTS AND DISCUSSION

Effect of DOP on styrene homopolymerization

The polystyrene particles with DOP incorporated were prepared with an SPG membrane pore size of 0.51 μm for emulsification. They were subsequently polymerized by suspension polymerization. The preparative conditions for a one-step emulsification are shown in Table I and the recipes of copolymer compositions in Table II.

The SEM micrograph [Fig. 1(a) for Run 2013] shows that polystyrene particles incorporating DOP have an average diameter of 3 μm and are irregular in shape.

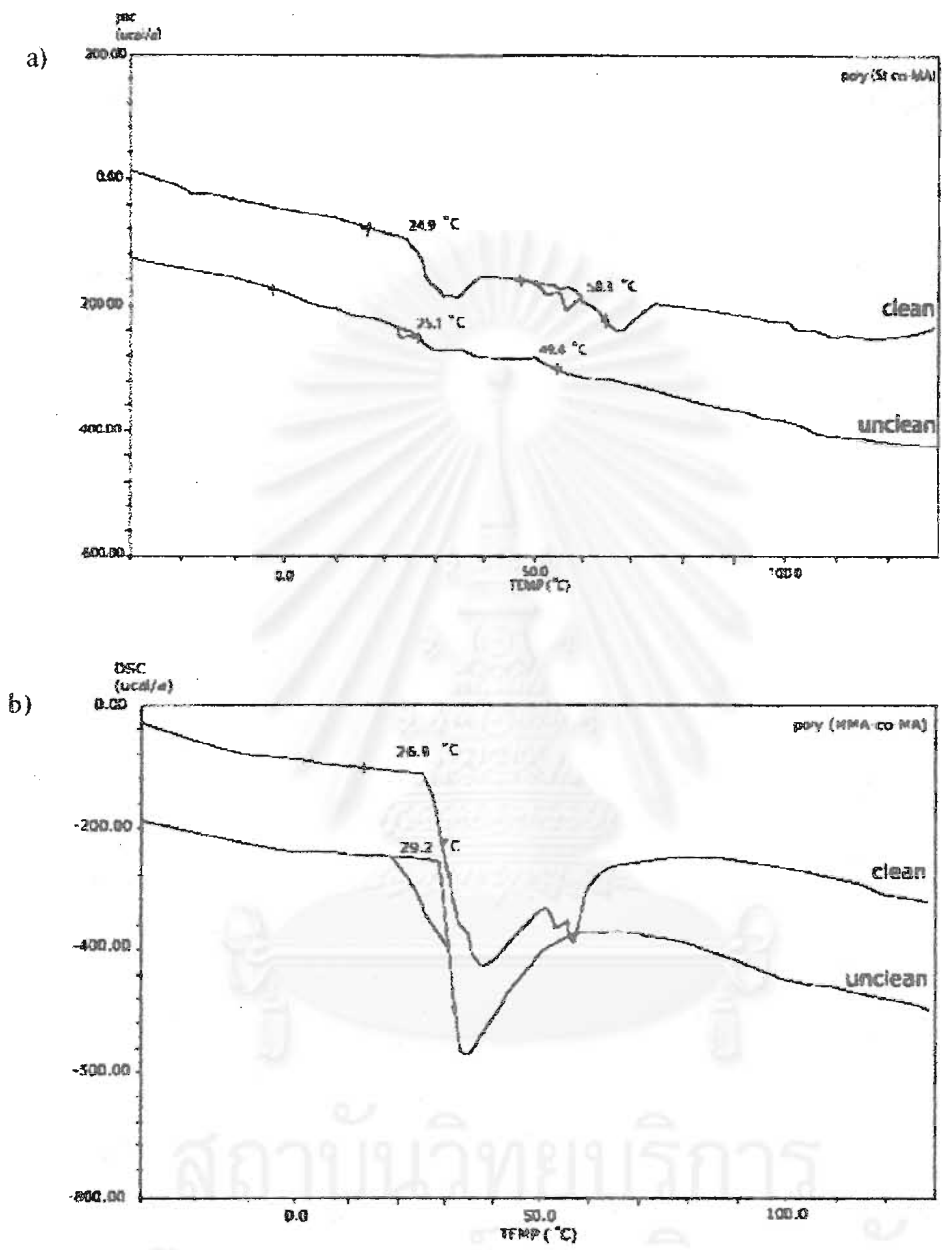


Figure 4 DSC thermograms of (a) poly(St-co-MA)-DOP and (b) poly(MMA-co-MA)-DOP.

A higher magnification of these particles revealed small particles with an average diameter of less than 0.1 μm . These small particles covered the surface of large particles. Very interestingly, we estimated that emulsion polymerization takes place at the expense of the suspension polymerization for the present case. Secondary particle nucleation in Run 2013 could take place at the longer emulsification time of 20 h using the SPG membrane pore size of 0.5 μm with low pressure (1.3 kgf cm^{-2}). Smaller emulsion droplets (4.1 μm) were obtained, leading to opalescence and forma-

tion of small polymer particles. This resulted in higher molecular weight and a bimodal molecular weight distribution. Because DOP and styrene monomers have relatively close solubility parameter values, both are thus compatible. As suspension polymerization proceeds, styrene polymerizes much faster and excludes DOP, leaving it in the aqueous phase because of the latter's moderate hydrogen bonding. The aqueous phase composition of dissolved styrene monomer and DOP then polymerized to give the minute amount of secondary particles deposited on the larger primary

TABLE V
Monomer Reactivity Ratios in Radical Copolymerization

| M_1 | r_1 | M_2 | r_2 | $r_1 r_2$ |
|---------------------|-------|---------------------|-------|-----------|
| Styrene | 0.84 | Butyl acrylate | 0.18 | 0.151 |
| Styrene | 0.19 | Methyl acrylate | 0.80 | 0.154 |
| Styrene | 0.56 | Butyl methacrylate | 0.31 | 0.174 |
| Styrene | 0.52 | Butyl methacrylate | 0.47 | 0.244 |
| Styrene | 0.74 | Butyl methacrylate | 0.59 | 0.437 |
| Styrene | 0.49 | Methyl methacrylate | 0.418 | 0.205 |
| Methyl methacrylate | 2.15 | Methyl acrylate | 0.40 | 0.86 |

particles. Glass-transition temperatures of the composite polymer as shown in Table II, corresponding to the highly and modestly plasticized portions, are 18 and 71°C, respectively. The glass-transition temperature results confirm the polymerization loci. We anticipate that DOP migration could probably take place during the temperature rise in the course of the DSC measurement.

Dependency of styrene homopolymerization on the initiator type

Two types of initiator, ADVN (a more aqueous type) and BPO (a nonaqueous type), were used to polymerize DOP plasticized styrene. Both initiators produced similar monomer conversions of 74.6 and 76.5%. The effects of the initiator on the particle size are shown in Table II. The average particle size obtained from ADVN initiation [Run 2012, Fig. 1(b)] was larger than that from BPO [Run 1014, Fig. 1(c)]. After the polymer latex had been kept for 24 h, we found that the plasticized polystyrene synthesized with BPO initiation gave one layer of precipitate residing at the bottom of the bottle. In contrast, two separate layers of precipitate were observed for the ADVN initiation. The BPO-initiated polystyrene preferred not to suspend in the aqueous phase because of the higher hydrophobicity of both initiator fragments. For the ADVN initiation system, the polystyrene particles with the more polar initiator fragments could better remain in the aqueous phase. Therefore, BPO initiation gave polymer with lower average molecular weights and a narrow molecular weight distribution than those from the ADVN initiation because the former terminated faster than did the latter. However, the surface morphology of the polymer particles was still similar because a smooth surface was obtained as shown in Figure 1(b)–(d).

The glass-transition temperature of DOP plasticized polystyrene is presented in Table II. For all experiments, two separate T_g values were found, indicating increasing immiscibility of the styrene monomer (dissolving PS) and DOP during polymerization. At the beginning stage of the polymerization, more DOP concentration was used along with styrene conversion

because the polymer chain lengths were still short, which eased the inclusion of DOP between these chains. At this stage, highly plasticized polystyrene was obtained, yielding a lower glass-transition temperature. At the later stage of polymerization, less DOP was retained in the monomer droplets. Less-plasticized polystyrene particles (chains) resulted, yielding a higher glass-transition temperature.

Effect of the inhibitor on polymerization and polymer particles

Two types of water-soluble inhibitors, NaNO_2 and PDA, were used.¹⁶ From Table II it may be observed that the inhibitors did not significantly affect the monomer conversion, molecular weights and distribution, and particle morphology. All the synthesized particles had smooth surfaces and were spherical with

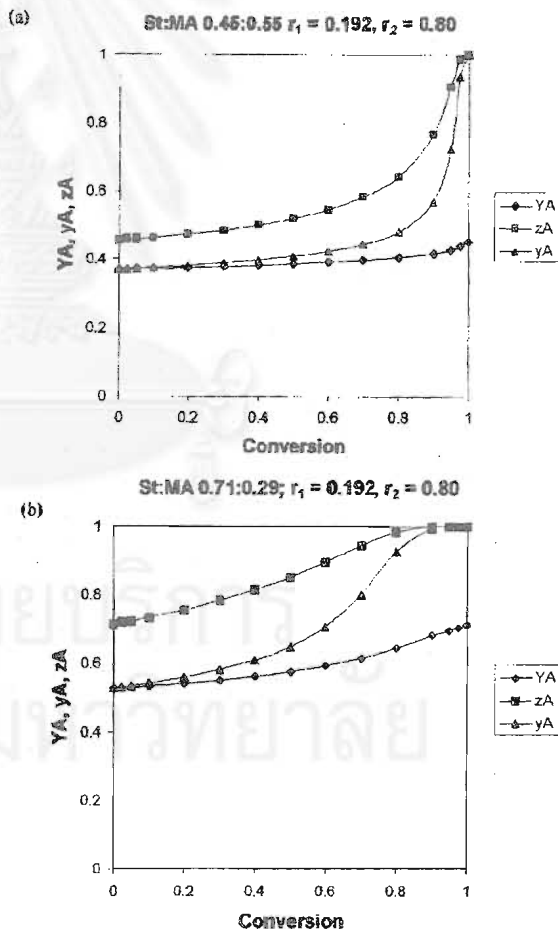


Figure 5 Composition drift of poly(St-co-MA): (a) St : MA, 50 : 50 wt %; (b) St : MA, 75 : 25 wt % (YA, cumulative composition of styrene in copolymer; yA, composition of styrene in unreacted monomer; zA, instantaneous composition of styrene in copolymer).

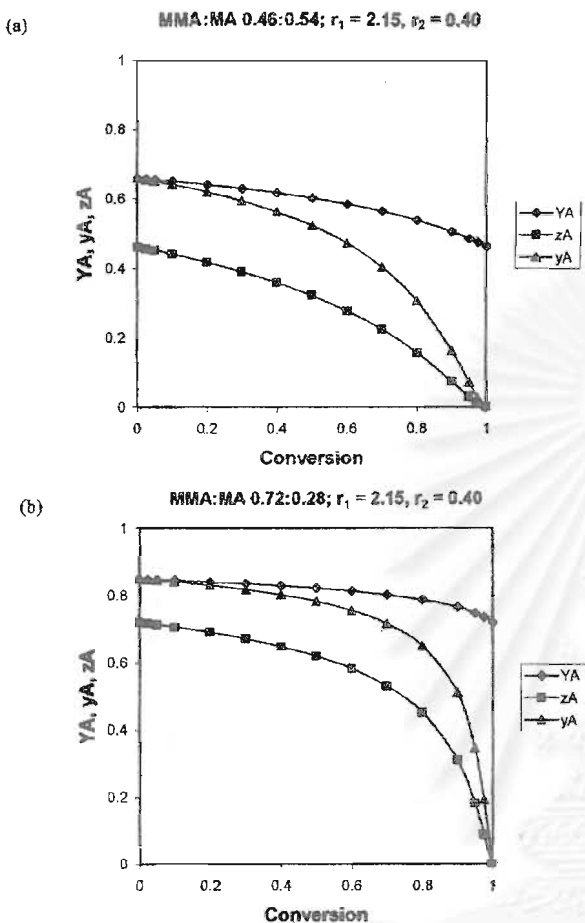


Figure 6 Composition drift of poly(MMA-co-MA): (a) MMA : MA, 50 : 50 wt %; (b) MMA : MA, 75 : 25 wt % (YA, cumulative composition of MMA in copolymer; yA, composition of MMA in unreacted monomer; zA, instantaneous composition of MMA in copolymer).

an average particle size of 8 μm . One must mention that the latex with a PDA inhibitor exhibited a dark violet color [Fig. 1(d)], from which dark brown polystyrene particles resulted. For the forthcoming syntheses of plasticized copolymers, only NaNO_2 was used as an inhibitor.

Effect of DOP on properties of poly(styrene-co-MA) and poly(MMA-co-MA) particles

Particle morphology

DOP plasticizer of 5% by weight of monomer was added to 16 g of total monomer mixtures. Poly(St-co-MA) and poly(MMA-co-MA) particles were then synthesized as shown in Tables III and IV. SEM micrographs for all copolymer particles obtained in each run are shown in Figure 2. The particles of poly(St-co-

MA) remained spherical in shape as shown in Figure 2(a)–(d). In the absence of DOP, pinholes on the particle surface were observed in Figure 2(a) for Run 2022. In addition, small flakes were attached to the particle surfaces in Run 2023 [Fig. 2(b)] when the amount of styrene monomer increased in the absence of DOP. With the addition of DOP, the polymer particles retained a spherical shape with a smooth surface. Poly(MMA-co-MA) was synthesized by use of the same experimental methods as for the poly(St-co-MA). A smooth, spherical particle surface was obtained for all recipes. However, the particles were soft and easily deformed when exposed to a strong electron beam from the SEM apparatus as shown in Figure 3. Poly(St-co-MA) particles are rather strong and rigid because its vinyl backbone contains the bulky phenyl group moiety as a substituent group for the hydrogen atom, whereas poly(MMA-co-MA) particles are relatively flexible, with the less-stiff and weaker aliphatic functional group. This difference in chain stiffness could be the reason for the polymer surface hardness and resistance to high energy irradiation.

Glass-transition temperature

The secondary (higher) T_g value of the unclean poly(St-co-MA) particles was found (Table III and Fig. 4) to be lower than that of the clean polymer. The glass-transition temperature of polymers is of course affected by the addition of DOP plasticizer (5 wt % of monomer). In general, DOP resides physically inside the polymer chains and reduces the repulsion force between intermolecular chains. It can thus ease the motion of the rigid chains of styrene-MA copolymer. In comparison, some portions of DOP in the polymer latex cleaned with methanol were washed out from the particles during the treatment. The secondary T_g of the clean polymer particles was higher than that of the unclean latex, which was close to the T_g value of neat polystyrene homopolymer. Besides the removal by methanol cleaning, migration of the DOP plasticizer to the particle surface according to its general nature may assist in the removal during the cleaning. On the other hand, the primary (lower) T_g values were located close to the T_g of the MA homopolymer, depending on the MA monomer content in the copolymer. The different increments in T_{g1} (the lower T_g) and T_{g2} (the higher T_g) depended greatly on the sample preparation methods and the incorporated amount of DOP. The difference between T_{g1} and T_{g2} of the clean particles was greater than that of the unclean particles. In addition, the T_{g1} and T_{g2} of the DOP plasticized polymer particles were narrower than those of particles without DOP.

Table V shows the reactivity ratios of the comonomers in the present research. Figure 5 shows the composition drift of St in the copolymer of poly(St-co-MA).

TABLE VI
Recipe and Experimental Results of Styrene and Butyl Methacrylate Copolymerization

| Run no. | Composition | Monomer composition (wt %) | Monomer conversion (%) | D_e (μm) | CV_e (%) | D_p (μm) | CV_p (%) | \bar{M}_n ($\times 10^{-4}$) | \bar{M}_w ($\times 10^{-4}$) | PDI | T_g ($^{\circ}\text{C}$) | |
|-------------------|------------------|----------------------------|------------------------|-------------------------|------------|-------------------------|------------|----------------------------------|----------------------------------|-------------------|------------------------------|------------------------|
| | | | | | | | | | | | Clean | Unclean |
| 2002 ^a | P(St-co-BMA) | 80/20 | 63.8 | 7.1 | 25.9 | 5.8 | 16.1 | 4.9 | 57.9 | 11.9 ^b | na | 26.1/45.7 ^c |
| 2008 ^a | P(St-co-BMA) | 50/50 | 71.8 | 8.4 | 21.6 | 3.8 | 13.1 | 1.5 | 5.2 | 4.0 | 12.2/43.8 ^c | -3.0 |
| 2051 ^d | P(St-co-BMA)/PSt | (62.5/25)/12.5 | 75.4 | 8.4 | 14.7 | 6.1 | 20.9 | 0.5 | 3.4 | 6.9 | 23.8/58.4 ^c | 17.2/65.7 ^c |
| 2052 | P(St-co-BMA)/PSt | (62.5/25)/12.5 | 52.0 | 6.2 | 17.5 | 5.5 | 21.2 | 0.5 | 2.8 | 5.2 | 21.2/50.0 ^c | 17.3 |

^a SPG pore size 0.51 μm ; otherwise, 0.90 μm .

^b Bimodal peak.

^c Two separate T_g values were observed.

^d Recipe without DOP. na, not available.

The reactivity ratios of the two monomers, r_1 (St = 0.192) and r_2 (MA = 0.80),^{17,18} indicate that MA is consumed faster than St [Fig. 5(a)]. The reaction mixture is short of MA, that is, the polymer propagation chains are rich in MA units at the beginning [Fig. 5(b)], and the subsequently growing chains are terminated by the St monomer units when approaching a complete conversion. The composition drift of styrene was more pronounced at the higher styrene concentrations. Based on $r_1 r_2 \approx 0.15$, this copolymer lies between the two extremes of ideal and alternating copolymerization.¹⁸ As the $r_1 r_2$ product decreases from unity (1 for an ideal copolymerization) toward zero, there is an increasing tendency toward alternation. However, the copolymer is still of a random type. Copolymer composition drift could be an attribute determining the extent of T_g in 50/50 wt % of poly(St-co-MA) as shown in Table III.

In the case of poly(MMA-co-MA), a single T_g value with a sharp transition was observed for all copolymer compositions as shown in Figure 4(b). The T_g value was close to room temperature. T_g values of the copolymers with and without DOP were observed in the same range, as shown in Table IV. Likewise, the T_g value is also controlled by the composition drift in the copolymer. Moreover, a much greater composition drift in the copolymer is also found in the case of MMA-MA monomers. The reactivity ratios of MMA (r_1) and MA (r_2) are 2.150 and 0.400,^{17,18} respectively, as shown in Table V. Based on the $r_1 r_2$ product of 0.86 (approaching 1), poly(MMA-co-MA) is an ideal (random) type of copolymer. Figure 6 shows the composition drift of MMA in the copolymer. Because the MMA reactivity ratio is greater than unity, the copolymer contains a larger proportion of MMA [Fig. 6(a)]. The very high value of r_1 produces the MMA-rich chains at the beginning of the copolymerization [Fig. 6(b)], which causes MMA starvation in the reaction mixture. At the end of the copolymerization, MA units are thus preferentially consumed, depending on the reaction time. Because the difference in reactivity of the two monomers is very high, it becomes more difficult to produce copolymers having appreciable amounts of the less-reactive monomer, unless the copolymerization approaches the end of conversion. Composition drift in the copolymer is thus another factor that controls the glass-transition temperature of the copolymer.

Compared with poly(St-co-MA), poly(MMA-co-MA) copolymers achieved better compatibility than that of St-MA copolymers. This could result from the similar chemical structure of DOP and acrylate monomer. In other words, the DOP mixes more homogeneously in the matrix of poly(MMA-co-MA) than it does in the matrix of poly(St-co-MA), according to the DSC thermograph shown in Figure 4.

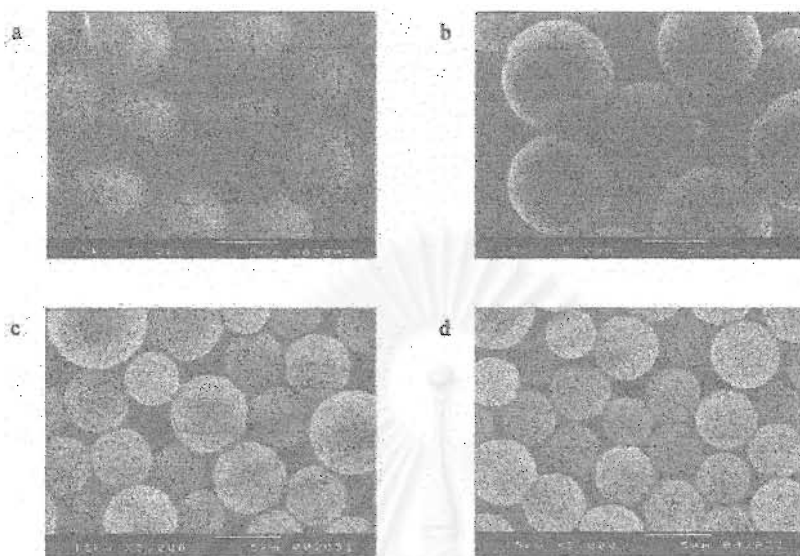


Figure 7 SEM micrographs of poly(St-co-BMA)-DOP: (a) St:BMA = 80:20; (b) St:BMA = 50:50; (c) St:BMA:PSt = 62.5:25:12.5 (without DOP); (d) St:BMA:PSt = 62.5:25:12.5.

However, other factors influencing T_g may include the surfactant and stabilizer in the polymer latex,¹⁹ given that the PVA and SLS can physically adsorb onto the polymer surface. If possible, it might be necessary to separate the particles from their serum before proceeding to the subsequent processes. The heating rate during the DSC scanning is also undoubtedly one of the factors that governs the T_g value.

Effect of the addition of polystyrene on properties of poly(St-co-BMA) copolymers

The SPG membrane pore size of 0.90 μm was used for the emulsification of St and BMA, with results as shown in Table VI. The amount of the BMA phase was varied from 20 to 50% in the monomer mixture in the presence of 5 wt % DOP of total monomer mixture. When the BMA phase is present at more than 50 wt %, the particles become flattened, which is in agreement with our previous work.^{15,20} SEM micrographs of the poly(St-co-BMA) particles are shown in Figure 7. Spherical particles having smooth surfaces were synthesized without a phase separation. Upon the addition of 12.5 wt % polystyrene (with $M_n = 4000$; $M_w = 40,000$) into the St-BMA mixture, the viscosity of the dispersion phase significantly increased. The number-averaged molecular weight of the resulting copolymer was close to 5000 as shown in Table VI (Runs 2051 and 2052). We anticipate that added polystyrene functions as if it were a macromonomer (a bulky molecule), which diffuses rather slowly in the monomer mixture. Because it is of rather high molecular weight, polystyrene thus retards the propagation step of St and BMA monomers. Therefore, the higher molecular weight

polystyrene can be considered as a kind of molecular spacer to prevent the propagating radicals from adding more monomers. The most likely outcome for these short propagating radicals is to terminate, which ultimately results in a low average molecular weight.

When methanol was added into the reaction mixture, all the polymer components containing styrene units were precipitated to result in a mixture of poly(St-co-BMA) and polystyrene beads. This mixture of the plasticized poly(St-co-BMA) and polystyrene increased the glass-transition temperatures of the particles. As shown by the second T_g of the clean particles in Runs 2051 and 2052, the addition of polystyrene into the reaction mixture does not significantly alter the efficiency of DOP in poly(St-co-BMA)/PSt. Thus it is not necessary to include DOP in the composite particles of poly(St-co-BMA) when polystyrene is added before the polymerization.

Glass-transition temperature of poly(St-co-BMA)

A single-stage glass-transition temperature was revealed in the unclean poly(St-co-BMA) copolymer as shown in Table VI. The presence of DOP in the copolymer enhances the free volume of the hard phase. Because both DOP and BMA contain a similar ester functional group, the DOP can be compatible with the BMA soft domain. In each domain, the DOP molecular chains lubricate the St backbone, resulting in a low single T_g in both poly(St-co-BMA)/PSt and poly(St-co-BMA) copolymers. For the clean polymers, the two separate T_g values were observed. This result can be explained as follows. The presence of DOP plasticizer

TABLE VII
Recipe and Experimental Results of Styrene and Butyl Acrylate Copolymerization Using an SPG Pore Size of 0.90 μm

| Run no. | Composition | Monomer composition (wt %) | Monomer conversion (%) | D_e (μm) | CV_e (%) | D_p (μm) | CV_p (%) | \bar{M}_n ($\times 10^{-4}$) | \bar{M}_w ($\times 10^{-4}$) | PDI | T_g ($^{\circ}\text{C}$) | |
|---------|-----------------------|----------------------------|------------------------|-------------------------|------------|-------------------------|------------|----------------------------------|----------------------------------|-----|------------------------------|------------------------|
| | | | | | | | | | | | Clean | Unclean |
| 2048 | P(St-co-BA) | 75/25 | 71.3 | 8.7 | 13.9 | 6.2 | 15.8 | 2.6 | 6.2 | 2.4 | 22.7/58 ^a | 17.4/51.6 ^a |
| 2047 | P(St-co-BA)/DOP | 75/25 | 65.1 | 8.1 | 15.1 | 6.5 | 16.3 | 2.1 | 4.9 | 2.3 | 40.2 | 16.8 |
| 2049 | P(St-co-BA)/PSt | (62.5/25)/12.5 | 86.0 | 7.6 | 13.5 | 5.3 | 17.4 | 0.7 | 3.9 | 5.4 | 17.2/55 ^a | 18.8/52.0 ^a |
| 2050 | [P(St-co-BA)/PSt]/DOP | (62.5/25)/12.5 | 67.9 | 6.8 | 21.7 | 5.2 | 23.3 | 0.6 | 3.7 | 5.9 | 22.2/53.3 ^a | 19.7 |

^a Two separate T_g values were observed.

in the copolymer depends largely on the physical interaction between the copolymer and the plasticizer. After the solvent washing, DOP could remain partially in the polymer particles, if this interaction is strong enough.

Effect of DOP on properties of poly(St-co-BA) copolymer

The SPG membrane with a pore size of 0.90 μm was used for emulsification of the St and BA monomers. The experimental results are shown in Table VII and Figure 8. The presence of the soft BA phase in the copolymer synergistically enhances the plasticizing effect of DOP. Because BA itself behaves like a plasticizing monomer, the expected single glass-transition temperature was found in poly(St-co-BA) particles for both clean and unclean samples (Run 2047). However, when PSt was added into the St-BA monomer mixture, the synthesized poly(St-co-BA)/PSt gave a single T_g value in the unclean particles. For the clean particles, two separate T_g values were found. Likewise, a

low number-averaged molecular weight was also found, as in the above-mentioned case of poly(St-co-BMA).

Internal morphology of poly(St-co-MA)

The microtomes and stained polymer particles (Runs 2018 and 2019) reveal their internal morphology as shown in Figure 9. The internal particle morphology was observed by varying the monomer composition. The transmission electron micrographs of poly(St-co-MA) with St/MA of 75/25 and 50/50 are shown in Figure 9(a), (b). Inside the particles, the small white granules of MA were revealed. The granules did not appear at the outermost submicron thickness at the circumference of the particle. When a higher concentration of styrene was incorporated, larger sizes of white granules were produced as shown in Figure 9(b).

When the emulsion droplets are formed, there is a time lapse before the subsequent suspension polymer-

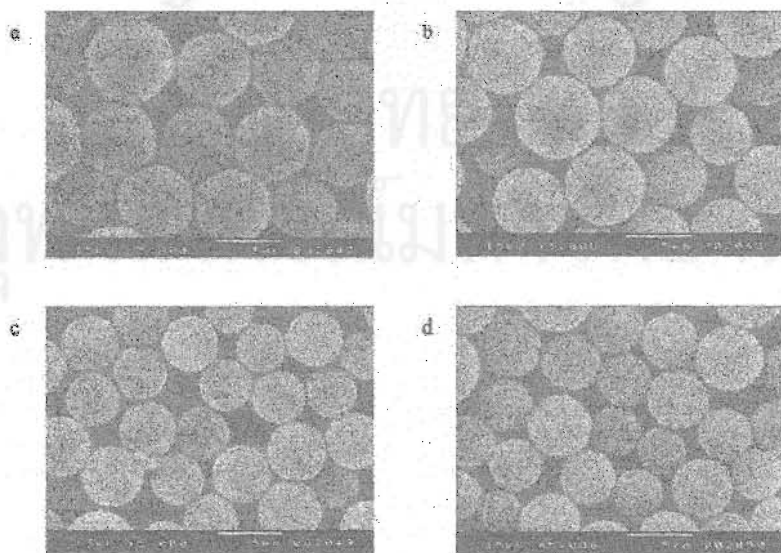


Figure 8 SEM micrographs of polymer particles: (a) poly(St-co-BA), St:BA = 75:25; (b) poly(St-co-BA)-DOP, St:BA = 75:25; (c) poly(St-co-BA)/PSt, St:BA:PSt = 62.5:25:12.5; (d) poly(St-co-BA)/PSt, St:BA:PSt = 62.5:25:12.5.

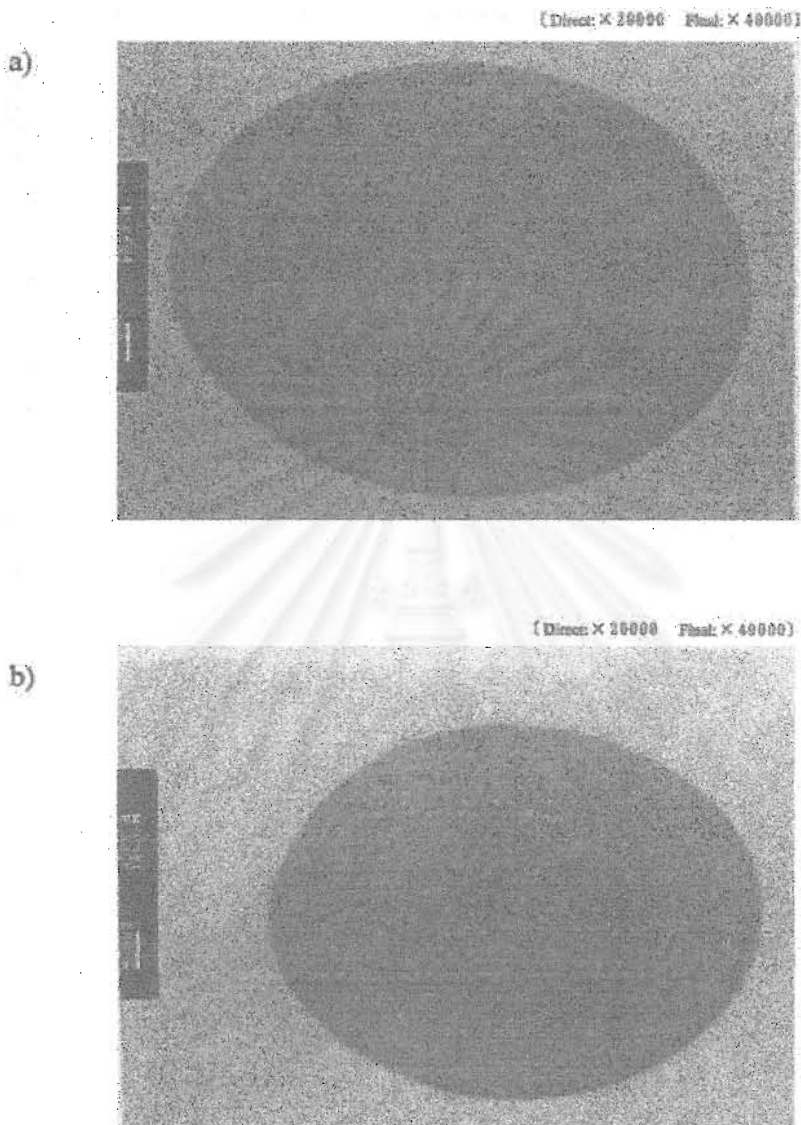


Figure 9 TEM micrographs of poly(St-co-MA): (a) St : MA = 50 : 50; (b) St : MA = 75 : 25.

ization. We observed some droplet separation and their suspension inside the larger drops. Given that the MA reactivity ratio is greater than that of styrene, MA monomer droplets were consumed faster at the beginning of the polymerization to become the small domains. The styrene-rich phase was subsequently produced, which later became the matrix for the MA domains. The TEM micrographs also suggest that some diffusion of MA-rich domains into the styrene-rich polymer matrix probably occurs.

CONCLUSIONS

SPG emulsification and subsequent suspension polymerization were employed for preparation of two-

phase styrene-acrylate copolymer particles incorporating DOP plasticizer. Both suspension and emulsion polymerizations took place, but the former controls the polymer behavior. The presence of DOP on the polystyrene-based particles significantly enhances the mobility of the styrene backbone and yields lower T_g values of the copolymers. The slightly nonpolar DOP preferentially plasticizes the matrix phase of both the hard PS-phase and the soft (meth)acrylate-phase. Regardless of the monomer concentration ratios, the resulting spherical polymer particles range in size from 3 to 7 μm . Upon washing the polymer particles with methanol, DOP in the polymers was washed out and two separate T_g peaks resulted. Microphase separation was found when the monomer droplets were formed

at a later stage in the emulsification process. Small particles were then produced to give a broad molecular weight distribution.

All the comonomer pairs under study exhibited composition drift during the copolymerization because of their substantial difference in monomer reactivity ratios, which was evidenced by the T_g values of the copolymers. In comparison, poly(MMA-co-MA) revealed that they were well compatibilized with DOP. A single T_g value with a sharp transition was found in both clean and unclean particles, given that the presence of a similar functional group (ester) significantly enhances the physical interaction between them and yields more compatible behavior. When the low T_g polymers are carefully produced, the polymer particles can be used for surface-coating purposes without the inclusion of plasticizers because film flexibility and a low glass-transition temperature can be obtained directly from the inherent properties of the designed monomers and their corresponding copolymer. In addition, the inclusion of moderately high molecular weight polystyrene in the polymerization solution and the effect of DOP as a plasticizer for the copolymer, based on the polymer particle properties and glass-transition temperature, are not significant.

The authors express their sincere appreciation to the Golden Jubilee Program of the Thailand Research Fund for providing a scholarship through Contract Number 2.M.CU/42/E.1, and to the Graduate School of Bio-Applications and Systems Engineering (BASE), Tokyo University of Agriculture and Technology, Tokyo, Japan for providing research facilities to the first author to carry out this research.

References

1. Landfester, K.; Spiess, H. W. *Acta Polym* 1998, 49, 451.
2. Winnik, M. A.; Feng, J. *J Coat Technol* 1996, 68, 39.
3. Cho, I.; Lee, K. W. *J Appl Polym Sci* 1985, 30, 1903.
4. Min, T. I.; Klein, A.; El-Aasser, M. S.; Vanderhoff, J. W. *J Polym Sci Polym Chem Ed* 1983, 21, 2845.
5. Nelliappan, P.; El-Aasser, M. S.; Klein, A.; Daniels, E. S.; Robert, J. E. *J Polym Sci Part A: Polym Chem* 1996, 34, 3173.
6. Chen, Y. C.; Dimonie, V. L.; El-Aasser, M. S. *J Appl Polym Sci* 1991, 42, 1049.
7. Jonsson, J. E.; Hassander, H.; Tornell, B. *Macromolecules* 1994, 27, 1932.
8. Jonsson, J. E.; Karlsson, O. J.; Hassander, H.; Tornell, B. *Macromolecules* 2001, 34, 1512.
9. Stubbs, J.; Larsson, O.; Jonsson, J. E.; Sundberg, E.; Durant, Y.; Sundberg, D. *Colloids Surf A: Physicochem Eng Aspects* 1999, 153, 255.
10. Shieh, Y.; Liu, C. M. *J Appl Polym Sci* 2002, 83, 2548.
11. Hsu, S. C.; Lee, C. F.; Chiu, Y. C. *J Appl Polym Sci* 1999, 71, 47.
12. Feng, J.; Winnik, M. A.; Shivers, R. R.; Clubb, B. *Macromolecules* 1995, 28, 7671.
13. Tamai, T.; Pinenq, P.; Winnik, M. A. *Macromolecules* 1999, 32, 6102.
14. Kirsch, S.; Pfau, A.; Stubbs, J.; Sundberg, D. *Colloids Surf A: Physicochem Eng Aspects* 2001, 183, 725.
15. Nuisin, R.; Ma, G. H.; Omi, S.; Kiatkamjornwong, S. *J Appl Polym Sci* 2000, 77, 1013.
16. Sudoi, E. D.; El-Aasser, M. S.; Vanderhoff, J. W. *J Polym Sci Part A: Polym Chem* 1986, 24, 3515.
17. Brandrup, J.; Immergut, E. H. *Polymer Handbook*, 3rd ed.; Wiley: New York, 1989; Sec. II, pp. 182-216.
18. Odian, G. *Principles of Polymerization*, 3rd ed.; Wiley: Singapore, 1991; pp. 460-466.
19. Zhao, Y.; Urban, M. W. *Macromolecules* 2000, 33, 8426.
20. Kiatkamjornwong, S.; Nuisin, R.; Ma, G. H.; Omi, S. *Chin J Polym Sci* 2000, 18, 309.

สถาบันวิทยบริการ
จุฬาลงกรณ์มหาวิทยาลัย